

**A Novel Microencapsulation System: Preparation and  
Characterization of Genipin Cross-linked Alginate-Chitosan  
Microcapsules for Live Cell Oral Delivery and Other Applications**

Hongmei Chen

*Biomedical Technology and Cell Therapy Research Laboratory  
Department of Biomedical Engineering  
Faculty of Medicine  
McGill University  
Montreal, Quebec, Canada*

A thesis submitted to McGill University in partial fulfillment of the  
requirements of the degree of

**Doctor of Philosophy**

**June, 2006**



**McGill**

©Hongmei Chen, 2006



Library and  
Archives Canada

Bibliothèque et  
Archives Canada

Published Heritage  
Branch

Direction du  
Patrimoine de l'édition

395 Wellington Street  
Ottawa ON K1A 0N4  
Canada

395, rue Wellington  
Ottawa ON K1A 0N4  
Canada

*Your file* *Votre référence*  
ISBN: 978-0-494-27764-5  
*Our file* *Notre référence*  
ISBN: 978-0-494-27764-5

#### NOTICE:

The author has granted a non-exclusive license allowing Library and Archives Canada to reproduce, publish, archive, preserve, conserve, communicate to the public by telecommunication or on the Internet, loan, distribute and sell theses worldwide, for commercial or non-commercial purposes, in microform, paper, electronic and/or any other formats.

The author retains copyright ownership and moral rights in this thesis. Neither the thesis nor substantial extracts from it may be printed or otherwise reproduced without the author's permission.

#### AVIS:

L'auteur a accordé une licence non exclusive permettant à la Bibliothèque et Archives Canada de reproduire, publier, archiver, sauvegarder, conserver, transmettre au public par télécommunication ou par l'Internet, prêter, distribuer et vendre des thèses partout dans le monde, à des fins commerciales ou autres, sur support microforme, papier, électronique et/ou autres formats.

L'auteur conserve la propriété du droit d'auteur et des droits moraux qui protègent cette thèse. Ni la thèse ni des extraits substantiels de celle-ci ne doivent être imprimés ou autrement reproduits sans son autorisation.

---

In compliance with the Canadian Privacy Act some supporting forms may have been removed from this thesis.

Conformément à la loi canadienne sur la protection de la vie privée, quelques formulaires secondaires ont été enlevés de cette thèse.

While these forms may be included in the document page count, their removal does not represent any loss of content from the thesis.

Bien que ces formulaires aient inclus dans la pagination, il n'y aura aucun contenu manquant.

  
**Canada**

*To my daughter Hiaojuan*

## ABSTRACT

Oral therapy utilizing artificial cell microencapsulation has shown promise in the treatment of many diseases. The key requirements of microcapsules for such applications include biocompatibility, mechanical stability, permeability and resistance to the human gastrointestinal (GI) environment. In particular, preservation of structural integrity is crucial when live genetically engineered cells are used. One of the main obstacles in the progress of this strategy is attaining biocompatible and stable microcapsules.

This thesis aims to develop a suitable microcapsule system, the genipin cross-linked alginate-chitosan (GCAC) microcapsule, for live cell oral delivery. The preparation procedure, including calcium-alginate ionotropic gelation, coacervative chitosan coating and covalent cross-linking by genipin, was established and optimized. Control factors affecting the formation of microcapsule membrane were identified. The structural and physical characteristics of GCAC microcapsules, such as mechanical stability, swelling characteristics, permeability, controlled release, degradation, and others were investigated and compared with earlier established microcapsule systems including alginate-chitosan and alginate-poly-L-lysine-alginate (APA). In addition, live cell oral delivery features were evaluated with a computer controlled dynamic simulated human GI model using genetically engineered *Lactobacillus plantarum* 80 cells as an example.

Results show that by incorporating genipin, a new class of GCAC microcapsule system can be formulated. Results also show that covalent cross-linking by genipin considerably enhanced the microcapsule stability and durability while maintaining permeability similar to that of the APA membrane. The GCAC membrane possessed strong resistance to structural degradation and GI impediments, while providing a favorable microenvironment for cell proliferation and survival in harsh GI conditions.

In addition, this research found that the fluorogenic attributes of genipin can be exploited to characterize the microcapsule membrane by confocal laser scanning microscopy. A simple, *in situ*, and non-destructive approach was established and extended to assess other microcapsule systems. Rapid determination of coating material distribution, binding intensity, and membrane thickness on a routine basis was achieved using this novel and superior method.

This work highlights the immense potential of the novel genipin cross-linked alginate-chitosan microcapsule as an oral delivery vehicle for live therapeutic cells and other important applications. Further studies will investigate its full potential for artificial cell oral therapy.

## RÉSUMÉ

La cellule artificielle microencapsulation d'utilisation de thérapie oral a pu faire croire dans le traitement de plusieurs maladies. Les requis majeurs de caractéristiques de microcapsule pour telle application incluent la biocompatibilité, la stabilité mécanique, la perméabilité et la résistance à l'humain gastro-intestinal (GI) environnemental. En particulier, la préservation d'intégrité structurale est cruciale quand nous utilisons de nouvelles cellules. Un des obstacles principaux dans le progrès de cette stratégie est d'atteindre des microcapsules stable et biocompatible.

Cette thèse a cherché à développer un système de microcapsule convenable, le l'alginate-chitosan croix-relié genipin (GCAC), pour la livraison orale d'une cellule vivante. La procédure de préparation, y compris le calcium-alginate ionotropic gelation, le revêtement de chitosan et le croix-relier covalent par genipin, a été établi et optimisé. Les facteurs de contrôle affectant la formation de membrane de microcapsule ont été identifiées. Les caractéristiques structurales et physiques es microcapsules GCAC, telle que la stabilité mécanique, caractéristiques d'enflure, la perméabilité, le relâchement contrôlé, la dégradation, et les autres ont été examiné et comparé à l'alginate-chitosan antérieurement proposé (alternatif courant) a même les membranes bien établi d'alginate-L-polysine-alginate (APA). Aussi, caractéristiques de livraison orales les cellules en vie ont été évaluées en utilisant un ordinateur contrôlé et dynamiquement simulé par des gastro-intestinal humaine (GI) le modèle utilisait comme un exemple les cellules *Lactobacillus plantarum* génétiquement organisé 80 (LP80).

Les résultats ont montré qu'en utilisant le genipin, une nouvelle classe de microcapsule (le système de GCAC) peut être formulé. Les résultats ont aussi montré le croix-relier covalent par genipin a amélioré considérablement la stabilité de microcapsule et la durabilité toute en maintenant la perméabilité similaire à la membrane de APA. La membrane de GCAC a possédé la résistance forte à la dégradation structurale et les entraves de GI, et pendant ce temps a fourni un microenvironnement favorable pour la survie de cellule, la prolifération, et la protection suffisante contre l'environnement rugueux de GI.

En plus, cette recherche a trouvé que l'approche de genipin de fluorogénic récemment développée peut être utilisée pour caractériser la membrane de microcapsule par le laser de confocal scrutant la microscopie (CLSM). Une approche simple, *in situ*, non destructive a été établie et a été étendue à évaluer les autres systèmes de microcapsule. Cette méthode, nouvelle et supérieure, a permis la détermination rapide de revêtement de la distribution matérielle, l'intensité liante, et l'épaisseur de membrane sur une base routinière, qui a facilité la compréhension et l'amélioration des microcapsules.

Les présentes conclusions ont révélé que ce nouveau genipin l'alginate-chitosan croix-relié (GCAC) microcapsules a le potentiel significatif comme un véhicule de livraison oral pour les cellules thérapeutiques vivantes. Plus de travail est exigé afin d'examiner le potentiel complet du GCAC microcapsule pour la livraison orale et les autres applications.

## ACKNOWLEDGEMENTS

I would like to express my sincere gratitude to my supervisor Dr. Satya Prakash for the opportunity to conduct this research at the Biomedical Technology and Cell Therapy Research Laboratory of the Biomedical Engineering Department, and for his advice, support and encouragement throughout the duration of my Ph. D. study.

I wish to acknowledge the laboratory assistance and suggestions given by Dr. Wei Ouyang, Mitchell Jones, Terrence Metz, Christopher Martoni, Tasima Haque, Bisi Lawuyi, Trisna Lim, Fatmeh Afkhami, and Rebecca Cohen as well as their contributions as co-authors to the original articles presented in the thesis.

I am also thankful to all other colleagues working in the Biomedical Technology and Cell Therapy Research Laboratory (Maryam, Jasmine, Mehrnous, Pavan, Tin, Leonard, and Tahilia). I give special thanks to Dr. Wei Ouyang, Bisi Lawuyi, Christopher Martoni, and Mitchell Jones for their constructive ideas, help and important support.

A big thank you goes particularly to Professor T. M. S. Chang, from whom I got to know artificial cells and McGill University, and for his persistent encouragement and interest with my research. In addition, I extend my appreciation to Dr. Maryam Tabrizian for the access to the research facilities in her laboratory. I also wish to thank Ms. Lina Vuch for the French translation. Moreover, my thanks go to all the people with whom I have worked during the course of this thesis work. Specifically, I am thankful to Ms. Line Mongeon, Ms. Jacynthe Laliberte, Dr. Hojatollah Vali, Mr. Petr Fiurasek, Dr. Frederick Morin, and Ms. Suzie Poulin for their technical assistance, as well as to Professors Zhenqiu Chen and Bo Deng for fruitful discussions on several scientific matters.

This work was supported by the Natural Sciences and Engineering Research Council (NSERC) of Canada and the Canadian Institutes of Health Research (CIHR). I gratefully acknowledge the doctoral scholarships from NSERC, Fonds Québécois de la Recherche sur la Nature et les Technologies (FQRNT), and Greville Smith McGill Major.

Last, but certainly not the least, I would like to dedicate this thesis to my family, my husband and parents, for their everlasting love, support, understanding, encouragement, and patience, to whom I am indebted all the time and without whom none of this would be possible.

## **PREFACE**

In accordance with the McGill University Thesis Preparation and Submission Guidelines, I have taken the option of writing the experimental section in the form of original papers either published or appropriate for publication. These papers comprise chapters 3-10 of this thesis, and are each divided into sections consisting of an abstract, introduction, material and methods, results, discussion, and conclusions. In addition, this thesis contains an overall abstract, introduction and literature review, as well as a summary of results, final conclusions, claims to original contributions, and recommendations.

## TABLE OF CONTENTS

ABSTRACT.....	I
RÉSUMÉ .....	III
ACKNOWLEDGEMENTS .....	V
PREFACE .....	VI
TABLE OF CONTENTS .....	VII
LIST OF TABLES.....	X
LIST OF FIGURES.....	XII
LIST OF ABBREVIATIONS AND TERMINOLOGY.....	XVIII
<b>CHAPTER 1: GENERAL INTRODUCTION .....</b>	<b>1</b>
1.1 OVERVIEW .....	1
1.2 THESIS RESEARCH OBJECTIVES.....	3
1.3 THESIS OUTLINE.....	3
<b>CHAPTER 2: LITERATURE REVIEW .....</b>	<b>4</b>
2.1 INTRODUCTIN TO ARTIFICIAL CELLS .....	4
2.2 DESIGN CONSIDERATIONS OF ARTIFICIAL CELLS FOR LIVE CELL APPLICATIONS.....	6
2.3 ARTIFICIAL CELL PREPARATION TECHNIQUES .....	7
2.4 MICROCAPSULE MEMBRANES AND ARTIFICIAL CELL SYSTEMS CONTAINING LIVE CELLS .....	12
2.5 MICROCAPSULE AND MEMBRANE CHARACTERIZATION.....	35
2.6 ARTIFICIAL CELLS CONTAINING LIVE MICROBES FOR ORAL THERAPY .....	46
<b>PREFACE FOR CHAPTERS 3 TO 10.....</b>	<b>48</b>
<b>CONTRIBUTIONS OF AUTHORS .....</b>	<b>53</b>
<b>CHAPTER 3: <i>IN-VITRO</i> ANALYSIS OF APA MICROCAPSULES FOR ORAL DELIVERY OF LIVE BACTERIAL CELLS .....</b>	<b>54</b>
3.1 ABSTRACT.....	55
3.2 INTRODUCTION .....	55
3.3 MATERIALS AND METHODS .....	56
3.4 RESULTS AND DISCUSSION .....	59
3.5 CONCLUSIONS.....	60
3.6 ACKNOWLEDGEMENTS.....	61
<b>CHAPTER 4: PREPARATION AND CHARACTERIZATION OF NOVEL POLYMERIC MICROCAPSULES FOR LIVE CELL ENCAPSULATION FOR THERAPY .....</b>	<b>69</b>
4.1 ABSTRACT.....	70
4.2 INTRODUCTION .....	70
4.3 MATERIALS AND METHODS .....	72
4.4 RESULTS AND DISCUSSION.....	75
4.5 CONCLUSIONS.....	78
4.6 ACKNOWLEDGEMENTS.....	79
<b>CHAPTER 5: REACTION OF CHITOSAN WITH GENIPIN AND ITS FLUOROGENIC ATTRIBUTES FOR POTENTIAL MICROCAPSULE MEMBRANE CHARACTERIZATION .....</b>	<b>86</b>
5.1 ABSTRACT.....	87
5.2 INTRODUCTION .....	87
5.3 MATERIALS AND METHODS .....	89
5.4 RESULTS .....	90

5.5 DISCUSSION .....	94
5.6 ACKNOWLEDGEMENTS.....	97
<b>CHAPTER 6: A NEW METHOD FOR MICROCAPSULE CHARACTERIZATION: USE OF FLUOROGENIC GENIPIN TO CHARACTERIZE POLYMERIC MICROCAPSULE MEMBRANES .....</b>	<b>108</b>
6.1 ABSTRACT.....	109
6.2 INTRODUCTION .....	109
6.3 MATERIALS AND METHODS .....	111
6.4 RESULTS .....	114
6.5 DISCUSSION .....	117
6.6 ACKNOWLEDGEMENTS.....	120
<b>CHAPTER 7: GENIPIN CROSS-LINKED ALGINATE-CHITOSAN MICROCAPSULES: MEMBRANE CHARACTERIZATION AND OPTIMIZATION OF CROSS-LINKING REACTION .....</b>	<b>126</b>
7.1 ABSTRACT.....	127
7.2 INTRODUCTION .....	127
7.3 MATERIALS AND METHODS .....	128
7.4 RESULTS .....	130
7.5 DISCUSSION .....	133
7.6 CONCLUSIONS.....	136
7.7 ACKNOWLEDGEMENTS.....	136
<b>CHAPTER 8: INVESTIGATION OF STRUCTURE AND RELEVANT PROPERTIES OF THE ALGINATE-CHITOSAN MICROCAPSULES COVALENTLY CROSS-LINKED BY GENIPIN .....</b>	<b>150</b>
8.1 ABSTRACT.....	151
8.2 INTRODUCTION .....	151
8.3 MATERIALS AND METHODS .....	153
8.4 RESULTS AND DISCUSSION.....	158
8.5 CONCLUSIONS.....	165
8.6 ACKNOWLEDGEMENTS.....	165
<b>CHAPTER 9: EVALUATION OF MICROCAPSULES FOR POTENTIAL GASTROINTESTINAL APPLICATIONS USING A DYNAMIC SIMULATED HUMAN GASTROINTESTINAL MODEL .....</b>	<b>184</b>
9.1 ABSTRACT.....	185
9.2 INTRODUCTION .....	185
9.3 EXPERIMENTAL .....	187
9.4 RESULTS .....	190
9.5 DISCUSSION .....	192
9.6 ACKNOWLEDGEMENTS.....	195
<b>CHAPTER 10: MICROENCAPSULATION OF <i>LACTOBACILLUS</i> IN COVALENTLY CROSS-LINKED MICROCAPSULES FOR POTENTIAL GASTROINTESTINAL APPLICATIONS .....</b>	<b>204</b>
10.1 ABSTRACT.....	205
10.2 INTRODUCTION .....	205
10.3 MATERIALS AND METHODS .....	208
10.4 RESULTS .....	211
10.5 DISCUSSION .....	215
10.6 CONCLUSIONS.....	218
10.7 ACKNOWLEDGEMENTS.....	218

<b>CHAPTER 11: SUMMARY OF OBSERVATIONS, CONCLUSIONS AND CLAIMS TO ORIGINAL CONTRIBUTIONS</b> .....	<b>231</b>
11.1 SUMMARY OF OBSERVATIONS .....	231
11.2 CONCLUSIONS.....	236
11.3 CLAIMS TO ORIGINAL CONTRIBUTIONS .....	237
<b>CHAPTER 12: RECOMMENDATIONS</b> .....	<b>238</b>
<b>REFERENCES</b> .....	<b>240</b>
<b>APPENDICES</b> .....	<b>277</b>

## LIST OF TABLES

<b>Table 2.1</b>	Some promising applications of artificial cell technology utilizing live cells.....	5
<b>Table 2.2</b>	Artificial cell design considerations for microencapsulation of live cells.....	6
<b>Table 2.3</b>	Polyelectrolyte materials used for cell encapsulation.....	9
<b>Table 2.4</b>	Parameters affecting polyelectrolyte complexation.....	10
<b>Table 2.5</b>	Summary of major modifications on the APA membrane for cell encapsulation (1997-2006).....	21
<b>Table 2.6</b>	Examples of artificial cell microcapsule formulations alternative to the APA membrane for cell encapsulation.....	33
<b>Table 3.1</b>	Exposure duration and morphological changes of the alginate-poly-L-lysine-alginate (APA) microcapsules to the media of the simulated human gastro-intestinal model.....	62
<b>Table 3.2</b>	Media and incubation conditions used for microbial enumeration of the simulated GI model.....	63
<b>Table 5.1</b>	Effect of temperature and reaction time on the physical appearance of the chitosan-genipin reaction mixture.....	98
<b>Table 6.1</b>	Thickness and relative fluorescence intensity of polyamine coating on genipin-treated microcapsules.....	121
<b>Table 7.1</b>	Control factors and their levels for the cross-linking reaction.....	138
<b>Table 7.2</b>	Range tests on the fluorescence intensity of the GCAC microcapsule membranes.....	139
<b>Table 7.3</b>	Membrane thickness of GCAC microcapsules cross-linked under varied conditions.....	140
<b>Table 7.4</b>	Range tests on membrane thickness of the GCAC microcapsule membranes.....	141

<b>Table 8.1</b>	Characteristics of FITC-dextran used for the measurement of microcapsule permeability.....	167
<b>Table 9.1</b>	Exposure of GCAC microcapsules to the simulated human GI transit (72 h in total) and the corresponding morphological changes.....	196
<b>Table 9.2</b>	Media and incubation conditions used for enumeration of representative microbes in the simulated human colon.....	197
<b>Table 9.3</b>	Effects of microcapsules on selected microbes in the simulated transverse colonic medium .....	198
<b>Table 10.1</b>	Summary of the optimized encapsulator settings for <i>Lactobacillus plantarum 80</i> encapsulation.....	220
<b>Table 10.2</b>	Initial loading of <i>Lactobacillus plantarum 80</i> in microcapsules...	221

## LIST OF FIGURES

<b>Figure 2.1</b>	Schematic representation of the egg-box structure of calcium-alginate gel.....	15
<b>Figure 2.2</b>	Molecular structures of poly-L-lysine (left) and chitosan (right)..	25
<b>Figure 2.3</b>	Chemical structure of methacrylic acid copolymer.....	28
<b>Figure 3.1</b>	Schematic representation of the dynamic simulated human gastro-intestinal (GI) model. Vessel 1: stomach; Vessel 2: small intestine; Vessel 3: ascending colon; Vessel 4: transverse colon; and Vessel 5: descending colon.....	64
<b>Figure 3.2</b>	Microphotographs of the APA microcapsules. a, freshly prepared; b-e, during transit in the simulated human GI model: b, 2 h of exposure (in the simulated stomach); c, 6 h of exposure (2 h in the simulated stomach and 4 h in the simulated small intestine); d, 48 h of exposure (2 h in the simulated stomach, 4 h in the simulated small intestine, 18 h in the simulated ascending colon and 24 h in the simulated transverse colon); e, 72 h of exposure (2 h in the simulated stomach, 4 h in the simulated small intestine, 18 h in the simulated ascending colon, 24 h in the simulated transverse colon and 24 h in the simulated descending colon).....	65
<b>Figure 3.3</b>	Effects of the presence of the APA microcapsules on the microbial populations of <i>enterococcus sp.</i> , <i>staphylococcus sp.</i> , and <i>lactobacillus sp.</i> in the simulated ascending colon (a) and descending colon (b) of the simulated human GI model.....	66
<b>Figure 3.4</b>	Effects of the presence of the APA microcapsules on enzymatic activities of the simulated small intestine (a) and transverse colon (b) medium in the simulated human GI model.....	67
<b>Figure 3.5</b>	Viability of encapsulated <i>LP80</i> bacteria in simulated gastric medium.....	68
<b>Figure 4.1</b>	a, Schematic representation of the GCAC microcapsule structure; b-c, visualization of the GCAC microcapsule membrane by CLSM; b, Micrographs of an optical section taken through the equation of the microcapsules showing the fluorescent genipin cross-linked chitosan membrane; c, 3D reconstruction of optical sections of the GCAC microcapsule showing the shell-like genipin cross-linked chitosan membrane...	80

<b>Figure 4.2</b>	Preparation of the genipin crosslinked alginate-chitosan (GCAC) microcapsules.....	81
<b>Figure 4.3</b>	Optical photomicrographs of the GCAC microcapsules. a, freshly made and b, after 1-week incubation in PBS.....	82
<b>Figure 4.4</b>	Optical photomicrographs of the GCAC microcapsules containing <i>LP80</i> bacterial cells. a, freshly made; b, after 1 month of storage in minimal broth media at 4 °C; and c, after 6 months of storage in minimal broth media at 4 °C.....	83
<b>Figure 4.5</b>	(a): optical photomicrographs of the GCAC microcapsules containing HepG2 cells; and (b): HepG2 encapsulated GCAC bead subject to the viability test using a trypan blue assay.....	84
<b>Figure 4.6</b>	Metabolic activity of the encapsulated HepG2 cells after the process of capsule formation.....	85
<b>Figure 5.1</b>	Absorption and fluorescence spectra of the chitosan-genipin mixture, chitosan and genipin solution acquired at excitation 369 nm and emission 469 nm, respectively.....	99
<b>Figure 5.2</b>	Linear relationship between fluorescence intensity and concentration of the chitosan-genipin reaction product.....	100
<b>Figure 5.3</b>	(a): Fluorescence spectra of the chitosan-genipin mixture composed of varied reactant ratios; and (b): Fluorescence intensities of the chitosan-genipin mixture at $\lambda_{em}^{max}$ as a function of component ratios.....	101
<b>Figure 5.4</b>	Effect of the reaction temperature on the fluorescence spectra of the chitosan-genipin mixture incubated for 4 h. Aliquots were diluted 10 times and scanned with the excitation wavelength set at 369 nm.....	102
<b>Figure 5.5</b>	Fluorescence spectra (a) and intensity profile (b) of the chitosan-genipin mixture incubated at 20°C. At designated time points, aliquots of the mixture were diluted 10 times and scanned with the excitation wavelength set at 369 nm. The fluorescence intensities at $\lambda_{em}^{max}$ were plotted as a function of time.....	103
<b>Figure 5.6</b>	Confocal laser scanning microscopic (CLSM) images of the alginate-chitosan microcapsules after genipin treatment (ACG) (a & b); alginate-chitosan (AC) microcapsules (c & d); and alginate beads after genipin treatment (AG) (e & f) viewed at the transmission light channel (left) and at the fluorescence channel	

	(right).....	104
<b>Figure 5.7</b>	Fluorescence intensity profiles corresponding to the white lines across the microcapsule images at the focal planes. (a): alginate-chitosan microcapsules after genipin treatment (ACG); (b): alginate-chitosan microcapsules (AC); and (c): alginate beads after genipin treatment (AG).....	105
<b>Figure 5.8</b>	Predicted mechanism of the reaction between chitosan and genipin. (a), formation of highly conjugated genipin derivative; and (b), formation of secondary amide linkage.....	106
<b>Figure 5.9</b>	Solid state <sup>13</sup> C NMR spectra (a) and FTIR spectra (b) of chitosan before and after genipin treatment.....	107
<b>Figure 6.1</b>	Absorption and fluorescence spectra of PLL, genipin, and their reaction mixture.....	122
<b>Figure 6.2</b>	CLSM images of APA microcapsules and representative fluorescence intensity profile.....	123
<b>Figure 6.3</b>	Quantification of PLL binding to APA microcapsules.....	124
<b>Figure 6.4</b>	Fluorescence intensity profiles corresponding to a line across the optical equatorial sections of various polyamine-based microcapsules after genipin treatment.....	125
<b>Figure 7.1</b>	(a): Schematics of the chemical structures of alginate (top), chitosan (middle) and genipin (bottom) used in microcapsule preparation. (b): Schematic molecular structure of the genipin cross-linked alginate-chitosan (GCAC) microcapsules.....	142
<b>Figure 7.2</b>	Photomicrographs of the GCAC (a-b), the control alginate-chitosan (c-d) and the control alginate-genipin (e-f) microcapsules viewed from the transmitted light channel (upper row) and the fluorescence channel (lower row) of CLSM. Genipin treatment (1.0 mg/ml) on microcapsules was performed at 37°C for 24 h.....	143
<b>Figure 7.3</b>	CLSM images of the GCAC microcapsules. The microcapsule membrane was cross-linked at varied genipin concentrations (1.0, 2.5, or 5.0 mg/ml) and temperatures (4, 20, or 37°C) for different reaction time (5, 24, 48, or 72 h).....	144
<b>Figure 7.4</b>	Fluorescence intensity profiles corresponding to the lines drawn across the focal plane of the GCAC microcapsules cross-linked	

	by genipin at a concentration of 2.5 mg/ml for 24 h at (a) 37, (b) 20, and (c) 4°C. (d) shows the fluorescence intensity of the membrane corresponding to a red line of 500 $\mu\text{m}$ in length indicating homogeneous distribution of the cross-linked chitosan membrane.....	145
<b>Figure 7.5</b>	3-D diagrams representing the intensity distribution over the scan areas and the relative fluorescence intensity of the GCAC microcapsule membranes.....	146
<b>Figure 7.6</b>	Fluorescence intensity of the GCAC microcapsules as a function of cross-linking time. The reaction temperatures used: (a) 4, (b) 20, and (c) 37°C.....	147
<b>Figure 7.7</b>	Effects of control factors on the fluorescence intensity of the GCAC microcapsule membranes. Control factors: (a) cross-linking temperature; (b) cross-linking time; and (c) genipin concentration. ....	148
<b>Figure 7.8</b>	Topography and roughness analysis of the cross-sectioned GCAC microcapsule membrane obtained by AFM.....	149
<b>Figure 8.1</b>	SEM images show the general appearance (a-b) and surface structure (c-f) of the AC (left) and GCAC (right) microcapsules.	168
<b>Figure 8.2</b>	SEM images show different structure of the surface and interior of the AC microcapsules. Red boxes indicate selected areas for detailed investigation.....	169
<b>Figure 8.3</b>	SEM images show the different structure of the surface and interior of the GCAC microcapsules.....	170
<b>Figure 8.4</b>	TEM images of the microcapsules. a-b, alginate bead; c-d, AC microcapsule; e-f, GCAC microcapsule.....	171
<b>Figure 8.5</b>	Microphotographs of the GCAC (a, c) and AC (b, d) microcapsules before (a- b) and after (c- d) chelation by sodium citrate (50 mg/mL) for 24 h.....	172
<b>Figure 8.6</b>	Morphological stability of the GCAC (upper row) and AC (lower row) microcapsules containing blue dye after incubation in saline for 6 months. Red arrows indicate defects of the capsules.....	173
<b>Figure 8.7</b>	Microphotographs of microcapsules after subject to magnetically stirring at 600 rpm for 3 h.....	174

<b>Figure 8.8</b>	Analysis of fluorescence intensity inside and outside the microcapsule. The GCAC microcapsules were cross-linked by genipin (2.5 mg/mL, at 20 °C for 5 h) and incubated in a FITC-dextran solution (20 KD, 250 µg/mL) at room temperature overnight.....	175
<b>Figure 8.9</b>	Visualization of FITC-dextran permeation into microcapsules by CLSM .....	176
<b>Figure 8.10</b>	Diffusion of FITC-dextran into microcapsules as a function of dextran molecular weight.....	177
<b>Figure 8.11</b>	Penetration of BSA into microcapsules as a function of incubation time.....	178
<b>Figure 8.12</b>	Cumulative release of encapsulated BSA from microcapsules as a function of incubation time.....	179
<b>Figure 8.13</b>	HPLC chromatographs of the encapsulated BSA in the GCAC and AC microcapsules as compared to BSA standard.....	180
<b>Figure 8.14</b>	Leaking of the entrapped FITC-dextran (MW 2000 KD) from microcapsules incubated in lysozyme solution .....	182
<b>Figure 8.15</b>	Microphotographs of microcapsules after sequential incubation in the simulated gastric fluid and the simulated intestinal fluid .....	183
<b>Figure 9.1</b>	Microphotographs of the GCAC microcapsules cross-linked at 4 (a-h) and 20 °C (i-p) during the simulated human GI transit through the simulated stomach, small intestine, transit, and descendent colons.....	199
<b>Figure 9.2</b>	Recovery of microcapsules after 72 h of simulated human GI transit.....	200
<b>Figure 9.3</b>	Leaching of the encapsulated FITC-dextran into the simulated intestinal medium following 1-hour simulated gastric exposure...	201
<b>Figure 9.4</b>	Enzymatic activities retained in the suspension of the simulated human transverse colon in the presence of microcapsules relative to those in the absence of microcapsules (control) .....	203
<b>Figure 10.1</b>	Microphotographs of the GCAC microcapsules: a, plain and freshly made; b, containing <i>LP80</i> cells and freshly made; c, plain and after 2 yr of storage in deionized H <sub>2</sub> O at 4 °C; and d,	

	containing <i>LP80</i> cells and after 2 yr of refrigerated storage in minimum medium (1: 1 = broth: PS) at 4 °C.....	222
<b>Figure 10.2</b>	Resistance of <i>LP80</i> enclosed microcapsules to osmotic pressure shock.....	223
<b>Figure 10.3</b>	Microphotographs of microcapsules containing <i>L. plantanrum 80</i> ( <i>pC</i> BH1) post exposure to mechanical stress in MRS broth (175 rpm, 37 °C) for 3 days.....	224
<b>Figure 10.4</b>	Microphotographs of microcapsules containing <i>L. plantanrum</i> ( <i>pC</i> BH1) post exposure to mechanical stress in PS (175 rpm, 37 °C) for 3 days.....	225
<b>Figure 10.5</b>	Microphotographs of the GCAC microcapsules containing <i>L. plantanrum</i> ( <i>pC</i> BH1) after exposure to mechanical stress and sequential incubation in SGF (pH 1.2) and SIF (pH 7.5) at 175 rpm, 37°C.....	226
<b>Figure 10.6</b>	Growth profiles of encapsulated and free <i>Lactobacillus plantarum</i> 80 incubated in MRS broth, 37 °C.....	227
<b>Figure 10.7</b>	Survival of <i>LP80</i> cells as a function of exposure time in the simulated human gastric medium (pH 2.0, 37 °C).....	228
<b>Figure 10.8</b>	Tolerance of the GCAC encapsulated <i>LP80</i> cells to the simulated human GI media taken from the simulated a, stomach (V1, pH 2.0); b, small intestine (V2, pH 7.4); and c, large intestine (V 3: ascending colon, pH 5.6; V 4: transit colon, pH 6.2; and V5: descending colon, pH 6.8) under mechanical agitation (175 rpm) and in anaerobic conditions at 37 °C.....	229
<b>Figure 10.9</b>	Survival of microencapsulated <i>Lactobacillus plantarum</i> 80 during long term storage in physiological solution at 4 °C.....	230

## LIST OF ABBREVIATIONS AND TERMINOLOGY

AC	Alginate-chitosan
ACG	Alginate-chitosan microcapsules with genipin treatment
AC-PEG-A	Alginate-chitosan-polyethylene glycol-alginate
AC-PEG-PA	Alginate-chitosan-polyethylene glycol-poly-L-lysine-alginate
AFM	Atomic force microscopy
AG	Ca-alginate beads with genipin treatment
AP	Alginate- poly-L-lysine
APA	Alginate- poly-L-lysine –alginate
AP-PEG-A	Alginate-poly-L-lysine-polyethylene glycol-alginate
AP-PEC-PA	Alginate-poly-L-lysine-pectin-poly-L-lysine-alginate
BSA	Bovine serum albumin
BSH	Bile salt hydrolase
CLSM	Confocal laser scanning microscopy
Ctrl	Control
CFU	Colony forming unit
DMSO	Dimethyl sulfoxide
em	Emission
ex	Excitation
FBS	Fetal bovine serum
FITC	Fluorescein isothiocyanate
FTIR	Fourier transform infrared (spectroscopy)
GCAC	Genipin cross-linked alginate-chitosan
GE	Genetically engineered

GI	Gastrointestinal
HMW	High molecular weight
HPLC	High-performance liquid chromatography
LP80	<i>Lactobacillus plantarum</i> 80 (ρCBH1)
LSM	Laser scanning microscopy
MEM	Minimum essential medium
MRS	De Man Rogosa Sharpe (broth or agar)
MTT	3-(4,5-dimethylthazol-2-yl)-2,5-diphenyl tetrazolium bromide
<i>M<sub>n</sub></i>	Number average molecular weight
<i>M<sub>v</sub></i>	Viscosity average molecular weight
<i>M<sub>w</sub></i>	Weight average molecular weight
MWCO	Molecular weight cutoff
NMR	Nuclear magnetic resonance (spectrometry)
PBS	Phosphate buffer saline
PEC	Polyelectrolyte complexation
PEG	Polyethylene glycol
pI	Isoelectric point
PLL	Poly-L-lysine
PS	Physiological solution
$R_{\eta}$	Viscosity radius
s.d.	Standard deviation
SEM	Scanning electron microscopy
SGF	Simulated gastric fluid
SIF	Simulated intestinal fluid

TEM	Transmission electron microscopy
$\lambda_{ex}^{max}$	Wavelength of maximum excitation
$\lambda_{em}^{max}$	Wavelength of maximum emission
cm	centimeter
CPS	counts per second
d	day
h	hour
mg	milligram
min	minute
mL	milliliter
mm	millimeter
nm	nanometer
rpm	rotation per minute
$\mu$ l	microliter
$\mu$ m	micrometer
yr	year

## 1.1 Overview

Advances in molecular biology research have introduced a wide range of genetically engineered cells with desired metabolic activities to produce disease modifying substrates, such as cytokines, enzymes, antibodies, growth factors and others<sup>1,2</sup>. The use of these materials opens up new hope in the treatment of a wide array of human diseases. However, these biologics are generally fragile and may easily become degraded or denatured<sup>3</sup>. To overcome the delivery obstacles, Prakash and Chang proposed the concept of artificial cell oral therapy<sup>4</sup>, wherein live functional cells encapsulated in the confines of a semi-permeable membrane are administered orally. The polymeric membrane isolates the cells from the host gastrointestinal (GI) environment, allowing the bi-directional exchange of small molecules, such as nutrients, wastes, selected substrates and other products, while preventing the passage of large substances, for instance cells, immunocytes and antibodies<sup>5</sup>. When given orally, viable cells, being protected by microencapsulation, can reach the intestine in a large controlled number. They can be designed to secrete small biologics (peptides, enzymes, growth factors, etc.) to be released into the gut lumen for therapy. Alternatively, artificial cells can act as bioreactors during their GI transit by metabolizing undesirable small substances (amino acids, bile acids, ammonia, etc.) present in the gut and eventually eliminate them from the body<sup>6</sup>. Previous research has demonstrated the potential of oral delivery of microencapsulated genetically engineered (GE) cells as an alternative oral therapy for a number of human diseases<sup>4,7-10</sup>. The range of therapeutic opportunities for this approach is very broad.

It is known that any orally administered biologics are challenged in the human GI system<sup>11</sup>. Effective oral therapy utilizing live cells requires the cells to remain viable and functional during GI transit. Furthermore, GE microorganisms should be retained in the microcapsules and not leak into the GI tract. It has been shown that novel cells may, if prolonged and repeated large doses are taken, stimulate a host immune response, systematically propagate in the intestine, disrupt the indigenous microflora, and have risks of

immuno-modulation, translocation and gene transfer<sup>2,12-18</sup>. Therefore, it is essential that GE bacteria be encased in the microcapsules, perform the therapeutic functions during the GI transit, and be excreted along with the intact microcapsules in feces without being retained in the body even though they are classified as nonpathogenic<sup>19</sup>. To fulfill these requirements, it is important to maintain the structural integrity of microcapsules, which in turn is strongly dependent on the membrane stability and other microcapsule features.

Designing an appropriate microcapsule membrane for oral delivery of live cells is challenging. On one hand, there is a need for creating a robust isolating barrier between the cells and the host gut. On the other hand, cell viability, metabolism, and functions should be sustained during processing and GI transit. In addition, targeted substrates and products should be able to freely pass through the microcapsule membrane for therapy. Although numerous microcapsule systems have been studied for oral delivery, such devices are used for the controlled release of curative agents, for instance drugs and probiotics<sup>20-26</sup>. Relevant research on developing a microcapsule system for oral delivery of live cells intended to function during the GI transit while needing to be retained in the microcapsules is scarce in the literature<sup>27</sup>.

Though many methods exist for the preparation of artificial cells, polyelectrolyte complexation, by which the semi-permeable membrane is formed by ionic interactions between two or more oppositely charged polyelectrolytes in an aqueous solution, is the preferred one, ensuring mild reaction conditions and avoiding the use of solvents and toxic monomers<sup>28,29</sup>. In addition, as most synthetic polyelectrolyte materials are, to some extent, cytotoxic, natural materials are preferential for cell encapsulation<sup>30,31</sup>. Alginate, a naturally occurring polysaccharide extracted from brown seaweed, is by far the most commonly used polymer because of its excellent cell-compatibility, its status as an FDA approved food additive, ease of operation, and mild process conditions<sup>29,32,33</sup>. The incorporation of other polymers to envelope the alginate bead is necessary to create a stable and semi-permeable membrane. Chitosan is a polysaccharide obtained by alkaline deacetylation of chitin (a natural component of shrimp or crab shells). It is one of the few polycations available in nature, and can form strong complexes with negatively charged alginate<sup>34,35</sup>. The alginate-chitosan (AC) microcapsule has been investigated for the controlled release of therapeutic agents<sup>20,36-39</sup>, enzyme immobilization<sup>40-42</sup> and cell encapsulation<sup>43-47</sup>. It was reported that the AC membrane

protected probiotics from the gastric environment and enhanced their intestinal release<sup>48,49</sup>. Previous research also suggested the limitations associated with this ionically linked membrane, for instance, inadequate stability, susceptibility to degradation and cell leakage<sup>49-53</sup>.

To elevate the concept of artificial cell oral therapy towards applications, there is an urgent need to develop a suitable microcapsule system for oral delivery of live cells, which is the main goal of this thesis research.

## **1.2 Thesis research objectives**

The primary objective of this thesis is to develop a microcapsule system suitable for oral delivery of live engineered cells. The specific research objectives are:

- To design a new alginate-chitosan microcapsule system
- To establish the preparation procedure and optimize reaction parameters of the new microcapsule system
- To investigate the membrane structure and the physical properties of the novel microcapsule
- To examine the suitability of the GCAC microcapsule system for oral delivery applications
- To discern the capability of the GCAC microcapsule system for live cell encapsulation
- To investigate the potential of the GCAC microcapsule system for oral delivery of live engineered cells

## **1.3 Outline of thesis**

This thesis is parted into 12 chapters. Chapter 1 describes the background and research objectives of this thesis, followed by an extensive literature survey of the subject matter in Chapter 2. Chapters 3-10 are 8 original papers published or to be submitted. These research articles include the main studies performed to achieve the thesis objectives. Chapter 11 summarizes the findings of this thesis work, and the claims to original contributions to knowledge. Recommendations for future research are included in Chapter 12 of this thesis.

## 2.1 Introduction to artificial cells

Microencapsulation in artificial cells<sup>5</sup> describes the envelopment of biologically active materials within a polymeric matrix surrounded by a semi-permeable membrane for the purposes of protection, isolation, controlled release and/or targeted delivery. Since the pioneering discovery by T. M. S. Chang<sup>5</sup>, this concept has been extensively developed and used in numerous areas<sup>19</sup>. The principle of cell encapsulation is that the semi-permeable membrane separates the cells from the external milieu, allows bi-directional exchange of small molecules including oxygen, nutrients, and wastes for cell survival, and selected substrates and products for therapeutic functions, but prevents the entry of immunocytes, antibodies and other immune molecules that might destroy the enclosed cells<sup>5</sup>. This strategy potentially permits allogenic and xenogenic transplantation without the need for immunosuppression, and allows the continuous secretion and delivery of therapeutic products to the host at a more physiological and effective concentration. It also eliminates the tedious isolation processes usually associated with conventional biotechnology and ensures the chemical stability of the 'de novo' biologics<sup>54</sup>.

Since artificial cells can be extensively varied in content (e.g. cell type) and membrane features (e.g. composition, configuration, fabrication method, etc.), there are almost infinite microcapsule architecture possibilities. Similarly, the potential therapeutic applications are enormous<sup>19,22,55-62</sup>. Over the past two decades, artificial cells have been investigated for direct implantation, intravenous injection, oral delivery, or as an extracorporeal device and bioreactor<sup>19,63</sup>. Significant progress has been made, for instance in clinical trials for the treatment of type 1 diabetes<sup>64</sup>, cancers<sup>65</sup>, hypoparathyroidism<sup>66</sup>, amyotrophic lateral sclerosis<sup>67</sup> and Huntington's diseases<sup>68</sup>, that has brought this technology closer to a realistic clinical application. Some promising applications of artificial cell technology are listed in Table 2.1.

Table 2.1. Some promising applications of artificial cell technology utilizing live cells.

Disorder	Enclosed cells and functions	Route of administration	Ref.
Diabetes	Pancreatic islets for insulin secretion	Implantation	64,69-76
Renal Failure	<i>E. coli</i> DH5 transfected with the urease gene; metabolic induced <i>Lactobacillus delbrueckii</i> , for urea removal	Oral delivery	4,26,77
Liver Failure	Hepatocytes for liver function support	Implantation	47,78-80
Hemophilia	Recombinant C2C12 myoblasts secreting factor IX	Implantation	81,82
Hyperlipidaemia and atherosclerosis	Recombinant CHO-E3 cells secreting wild-type apoE3 protein	Injection	83
Dwarfism	Non-autologous C2C12 cells secreting human growth hormone	Implantation	84
MPS VII	Recombinant 2A-50 fibroblasts secreting $\beta$ -glucuronidase	Injection	85
ADA deficiency	Human fibroblasts expressing ADA	Implantation	86
Cancers	Varied recombinant cells secreting endostatin, cytokines, antibodies, etc for tumor suppression	Implantation	65,87-94
CNS diseases (Parkinson's, Huntington's, ALS, chronic pain, etc.)	Recombinant cells secreting CNTF, GDNF, dopamine, CSF-1, and $\beta$ -endorphin; chromaffin cells	Implantation	43,45,67,68,95-101
Gastric disorders	<i>Lactobacillus</i> and <i>bifidobacterium</i> to for gastric health improvement	Oral delivery	102,103
Hypercholesterolemia	<i>Pseudomonas pictorum</i> , <i>Lactobacillus plantarum</i> 80 for cholesterol lowering	<i>In vitro</i> study	9,10

Abbreviations: ADA, adenosine deaminase; ALS, amyotrophic lateral sclerosis; CNS, central nervous system; MPS VII, mucopolysaccharidosis type VII.

## 2.2 Design considerations of artificial cells for live cell applications

Despite being very promising, cell encapsulation has not yet been applied in routine clinical practice. Conflicting reports of success illustrate the complexity of developing suitable microcapsule designs to implement this technology<sup>22,74,76,104</sup>. Successful artificial cell design must fulfill a number of criteria<sup>22</sup>. Firstly, the material should be biocompatible, non-toxic and benign to the immune system. Secondly, the process for cell encapsulation should be mild enough to preserve adequate cell viability and retain a high initial seeding density of cells. Thirdly, microcapsules should be able to bear shear stress, culture media or other environmental constraints. Finally, microcapsule characteristics including size, mechanical strength, permeability, degradability and other host-related factors require a subtle balance to optimize clinical features. Choice of matrix/membrane materials and formulation methods dictates the performance of live artificial cells, and is thus critical in developing new microcapsules. Table 2.2 summarizes main considerations in selecting suitable materials and processing techniques for cell encapsulation.

Table 2.2. Artificial cell design considerations for microencapsulation of live cells

---

### Material characteristics/chemistry

- availability of clinical grade materials with reproducible characteristics
- potential impurities and leachable residues, e.g. endotoxin, solvent, additive, initiator, cross-linker, pore-forming agent, precipitating agent
- biocompatibility, non-cytotoxicity to both host and encapsulated cells
- non-thrombogenic if in contact with blood, non-tumorigenic
- not trigger host immune response
- no interference with cell functions *in vitro* and *in vivo*
- sterilization options for materials
- cost

---

### Formulation and processing

- ease of processing
  - reproducibility of critical desired features
-

- 
- complete encapsulation
  - lack of harsh chemicals, temperatures or pH needed for preparation
  - maintenance of cell survival and function during processing and storage (for pre-formed device)
  - Sterilization during processing and after manufacture
  - Ease of sealing
- 

#### Artificial cell features

- Geometry, surface morphology and charge, dimensions scaled between species and implant sites
  - adequate mechanical integrity to withstand handling, application and retrieval (if needed), minimize defects
  - provide suitable extra-cellular microenvironment for cell growth and proliferation
  - highly selective permeability (high diffusion in the low MW nutrient range and low diffusion in the high MW immunoglobulin range)
  - adequate stability of critical properties (e.g., membrane transport and resistance to biodegradation) in the host environment for the implant lifetime
  - appropriate biodegradability if desired
  - alternation of the host physiology of the biological fluids/tissue environment (material itself and potential degraded substance)
- 

## **2.3 Artificial cell preparation techniques**

### **2.3.1 Commonly used microencapsulation methods**

Numerous microencapsulation techniques, fundamentally different in the nature of the entrapment mechanism, have been developed for cell encapsulation<sup>32,105-110</sup>. A typical encapsulation process starts with a scheme to generate a controlled-size droplet from a liquid cell suspension, followed by a rapid solidification or gelation to stabilize the droplet, and if needed, by further interfacial processes to obtain a solid microcapsule membrane surrounding

the droplet. Gelation or solidification can occur through a change in temperature for thermo-reversible gels such as agarose, or by the formation of an insoluble complex via chemical or ionic cross-linking, or by solvent extraction. The commonly used techniques encompass:

- ionic gelation (e.g., calcium-alginate beads)
- complex coacervation (e.g., alginate-poly-L-lysine-alginate microcapsules)
- interfacial precipitation (e.g. HEMA-MMA system)
- phase separation (e.g., gelatin and agarose capsules)
- solvent extraction or evaporation method (e.g., spray-drying for probiotic encapsulation)

### **2.3.2 Microencapsulation by polyelectrolyte complexation**

Though many methods exist for the preparation of artificial cells, polyelectrolyte complexation (PEC) by which the semi-permeable membrane is formed by complex coacervation between two or more oppositely charged polyelectrolytes in an aqueous solution, is the simplest and most preferable method because it allows for mild reaction conditions and avoiding the use of toxic solvents and monomers<sup>28,29</sup>. The best example is the well-known alginate-poly-L-lysine-alginate (APA) microcapsule<sup>69</sup>, which can be formed by immersion of the calcium alginate beads in an aqueous solution of poly-L-lysine (PLL). The  $-NH_3^+$  groups of PLL couples with the  $-COO^-$  groups of alginate, providing a PEC membrane around the alginate beads. It requires only short processing time at ambient or lower temperature, thereby providing well-controlled manipulation and high maintenance of biological activity. This PEC microcapsule system has been widely investigated as an immuno-protection container in cell transplantation applications<sup>75,107,111-115</sup>.

A wide variety of other polyelectrolytes have been investigated for cell encapsulation and immunoisolation<sup>30</sup>. Prokop et al examined more than one thousand binary polyelectrolyte combinations, from which 47 pairs were identified as alternatives to the standard alginate-PLL chemistry<sup>28,30</sup>. The properties of these PEC microcapsules were dependent on the polyelectrolyte characteristics and processing conditions, which in turn, can be used to modulate the microcapsule performance<sup>30,44</sup>. Some of the polyelectrolyte materials investigated for cell encapsulation are listed in Table 2.3

Table 2.3. Polyelectrolyte materials used for cell encapsulation

<b>Polymer</b>	<b>Type</b>	<b>Source</b>
Alginate	Polyanion	Natural
Carboxymethylcellulose	Polyanion	Natural
Carrageenan	Polyanion	Natural
Cellulose sulfate	Polyanion, permanently charged	Natural
Heparin	Polyanion, permanently charged	Natural
Pectinate	Polyanion	Natural
Xanthan	Polyanion	Natural
Polyacrylic acid	Polyanion	Synthetic
Poly(styrene sulfonate)	Polyanion, permanently charged	Synthetic
Chitosan	Polycation	Natural
Poly-L-lysine	Polycation	Natural
Hydroxyethyl cellulose	Polycation	Synthetic
Poly(allylamine) hydrochloride	Polycation	Synthetic
Poly(diallyldimethyl ammonium) chloride	Polycation, permanently charged	Synthetic
Poly(ethyleneimine)	Polycation	Synthetic
Poly(methylene co-guanidine) (PMCG) hydrochloride	Polycation, oligomeric	Synthetic
Poly(vinylamine) hydrochloride	Polycation	Synthetic
Protamine sulfate	Polycation	Synthetic

In recent years, a novel approach of micro- and nanoencapsulation using a self-assembly technique has emerged. Ultrathin multilayered capsule membranes can be fabricated by means of step-wise adsorption of polyelectrolytes on the template substrate<sup>116,117</sup>. The size

of the capsules, defined by the size of the template used, can be varied from 0.1 to tens of micrometers. The layer-by-layer (LbL) assembled shells can be tailor-made, by selecting appropriate shell materials and by controlling the number of polyelectrolyte layers. Desired thickness (usually in nanoscale), tunable permeability, mechanical strength, and other features are obtainable<sup>116,118,119</sup>. Factors controlling the absorption of PEC layers are listed in Table 2.4.

Table 2.4. Parameters affecting polyelectrolyte complexation

<b>Polyelectrolyte chemistry</b>	<b>Solution properties</b>	<b>Processing conditions</b>
Molar mass	Polymer concentration	Reaction time
Type of charge group	pH (affected by pKa)	Template diameter
Charge density	Solvent	Method of formation
Chain architecture	Ionic strength	Temperature
Hydrophobicity	Additives	

These multilayered capsule systems are of special interest for drug delivery, biosensors, micro-reactors and live cell encapsulation, which has been shown in a number of recent reports<sup>120-125</sup>. Alginate microspheres have been used as negatively charged templates for polyelectrolyte LbL assembly<sup>126</sup>. Positively charged macromolecules, for instance peroxidase, can be spontaneously loaded into the alginate beads with high efficiency; whereas, the nanofilm coatings provided protection for the encapsulated biomolecules and prolonged the life-span of the capsules in biological environments<sup>127</sup>. Schneider et al microencapsulated pancreatic islets by LbL assembly and transplanted them in animal models<sup>125</sup>. Results obtained demonstrated advantages of multilayer-membranes over the conventional single plain preparations. The authors claimed that these PEC assembled beads were biocompatible and mechanically stable with precisely controllable membrane cut-offs and excellent insulin-response even though the thickness of the multilayer membranes was only 145 nm in total. Most recently, the LbL technique was utilized to protect mammalian cells, used in implantable biosensors, by alternating the layers of polycation poly-diallyldimethyl

ammonium chloride and negatively charged poly-styrene sulfonate on MELN cells<sup>120</sup>. Although relevant research involving living cells was still limited in the literature, it is envisaged that the LbL self-assembly technique will play a role in advancing the development of artificial cells as novel micro-carriers of therapeutic cells.

### **2.3.3 Advance and challenges in the preparation of microcapsules**

The development and therapeutic benefit of artificial cells have brought forth the need to prepare microcapsules in large quantities and in sufficient quality suitable for clinical trials and widespread applications. While initial lab-scale experiments are frequently performed in simple beaker/stirrer setups, clinical trials and market introduction require more sophisticated technologies, allowing for economic, robust, aseptic, well-controllable and reproducible manufacture of microcapsules. In the past few years, significant progress has been made in the innovation of more advanced technologies for the production of uniform microbeads and to ensure repeatability and reproducibility both within and between batches<sup>110</sup>. Among those investigated are extrusion through needles<sup>128</sup>, air-jet<sup>129</sup> and vibrating nozzle<sup>130</sup>, spinning disk atomization<sup>131,132</sup>, dripping using electrostatic forces and ultrasonic jet excitation<sup>129,130,133</sup>, membranes and microfabricated microchannel devices<sup>134,135</sup>, emulsification<sup>136,137</sup> as well as coacervation<sup>138</sup>. Anilkumar et al developed an automated chemical reactor able to generate uniform capsules continuously and at a high rate of production<sup>139</sup>. Several encapsulation devices, for example, Inotech Encapsulator (<http://www.inotechintl.com>) and JetCutter system (<http://www.geniaLab.com>), are commercially available for the controlled microencapsulation of drugs, enzymes, microorganisms, plant and animal cells. The size of the beads produced by the JetCutter system can be varied from 120  $\mu\text{m}$  to larger than 3 mm<sup>140</sup>. These apparatus highlight the high productivity, uniformity of the particles (with a size distribution below 5%), reproducibility in terms of shape, size and morphology, and the capability for being scaled up<sup>130,141</sup>, though achieving mono-dispersion in size is still challenging. Artificial cells can now be made ranging in size from macro-dimensions, micron-dimensions, nano-dimensions, and to molecular dimensions to fit various applications<sup>63</sup>. Generally, achieving uniformity with smaller beads is more difficult than with larger ones.

In cell encapsulation, smaller capsules offer a number of distinct advantages. They promote rapid mass transfer, better cell functions, and a higher rate of product secretion owing to a larger surface area-to-volume ratio<sup>104,142</sup>. They also favor smaller implant volume, easy *in vivo* application and potential access to a certain implantation sites<sup>39,143-145</sup>. Previous research showed that in order to maintain a non-limiting oxygen concentration throughout the gel matrix, cells must be immobilized in capsules with a diameter less than 300  $\mu\text{m}$ <sup>146</sup>. However, reduction in capsule size presents a risk of inadequate and incomplete cell encapsulation. Protruding xeno-cells through the capsule membranes may lead to immune response<sup>80,147</sup>. Thus more work has to be done on the development of conceivable approaches to prepare uniform and small capsules while ensuring complete and sufficient cell encapsulation.

## **2.4 Microcapsule membranes and artificial cell systems containing live cells**

In all *in vivo* applications using microencapsulated live cells, the effectiveness of immuno-protection strongly depends on the engineering of microcapsule membrane<sup>104,148</sup>. The use of different membranes allows for variations in permeability, mass transfer, mechanical stability, durability, and biocompatibility that can be exploited to fit a desired application.

### **2.4.1 Selection of microcapsule materials for cell encapsulation**

Hydrogel-based biomaterials are favored for artificial cell formulation and have been typically utilized for bioencapsulation and immunoisolation for a number of reasons<sup>108,149,150</sup>. Hydrogels are soft polymeric materials composed of either covalently or electrostatically cross-linked networks containing a high percentage of water. Their hydrophilic nature minimizes protein adsorption and cell adhesion by virtually eliminating interfacial tension with the recipient's tissues. The soft and pliable features of hydrogels reduce the mechanical or frictional irritation to surrounding tissues. In addition, some structural characteristics of hydrogels are, to a certain extent, similar to the extra-cellular matrix of many tissues<sup>149,151</sup>.

As has been noted in the previous section, utilizing polyelectrolyte hydrogels is preferable for cell encapsulations<sup>28-30</sup>. The selection of polyelectrolyte materials must essentially meet the following requirements: (1) should allow for processing in water and physiological solution, avoiding the use of organic solvents, which, in many cases are cytotoxic; (2) should have sufficiently high electric charges, either permanent or pH inducible at a tolerable range; (3) the functional groups in the polymer chains should be benign, not induce immune response; and (4) should ensure rapid gelation in the presence of cross-linking counterions or by coacervation. With respect to the source of materials, natural polymers have been extensively used due to their satisfactory biocompatibility and tissue tolerance, though their physicochemical characteristics may perhaps vary from different natural sources<sup>152</sup>. Synthetic hydrogels, on the other hand, can be produced in large quantities with easy control over their structure and properties, and they tend to be more durable *in vivo*<sup>148</sup>. However, most synthetic polyelectrolyte materials, particularly polycations, exhibit a moderate level of cytotoxicity. A recent study by Germain et al<sup>153</sup> showed a toxic effect of polyelectrolyte deposition on living and adherent mammalian cells. Decreased cell viability was found when a polycation was coupled with polyanion poly(sodium 4-styrene sulfonate), with a greater toxic effect for poly(ethylene imine), polyphosphoric acid, poly(allylamine hydrochloride), and protamine sulfate than for PLL and poly(diallyldimethyl ammonium) chloride. This suggests that the adsorption of some polyelectrolytes onto the cell membrane may perturb membrane fluidity and subsequently alter vital trans-membrane systems. It is therefore important to carefully select cell compatible materials to minimize stress for the encapsulated cells.

A number of natural polymers have been identified as suitable components for live cell microencapsulation<sup>28</sup>. Polyanions may act as extra-cellular matrix analogues and are often used as inner materials that directly contact with cells. There are relatively few naturally occurring polycations available and thus the selection of the appropriate polycation is more limiting (Table 2.3). The following section is a review on microcapsule systems used for cell encapsulation, with a focus on APA and alginate-chitosan (AC) microcapsule systems, and also covering several synthetic microcapsule systems being investigated.

## 2.4.2 Alginate as encapsulation matrix

In cell encapsulation, the main function of the core material is to entrap cells and form a perfect spherical bead while preserving cell viability. The biomatrix used should be totally biocompatible, neither interfering with cell function nor triggering host immune responses. In this regard, alginate is the most suitable biopolymer.

Alginate is an anionic polysaccharide extracted from brown seaweed. It is composed of linear  $\beta$ -D-mannuronic (M blocks) and  $\alpha$ -L-guluronic (G blocks) acids interspersed with regions of mixed sequences (MG blocks)<sup>32</sup>. Its popularity is due to its excellent biocompatibility, acceptability as an FDA approved food additive, ease of operation, and mild process conditions suitable for both the host and the enclosed cells<sup>32,33</sup>.

To prepare a cell-entrapped alginate bead, droplets of alginate-cell suspension are gelled in the presence of multivalent ions, which cross-link alginate chains to form rigid gel beads<sup>154</sup>. The affinity of alginate for alkaline earth metal ions increases in the order of  $Mg^{2+} \ll Ca^{2+} < Sr^{2+} < Ba^{2+}$ . The use of  $Ba^{2+}$  results in strong alginate beads<sup>155</sup>, but is less likely to be acceptable for clinical applications due to the known neurotoxicity of ionized barium<sup>156</sup>. Calcium ions bind preferentially to the G blocks of more than 20 monomers in alginate chains. The composition and sequence variations of alginate molecules affect the functionality<sup>32</sup>. Alginate beads made from high G content ( $> 70\%$ ) tend to form a more rigid structure with higher mechanical strength and porosity, while the reverse is observed for alginate rich in M blocks. Figure 2.1 represents the schematic interactions between alginate and  $Ca^{2+}$  ions, leading to the formation of the so-called egg-box structure.

Alginates are a family of heterogeneous polymers with a wide range of variations in chemical compositions and hence, functional characteristics. A large amount of research has shown that the source, M/G ratio, purity, molecular weight, concentration of alginate, the nature of gelling reagents ( $Ca^{2+}$  or  $Ba^{2+}$ , external or internal introduction), and the distribution of alginate gel (homogeneous or heterogeneous), all significantly impact the properties of alginate beads, particularly in mechanical stability and biocompatibility<sup>32,126,154,157-160</sup>. In cell encapsulation, it is recommended to use highly purified alginate with intermediate guluronic acid content at higher concentrations ( $\geq 1.5$  wt%)<sup>33</sup>.

Alginate is a highly hydrophilic polymer due to the presence of  $-OH$  and  $-COOH$  groups in its chain. At neutral pH, water from the environment penetrates into alginate beads to form hydrogen bridges with their available  $-OH$  and  $COO^-$  groups, and fills up the space among the chains and/or the centre of wide pores or voids<sup>32</sup>. As a consequence, the beads tend to swell substantially. Additional swelling and eventual destabilization are promoted by the presence of non-gelling ions and chelators, such as sodium, magnesium, phosphate, lactate, and citrate, due to ions exchange with the non-cooperatively bound calcium ions and the loss of the egg-box structure in alginate matrix<sup>32,154,161</sup>. A substantial quantity of sodium and phosphate ions in physiological conditions induce osmotic swelling, which presents one of the main causes of alginate-based microcapsule breakage<sup>162</sup>. Moreover, at low pH, alginate undergoes acidic hydrolysis, causing polymeric degradation and release of enclosed ingredients<sup>163</sup>. Previous studies suggest that alginate beads can be stabilized by creating a strong membrane and keeping a low swelling gel network<sup>156,162,164,165</sup>. This is imperative in cell transplantation to envelope the cells by semi-permeable membranes for immuno-isolation. Ideally, the microcapsules remain stable under physiological conditions over extended periods, i.e., for several years<sup>162</sup>.

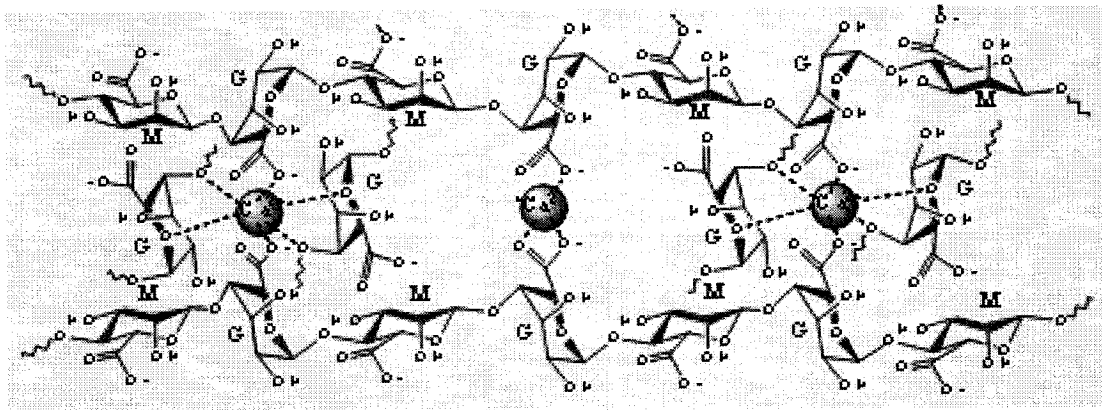


Figure 2.1. Schematic representation of the egg-box structure of calcium-alginate gel.

### 2.4.3 APA microcapsule membrane

#### 2.4.3.1 Preparation and applications of APA microcapsules

Over the past two decades, the alginate-poly-L-lysine-alginate (APA) complex, originally developed by Lim et al<sup>69</sup>, represents the most widely studied membrane for constructing artificial cells. This membrane is formed via polyelectrolyte complexation between alginate and PLL. Binding of PLL to the pre-formed Ca-alginate bead is driven by electrostatic interactions between the carboxyl groups of alginate and the long-chain alkyl amino groups extending from the polyamide backbone of PLL. Subsequent exposure of this PLL coated bead to a dilute alginate solution neutralizes positively charged PLL residues still present at the capsule surface. Finally, the citrate treatment chelates the calcium ions and liquefies the Ca-alginate core<sup>113</sup>.

The APA microcapsule membrane stabilizes the ionic gel network and reduces gel porosity. Depending on the polymer chemistry and coating conditions, microcapsule membranes, thick or thin, dense or loose, can be formed. The membrane characteristics, in turn, affect the properties of the microcapsule, such as stability and permeability. Since its discovery, the APA membrane has widely fueled the field of cell encapsulation and has been used as a means to prevent immune rejection problems when utilizing non-autologous cells for therapy<sup>64,68,69,71,73</sup>. Previous research showed that the APA system allowed for proliferation of encapsulated cells and prolonged the survival of xeno-grafts implanted both intraperitoneally and subcutaneously. Reversal of hyperglycemia in various diabetic animal models and human subjects by using APA microencapsulated islets has been reported<sup>64,69,71-73,75,107,166</sup>. The principle applicability of the APA microencapsulation technique for gene therapy, cell therapy and enzyme therapy has been demonstrated by the success in numerous animal studies for the treatment of a wide variety of diseases<sup>19</sup>, for instance hemophilia<sup>82</sup>, kidney and liver failure<sup>4,78,167</sup>, central nervous system insufficiencies<sup>68</sup>, diabetes mellitus<sup>64,168</sup> and others<sup>83,169,170</sup>. However, serious limitations persisted regarding long-term *in vivo* applications, causing graft failures<sup>76,115,115,156,171-174</sup>.

#### 2.4.3.2 Limitations of APA microcapsule system

The major obstacle encountered was the capsular fragility and short-term durability of the APA system. Under physiological conditions, the microcapsules are exposed to a combination of destructive forces comprising slow dissociation of the polyelectrolyte complex, chemical or biological degradation of the polyamino acid coating and polysaccharide matrix, osmotic swelling of the alginate core, shear forces causing capsule damage and abrasion, and so forth. Owing to the high water content and ionic interactions instead of covalent bonds, the APA membrane is poor in mechanical strength and is prone to degradation *in vivo*. The membrane fragility and inadequate long-term stability may instigate undesirable cell leaching and limit its clinical applications. Leaking of microbes such as *E coli* and *Lactococcus spp.*, yeast, and animal cells for instance, erythrocytes and HT29 tumor cells, from the APA microcapsules was observed<sup>6,102,141,175</sup>. Research has shown that APA microcapsules containing hepatocytes underwent physical breakdown 4-6 weeks post intraperitoneal transplantation with considerable loss of cell viability and functions<sup>176</sup>. Significant deterioration of the APA capsules was also found after only 2 weeks of intraperitoneal implantation in dogs<sup>156</sup>. The retrieved capsules became ghost-like and poorly defined, accounted for only 10% of the original implanted, and were found deprived of PLL coating. In the simulated human GI environment, APA capsules gradually lost structural integrity, and only traces of membrane debris were retrieved after 72 h<sup>27</sup>. Rokstad et al<sup>115</sup> investigated the parameters affecting the capsule integrity in relation to cell functions and found that the APA microcapsules were not strong enough to keep proliferating cells within the microcapsules for prolonged time periods.

Moreover, recent studies revealed the incomplete covering of PLL by the second alginate incubation, being exposed at the surface of the APA microcapsule in considerable amount<sup>75,177-179</sup>. Cationic poly-L-lysine is reported to be immunogenic and inflammatory<sup>22,180</sup>. The exposure of PLL may cause fibrotic reaction, cellular overgrowth and necrosis of the grafts, giving rise to biocompatibility problems<sup>174,181-183</sup>. Toso<sup>172</sup> found that microcapsules with PLL coating induced more host reaction and fibrotic overgrowth than the uncoated alginate beads<sup>172</sup>. A recent study by Robitaille *et al* demonstrated that macrophages, lymphocytes, TNF-alpha, IL-1beta and TGF-beta(1) all played a role in the pathogenesis of the host response to the APA microcapsules, which involved chronic inflammatory and fibrogenic processes<sup>174</sup>. PLL can also be recognized by the fibrinolytic system, leading to

plasmin-mediated degradation of PLL and subsequent weakening of the capsules<sup>184</sup>. Van Raamsdonk *et al* showed that the loss of long-term stability of the APA microcapsules was associated with activation of the complement system<sup>156</sup>. In contrast, De Vos *et al* found that APA capsules were highly biocompatible when implanted in rats for up to 2 years. Prolonged survival of APA encapsulated islets allografts was sustained for up to 200 days<sup>75</sup>. It is worth noting that the success of grafts is dependent on different animal models and implantation sites, and may also be related to the administration of sub-therapeutic levels of immunosuppression in some *in vivo* studies<sup>156,185</sup>.

Additionally, the reported permeability of the APA capsules varied considerably. The standard APA membrane was thought to have a molecular weight cutoff below 100 KD, thus excluding immunoglobins. However, discrepant reports were found in the literature. A study on DNA encapsulation by the APA membrane suggested a molecular weight cut-off of the PLL membrane slightly greater than the 31 KD nuclease<sup>186</sup>. Some reports showed the membrane exclusion limit at 60-70 KD<sup>6,107,113,187,188</sup>. Other researchers found a higher permeability threshold than expected<sup>155,189-191</sup>. Awrey *et al*<sup>189</sup> reported that the APA membranes were permeable to immunoglobulins of IgG class and could not provide a MWCO below 300 KD. Increasing the thickness of PLL membrane did not lower the exclusion limit. Although double-coated microcapsules decreased the leaking of large molecular species, the effect was short-lived (only 2 weeks). A similar study also suggested that the APA membrane could inhibit cell-cell contact between enclosed cells and the host's lymphocytes, but could not completely protect the enclosed cells from xenogeneic humoral immunity. In this study, an extensive fibrotic reaction was found one week after transplantation against APA microcapsules containing human cells. And the secretion of therapeutic protein endostatin ceased<sup>114,192</sup>.

#### **2.4.3.4 Modifications on APA microcapsule membrane**

Currently alginate-PLL-alginate complexed artificial cells are the most widely used for cell encapsulation. However, as has been discussed above, limitations of long-term mechanical instability, possible immunogenicity, coupled with high cost have restricted its applications. To address the physicochemical problems, a number of adaptations to the initial APA chemistry and technique have been made (Table 2.5). Many studies were undertaken to

examine the effects of alginate chemical composition and purity, modulation of PLL coating, and bead size in relation to *in vivo* behaviors of the capsules, as has been summarized in a recent review<sup>168</sup>. In addition, a host of other modifications incorporating various materials were explored to improve membrane stability and surface properties, some of which are discussed below.

Dusseault et al<sup>164</sup> used a bifunctional photoactivatable cross-linker to create covalent links between adjacent layers in the APA membrane. The resulting membrane possessed strong resistance against disintegration to mechanical shear forces. The physical integrity of these microcapsules was upheld after being challenged to extremely harsh chemical stresses in an alkaline buffer at pH 12 for up to 3 years. The MWCO of the cross-linked membrane remained similar to the standard APA capsules. The viability of encapsulated cells was maintained. This modified APA membrane shows potential for cell transplantation applications, though *in vivo* investigations have not been reported.

An interesting strategy to improve membrane strength is to incorporate an inorganic component to the microcapsule membrane<sup>193-195</sup>. Coradin and coworkers<sup>195</sup> have successfully coated alginate-poly(L-lysine) beads with sodium silicate, and the resulting composite particles have shown enhanced mechanical resistance. These novel silica-containing systems have been investigated for protein/enzyme immobilization and diffusion. Though cell viability and cytotoxicity were yet to be evaluated, these alginate-inorganic hybrid composites were considered to hold some promise for cell encapsulation.

Another attempt to form hybrid microcapsules, reported by Sakai et al<sup>193,194</sup> involved the sol-gel reaction and polyelectrolyte complexation to produce alginate/aminopropyl-silicate/alginate (Alg/AS/Alg) membrane. The preparation process was similar to that for the APA capsules. The hybrid membrane strength was enhanced by the Si-O-Si bonds. Small molecules such as insulin, glucose remained freely diffusive across the membrane, and the MWCO was observed at 70-150 KD. Xenotransplantation of microencapsulated rat islets in induced diabetic mice models showed the maximum maintenance of normoglycemia up to 105 days without immunosuppression. However, the authors also found that the siliceous precursors affected the insulin secretion activity of the encapsulated islets<sup>193</sup>.

PEGylation is an effective way to improve the biocompatibility of biomaterials. Polyethylene glycol (PEG) is a biocompatible and non-ionic polymer. It has been reported

that by incorporating PEG to microcapsule surface, the absorption of proteins can be reduced, which in turn may minimize cell adhesion and consequent inflammatory responses and fibrous overgrowth. Earlier, Sawhney et al<sup>196,197</sup> reported the excellent anti-fibrotic effects of PEGylation on AP capsules with PLL-graft-PEG surface. However, the improved biocompatibility compromised the membrane strength and increased the permeability. In another study, positively charged PEG-amine derivatives were used to complex with negatively charged surface of the APA capsules, resulting in a smoother surface than the APA capsules. Intraperitoneal transplantation of the microencapsulated islets using this PEGylated membrane allowed for restoration of normal glycaemia levels in tested animals for up to 200 days without immunosuppression. As well these surface-modified capsules were free of cellular overgrowth after the same period of being implanted *in vivo*<sup>198</sup>. More recently, Lee et al described the fabrication of microcapsules with a three-layer structure of alginate/photosensitive poly(L-lysine)/short chain alginate-co-MPEG, aiming for the improvements in mechanical strength and biocompatibility. They further investigated the encapsulation of human parathyroid tissue using this system and found that this PEG modified APA system retained structural stability and was free of cell adhesions 12 weeks after transplantation, and the functionality of the encapsulated parathyroid glands was sustained both *in vitro* and *in vivo*, the results of which implied potential application in endocrine surgery<sup>169</sup>.

To address the problem of the inflammatory PLL, other alternative materials, such as poly-L-ornithine, poly-L-arginine, or poly-L-histidine, was also investigated<sup>156,199,200</sup>. However, Van Raamsdo et al found the *in vivo* stability of the polyamino acid coating was very limited<sup>156</sup>. A recent report also suggested the inadequate membrane durability of alginate-polyornithine microcapsules as evidenced by the physical deformation and membrane erosion post intraperitoneal implantation<sup>201</sup>.

The aforementioned modifications as well as others being studied show that significant improvements in the traditional APA microcapsule are achievable. However, more research must be undertaken to assess the short and long term *in vivo* effectiveness of these modified formulations for artificial cell applications.

Table 2.5 Summary of major modifications on the APA membrane for cell encapsulation (1997-2006)

Method	Major outcomes and results	Ref
Modified alginate matrix (purification, G/M content)	Excluded inflammatory contaminants; more PLL bound; reduced biological responses; improved biocompatibility; but insufficient immunoprotection.	112,182,202
Surface modification by cross-linking PLL with polyacrylic acid	Smoother surface; better covering of PLL; improved biocompatibility	203
PEGylation of APA membrane	Low immunogenicity; reduced fibrotic overgrowth; improved biocompatibility	169,198
Replacement of PLL with other polyamino acids (poly-L-ornithine, poly-L-arginine or poly-L-histidine)	Less immunogenic; improved perm-selectivity; but inadequate <i>in vivo</i> stability	156,199,200
Ba <sup>2+</sup> for alginate gelation	Stabilized alginate matrix; but potentially cytotoxic	179
Incorporation of PEG, PVA, pectin, and/or chitosan to membrane	Improved stability and durability; but limited in multiple preparation steps	167,204-207
Na <sub>2</sub> SO <sub>4</sub> treatment on APA capsules	Reduced capsule swelling; improved membrane durability	165
Collagen matrix enveloped by a 3-layer alginate-PLL-alginate membrane	Supported anchorage-dependent cell growth; preserved hepatocyte functions <i>in vivo</i> ; reduced inflammatory and lymphocytic reactions	78

Table 2.5 (continued)

Coating with sodium silicate	Enhanced mechanical resistance and diffusion property; yet to test for cell encapsulation and cytotoxicity	195
Alginate-aminopropyl-silica-alginate capsules	Incorporated sol-gel process and electrostatic complexation; improved stability; permeable to glucose and insulin; normoglycemia achieved using encapsulated islets; but siliceous precursors affect insulin secretion	193,194
Addition of polyethylenimine (PEI) in core and bis(polyoxyethylene bis[amine]) (PEGA) on membrane	Enhanced mechanical stability while not affecting coating process and mass transfer property	208
Alginate-PLL-propylene-glycol-alginate (PGA)-BSA capsules	Incorporated electrostatic interactions and covalent links; improved long term stability; cell survival enhanced by addition of BSA	209
Covalently cross-linked APA	Improved membrane strength; MWCO comparable to APA; remained cell compatible	164,210
Covalent cross-links by Na-acrylate and N-vinylpyrrolidone	Improved mechanical and chemical stability; biocompatible <i>in vivo</i> ; cell survival limited by photopolymerization	128

## 2.4.4 Chitosan and alginate-chitosan complexed microcapsules

### 2.4.4.1 Chitosan chemistry and its membrane forming potentials

Chitosan, a linear polysaccharide of (1–4)-linked D-glucosamine and *N*-acetyl-D-glucosamine, is one of the few abundantly available cationic polysaccharides. It is obtained by partial deacetylation of chitin found in the exoskeleton of marine crustaceans<sup>211</sup>. Chitosan has attracted considerable interest from both fundamental research and industrial applications for a variety of reasons. Attributes including low toxicity, non-antigenicity, good biocompatibility, controllable biodegradability and cationic nature make chitosan a good candidate in numerous pharmaceutical and biomedical applications<sup>212</sup>. Chitosan is also readily converted to fibers, films, coatings, beads, powders and solutions, which further enhances its applicability. Over the last 20 years, chitosan has been extensively investigated in the fields of conventional and novel drug delivery, tissue engineering, microencapsulation, has been used as a biologically active agent, and so forth<sup>213-215</sup>.

Chitosan is a positively charged biopolymer, with the charge density directly related to the degree of deacetylation and the environmental pH. Though some research found that cationic materials tend to attract host inflammatory cells and may limit their applications in cell encapsulation, recent research by De Rosa suggested that PEC hydrogels with a partial positive charge may favor the functions of certain cell types such as fibroblasts<sup>216</sup>. The chitosan membrane modified with gelatin was found to encourage cell proliferation<sup>217</sup>. A number of other research also demonstrated the ability of chitosan to support various cell types as well as the compatibility of chitosan with soft tissues<sup>43,45,218-226</sup>.

A major disadvantage of chitosan is its poor solubility in physiological pH<sup>213</sup>. Since the  $pK_a$  of the D-glucosamine residue is around 6.5, chitosan is soluble only in dilute acetic acid or hydrochloric acid solutions, which limits its application and processing convenience, in particular as a matrix material for direct cell immobilization. Considerable efforts have been made on developing a water-soluble chitosan to overcome this drawback. Versatile modifications are performed on the hydroxyl and amino groups on glucosamine units of chitosan, or by depolymerization to form water soluble oligomeric chitosan<sup>227-232</sup>.

Because of the presence of amino groups, cationic chitosan has been used to interact with negatively charged materials via coacervation to form ionically linked hydrogels<sup>28</sup>. In

addition, chitosan may be readily obtained in large quantities from crab and shrimp shells, and hence presents a more cost-effective alternative to PLL in polyelectrolyte applications. Chitosan can complex with natural polyanions such as alginate, carboxymethylcellulose, cellulose sulphate, dextran sulphate, carboxymethyl-dextran, heparin, carragenen, xanthan, and pectin.

#### 2.4.4.2 AC membrane

Many reports demonstrate the effectiveness of chitosan-coated alginate microcapsules for sustained drug release and for live cell therapy<sup>20,34,37,51,233,234</sup>. Several research groups have investigated the alginate-chitosan (AC) polyelectrolyte complexation<sup>35,234-238</sup> with respect to the kinetic binding of chitosan to alginate beads, the effects of chitosan characteristics and preparation parameters on microcapsule properties, as well as the diffusion mechanism of the enclosed drugs.

The basic principle in the formation of AC complex is the electrostatic interactions between the protonated amino groups of chitosan and the carboxyl groups of alginate molecules<sup>35</sup>. Other intermolecular attractions such as hydrogen bonds and van der Waals forces also exist. The complexation between alginate and chitosan is considered stronger than that between alginate-PLL, probably due to the higher affinity of chitosan to the mannuronic and guluronic acid residues on the alginate bead surface<sup>162,235</sup>. In addition, similarity in charge distance, charge distribution and other structural features of the two polysaccharide molecules may also account for stronger cooperative ionic bounds. On the other hand, PLL has higher charge density and greater flexibility than chitosan due to its shorter monomer length (Fig. 2.2), which could lead to a stronger electrostatic attraction with alginate and thus an increased PLL binding<sup>35</sup>. Nevertheless, it is reported that AC microcapsules form a thicker membrane than alginate capsules coated with PLL (30 versus 10  $\mu\text{m}$ )<sup>239-241</sup>.

In the preparation of microcapsules with an alginate core and a coacervate AC membrane, variations in the procedures and the materials applied are wide. One method involves a one-step procedure, where alginate is dropped into a calcium/chitosan solution. Another approach for preparing AC complex capsules utilizes two steps, in which capsules are produced from a preformed calcium alginate bead and subsequently coated with chitosan.

Studies have shown that the stability of AC capsules strongly depends on the amount of chitosan bound to the alginate beads, which in turn is affected by several factors<sup>34,235,236</sup>.

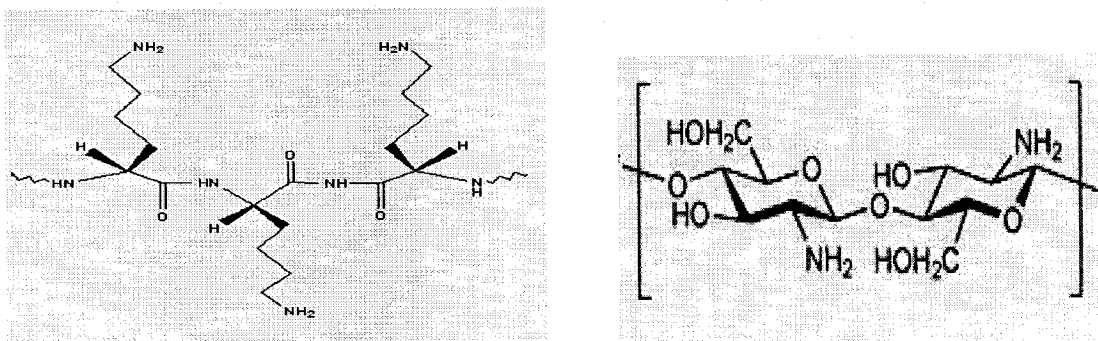


Figure 2.2. Molecular structures of poly-L-lysine (left) and chitosan (right)

Gaserod et al<sup>235</sup> found that the two stage procedure resulted in 100 times more chitosan binding to the microcapsules than the one-stage process. It was hypothesized that in a one-step procedure, the initial AC complex creates a membrane with small pores that restricts further diffusion of chitosan into the beads; whereas, in the two-step procedure, the porous calcium alginate gels allow chitosan to not only bind on the surface but also diffuse into the interior gel network, and in some cases, to form a solid complex gel. The findings by Gaserod et al<sup>35</sup> using radioactive labeled fractions of chitosan and by Chen et al using genipin as a fluorogenic marker via confocal laser scanning microscopy (unpublished results) support this hypothesis.

With respect to the material applied, alginates with large extended backbones or high molar mass in the range of  $10^5 - 10^6$  dalton are used as an inner material to ensure a sufficient number of intermolecular ionic bridges between the chains and facilitate the interaction with oppositely charged molecules<sup>28</sup>. Porous alginate gel favors chitosan binding, which can be achieved by selecting an alginate with a high G/M ratio, including gelling calcium ions in the chitosan solution, and/or by making the alginate beads homogeneous<sup>35,242</sup>. Concerning the chemistry of chitosan, chitosan with low molecular mass (below 20 KD) is preferable<sup>232</sup>. This is in large part due to the fact that the chain entanglement in high molecular weight polymers, such as alginate, may restrict the accessibility of amino groups on chitosan for reaction. Low molecular mass chitosan, with its shorter and more mobile chains, would undergo

conformational changes with greater ease, bringing the reactive groups to close proximity, and thereby facilitating the binding with alginate. Specifically, the use of oligomeric chitosan (MW < 3KD) permits the formation of AC capsules with good mechanical properties at a physiological pH<sup>243</sup>. Chitosan with a high degree of N-deacetylation provides more reactive amino groups to interact with alginate and form a more tightly bound network. It has been reported that a very strong polyelectrolyte complex could be achieved between fully deacetylated chitosan and negatively charged polysaccharides<sup>244</sup>. Furthermore, since both alginate and chitosan are weak polyelectrolytes, the environmental pH may influence the degree of ionization and thus the chitosan binding and the stability of AC complex. According to the intrinsic pKa of chitosan (~ 6.3) and alginate (~ 3.5), AC complexation is favorable at a pH of around 5.0, where both amine or carboxylic groups in both polyelectrolytes have about 70-80 % of the degree of dissociation, and each polysaccharide may sustain the relatively rigid, linear conformation, leading to a dense complex membrane<sup>34</sup>.

Bartkowiak and Hunkeler studied the permeability of the AC capsules by detecting the permeation of polymer standard dextran (70 and 110 KD) into the capsules<sup>243</sup>. It was found that the membrane was highly permeable, with a cutoff above 110 KD for dextran. Furthermore, the alginate core density, or the polyanion concentration, influenced the extent of dextran diffusion. Specifically, a thinner and less permeable capsule wall is formed at higher polyanion levels. Another study examined the membrane permeability using hemoglobin and immunoglobulin G (IgG) as permeants<sup>235</sup>. Results showed that the AC capsules formed by either the one-step or two-step procedure can not block the diffusion of IgG. The capsule permeability can be reduced by utilizing chitosan with higher MW and degree of deacetylation on a more heterogeneous alginate core. It was also suggested that building an additional multilayer of chitosan-alginate on the two-stage capsules may be required to create a wall impermeable to immunoglobulin class, therefore not elicit an immune reaction if used in cell transplantation.

Microencapsulation by AC complexation has been the topic of many investigations for the delivery of drugs<sup>36,38,238</sup>, proteins<sup>39,245</sup>, enzymes<sup>40</sup>, growth factors<sup>37</sup>, DNA<sup>186,246</sup>, live microbes<sup>48,49,233</sup>, and cells<sup>46,47</sup>. A recent interesting study by Green et al<sup>46</sup> successfully encapsulated a wide range of human cell types, including promyoblasts, chondrocytes, adipocytes, adenovirally transduced osteoprogenitors, immunoselected mesenchymal stem

cells, and the osteogenic factor, rhBMP-2 (BMP: bone morphogenic protein) into calcium phosphate/alginate/chitosan membranes using a facile procedure without loss of cell viability. One of the distinct features of this preparation is that the encapsulated growth factors can be delivered to human bone marrow stromal cells *in situ* by co-encapsulation to generate a new collagen matrix within the AC beads both *in vitro* in culture, and *in vivo*, where new bone matrix is generated. The degradation of polysaccharide-based membrane could be controlled by varying the mineral content so as to release cell types and growth factors for tissue regeneration and repair.

Despite being widely used, alginate-based microcapsules formed via ionic interactions are sensitive and “soft” hydrogels. The mechanical stability of the AC membrane was found to be sub-optimal in some applications<sup>43,49-52</sup>.

#### **2.4.5 Synthetic microcapsule systems**

Although alginate-based technology is still receiving a great deal of attention, research has been undertaken to develop alternative microcapsule systems attempting to improve certain physicochemical limitations in the classic alginate system. The use of synthetic polymers provides greater flexibility in molecular design and in principle, allows for a precise tailoring of mechanical and transport properties of the hydrogels. It also has the advantage of a precise control in material purification. Four synthetic microcapsule systems investigated for cell encapsulation are discussed in this section as follows.

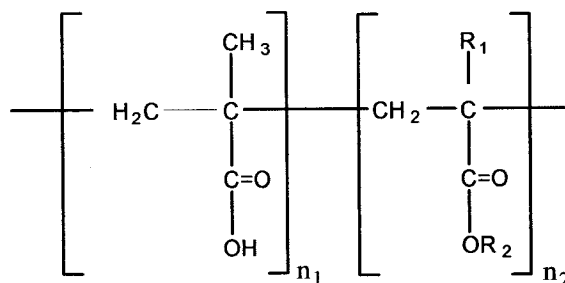
##### **2.4.5.1 PHEMA-MMA system**

A variety of acrylic acid copolymers have been developed for sustained release applications and cell encapsulation<sup>108</sup>. Figure 2.3 shows the chemical structure of the methacrylic acid copolymer. This synthetic microcapsule system offers more flexibility for modifying key components and allows one to control over needed properties, for example, by balancing hydrophilicity (i.e., membrane permeability) and hydrophobicity (i.e., membrane strength and durability), and easy scale-up. Eudragit® is the commercially available delivery system made from methacrylic acid copolymers and used for sustained release applications<sup>247</sup>.

Sefton and co-workers studied the encapsulation of viable cells, such as Chinese hamster ovary fibroblasts, human embryo kidney transfected cells, HepG2 cells, and dopamine secreting PC12 cells, into hydroxyethyl methacrylate-methyl methacrylate (HEMA-MMA) microcapsules via interfacial precipitation<sup>108</sup>. These membranes have an approximate exclusion limit of 100 KD. Although the encapsulated cells remained viable, *in vivo* studies have demonstrated the formation of cell aggregation and the risk of capsule clumping after implantation, likely due to hypoxia and central necrosis.

To prevent aggregation and preserve cell functions, the combination of extra-cellular matrix analogues, such as collagen, alginate, chitosan and hyaluronic acid, together with an immunisolating membrane was proposed. A research group from Singapore configured a 3D microenvironment for cultivation of sensitive anchorage-dependent cells by using chitosan or collagen as the core matrix, which complexed with methacrylic acid (MAA), HEMA and MMA to form a terpolymeric membrane<sup>225,248,249</sup>.

A four-layer microcapsule design based on this terpolymer system was also investigated as an improvement in the mechanical strength and cell functions for immobilizing hepatocytes as a bioartificial liver assist device<sup>250</sup>. Despite some success using this methacrylate-based hydrogel system for mammalian cell encapsulation, there exist several limitations to this system, for instance, the exposure to organic solvents, possible presence of residual monomers used in their manufacture and potential impairment by irradiation, which are undesirable for use in some cell cultures.



Methacrylic acid (MAA):  $\text{R}_1 = \text{CH}_3$ ,  $\text{R}_2 = \text{H}$ ;

Methyl methacrylate (MMA):  $\text{R}_1 = \text{CH}_3$ ,  $\text{R}_2 = \text{CH}_3$ ;

Hydroxyethyl methacrylate (HEMA):  $\text{R}_1 = \text{CH}_3$ ,  $\text{R}_2 = \text{OCH}_2\text{CH}_2\text{OH}$

Figure 2.3. Chemical structure of methacrylic acid copolymer

#### 2.4.5.2 Poly(methylene co-guanidine) and cellulose sulfate system

Poly(methylene co-guanidine) (PMCG) hydrochloride is a synthetic oligomeric cation with several unique features: low molecular weight, high charge density, high mobility and reactivity. It can form a strong ionic complex with negatively charged alginate and cellulose sulfate (CS). Being low in molecular weight, it may readily diffuse into the gel matrix, coacervate with polyanions and reduce the bead porosity. Orive et al<sup>251</sup> used PMCG as an alternative to PLL and produced a mechanically more resistant alginate-PMCG-alginate for islet encapsulation. Exposure of alginate beads to PMCG solution for 1 minute sufficiently formed a stable coating and may reduce the risk of cytotoxicity for the encapsulated cells induced by oligomeric PMCG<sup>30</sup>. Another type of polymeric capsule based on the use of this oligomer is the multicomponent alginate/CS//PMCG/Ca<sup>2+</sup> system<sup>252,253</sup>. For the preparation, a suspension of living cells and alginate/CS polyanion mixture was gelled in the polycation solution containing calcium chloride and PMCG. CS upholds the capsule network structure; alginate influences the droplet rheology; whereas PMCG forms the external membrane. The capsule size, mechanical strength, membrane thickness, and permeability can be controlled independently. This alginate-CS-PMCG microcapsule chemistry can also be adapted to hollow fiber geometry rendering it a valuable vehicle for many microencapsulation applications. Most recently, Bucko explored the encapsulation of a whole-cell epoxide-hydrolyzing biocatalyst in this membrane system and found five-fold preservation of the catalytic activity of the encapsulated nocardia tartaricans bacterial cells compared to free cultures, and 3-20-fold increase in the cis-epoxysuccinate hydrolase activity during storage compared to those entrapped in calcium pectate gels<sup>254,255</sup>. However, synthetic oligomeric cations remain potentially toxic to cells and contact time should be minimized.

#### 2.4.5.3 NaCS/PDADMAC capsules

Dautzenberg et al<sup>256</sup> established an encapsulation system based on sodium cellulose sulfate (NaCS) and polydiallyldimethyl ammonium chloride (PDADMAC) for the encapsulation of mammalian cells. NaCS and PDADMAC, both having permanent negative charges on the molecular chains, were used to build the capsule core and polyelectrolyte complex membrane, respectively. This preparation offers the advantages of having outstanding mechanical properties coupled with rapid preparation procedure. Also, it allowed

the preparation of microcapsules under physiological reaction conditions. Permeability of the capsules can be controlled over a wide range. The *in vivo* release of antibodies was achieved by using NaCS-PDADMAC encapsulated hybridoma cells. Results also showed the therapeutic relevance of encapsulated genetically modified cells as an activation center for cytostatic drugs during tumor therapy<sup>256,257</sup>. The drawback of this system is the limited life span of the encapsulated cells, which restricts the application to disease models requiring a long-term supply of therapeutic agents. Adaptation to this microcapsule system is under study<sup>258</sup>.

#### **2.4.5.4 Silanization of microcapsules**

Boninsegna et al<sup>259</sup> proposed the silanization of cells as a method of microencapsulation for prospective cellular grafts. In this method, silanes react with the exposed hydroxides on the cell surface and form a thin siliceous layer homogeneously surrounding individual cells. In this way, layer thickness can be controlled in the 0.1 -2.0  $\mu\text{m}$  interval. The process preserves original islet dimensions and does not suppress viability or function. Results from the transplantation studies using encapsulated islets in diabetic rats indicated prolonged restoration of normal glycaemia levels and protection from immunological attack.

#### **2.4.5.5 Nanoporous microsystem**

Desai et al described a microfabrication approach to cellular delivery based on micro- and nanotechnology<sup>134,260</sup>. The nanoporous biocapsules are bulk and surface micromachined to present uniform and well-controlled pore sizes. Such a design with tailored surface chemistries and precise microarchitectures may have potentials for immunoprotection in cell therapy and overcome some limitations associated with conventional encapsulation and delivery technologies<sup>135</sup>.

#### **2.4.6 Cross-linking of microcapsule membrane**

Maintaining integrity of microcapsules containing live cells is critical for effective *in vivo* immunoisolation and survival of transplanted grafts. Previous research has shown that microcapsules with sufficient membrane strength improve and prolong the *in vivo* functions

of encapsulated cells<sup>156</sup>. Microcapsules made of ionically linked hydrogels have several good characteristics and have been used for entrapment of a variety of bioactive materials and living cells, however they are prone to environmental constraints. Limitations such as chemical instabilities, material degradation or fracture, and broad membrane pore sizes persist. To improve mechanical stability of these microcapsule systems, exogeneous cross-links were introduced to membrane structure. Covalent cross-linking of microcapsules constitutes an effective way to generate polymeric networks with high gel strength and strong resistance to chemical, proteolytic and mechanical stresses<sup>261,262</sup>. Different cross-linking strategies have been investigated, for instance the use of bifunctional aldehydes<sup>40,51,263-268</sup>, carbodiimide (EDC)<sup>51</sup>, photo-cross-linkable molecules such as PEG<sup>269</sup>, methacrylate<sup>249</sup>, N-vinylpyrrolidone (NVP)<sup>210</sup> and other polyelectrolytes<sup>121,164,270,271</sup>. More recently, multi-functional cross-linking reagents<sup>272</sup>, UV sensitive diazo-resin nano-films<sup>273,274</sup>, as well as other methodologies<sup>263,275-277</sup> were proposed. Although the improvements in microcapsule stability using these synthetic cross-linking reagents have been reported in the literature, concerns about their cytotoxicity persist<sup>210,278-281</sup>.

Genipin is an iridoid glucoside extracted from Gardenia fruits<sup>282</sup>. It has long been used in Chinese herbal medicine for its anti-inflammatory, anti-thrombotic effects and liver protection activity<sup>283-287</sup>. Genipin is known to react rapidly with amino acids to make blue pigments, which are currently used as a natural colorant in the food and fabric industries<sup>288</sup>. As an alternative cross-linker, genipin was reported to be much less cytotoxic than synthetic counterparts such as glutaraldehyde. It allows for mild, but effective and covalent coupling with a variety of biomaterials containing primary amines<sup>279,289,290</sup>. These findings have prompted growing research interests, with a large number of publications in recent years. Studies have investigated the cross-linking mechanisms, the characteristics of the cross-linked products, and various biomedical applications in the fields of tissue fixation, membrane reinforcements and tissue engineering<sup>290-303</sup>. In addition, the fluorogenic characteristics of genipin were recently reported<sup>239,304</sup>. However, the use of genipin in applications involving live cells is still rare in the literature<sup>294,305</sup>.

Recent research on improving current microcapsule formulations and designing new artificial cell systems is enhancing the applicability of this strategy in preventive and curative

medicine. Table 2.6 lists some of the numerous artificial cell microcapsule formulations being studied for the development of artificial cells containing live cells. Despite encouraging results, each membrane is not without its disadvantages. An optimized microcapsule system fulfilling all the requirements for clinical applications has yet to be developed<sup>55</sup>.

Table 2.6 Examples of artificial cell microcapsule formulations alternative to the APA membrane for cell encapsulation

Microcapsule system	Main features	Ref
Alginate-chitosan (AC) capsules	Low cost; thicker membrane than APA; improved mechanical resistance; reduced membrane cutoff and cell leakage; supported mammalian and microbial cell growth and functions	52,141,235,243
Genipin cross-linked AC capsules	Covalent links created by naturally occurring genipin; enhanced membrane strength and durability; yet to test <i>in vivo</i>	306
Alginate-agarose microcapsules	Cell survival dependent on cell lines; limited mechanical stability	307
Alginate-cellulose sulfate-poly(methylene-co-guanidine) (A-CS-PMCG) system	Improved mechanical strength; easy control over membrane thickness; oligomeric PMCG may be immunogenic; yet to test long term stability	254,255,308,309
Alginate-PMCG-alginate capsules	Improved membrane strength; easily adjusted capsule size and wall thickness; oligomeric PMCG may be cytotoxic	251
Polyvinlyamine hydrochloride-based microcapsules	Mechanically stable; permeability can be controlled over a wide range	310
PHEMA-MMA system	Water insoluble; better stability and durability; limited cell survival and mass transfer in some applications	97,105,247
Chitosan core-poly(MAA-HEMA-MMA) shell	Prepared in physiological conditions; controllable mechanical strength and permeability; supported hepatocyte growth; maintained cell functions	225

Collagen core complexed with terpolymer HEMA-MAA-MMA shell	Improved mechanical strength and chemical stability; enhanced cell functions	248-250
Sodium cellulose sulfate and poly(dimethyldiallyl-ammonium chloride) system (NaCS-PDMDAAC)	MWCO less than 2 KD if prepared by standard method; addition of pore forming agent (starch) increased cutoff to 70 KD for proteins; allowed secretion and release of therapeutics by the encapsulated cells.	256-258,311,312

## 2.5 Microcapsule and membrane characterization

To further elevate artificial cells toward clinical applications, it is essential to understand the structural and physical properties of microcapsules in order to optimize their *in vitro* performance and *in vivo* functions. In this section, several key microcapsule features and the methods of characterization are discussed.

### 2.5.1 Visualization and characterization of microcapsule membrane

Despite the fact that microcapsule membrane is a dominant factor governing overall microcapsule performance, its characterization is challenging due to the small size, spherical shape and hydrogel nature of microcapsules along with the fragility of the membrane and other factors.

Visualization techniques including conventional or stereoscopic light microscopy (LM), scanning electron microscopy (SEM) and transmission electron microscope (TEM) are frequently used to characterize the morphology and structure of microcapsule membranes<sup>313</sup>. Though receiving wide recognition in microcapsule research, each method has its own limitations. LM is simple to administer, however remains impeded by the scattered or emitted light from structures outside the optical focal plane, which in turn limits the resolution<sup>133,243,314</sup>. SEM, in contrast, usually requires a relatively complex sample pre-treatment (e.g. dehydration and gold sputtering) and does not provide information on the inner structure of objects<sup>315</sup>. On the other hand, TEM allows inspection of the microcapsule wall structure, but is typically destructive and requires elaborate sample treatment including embedment, mechanical sectioning and in some cases selective staining. Some structural features may be altered or lost during the microscopic sample pre-treatment<sup>49,316</sup>. Furthermore, electron microscopic methods in general require expertise for sample preparation and result interpretation.

In recent years, atomic force microscopy (AFM), a technique originally used to characterize the surfaces of insulating crystals, has attracted increasing interest in microcapsule research and has become a useful tool for investigating the surface structure on polymeric hydrogel microspheres, capsules and particles<sup>317</sup>. AFM measures the attractive or

repulsive forces between a probe and the sample under a wide variety of operating conditions, either in air, water or other solvents. Almost all materials can be tested without extensive sample treatment. AFM records the topography of the sample surface with a resolution on the nano-scale, thus the surface roughness can be quantitatively assessed. It provides friction force images to distinguish different materials, phases, and chemical properties. In addition, the adhesion forces on surfaces can be a measurement of surface energy, especially useful in revealing surface modifications.

Quantitative chemical mapping on microcapsule surface has been recently reported. Scanning transmission X-ray microscopy was used to probe the nature and location of the chemical modifications on the covalently cross-linked alginate capsule surface<sup>318</sup>. Tam et al analyzed the microcapsule membrane at the micrometric/nanometric scale using a combination of advanced techniques, namely attenuated total reflectance Fourier transform infrared spectroscopy, X-ray photoelectron spectroscopy, and time-of-flight secondary ion mass spectrometry. They successfully detected and quantified the presence of PLL on the surface of standard APA capsules, providing direct evidences for inadequate covering of immunogenic PLL<sup>178</sup>.

Although certain parameters such as membrane thickness, distribution and density correlate with the microcapsule permeability, stability and biocompatibility, precise determination of them is difficult, and related reports are limited in the literature<sup>49,241,250</sup>. Electron microscopic evaluation could not be used for the visualization of the membrane density and coated material distribution because the dehydration of hydrogel microcapsules may lead to artifacts. Ma *et al* used a gravimetric method to measure the PLL membrane on the APA microcapsules. Apart from being destructive and cumbersome, this method could not assess the distribution of the coating polymers<sup>241</sup>. Additionally, approaches using radio-labeled polymers and enzyme-linked sorption assays involve elaborate sample preparation<sup>235,242</sup>, and the availability of the particular materials needed may also impede the process. Other methods for analyzing the thickness of thin films and small particles, such as ellipsometry<sup>125</sup> and surface plasmon resonance spectroscopy<sup>319</sup>, may not be suitable for hydrogel microcapsule membrane systems.

Confocal laser scanning microscopy (CLSM), a non-destructive approach, offers several advantages over ordinary light microscopy and the technically more demanding

electron microscopy<sup>320,321</sup>. In CLSM, the light from out-of-focus structures is faded out. Provided the material is sufficiently translucent, a section through the center of the capsules is visualized by optical slicing. By using different fluorescence labels, the non-destructive view and unambiguous identification of the capsule wall and interior is possible. By collecting several coplanar cross sections, a three-dimensional reconstruction of the inspected objects can be performed. Hence, CLSM allows the visualization/localization of microcapsule core-shell structure and provides computational image analysis to quantify different encapsulated phases as well as polymer distribution throughout the capsule<sup>320,321</sup>. In many studies, the microcapsule core and/or membrane components were labeled with fluorescent markers, such as fluoresceine isothiocyanate or rhodamine B isothiocyanate prior to encapsulation and thereafter identified their distribution under CLSM<sup>179,188,320-322</sup>. The labeling approaches included covalently linking and basic blending of fluorescent markers with the polymers<sup>138,320</sup>. Covalent linking processes, however, present risks of blocking some of the functional groups in the involved polymers essential for polyelectrolyte complexation, leading to weak binding. By physical mixing, on the other hand, the markers may not bind firmly at the intended sites and may migrate into other sites leading to compromised results. For instance, a rather thick PLL membrane (40–120  $\mu\text{m}$  in thickness) in the conventional APA capsules was reported<sup>179,188</sup> using prior-labeled PLL, in contrast to the thin membrane ( $\sim 10 \mu\text{m}$ ) measured by other methods<sup>144,241,323</sup>. In addition, other issues pertaining to the stability and solubility of the labeled polymers, the control of labeling efficiency, the separation of free markers, as well as their influences on the encapsulation process still remain<sup>179,320</sup>.

To overcome these limitations, a new method by fluorogenic genipin treatment without prior labeling of polymers was proposed<sup>239,323</sup>. Genipin, non-fluorescent in its free form, can selectively interact with primary amines and generate fluorescent conjugates. The covalently coupled genipin-polyamine conjugates formed *in situ* within the microcapsule enable the visualization and quantification of membrane material, such as chitosan and/or PLL, with regard to distribution, binding density by CLSM examination and computational image analysis. Furthermore, this approach requires minimal sample treatment. It is thus possible to quickly determine the membrane thickness and coating density on a routine basis as to facilitate the understanding of microcapsule structure and improve the control over functional properties.

## 2.5.2 Assessment for mechanical stability of microcapsule membrane

For many applications, microcapsules are subjected to mechanical stresses exerted by their environments that may induce deformation and potential breakup. Microcapsules should be strong enough to withstand environmental constraints during processing, implantation, as well as both short-term and long-term *in vivo* utilization. However, the mechanical properties of microcapsules are an intriguing object to study for physical reasons. Though no standard testing is currently available, a number of assessment methods have been explored<sup>28,116,316,324,325</sup>. A review of several current methods is discussed below with a focus on the advantages and limitations of each.

Thickness of the capsule membrane was used as an indirect measurement for membrane strength<sup>199,241</sup>. While it may be true that for a given material a thick capsule wall is stronger than a thinner wall, it is not possible to generally associate the thickness of the capsule wall with the strength of the capsule when different materials are compared.

The mechanical stability of the membrane was semi-quantitatively assessed by applying a compression force via a micrometer, tweezers, or parallel plates on individual capsules<sup>30,326</sup>. While this test provides a rapid estimation of the capsule strength, it does not provide quantitative results and is mainly used for screening microcapsule formulations. More advanced techniques have become available to derive quantitative data on capsule membrane strength. These compression tests utilize special apparatus such as a Texture Analyzer and Mechanic Tester, to measure the load required to burst the capsule<sup>133,327,328</sup>. These methods can provide an accurate measure of capsule elasticity and fragility depending on the sensitivity of the force transducer, which is supposed to be tunable to fit the anticipated bead or capsule strength. However, compromised precision was reported from inter-laboratory testing<sup>328</sup>. Direct comparison of capsule mechanical properties based on bursting force values is impossible when the tested capsules undergo high deformation (strain at bursting above 95%)<sup>243</sup>. Moreover, it may be time consuming to test enough capsules to avoid sampling errors, and has limited applicability on testing small capsules (<300  $\mu\text{m}$ ).

An AFM approach was recently introduced to study microcapsule mechanics<sup>324</sup>. It directly assesses the deformation of microcapsules under applied load and probes the forces at

failure. The advantages of this technique include increased accuracy, ability to image at atomic resolution and potential to image a wide variety of samples in an aqueous environment. Moreover, it provides more detailed experimental information on microcapsule properties including load-deformation profiles, elasticity and plasticity of the capsule shell, swelling behaviors, permeability and so forth. A combination of AFM and CLSM was explored to study the deformation properties of multilayer microcapsules<sup>329</sup>. High-frequency scanning acoustic microscopy was also used to characterize the elasto-mechanical properties of microcapsules<sup>330</sup>.

Microcapsule strength can also be evaluated by exposing the capsule population to a well-defined shear-flow and measuring the fraction of capsules undergoing failure<sup>50,225,316,331</sup>. In the modified quantitative assessment described by Leblond et al<sup>331</sup>, microcapsules along with glass beads were exposed to continuous agitation. This mechanical test incorporates stresses of compressive, crushing, shearing and abrasive forces applied on microcapsules and allows easy measurement by detecting the leaking degree of encapsulated fluorescent macromolecules. Vigorous agitation may accelerate the breakage of the capsules so as to shorten the time needed for the test. But in an assay, only 10 % of hollow APA capsules broke after 20 h of agitation, indicating it is not appropriate for microcapsules with strong membranes.

Van Raamsdonk and Chang described an osmotic pressure test to quantify the strength of microcapsules by exposing beads to an osmotic pressure shock and assessing the percentage of broken microcapsules<sup>332</sup>. This osmotic swelling test induced the entrance of water within the capsule by an osmotic phenomenon that presents a main cause of microcapsule breakage under physiological conditions<sup>162</sup>. Moreover, a combination of destabilizing forces including osmotic pressure shock, citrate chelation and shear forces (by continuous rotation) comprise another method for assessing the mechanical stability of microcapsules with a strong membrane<sup>95</sup>.

### **2.5.3 Characterization of microcapsule permeability**

In cell microencapsulation, live cells are isolated from the external environment by an artificial membrane. The semi-permeability of this membrane dominates the supply of

essential nutrients and oxygen, the elimination of toxic metabolites, and the exchange of therapeutic factors (physiological signals used as input for cell functions and products secreted). The membrane also serves as an immune barrier preventing the entry of the host immune substance that may destroy the foreign cells. A fundamental understanding of microcapsule membrane permeability is thus critical for successful exploitation of live cell microencapsulation for therapy<sup>33</sup>.

The permeability characteristics of a microcapsule membrane consist of two factors: the MWCO and the diffusion rate of permeation molecules<sup>333</sup>. The MWCO of a membrane, defined as the lowest molecular weight of the substance that cannot permeate through the membrane of the capsules, is measured using high molecular weight markers in the equilibrium state where less than 5 % of the maximal possible amount of marker mass enters (or leaves) a microcapsule. Examining the diffusion of low molecular mass markers in the equilibrium state allows one to discern whether the microcapsule interior is accessible for small molecules like cell nutrients, metabolites and secreted biologics. The kinetic marker diffusion, on the other hand, is investigated using smaller size markers in the transient state to assess the diffusion coefficients, an index of mass transport rate of appropriate markers across the inter-phase boundary. Previous research investigated the mass transfer coefficient of Vitamin B12 on different microcapsule formulations, and ranked them according to increasing mass transfer rate<sup>42,328</sup>. An extended study by Rosinski et al included markers of high molecular weight for diffusion coefficient determination to cover the entire range of mass transport phenomena including free accessibility of a marker to capsule interior and its exclusion, and evaluated the differences in mass transport caused by different microcapsule membrane chemistries<sup>334</sup>.

Typical markers of various molecular weights include proteins, dextrans (labeled or unlabeled), or PEG molar mass standards<sup>309</sup>. Dextran is a linear and neutral polysaccharide, whereas globular BSA bears negative charges at pH > 5.0 (pI = 4.8) and hydrophobic character. In capsule permeability research, the use of neutral polysaccharide molecular weight standards precludes the problems of absorption, aggregation and other charge/hydrophobic interactions, while proteins are thought to be more appropriate in determining the permeability of capsules designed for biological systems<sup>190,335</sup>. Based on relationships between solute size and molecular weight, Brissova et al described a conversion

of the exclusion limit for dextran to the size and approximate molecular weight of protein<sup>155</sup>. To determine the MWCO of capsules, cell lysate can also be used as probes. This was done by encapsulating *E. coli* lysate composed of proteins with various molecular weights inside the microcapsules. The cell lysate components with molecular weight lower than the MWCO of the capsule membrane would diffuse out of the capsules. The molecular mass of the largest molecule that can penetrate the membrane represents the upper limit of permeation through the membrane, and can be determined by analyzing the solution outside the capsules by gel electrophoresis<sup>258</sup>.

Methods to determine the permeability include both ingress- and egress-based techniques, and measurements can be conducted either in batch when a decrease/increase of the markers in the surrounding medium was detected by means of UV spectrophotometry<sup>107,187</sup> and size exclusion chromatography (SEC)<sup>308,336,337</sup>, or with individual capsules using confocal fluorescence microscopy<sup>188,338,339</sup>. An advantage of encapsulation of probes to determine the MWCO is the possibility to detect a small number of leaking capsules. However, the probes may possibly diffuse out of the capsules during the preparation procedure. Addition of probes to the medium containing capsules also has disadvantages. The sensibility or detection limit of the measurements in the supernatant depends on the ratio of medium volume to capsule volume, and is limited by the volume of capsule suspension and the volume of supernatant needed for sampling. When mass transfer is assessed by detecting the increase/decrease in marker concentrations in the supernatant, binding of markers, in particular proteins, to the capsule membranes (rather than penetrating) may lead to artifacts. Evaluating the diffusion of fluorescent markers by CLSM on individual capsules offers several advantages<sup>225,338,339</sup>. These include: (1) allows for direct visualization of marker permeation and distinction of marker absorption onto the capsule surface; (2) can evaluate reproducibility within one batch; and (3) allows for detection and withdrawal of defected capsules, which is not achievable by detecting the marker concentrations in supernatant. However, it may be time consuming to examine a large number of capsules individually in order to obtain statistically significant data. Nevertheless, using a broad spectrum of solutes of various molecular masses is highly recommended for diffusion experiments<sup>333</sup>.

It was found that different techniques for measuring the permeability of standard APA capsules yield different results<sup>107,188,190,336</sup>. One of the reasons for the disparity may be related

to the supraphysiologic protein concentrations (1-10 mg/ml) required in these measures. At this concentration, protein self-association and oligomerization may occur, resulting in erroneous results. To overcome this limitation, Brissova et al<sup>308</sup> reported a new assessing method using protein A sepharose (PAS)-antibody complex. The protein under investigation is radio-labeled, and present at a low concentration (1 ng/ml) within the physiological range. The protein is specifically bound and accumulated by PAS-antibody complex, which can be quantified by detecting their radioactivity using a gamma counter. In this manner, the absorption of protein to the capsule is not a factor in measuring the permeability.

#### **2.5.4 Immunoprotection and biocompatibility of microcapsules**

As the driving force behind the idea of artificial cells, sufficient immunoprotection and biocompatibility are necessary for the success in clinical applications. The host immune system response to microencapsulated cells can be divided into two categories: response to encapsulated cells, which can be triggered by insufficient immunoprotection, and response to the capsular membrane, which is instigated by inadequate biocompatibility.

Immunoprotection by artificial cells concerns the isolation of transplanted live cells or tissues from the host system through a physical barrier by creating a membrane against the passage of immunologically active molecules and cells, thus preventing immune rejection of the transplant<sup>16</sup>. The permeability of the membrane controls the extent of immunoisolation, and the requirements for immuno-protection vary depending on the cells (allogenic or xenogenic) used for transplantation. The rejection of transplanted cells involves several pathways. In the case of allogenic transplantation, immune response is triggered by a direct pathway involving T-lymphocyte sub populations such as CD8+ which act on the donor cells. This interaction can be prevented provided the microcapsule membrane maintains structural integrity and prevents any direct contact between the enclosed cells and the surrounding host cells. If these criteria are satisfied, the graft can be accepted by the host. Apart from the unavoidable absorption of proteins on graft surface, xenografts trigger a more vigorous host response than allografts. They can release antigens that can penetrate the capsule membrane and activate the recipient's immune cells in the vicinity of the capsules, resulting in an overgrowth of the capsules by fibroblast-like and macrophage-like cells, as well as an

inflammatory response. The activated macrophages produce cytotoxic cytokines that can pass through the semi-permeable capsule membrane and damage the encapsulated cells<sup>16</sup>. Furthermore, if by any chance, antibodies in the host environment penetrate into microcapsules and bind to encapsulated cells, they may activate the complement system and eventually lead to the destruction of xenografts. In cell microencapsulation, blocking immune molecules is a complicated task. The semi-permeable membrane may exclude the entry of immunocytes, macrophages, antibodies and other large immune molecules; however, humoral immune components, such as cytokines and tissue antigens secreted by the encapsulated cells and the recipient's cells, are low in molecular mass and can not be blocked by the capsular membranes that allow the exchange of nutrient and wastes<sup>108</sup>. The exposure or release of these immune substances into adjacent tissue may result in the recognition of a foreign object causing immune rejection. Nevertheless, upholding the membrane integrity and controlling the membrane permeability, pore size and pore homogeneity are crucial to achieve effective immunoisolation and consequently satisfactory immunoprotection in cell transplantation.

Graft failure is interpreted as the consequence of overgrowth of the capsules and subsequent ischemia and necrosis of the enclosed cells<sup>76</sup>. The presence of thick fibrotic tissue presents a physical barrier for nutrient/oxygen supply and waste removal for the encapsulated cells, which leads to rapid loss of cell viability and functionality<sup>168</sup>. Material traces released from fibroblasts, macrophages and/or lymphocytes migrating over the microcapsule surface may initiate the primary foreign body reactions. These host reactions may be a result of insufficient immunoprotection and/or inadequate microcapsule biocompatibility, and from both the membrane material and the therapeutic cells.

Many factors including chemical composition, uniformity, morphology, topography and other surface properties of implanted microcapsules affect biocompatibility of grafts<sup>168</sup>. Previous studies have shown that using highly purified and biocompatible polymers can improve biocompatibility<sup>112,173,340-342</sup>. It is essential that all contaminants, notably endotoxins and proteins, be removed from capsule materials<sup>202</sup>. Geometric inhomogeneities or irregularities may trigger the growth of fibroblasts and macrophages after implantation. A larger capsule volume generally results in more frequent adverse side effects in recipients, thus the use of smaller capsules is recommended. The surface properties of microcapsules has been correlated directly to biocompatibility, with improved compatibility being found for

smoother and flawless surfaces<sup>203,343</sup>. It has been shown that cell adsorption is decreased when the charged surface is shielded by the use of a non-ionic polymer, like PEG, thereby reducing inflammatory responses<sup>168</sup>.

The biological acceptance of encapsulated cells can also be influenced by the surgical procedure, site of implantation, type of cell used and the cellular products being secreted. It is believed that the early post-transplantation period is vital for long term functionality of the transplant<sup>56</sup>. Sufficient oxygen transport is also crucial to maintain oxygen-dependent metabolism and cell functionality. Conceivable approaches to improve graft oxygenation include the use of smaller capsules, seeding at an optimal cell density, inclusion of hemoglobin-based or perfluorocarbon oxygen carriers, as well as promotion of vascularization at the implantation site<sup>29,144,168</sup>. The portal vein has been proposed to be a possible alternative to the peritoneal cavity for transplantation of encapsulated cells with higher nutrient and oxygen supply and close contact to blood. Cell-related interactions also account for the outcome of the application. Integrating chemical agents, such as vitamins D3 and E that can counter antibodies, were used to enhance the immuno-barrier capacity of microcapsules. Coencapsulation of steroids (dexamethasone) that can release immunomodulating factors was reported to reduce biological response and improve biocompatibility<sup>344</sup>. Coencapsulation of sertoli cells<sup>76,344,345</sup> and bone marrow stem cells<sup>346</sup>, or co-administration of fibrosis-inhibiting drugs<sup>185</sup> or other weak immunosuppressants during the first 7 days following transplantation<sup>168</sup> has been investigated to curb immune rejection. Liu and Chang<sup>347,348</sup> investigated the transplantation of bioencapsulated bone marrow stem cells intraperitoneally into syngeneic hepatectomized rats. They found that this strategy facilitated the hepatic regeneration with an efficacy similar to that of bioencapsulated hepatocytes or free hepatocytes transplantation. These findings suggest the potential for a new alternative to hepatocyte transplantation for the treatment of acute liver failure with no immuno-rejection against the donor hepatocytes.

To improve the quality of microcapsules, efficient methods need to be established and standardized for the evaluation of biocompatibility of microcapsules. Recently, many efforts have been made to address this issue. A study by Lekka<sup>149</sup> indicated the reliability of AFM (contact mode) to quantify local surface properties affecting the biocompatibility of alginate-based hydrogel materials. Zhang et al introduced a polarized light microscopic method to

quantify the fibrosis formation of the microcapsule surface<sup>349</sup>. CLSM was also used to investigate the cell survival within the microcapsules, and compare the fibrotic reactions against the microcapsules containing allo- and xenocells<sup>192</sup>. Roth et al scored the biocompatibility of transplanted microcapsules real time (over a six-week period) and *in situ* by monitoring immune response using bioluminescent technology and a nuclear factor-kappa beta (NF-kappa B) sensitive transgenic mouse model<sup>350</sup>. NF-kB is a transcription factor that coordinates the inflammatory and wound healing cascades by initiating the transcription of cytokines, chemokines, adhesion molecules, and proinflammatory genes. This imaging evaluation approach allows many measurements of NF-kB activity to be acquired for each animal, reduces the number of animals required to obtain statistically significant immune response data over time, and in turn reduces error associated with animal variability. It can detect significant differences in NF-kB activity on mice before and after operation, but is unable to discern the effect of capsule wall composition on NF-kB activity. Moreover, an encapsulation platform for systematically testing the effects of microenvironmental parameters on encapsulated islets was developed<sup>351</sup>. This PEG-based inert encapsulation matrix affords control over the biochemical and biophysical cellular microenvironment and the introduction of systematic changes to this environment.

In summary, sufficient mechanical stability, appropriate permeability, sufficient immunoprotection and biocompatibility are major considerations in developing new microcapsules for cell therapy. However, the exact requirements for artificial cells are dictated by the type of bioactive species of interest and the intended function, and are therefore not equal for all applications. For example, some delivery devices for the treatment of CNS diseases may require a lesser degree of immunoisolation and should be biodegradable, avoiding their retrieval after fulfilling their function<sup>89,100</sup>. Other cell delivery carriers, especially in xenogenic cell transplantation, should encase the viable cells and withstand *in vivo* degradation long enough for immunoisolation purposes<sup>16</sup>. Permeability of the capsular membrane is also application-dependent. The membrane should allow the diffusion of a particular agent for therapy, by either sustained diffusion or burst release, depending on which is desirable. The requirements for mechanical stability are varied with application sites. Blood compatibility is another parameter that needs to be considered if artificial cells are used

intravenously. Finally, for vaccine delivery systems, “non-biocompatibility” of the materials might be desired to a certain extent, thus resulting in an adjuvant effect<sup>352</sup>.

## 2.6 Artificial cells containing live microbes for oral therapy

Oral ingestion is the preferred route of administration for therapy. Research has demonstrated that oral delivery of live functional bacterial cells has potential in the treatment of many diseases<sup>353</sup>. However, the human GI tract is a prominent part of the immune system<sup>11</sup>. The low gastric acidity is fatal for many ingested microorganisms. Actions from GI enzymes, bile and microflora actions, as well as other chemical and biochemical forces also play a role in the GI immune functions<sup>3,11</sup>. In addition, mucus containing IgA antibodies presents another barrier for the ingestion of microorganisms. On the other hand, effective oral therapy utilizing live cells requires the cells to survive GI transit and overcome the biological stresses encountered. Recently, with the advent of genetic engineering, strategies have been developed to accelerate strain improvement<sup>2</sup>. However, GE microorganisms may, if prolonged and repeated large doses are taken, stimulate host immune response, systematically propagate in the intestine, disrupt the indigenous microflora, and have risks of immunomodulation, translocation and gene transfer<sup>2,12-18</sup>.

To overcome these delivery obstacles, Prakash and Chang proposed the concept of artificial cell oral therapy<sup>4</sup>, wherein live functional cells were encapsulated and taken orally. The cells are isolated from the host GI environment, protected by the polymeric membrane, and reach the intestine in a large controlled number. They can be designed to secrete small biologics (peptides, enzymes, growth factors, etc.) and release into the gut lumen for therapy. Alternatively, they can act as bioreactors during their GI transit by metabolizing undesirable small substance (amino acids, bile acids, ammonia, etc.) present in the gut and eventually eliminate them from the body<sup>6</sup>. Previous research has demonstrated the potential of oral delivery using microencapsulated GE cells to circumvent problems associated with free bacteria. Examples include microencapsulated *Escherichia coli* DH5 cells over-expressing the *Klebsiella aerogenes* urease gene for urea removal in renal failure<sup>4</sup>, *Oxalobacter formigenes* producing oxalate-degrading enzymes for removal of accumulated oxalate in urolithiasis<sup>7,8</sup>, and bile salt hydrolase-overproducing *Lactobacillus plantarum* 80 (pCBHI) BSH<sup>+</sup> to

promote elevated bile salt deconjugation and serum cholesterol lowering<sup>9</sup>, as well as others<sup>10</sup>. The range of therapeutic opportunities for this technique is extremely widespread.

Designing an appropriate microcapsule membrane for oral delivery of live cells is challenging. GE bacteria should be encased in microcapsules, perform their therapeutic functions during GI transit, and be excreted along with the intact microcapsules in feces without being retained in the body even though they are classified as nonpathogenic<sup>19</sup>. To fulfill these requirements, there is a need, on one hand, for creating a robust isolating barrier between the cells and the host gut. On the other hand, cell viability, metabolism, and functions should be sustained during processing and GI transit. In addition, targeted substrates and products should be able to freely pass through the microcapsule membrane for therapy. Although numerous microcapsule systems have been studied for oral delivery, such devices are mostly used for the controlled release of curative agents, for instance drugs and probiotics<sup>20-26</sup>. Relevant research on developing a microcapsule system for oral delivery of live cells intended to function during the GI transit while needing to be retained in the microcapsules is scarce in literature.

In brief, oral delivery of live cells has great potential in healthcare. However, currently obtainable microcapsule formulations are not sufficient to fulfill the requirements for widespread clinical uses. There is an urgent need to develop a suitable microcapsule system to withstand the harsh and destructive GI environment for artificial cell oral delivery applications. Building upon current literatures, this thesis research investigates the design, preparation and suitability of a new microcapsule system for potential live cell oral delivery and other applications.

## PREFACE FOR CHAPTER 3-10

Presented in the following eight chapters are the studies performed in order to achieve the research objectives. Each chapter discusses various important aspects of the thesis research project. Chapter 3 investigates the suitability of the conventional APA microcapsule system for oral delivery of live cells. It provides the grounds for developing stronger microcapsule membranes. Chapter 4 describes the membrane design and the preparation of the GCAC microcapsule. It also provides a preliminary evaluation of its suitability for live cell encapsulation. Chapter 5 presents the findings of genipin fluorogenic attributes, based on which a new approach to use genipin to characterize microcapsule membranes was developed; results are reported in Chapter 6. Chapter 7 presents the detailed studies on the GCAC microcapsule membrane characterization and genipin reaction optimization. Chapter 8 studies the structural and physical characteristics of the GCAC microcapsules. Chapter 9 focuses on the microcapsule behaviors in the simulated human GI environment. Chapter 10 is on the investigation of using the GCAC membrane system for live genetically engineered *Lactobacillus plantarum* 80 (LP80) cells oral delivery.

During this thesis research period, I was able to contribute to 20 original research articles, 17 abstract/proceedings, 1 book chapter, and 1 U.S. provisional patent, pertaining to the thesis research goal. Of these I have elected to use 8 articles, of which I am the first author, as thesis chapters.

### **Original research articles (published/in press/to be submitted) presented in this thesis:**

1. **H Chen**, W Ouyang, M Jones, T Haque, B Lawuyi and S Prakash. *In vitro* analysis of APA microcapsules for oral delivery of live bacterial cells. *Journal of Microencapsulation*. 22(5): 539-547 (2005).
2. **H Chen**, W Ouyang, M Jones, T Metz, C Martoni, T Haque, R Cohen, B Lawuyi and S. Prakash. Preparation and characterization of novel polymeric microcapsules for live cell encapsulation and therapy. *Cell Biochemistry & Biophysics*. (in press)
3. **H Chen**, W Ouyang, B Lawuyi, C Martoni and S Prakash. Reaction of chitosan with genipin and its fluorogenic attributes for potential microcapsule membrane characterization. *Journal of Biomedical Materials Research*. 75A (4): 917-927 (2005).

4. **H Chen**, W Ouyang, B Lawuyi, T Lim and S Prakash. A new method for microcapsule characterization: use of fluorogenic genipin to characterize polymeric microcapsule membranes. *J Applied Biochemistry & Biotechnology*. 134 (3): 207-221 (2006).
5. **H Chen**, W Ouyang, B Lawuyi and S Prakash. Genipin cross-linked alginate-chitosan microcapsules: membrane characterization and optimization of cross-linking reaction. *Biomacromolecules*. 7 (7): 2091-2098 (2006).
6. **H Chen**, W Ouyang, C Martoni and S Prakash. Investigation of structure and relevant properties of the alginate-chitosan microcapsules covalently cross-linked by genipin. (to be submitted to *Journal of Membrane Science*)
7. **H Chen**, W Ouyang, C Martoni, F Afkhami, T Lim and S Prakash. Evaluation of microcapsules for potential gastrointestinal applications using a dynamic simulated human gastrointestinal model. (submitted to *J of pharmaceutical sciences*; part of the results published in *IFMBE proceeding series* 12, 2005)
8. **H Chen**, W Ouyang, B Lawuyi, C Martoni and S Prakash. Microencapsulation of *Lactobacillus* in covalently cross-linked microcapsules for potential gastrointestinal applications. (to be submitted to *Pharmaceutical Research*)

**Original research articles not included in the thesis:**

9. **H Chen**, and S Prakash. Influences of complexation reaction on the structure and properties of the alginate-chitosan microcapsules: visualization and optimization. (manuscript under preparation, intended to submit to *Acta Biomaterialia*)
10. T Haque, **H Chen**, W Ouyang, C Martoni, B Lawuyi, A Urbenska and S Prakash. *In vitro* study of alginate-chitosan microcapsules: an alternative to liver cell transplants for the treatment of liver failure. *Biotechnology Letters*. 27(5): 317-322 (2005).
11. T Haque, **H Chen**, W Ouyang, C Martoni, B Lawuyi, A Urbenska and S Prakash. Superior cell delivery features of polyethylene glycol incorporated alginate, chitosan and poly-l-lysine microcapsules. *Molecular Pharmaceutics*. 2(1): 29-36 (2005).
12. T Haque, **H Chen**, W Ouyang, C Martoni, B Lawuyi, A Urbenska and S Prakash. Investigation of a new microcapsule membrane combining alginate, chitosan, polyethylene glycol and poly-l-lysine for cell transplantation applications. *International Journal of Artificial Organs*. 28(6): 631-637 (2005).
13. M Jones, **H Chen**, W Ouyang, T Metz and S Prakash. Deconjugation of bile acids with immobilized genetically engineered *Lactobacillus plantarum* 80 (pCBH1). *Applied Bionics & Biomechanics*. (in press).

14. T Metz, M Jones, **H Chen**, T Lim, M Mirzaei, T Haque, D Amre, SK Das and S Prakash. A new method for targeted drug delivery using polymeric microcapsules. *Cell Biochemistry & Biophysics*. 43(1): 77-85 (2005).
15. W Ouyang, **H Chen**, M Jones, T Metz, T Haque, C Martoni and S Prakash. Artificial cell microcapsule for oral delivery of live bacterial cells for therapy: design, preparation and *in vitro* characterization. *J Pharmaceutics & Pharmacology Science*. 7(3): 315-324 (2004).
16. M Jones, **H Chen**, W Ouyang, T Metz and S Prakash. Microencapsulated genetically engineered *Lactobacillus plantarum 80 (pCBHI)* for bile acid deconjugation and its implication in lowering cholesterol. *J Biomed & Biotechnol*. 1: 61-69 (2004).
17. T Metz, D Amre, M Jones, W Ouyang, **H Chen**, T Haque, C Martoni and S Prakash. Artificial cell microcapsule containing thalidomide as an alternative oral therapy method for Crohn's disease (CD). *Pediatric Gastroenterology, Hepatology and Nutrition*. 565-571 (2004).
18. M Jones, **H Chen**, W Ouyang, T Metz and S Prakash. Method for bile acid determination by HPLC. *J Med Sci*. 23(5): 277-280 (2003).
19. B Lawuyi, **H Chen**, F Afkhami, A Kulamarva and S Prakash. Microencapsulation of engineered *Lactococcus lactis* in alginate-poly-L-lysine-alginate capsules for heterologous protein delivery. *Applied Biochemistry and Biotechnology* (accepted).
20. B Lawuyi, **H Chen** and S Prakash. Survival of microencapsulated engineered *Lactococcus lactis* in experimental and simulated gastrointestinal conditions. (To be submitted to *World Journal of Microbiology and Biotechnology*).

#### **Book Chapters:**

1. S Prakash, J Bhatena and **H Chen**. The artificial cell design: hydrogel. In: S. Prakash, editor. Introduction to artificial cell: concept, history, design, current status and future prospective. Woodhead Publishing Limited, Cambridge, England. (in press).

#### **Proceedings, Abstracts and Presentations:**

1. **H Chen**, W Ouyang, F Afkhami, T Lim and S Prakash. *In vitro* evaluation of covalently cross-linked microcapsules for potential oral therapy. *12<sup>th</sup> Intl Conference in Biomedical Engineering*. Dec 2005. Singapore.
2. **H Chen**, W Ouyang, M Jones, T Haque, B Lawuyi and S Prakash. *In vitro* characterization of APA microcapsules for oral delivery of live bacterial cells. *28<sup>th</sup>*

- Canadian Medical and Biological Engineering Society Conference*. Sept 2004. Quebec City, Canada.
3. **H Chen** and S Prakash. Stability of APA microcapsules and their resistance to simulated GI fluids. *6<sup>th</sup> CBGRC*. Nov 2003. Montreal, Canada.
  4. **H Chen**, W Ouyang, M Jones, T Metz and S Prakash. Alginate-chitosan microcapsules cross-linked by naturally occurring genipin. *23<sup>rd</sup> Canadian Biomaterials Society Symposium*. May 2003. Montreal, Canada.
  5. **H Chen**, W Ouyang, M Jones and S Prakash. Preparation alginate/chitosan based multilayer microcapsules for biomedical application. *Polymer in medicine and Biology 2002, ACS Symposia*. Nov 2002. California, USA.
  6. **H Chen**, W Ouyang, M Jones and S Prakash. New artificial cells: preparation and *in vitro* characterization. *5<sup>th</sup> CBGRC*. Sept 2002. Montreal, Canada.
  7. F Afkhami, W Ouyang, **H Chen**, J Bhathena, T Lim and S Prakash. *In vitro* analysis of APPPA microcapsules for oral delivery: impact of microcapsules on GI model flora. *XXXII ESAO Congress & IFAO Intl Federation for Artificial Organs*. Oct 2005. Bologna, Italy.
  8. T Lim, W Ouyang, **H Chen**, C Martoni, F Afkhami and S Prakash. Activated charcoal and probiotics bacteria in microcapsules for creatinine reduction—adjunct therapy for kidney failure. *XXXII ESAO Congress & IFAO Intl Federation for Artificial Organs*. Oct 2005. Bologna, Italy.
  9. W Ouyang, F Afkhami, **H Chen** and S Prakash. Confocal laser scan microscopy (CLSM) for potential microcapsule membrane characterization. *XXXII ESAO Congress & IFAO Intl Federation for Artificial Organs*. Oct 2005. Bologna, Italy.
  10. T Haque, **H Chen**, W Ouyang, T Metz, C Martoni and S Prakash. Design of a novel microcapsule membrane combining alginate, chitosan, polyethylene glycol and poly-L-lysine for cell transplantation. *XXXI Congress of European Society for Artificial Organs*. Sept 2004. Warsaw, Poland.
  11. T Haque, **H Chen**, W Ouyang, T Metz, B Lawuyi and S Prakash. Effect of integrating polyethylene glycol to alginate-poly-L-lysine and alginate chitosan microcapsules for oral delivery of live cells and cell transplantation for therapy. *28<sup>th</sup> Canadian Medical and Biological Engineering Society Conference*. Sept 2004. Quebec City, Canada.
  12. T Haque, **H Chen**, W Ouyang, C Martoni and S Prakash. Investigation of a novel microcapsule membrane integrating polyethyleneglycol to alginate, poly-L-lysine and chitosan microcapsules for the application of liver cell transplantation. *XX International Congress of the Transplantation Society*. Sept 2004. Vienna, Austria. Published in: *Transplantation* (supplement).

13. T Metz, D Amre, M Jones, **H Chen**, W Ouyang, T Haque, C Martoni and Prakash S. Artificial cells containing thalidomide as an alternative oral therapy method for Crohn's disease. *Gastroenterology*. 126 (4): A288 Suppl. 2, April 2004.
14. W Ouyang, **H Chen**, M Jones, T Metz and S Prakash. Novel multilayer microcapsule and its GI stability. *23<sup>rd</sup> Canadian Biomaterials Society Symposium*. May 2003. Montreal, Canada.
15. T Metz, **H Chen**, W Ouyang, M Jones, P Magown and S Prakash. Polymer microcapsules for targeted oral drug delivery in Crohn's disease. *23<sup>rd</sup> Canadian Biomaterials Society Symposium*. May 2003. Montreal, Canada.
16. M Jones, **H Chen**, W Ouyang, T Metz and S Prakash. Deconjugation of bile acids with immobilized genetically engineered *Lactobacillus Plantarum 80 (pCBH1)* cells and their potential for live cell therapy. *6<sup>th</sup> International Congress of the Cell Transplant Society*. Mar 2003. Atlanta Georgia, USA. Abstract in: *Cell Transplantation*. 12 (2): 196-197, 2003.
17. W Ouyang, **H Chen**, M Jones and S Prakash. Novel artificial cell formulation: design, preparation and morphology studies. *Polymer in Medicine and Biology. ACS Symposia*. Nov 2002. California, USA.

**Patents:**

1. S Prakash, **H Chen**, O Nalamasu, P Raja and P M Ajayan. Microcapsule carbon nanotube device. 2004, OTT of McGill University. 2005, US provisional.

## **CONTRIBUTIONS OF AUTHORS**

In all the original research articles included in this thesis as individual chapters, I am the first author and was responsible for designing studies, conducting experiments, analyzing data and preparing manuscripts. Dr. S. Prakash, reported as the last author in all manuscripts, is the research advisor and also the corresponding author. Other reported co-authors have provided suggestions and assistance in performing experiments, and proofread the manuscripts.

***In vitro* analysis of APA microcapsules for oral delivery of live bacterial cells**

Hongmei Chen, Wei Ouyang, Mitchell Jones, Tasima Haque, Bisi Lawuyi and Satya Prakash\*

*Biomedical Technology and Cell Therapy Research Laboratory*

*Department of Biomedical Engineering and Physiology, Artificial Cells and Organs Research  
Centre, Faculty of Medicine, McGill University, Montreal, Quebec, H3A 2B4 Canada.*

\*Corresponding author: Tel: 514 398-3676; Fax: 514 398-7461;  
Email: satya.prakash@mcgill.ca

---

**Preface:** This paper investigates the suitability of the alginate-poly-L-lysine-alginate (APA) microcapsules for oral delivery of live bacterial cells, *in vitro*, using a dynamic simulated human gastro-intestinal (GI) model. Results suggested the stability and durability of such devices require significant improvements on the microcapsule polymer chemistry to withstand biological impediments encountered in the human GI tract.

Original article published in *Journal of Microencapsulation*. 22(5): 539-547 (2005)

### 3.1 Abstract

Oral administration of microcapsules containing live bacterial cells has potential as an alternative therapy for several diseases. This article evaluates the suitability of the alginate-poly-L-lysine-alginate (APA) microcapsules for oral delivery of live bacterial cells, *in vitro*, using a dynamic simulated human gastro-intestinal (GI) model. Results showed that the APA microcapsules were morphologically stable in the simulated stomach conditions, but did not retain their structural integrity after a 3-day exposure in simulated human GI media. The microbial populations of the tested bacterial cells and the activities of the tested enzymes in the simulated human GI suspension were not substantially altered by the presence of the APA microcapsules, suggesting that there were no significant adverse effects of oral administration of the APA microcapsules on the flora of the human gastrointestinal tract. When the APA microcapsules containing *Lactobacillus plantarum* 80 (LP80) were subjected to the simulated gastric medium (pH $\leq$ 2.0), 80.0 % of the encapsulated cells remained viable after 5 min of incubation; however, the viability decreased considerably (8.3 %) after 15 min and dropped to 2.6 % after 30 min and lower than 0.2 % after 60 min, indicating the limitations of the currently obtainable APA membrane for oral delivery of live bacteria. Further *in vivo* studies are required before conclusions can be made concerning the inadequacy of APA microcapsules for oral delivery of live bacterial cells.

**Key words:** Alginate, artificial cells, live bacteria, microcapsules, oral delivery

### 3.2 Introduction

The use of live bacterial cells for therapeutic purposes has generated considerable attention and excitement among clinicians and health professionals<sup>354-356</sup>. A major limitation in the use of bacteria is the complexity in delivering products to the target tissues. Oral delivery may be the easiest method of administration, but the bacterial cells are primarily incapable of surviving their passage through the gastrointestinal (GI) tract<sup>357,358</sup>. A potential solution is the use of the encapsulation process to provide a physical barrier against adverse environmental conditions. Previous studies have shown that oral administration of the

artificial cells containing bacteria has potential as an alternative therapy for several diseases<sup>359,360</sup>. However, the capability of APA microcapsules to resist degradation during human GI transit and to protect the enclosed cells are yet unknown. The present study examines the suitability of APA microcapsules for GI applications, *in vitro*, using a dynamic simulated human GI model and investigates the encapsulation of live *Lactobacillus plantarum* 80 as well as their survivability in simulated gastric solution.

### 3.3 Methods and materials

Sodium alginate (low viscosity) and poly-L-lysine (PLL) (*M<sub>v</sub>* 27,400) were purchased from Sigma-Aldrich. *Lactobacillus plantarum* (LP80) containing the bile salt hydrolase (BSH) multicopy plasmid (pCBH1) were obtained from LabMET, University of Gent, Belgium. All other reagents and solvents were of reagent grade and used as received without further purification.

#### 3.3.1 Preparation of the microcapsules

The APA microcapsules were prepared according to the standard protocol<sup>361</sup> with slight modifications. A Na-alginate solution (1.5 %, w/v) was extruded into a stirred CaCl<sub>2</sub> solution (0.1M) using an Encapsulator (Inotech Corp.). The rigid Ca-alginate beads formed were then immersed in a PLL solution (0.1 %, w/v) for 10 min, and subsequently coated by another Na-alginate solution (0.05 %, w/v) for 10 min. The resulting APA microcapsules were washed and subjected to testing.

#### 3.3.2 Preparation of the microcapsules containing *Lactobacillus plantarum* (LP80)

The LP80-encapsulated beads were made based on our earlier report<sup>360</sup> with a few modifications. BSH isogenic *Lactobacillus plantarum* 80 (pCBH1) were grown at 37 °C in MRS broth supplemented with 100 µg/mL erythromycin. After 10 min of a centrifugation at 10 000xg, bacterial pellets (0.94 g cell wet weight) were washed, suspended in 5 mL of physiological solution (PS) and mixed with 45 mL of sterile alginate solution, giving the final alginate concentration of 1.5 % (w/v) and cell density of 3.22x10<sup>8</sup> CFU/mL. The subsequent encapsulation, PLL and alginate coating, were performed as described above. The preparation

procedure was carried out in a biological containment hood. All solutions used were either 0.22  $\mu\text{m}$  filtered or autoclaved to ensure sterility.

### **3.3.3 Dynamic simulated human gastro-intestinal model set-up**

The human GI conditions used in this study were simulated *in vitro* by means of a series of bioreactors. As seen in figure 3.1, each reactor corresponds to a specific stage of digestion. Specifically, vessel 1 represents the stomach, vessel 2 the small intestine, vessel 3, 4 and 5 represent the ascending colon, the transit colon, and the descending colon, respectively. Human fecal slurries containing normal human GI bacterial cells were inoculated into the large simulated colon (vessel 3, 4 and 5). The whole system was then maintained under anaerobic conditions by flushing the headspace of each vessel with  $\text{N}_2$  and the temperature was kept constant at 37 °C. A carbohydrate-based diet, composed of arabinogalactan 1.0 g/L, pectin 2.0 g/L, xylan 1.0 g/L, starch 3.0 g/L, glucose 0.4 g/L, yeast extract 3.0 g/L, peptone 1.0 g/L, mucin 4.0 g/L and cystein 0.5 g/L, was fed to the first vessel 3 times a day. After feeding, acidification of the stomach (0.2N HCl) occurred, followed by neutralization (0.2N NaOH) and addition of simulated pancreatic juice (12 g/L  $\text{NaHCO}_3$ , 6 g/L oxgal and 0.9 g/L pancreatin in autoclaved water) to the second vessel. The suspension was then transferred to the simulated ascending colon, the transit colon, and the descending colon for further interactions, and finally excreted as effluent. The entire process, including pH conditions, fluid volume and retention time at each stage was simulated and under computer control.

### **3.3.4 Resistance of the microcapsules to the simulated media of the GI model**

Plain APA microcapsules were exposed to the simulated GI fluids for a time period based on the estimated maximum period of human GI transit (table 3.1). Microcapsule samples (~ 250 beads) were taken at varied stages of digestion for physical observation under a microscope (LOMO, PC). Microphotographs were taken as records using a digital camera (Canon Power shot G2).

### 3.3.5 Effects of the APA microcapsules on microbial population and enzymatic activities in simulated GI media

The APA microcapsules (0.8 g) were put in a sterile beaker containing 20 mL of the simulated stomach medium from the simulated GI model. After pre-designated periods of incubation at 37 °C (table 3.1), the medium was replaced by the suspension from the successive vessel in the GI model. Incubation medium was withdrawn right before replacing the medium and used for bacterial enumeration and enzymatic activity determination as described below. The simulated GI media containing no microcapsules served as the control.

**Bacteriological assays:** Samples of simulated GI media from the incubation beaker were serially diluted by physiological solution and plated (0.1 mL) in triplicate on selective agar media to enumerate specific fecal marker microorganisms, enterococcus sp., staphylococcus sp., and *lactobacillus sp.*. The plating media and incubation conditions used are listed in Table 3.2.

**Enzymatic assays:** The enzymatic activities of  $\beta$ -galactosidase,  $\beta$ -glucosidase,  $\beta$ -glucuronidase,  $\alpha$ -galactosidase and  $\alpha$ -glucosidase in media were analysed by a modified literature method (Berg *et al* 1978). One milliliter of samples was centrifuged at 10 000xg for 10 min. The cell free supernatant (100  $\mu$ l) was pipetted into a 96-well plate, followed by the addition of a substrate solution (100  $\mu$ l, 5.0 mmol/L in 0.1 mmol/L phosphate buffer, pH 6.5). The absorbance at 405 nm was recorded by a  $\mu$ Quant multi-plate reader (Bio-Tek Instruments) before and after 30 min of incubation at 37 °C. The enzymatic activity was expressed in  $\mu$ mol p-nitrophenol released/(L·min) or unit released (U/L·min) and can be calculated as follows:

$$\text{Activities (U/L}\cdot\text{min)}=(A_{30}-A_0)/a*10\ 000/30=(A_{30}-A_0)/a *333$$

Where  $A_0$  and  $A_{30}$  are the absorbances at time 0 and time 30 min, respectively, and  $a$  is the slope of the p-nitrophenol standard curve.

### 3.3.6 Survival of the encapsulated cells in simulated gastric medium

The *LP80* encapsulated beads (0.1 g) were exposed in 1.0 mL simulated gastric medium from vessel 1 in the GI model (pH 2.0). After incubated in an Environ Shaker (Lab-Line) at 37 °C, 175 rpm, for a designated period of time, the beads were manually ruptured using a tissue pestle. The number of live *LP80* cells was determined by plate count on

selective MRS agar plates, supplemented with 100 µg/mL of erythromycin. Free *LP80* cells and PS served as a positive and negative control respectively.

### **3.4 Results and discussion**

#### **3.4.1 Resistance of the microcapsules to the simulated human GI conditions**

To evaluate the suitability of the microcapsules for oral delivery, it is important to understand their behaviour under conditions that represent the digestion course. Rather than using the acid-base buffer simulation system, a dynamic computer-controlled simulated human gastro-intestinal model was employed. This unique apparatus provides simulated GI environments relatively close to the actual human situation. Microcapsules were exposed to the simulated GI fluids from different vessels for a time period based on the estimated maximum period of human GI transit (table 3.1), as to mimic the experience along the GI course including pH fluctuation, enzymatic stress and GI micro-flora effects. Figure 3.2 depicts the physical changes of the APA microcapsules before and after exposure to the simulated GI medium at different phases of digestion. The original APA microcapsules were spherical and uniform in shape with a smooth surface, as shown in Figure 3.2a. They remained intact during the 2 h of incubation in the simulated stomach ( $\text{pH} \leq 2.0$ ) (figure 3.2b) and appeared weak when leaving the simulated small intestine ( $\text{pH} > 6.8$ ) 4 h later (figure 3.2c). At the phase representing the transit colon, the microcapsule beads were found still intact, though forming a ghost like structure (figure 3.2d). The integrity of the microcapsules continued to decline as they passed through the colon and after 72 h of interaction with the simulated GI media, only traces of the microcapsules were detected at the descending colon (figure 3.2e). These results showed that the APA microcapsules maintained physical stability in the acidic environment and gradually lost their structural integrity during GI transit.

#### **3.4.2 Effects of APA microcapsules on flora and enzymatic activities in the simulated GI model**

Another important factor in oral administration of microcapsules is that they should not disturb the natural microflora of the GI tract; thus, the effects of microcapsules on the microbes in the simulated GI model were investigated. Since the simulated GI model is a

dynamic system, static experiments were performed to maximize the effects. It was found that there were no significant differences ( $p>0.05$ ) between the APA microcapsules and the control on the microbial populations of the three tested bacteria, *enterococcus sp.*, *staphylococcus sp.*, and *lactobacillus sp.*, in the simulated ascending and descending colon (figure 3.3). Similarly, the five tested enzymatic activities in the simulated GI suspension representing the small and large intestine were not altered by the presence of the microcapsules (figure 3.4). These results indicated that there were no significant adverse effects of oral administration of the APA microcapsules on the flora of the human GI tract.

### **3.4.3 Survival of the encapsulated cells in the simulated gastric medium**

Since therapeutic microorganisms are usually required at a target site in the intestine, it is essential that they withstand the host's natural barriers against ingested bacteria. The acidity of the stomach forms a major barrier when applying live bacteria by oral administration. To assess the protective capability of the APA microcapsules against the harsh gastric environment, live *Lactobacillus plantarum* 80 (*LP80*) were encapsulated. After exposure to the simulated gastric medium ( $\text{pH}\leq 2.0$ ) for 60 min, no severe morphological disintegration of the *LP80*-loaded APA microcapsules was found (data not shown). After 5 min of exposure, more than 80 % of the encapsulated *LP80* cells remained viable (figure 3.5); however, cell viable counts decreased considerably after a 15-min incubation, as only 8.3 % of these cells survived. After 30 min, the viability of the encapsulated cells dropped to 2.6 % and to lower than 0.2 % after 60 min. These results suggested that the APA system was effective but not completely adequate for protecting the enclosed bacterial cells for oral delivery applications. Further *in vivo* studies in experimental animal models are required before conclusions can be made concerning the inadequacy of APA microcapsule for oral delivery of live bacterial cells.

## **3.5 Conclusions**

A dynamic simulated human gastro-intestinal model was employed to evaluate the GI stability of the APA membrane. Live *Lactobacillus plantarum* 80 (*pCBH1*) cells were encapsulated in this system to investigate its protective capability for potential GI applications.

Results showed that the APA microcapsules maintained morphological stability in the acidic conditions; however they did not uphold their structural integrity after a 3-day exposure in the simulated GI media. The microbial populations of the 3 tested types of bacteria and the activities of the 5 tested enzymes in the suspension of the simulated GI model were not substantially altered by the presence of the APA microcapsules, suggesting that there were no significant adverse effects of oral administration of the APA microcapsules on the flora of the human GI tract. When the *LP80* encapsulated microcapsules were subjected to the simulated gastric medium ( $\text{pH} \leq 2.0$ ), 80.0 % of the encapsulated cells remained viable after 5 min incubation. However, the viability decreased considerably (8.3 %) after 15 min, and dropped to 2.6 % after 30 min and to less than 0.2 % after 60 min, indicating that encapsulation by the APA system was effective but may not be able to provide adequate protection for the enclosed bacterial cells for oral delivery applications. Further *in vivo* studies are required before the inadequacy of APA microcapsules for oral delivery of live bacterial cells can be concluded.

### **3.6 Acknowledgements**

This work was supported by the research grant from Dairy Farmers of Canada (DFC). Chen acknowledges the postgraduate scholarship from Natural Science and Engineering Research Council (NSERC) of Canada.

Table 3.1. Exposure duration and morphological changes of the alginate-poly-L-lysine-alginate (APA) microcapsules to the media of the simulated human gastro-intestinal model

GI Compartments	Stomach	Small Intestine	Ascend. Colon	Transverse Colon	Descend. Colon
Expos. Time (h)	2	4	18	24	24
Microcapsule Morphology	Intact	Intact	Ghost like-intact	Ghost like-intact	Poorly defined

Table 3.2. Media and incubation conditions used for microbial enumeration of the simulated GI mode

Microbial group	Medium	Incubation conditions
<i>Enterococcus sp.</i>	Enterococcus agar	Aerobic, 37°C, 48 h
<i>Staphylococcus sp.</i>	Mannitol salt agar	Aerobic, 37 °C, 48 h
<i>Lactobacillus sp.</i>	Rogosa agar	Anaerobic, 37°C, 72 h

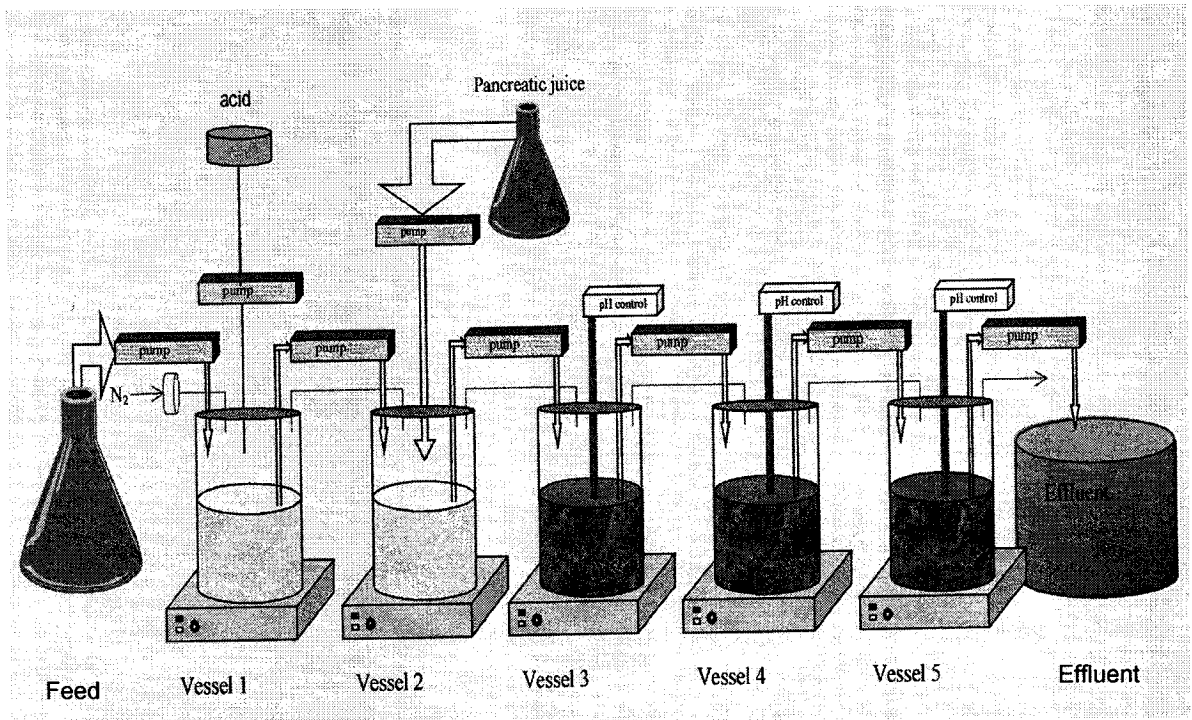


Figure 3.1. Schematic representation of the dynamic simulated human gastrointestinal (GI) model. Vessel 1: stomach; Vessel 2: small intestine; Vessel 3: ascending colon; Vessel 4: transverse colon; and Vessel 5: descending colon.

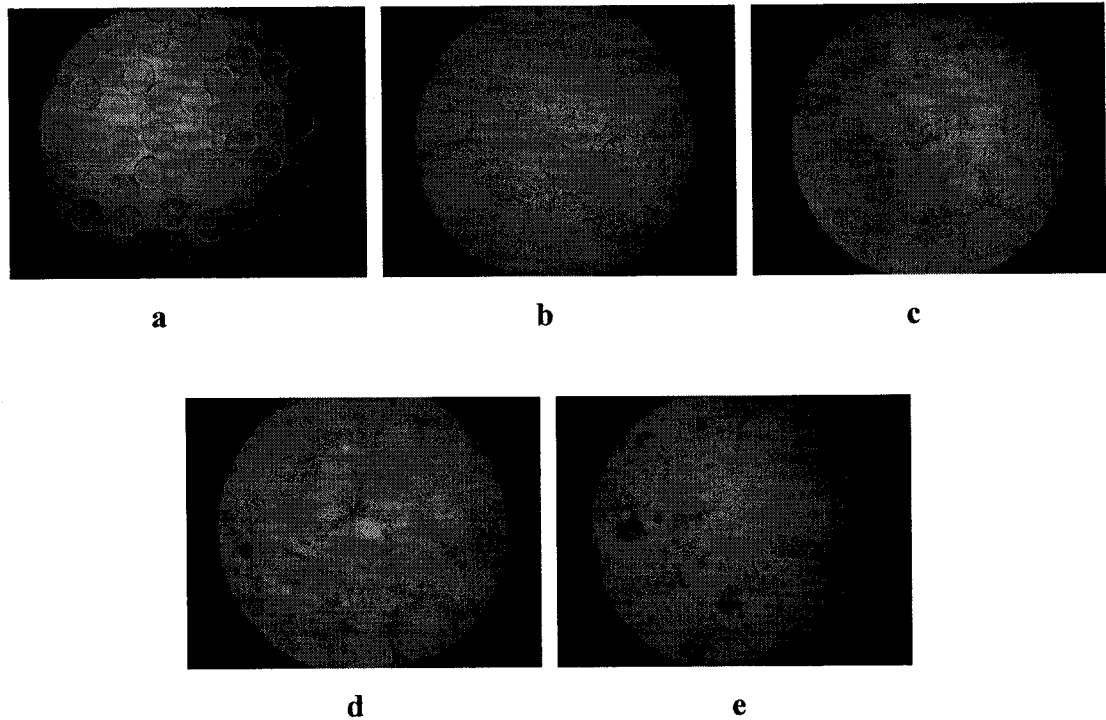


Figure 3.2. Microphotographs of the APA microcapsules. a, freshly prepared; b-e, during transit in the simulated human GI model: b, 2 h of exposure (in the simulated stomach); c, 6 h of exposure (2 h in the simulated stomach and 4 h in the simulated small intestine); d, 48 h of exposure (2 h in the simulated stomach, 4 h in the simulated small intestine, 18 h in the simulated ascending colon and 24 h in the simulated transit colon); and e, 72 h of exposure (2 h in the simulated stomach, 4 h in the simulated small intestine, 18 h in the simulated ascending colon, 24 h in the simulated transit colon and 24 h in the simulated descending colon) (original magnification: 35x).

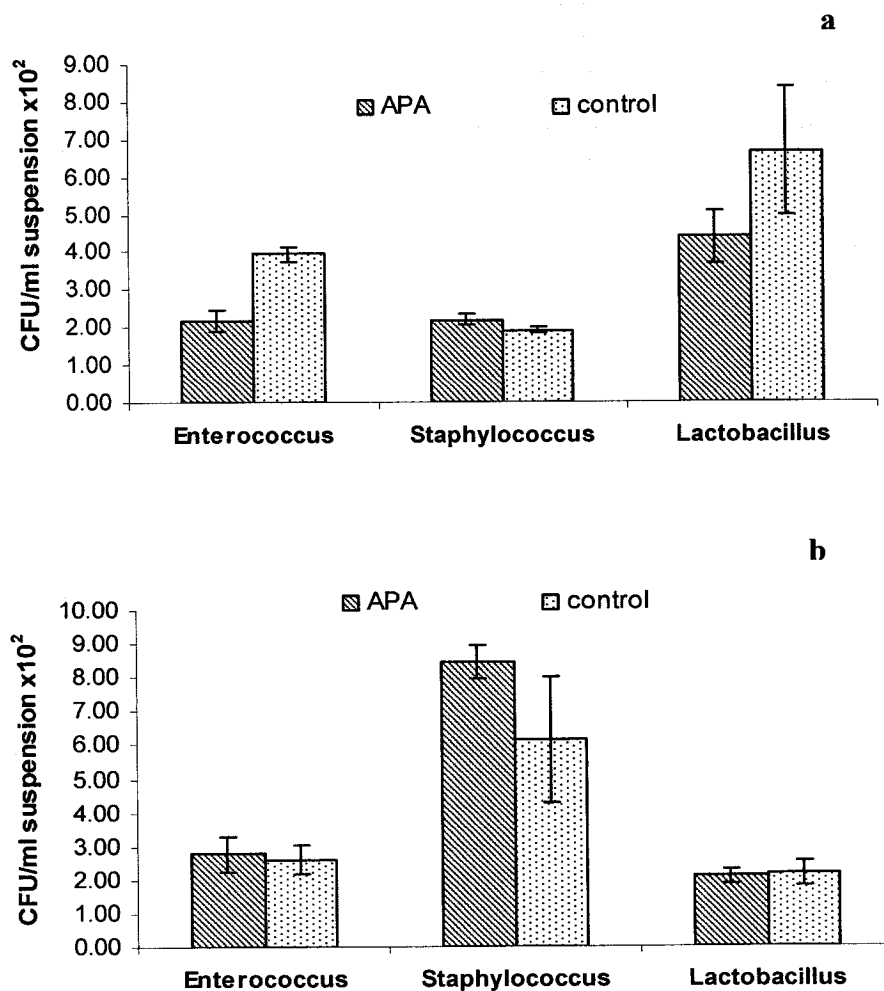


Figure 3.3. Effects of the presence of the APA microcapsules on the microbial populations of *enterococcus sp.*, *staphylococcus sp.*, and *lactobacillus sp.* in the simulated ascending colon (a) and descending colon (b) of the simulated human GI model.

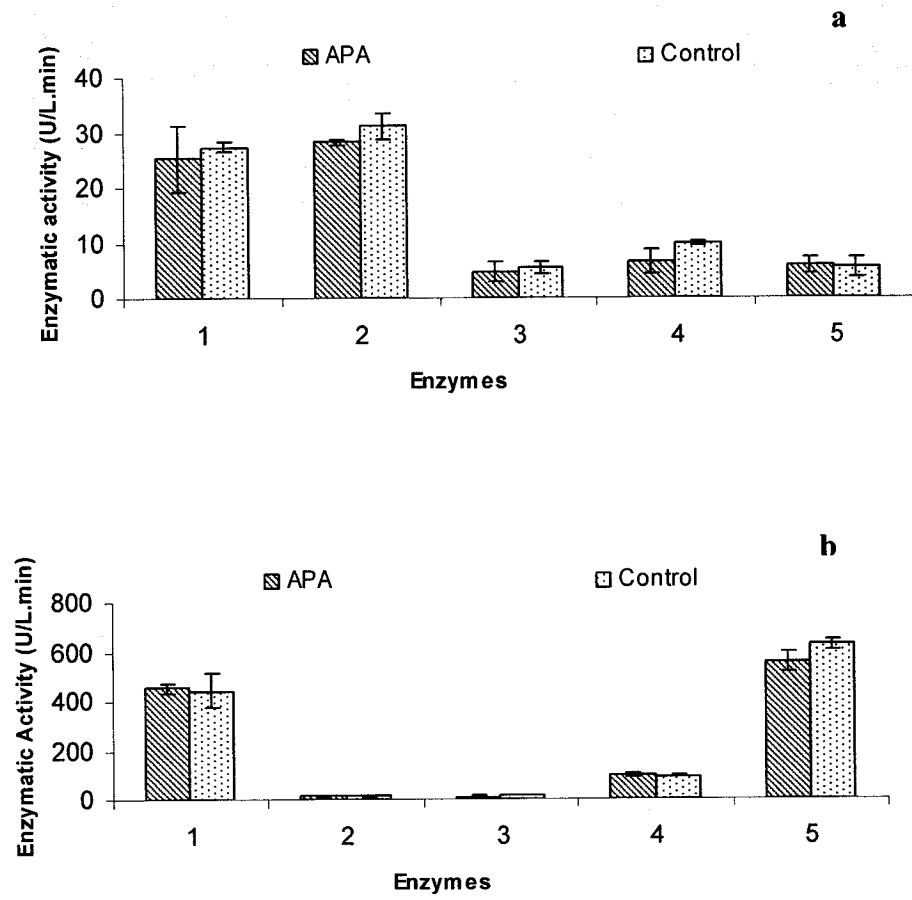


Figure 3.4. Effects of the presence of the APA microcapsules on enzymatic activities of the simulated small intestine (a) and transit colon (b) medium in the simulated human GI model. Type of enzymes: 1,  $\beta$ -galactosidase; 2,  $\beta$ -glucosidase; 3,  $\beta$ -glucuronidase; 4,  $\alpha$ -galactosidase; and 5,  $\alpha$ -glucosidase.

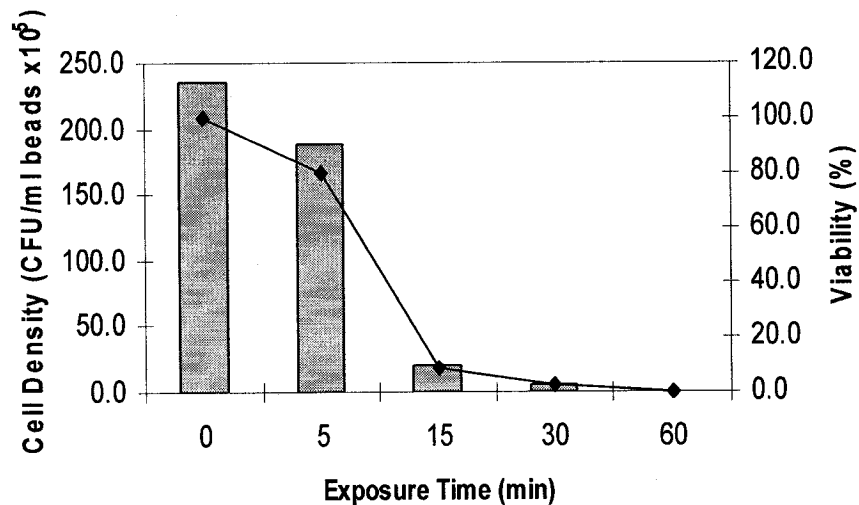


Figure 3.5. Viability of encapsulated *LP80* bacteria in simulated gastric medium. Nutrition for the simulated human GI model (1 mL, 37 °C, pH $\leq$ 2.0) was added to the micro-tube containing 0.1 mL of *LP80* encapsulated APA microcapsules and incubated at 37 °C, 175 rpm, for a designated period of time. After the beads were manually ruptured using a tissue pestle, the live *LP80* cells were determined by plate count on selective MRS agar plates in duplicate. Free *LP80* cells and PS served as a positive and negative control, respectively. Values of cell density represent an average of 2 replicates. Viability (%) was defined as cell density at different times in relation to that at time 0.

**Preparation and characterization of novel polymeric microcapsules for live cell encapsulation and therapy**

*Hongmei Chen, Wei Ouyang, Mitchell Jones, Terrence Metz, Christopher Martoni, Tasima Haque, Rebecca Cohen, Bisi Lawuyi and Satya Prakash\**

*Biomedical Technology and Cell Therapy Research Laboratory  
Department of Biomedical Engineering and Physiology, Artificial Cells and Organs Research  
Centre, Faculty of Medicine, McGill University, Montreal, Quebec, H3A 2B4 Canada.*

\*Corresponding author: Tel: 514 398-3676; Fax: 514 398-7461;  
Email: [satya.prakash@mcgill.ca](mailto:satya.prakash@mcgill.ca)

---

**Preface:** To improve mechanical stability and membrane resistance of microcapsules, exogeneous cross-linking in the membrane structure was introduced using a natural derived cross-linker genipin. This paper describes the membrane design and the preparation of the novel GCAC microcapsules. It also provides a preliminary evaluation of the feasibility of using this membrane for live cell encapsulation.

Original article published in *Cell Biochemistry & Biophysics* (in press)

## 4.1 Abstract

This article describes the preparation and *in vitro* characterization of novel genipin cross-linked alginate-chitosan (GCAC) microcapsules that have potential for live cell therapy applications. This microcapsule system, consisted of an alginate core with a covalently cross-linked chitosan membrane, was formed via ionotropic gelation between calcium ions and alginate, followed by chitosan coating by polyelectrolyte complexation and covalent cross-linking of chitosan by naturally derived genipin. Results showed that using this design concept and the three-step procedure, spherical GCAC microcapsules with improved membrane strength, suppressed capsular swelling and suitable permeability can be prepared. The suitability of this novel membrane formulation for live cell encapsulation was evaluated, using bacterial *Lactobacillus plantarum* 80 (*pCBHI*) (*LP80*) and mammalian HepG2 as model cells. Results showed that capsular integrity and bacterial cell viability were sustained six months post-encapsulation, suggesting the feasibility of using this microcapsule formulation for live bacterial cell encapsulation. The metabolic activity of the encapsulated HepG2 was also investigated. Results suggested the potential capacity of this GCAC microcapsule in cell therapy; however, further research is required.

**Key Words:** microcapsule, genipin, alginate, chitosan, artificial cell, live bacterial cells

## 4.2 Introduction

Artificial cell microencapsulation technology<sup>5</sup>, in which bioactive materials are retained inside the capsules and isolated from the extra-cellular environment, has shown promise in treatment of a number of diseases<sup>19,22,62,70,80,89,362</sup>. This strategy potentially allows cell implantation without the need for immuno-suppression and enables the controlled and continuous delivery of biological products to the host, giving rise to a more physiological and effective concentration of the therapeutic products. The scope of this application has now been extended to the use of recombinant cells<sup>68</sup>. Alginate-poly-L-lysine-alginate (APA) microcapsule<sup>69</sup> has been the most widely-investigated formulation for live cell encapsulation. However, serious limitations regarding mechanical insufficiency and biocompatibility

problems arose over long-term *in vivo* applications<sup>27,115,156,171,172</sup>. The membrane instability caused the eruption of capsules yielding undesirable leakage of encapsulated cells. This could severely damage the entire process, giving rise to many safety concerns. Therefore, design of a more suitable microcapsule formulation is needed for live cell therapy.

As most synthetic polyelectrolyte materials exhibit a moderate level of cell cytotoxicity, naturally occurring materials constitute optimal polymers for live cell encapsulation. Alginate, a linear copolymer of (1–4)-linked  $\beta$ -D-mannuronic acid and  $\alpha$ -L-guluronic acid, is a naturally occurring polysaccharide extracted from brown seaweed. Due to its ease of operation, mild processing conditions and good biocompatibility, alginate has shown distinct advantages in the field of cell encapsulation and is usually used as an inner polyanionic polymer<sup>32,33</sup>. Chitosan, a linear polysaccharide of (1–4)-linked D-glucosamine and *N*-acetyl-D-glucosamine, is one of the few abundantly available and cationic polysaccharides obtained by alkaline deacetylation of chitin. Low toxicity, good biocompatibility, controllable biodegradability, coupled with wide applicability make chitosan a good candidate not only for conventional and novel drug delivery systems but also as a biologically active agent. Because of the high affinity of chitosan for cell membranes, it has been used as a coating agent for liposome formulations<sup>363</sup>. Recently, it has been identified as a suitable substrate for biomimetic polymers owing to its structure similar to the glycosaminoglycans found in native tissue<sup>364</sup>. In the field of cell encapsulation, chitosan was used as an alternative to PLL in microcapsule membrane formation<sup>45,48,51,167,213,225</sup>.

To further increase capsular strength and resistance, chitosan can be chemically cross-linked by a bi-functional reagent, usually glutaraldehyde (GA)<sup>51</sup> or epoxy compounds (DEO)<sup>278</sup>, leading to the formation of a three-dimensional network in the capsular structure. However, these synthetic cross-linkers have a recognized disadvantage of potential cytotoxic effects and are not preferable in case of live cell encapsulation<sup>278</sup>. Genipin is an iridoid glucoside extracted from Gardenia fruits<sup>282</sup>. Earlier it has been reported that genipin can be used for cross-linking<sup>296</sup>, tissue fixation<sup>297</sup>, membrane reinforcements<sup>298,299</sup> and tissue engineering<sup>300-303</sup>. The objective of present study is to prepare and characterize a novel alginate-chitosan microcapsule formulation using genipin cross-linking and to test its feasibility for live cell encapsulation and therapy.

## 4.3 Materials and methods

### 4.3.1 Chemicals

Sodium alginate (low viscosity), trypan blue solution (0.4 %), MTT (thiazolyl blue) and sodium citrate were obtained from Sigma-Chemicals (St. Louis MO). Chitosan (low viscosity, 73.5 % deacetylation) and genipin were purchased from Wako BioProducts, USA. All other reagents and solvents were of reagent grade and used as received without further purification.

### 4.3.2 Bacterial strain, cell line and growth conditions

The bacterial strain used in this study was bile salt hydrolytic (BSH) isogenic *Lactobacillus plantarum* 80 (*pCBH1*) (*LP80*) obtained from LabMET, University of Gent, Belgium. This strain was genetically engineered and carries the multicopy plasmid *pCBH1* carrying the *L. plantarum* 80 chromosomal *bsh* gene and an erythromycin resistance gene, the former of which can overproduce the enzyme of bile acid hydrolase with noted potential in cholesterol lowering<sup>365</sup>. The stock cultures of *LP80* were kept in MRS broth containing 20 % (v/v) glycerol at -86 °C. The microorganisms were revived twice in MRS broth, followed by sub-culture of 1 % inoculum anaerobically in MRS broth supplemented with 100 µg/mL of erythromycin at 37°C.

The cell line HepG2 used in the present study was epithelial hepatocellular carcinoma tissues derived from human organisms and purchased from ATCC. The cells were routinely sub-cultured in MEM (minimum essential eagle media) supplemented with 10 % FBS and 1 % penicillin-streptomycin (obtained from Sigma Aldrich) at 37°C in a Sanyo MCO-18M multi-gas incubator with an air atmosphere of 5 % CO<sub>2</sub>. The cells were detached and sub-cultured every 10 days using Trypsin 0.53mM/EDTA (purchased from ATCC).

### 4.3.3 Preparation of genipin cross-linked alginate-chitosan (GCAC) microcapsules

#### a) Preparation of plain GCAC microcapsule

Ca-alginate beads were generated using an Encapsulator (Inotech. Corp. USA) which dispensed droplets of Na-alginate solution (1.5 % wt/v) into a stirred solution of 0.1M CaCl<sub>2</sub>,

where a gelation process took place. The alginate beads obtained were exposed to a chitosan solution (low viscosity, 2 % wt/v) containing 0.1M CaCl<sub>2</sub> for 30 min of coating, washed and then immersed in a genipin solution (5 mg/mL) for cross-linking for 48 h. The resulting microcapsules were washed and collected.

#### **b) Preparation of GCAC microcapsule containing LP 80 cells**

BSH isogenic *Lactobacillus plantarum* 80 (*pCBHI*) cells were grown for 1.5 days in broth and isolated from cultures after 10 min of a centrifugation at 10 000 g. The collected cell pellets (1.28 g cell wet weight) were washed with physiological saline (PS), pooled and mixed carefully with 50ml sterile alginate solution (1.5 % wt/v). The subsequent microencapsulation, coating and cross-linking reactions were performed using similar procedures to the plain microcapsules as described above, except that the cross-linking reaction was carried out at 4°C to maintain low level of metabolism. Finally, the microcapsules were rinsed with PS five times to remove excess genipin and stored at 4°C in either PS or a minimal broth media (50 % MRS broth and 50 % PS) to maintain low metabolism of the microorganisms. The preparation procedures including microencapsulation, coating and washing were carried out in a Microzone Biological Containment Hood (Microzone Corporation ON, Canada), and all solutions used were either 0.22 µm filtered or autoclaved to ensure sterility.

#### **c) Preparation of GCAC microcapsule containing HepG2 cells**

HepG2 cells were encapsulated in alginate microcapsules using previously established procedures<sup>167</sup>. Briefly, HepG2 cells were trypsinized and then centrifuged at 1000 rpm for 10 min at 20°C. The media was decanted and the cells were mixed with 0.5 mL of fresh media and 30 ± 10 mL of sterile filtered 1.5 % alginate solution to attain a concentration of 1.5x10<sup>6</sup> cells/mL. The encapsulation process and chitosan coating followed the same procedure as aforementioned. The genipin cross-linking was performed for either 2 h or 12 h at 37°C to produce the GCAC capsules. The microcapsules obtained were stored in complete growth media used for culturing free cells at 37°C and 5 % CO<sub>2</sub>. All the procedure was performed under sterile conditions and all solutions were either autoclaved or 0.22µm sterile filtered prior to usage.

#### **4.3.4 Visualization of the GCAC microcapsule membrane using confocal laser scanning microscopy (CLSM)**

The interior and membrane of the GCAC microcapsules were investigated using a Laser Scanning Confocal Imaging System (LSM 510, Carl Zeiss, Jena, Germany) equipped with a Zeiss Axiovert 100M microscope. For image acquisition, the microcapsules in storage solution (deionized H<sub>2</sub>O) were directly placed in a chambered coverglass system (Lab-Tek). A 488 nm argon laser was used in the single green fluorescence mode and the fluorescence was detected with the filter block BP500-550IR. The focal planes were set at the equatorial sections of the microcapsules. An average of 8 consecutive scans of a single field was taken. The microcapsule membrane was also imaged by performing Z-stack scanning of total 174.4 µm in Z-direction and reconstructed in a 3D projection.

#### **4.3.5 Method of testing viability of encapsulated *LP80* cells**

To determine the viability of the encapsulated bacteria, the *LP80* containing microcapsules (0.1 mL) were mechanically ruptured using a sterile tissue pestle. Aliquots of bacteria suspension from 10-fold serial dilutions with autoclaved physiological saline were plated in selective MRS agar plates supplemented with 100 µg/mL of erythromycin. The colonies formed were enumerated after 3-day incubation at 37 °C in an anaerobic condition. Free *LP80* cells and plain microcapsules served as positive and negative control, respectively. Triplicate experiments were performed.

#### **4.3.6 Identification of viable encapsulated HepG2 cells by trypan blue exclusion assay**

The GCAC microcapsules containing HepG2 cells (0.1 mL) were first subjected to citrate treatment (5 %, wt/v), then exposed to trypsin solution facilitating the cell detachment from the membrane, followed by extruding through a 27G needle. The contents were stirred with a micropipette and dyed with trypan blue solution (1:1 by volume). The viable and dead cells shown as bright and dark dots respectively were observed under an inverted light microscope (LOMO PC).

#### **4.3.7 Method of testing metabolic activity of encapsulated HepG2 cells**

The metabolic activity of the HepG2 cells within the GCAC microcapsules was determined using an MTT calorimetric assay. For this, approximately  $15 \pm 2$  capsules were incubated with 100  $\mu$ l of media and 25  $\mu$ l of an MTT solution (1 % MTT in PBS) for 24 h in 96 well plates. The media and MTT solution were removed from the wells and the microcapsules were washed once with physiological saline. The formazan crystals formed by the conversion of MTT were dissolved in 100  $\mu$ l of DMSO. After 30 min of incubation, the absorbance at 570 nm was recorded by a  $\mu$ Quant Universal Microplate Spectrophotometer (Bio-Tek Instruments, Inc.). Plain microcapsules without HepG2 cells were used as references. Results were expressed as mean  $\pm$  standard deviation from triplicate experiments, and compared with the metabolic activity of HepG2 cells encapsulated in uncross-linked alginate-chitosan (AC) microcapsules.

#### 4.4 Results and discussion

In recent years, there has been growing interests of using genipin, a chemical naturally derived from the gardenia fruit, as a new cross-linking reagent in biomedical research<sup>245,298,302,303</sup>. The findings that this substance can effectively cross-link polyamines with substantially less cytotoxicity<sup>296</sup> prompted us to design and formulate new microcapsules with genipin covalently cross-linked membrane. Figure 4.1-A shows the schematic diagrams for the genipin cross-linked alginate-chitosan (GCAC) microcapsule structure. The hypothesis is that chitosan will bind to the calcium-alginate gels via electrostatic interactions between the unused carboxyl groups in alginate and the primary amine groups in chitosan. This alginate-chitosan (AC) complex was considered to be irreversible and stronger than the binding of alginate and poly-L-lysine<sup>162</sup>. Genipin, an iridoid glucoside, can react with nucleophilic reagents such as chitosan via attacks by amine groups in the chitosan molecules<sup>291</sup> and form a denser chitosan coating on the microcapsule membrane. It was found that the reaction between chitosan and genipin generated fluorescent products<sup>239,306</sup>, which made the cross-linked chitosan membrane clearly visualized under CLSM. As can be seen in Fig. 4.1-B, the alginate cores were shown as the black interior of the microcapsules, while the genipin cross-linked chitosan coating was clearly identified by the appearance of distinguishing bright circles, each circumscribing an alginate core. Figure 4.1-C further illustrates the shell-like

fluorescent genipin cross-linked chitosan membrane. These findings strongly confirmed the proposed capsular design and structure. A three-step preparation procedure was established to make the GCAC microcapsules, which involved the formation of calcium-alginate beads by ionotropic gelation, coating of chitosan via polyelectrolyte complexation, and the subsequent chitosan cross-linking by genipin (Fig. 4.2). The resulting microcapsules were found spherical in shape with high homogeneity ( $450 \pm 10 \mu\text{m}$  in diameter) and in a shade of blue color (Fig. 4.3-A). The color change was attributed to the establishment of chitosan derivatives produced by the cross-linking reaction of genipin with the remaining amine groups in the polymeric chains of chitosan<sup>291</sup>. It was found that the capsular swelling in water at a wide range of pH and in PS was substantially suppressed (swelling ratio < 10 %, data not shown). Moreover, the GCAC microcapsules exhibited strong resistance to chelating disintegration in phosphate buffered saline (PBS) or sodium citrate. As illustrated in Figure 4.3-B, after a week of incubation in PBS, a clear membrane was seen on the margin of the spherical GCAC bead, enclosing the gel-like alginate core, suggesting the proposed membrane structure for the GCAC microcapsules. These results indicated considerable improvement on microcapsule membrane stability by genipin cross-linking over the non cross-linked counterparts described elsewhere<sup>50,234,235,366</sup>.

To evaluate the suitability of this new microcapsule formulation for live cell encapsulation with potentials in therapy, bacteria *Lactobacillus plantarum* 80 (*pCBH1*) (*LP80*) and mammalian HepG2 cells, which have shown noted potential in cholesterol lowering<sup>365</sup> and liver transplantation<sup>167</sup>, respectively, were selected to be encapsulated and examined. Morphologically, microcapsules containing *LP80* bacterial cells were not different from the cell free beads except for the apparent color change, ranging from milky white (AC beads) to grey-blue (GCAC beads) depending on the degree of cross-linking. The physical integrity and morphological stability of the *LP80* loaded GCAC microcapsules were maintained more than 6-month post-encapsulation (Fig.4.4), which may be attributed to the formation of strong cross-linked membranes. On the other hand, HepG2 cells were also successfully encapsulated in the GCAC beads. As can be seen from Figure 4.5-A, the morphology of the GCAC microcapsules was not affected by the presence of HepG2 cells and the microcapsule integrity was sustained during storage.

As it is important to maintain the viability of the encapsulated cells for therapy, we examined the viable counts of the encapsulated *LP80* after 6 months of storage at 4 °C. High *LP80* cell viability, 9.03 log CFU/mL beads, was achieved for the GCAC microcapsules stored in medium with 50 % broth. Although stocking encapsulated *LP80* in PS without nutrient supply caused a reduction in cell viability, a considerable number of viable cells (5.38 log CFU/mL beads) were preserved 6 months post-encapsulation. In contrast, free *LP80* did not survive under similar storage conditions (data not shown). These data demonstrated that *LP80* cells could be encapsulated by the established preparation procedure and that the microencapsulation by GCAC chemistry effectively protected the live microorganisms against death during storage. It could be inferred that the activity of the encapsulated *LP80* cells was not altered during storage. Furthermore, the apparent increased survival of the encapsulated *LP80* bacteria over the free cells during storage suggested that the GCAC microcapsule formulation provided favorable microenvironments for cell proliferation. It is known that cell-cell communication through the production of extra-cellular signals plays a role in the cell growth of *L. lactics*<sup>367</sup>, which may differ in the confines of a microcapsule from in free bacteria suspension. More recently, chitosan was reported to possess biomimetic activity to enhance cell-biomaterial interactions by the covalent attachment of molecules with free carboxylic acids<sup>368</sup>. It might be possible that the genipin cross-linked alginate-chitosan chemistry favored the cell adhesion and cell-polymer interactions that promoted cell proliferation.

To investigate the survival of encapsulated mammalian cell, trypan blue exclusion assay, a generally accepted method, was performed. Since hepatocytes are anchorage-dependent cells, they tended to attach to the capsular matrix. To quantify the cell viability by trypan blue exclusion assay, the microcapsules must be destroyed to liberate the HepG2 cells, allowing for trypan blue to dye on the cells. However, the GCAC microcapsules were not readily dissolved in many reagents including sodium citrate, nor could it be completely ruptured by passing through a 27G needle. Though quantitative results were not obtainable using this approach, it appeared that a plentiful of the HepG2 cells inside the GCAC microcapsule debris remained viable after the process (Fig. 4.5-B). Moreover, the metabolic activity of the encapsulated HepG2 cells was measured using the tetrazolium assay (MTT) using known numbers of capsules. The transformation of MTT to insoluble purple formazan,

as a result of succinic dehydrogenase activity, was used as a quantitative estimate of total metabolic activity of the encapsulated cells<sup>369</sup>. Results shown in Figure 4.6 suggested that despite harsh conditions in chitosan coating (pH < 6) and prolonged cross-linking procedure, the microcapsules retained the metabolic activity of the encapsulated cells post-encapsulation, though a reduction in cellular activity was apparent in those capsules cross-linked for prolonged period of time. This could be due to the exposure to unfavorable conditions during genipin treatment. A previous study has suggested that by choosing appropriate genipin concentration, one could obtain suitable cross-linked gel structure without producing cytotoxicity on osteoblast proliferation<sup>294</sup>. We speculated that the survival and metabolic activity of the encapsulated mammalian cells could be optimized by varying reaction parameters during the cross-linking process in the GCAC microcapsule preparation.

#### 4.5 Conclusions

This article describes the utilization of naturally occurring genipin as a cross-linking agent to form novel alginate-chitosan microcapsules in a manner that facilitate live cell encapsulation for potentially therapeutic applications. The genipin cross-linked alginate-chitosan (GCAC) microcapsule was prepared and tested for encapsulating live bacteria and mammalian cells. Results show that *Lactobacillus plantarum* 80 (*pCBH1*) and HepG2 cells can be encapsulated in the GCAC microcapsules via the established three-step procedure. Microcapsule integrity was attained after exposure to physiological medium and during long-term storage. The encapsulated *LP80* maintained high survival six months post-encapsulation, demonstrating that the GCAC microcapsule chemistry offered a favorable microenvironment for bacteria growth and proliferation, probably due to encouraging cell-cell communication and cell-biopolymer interactions. Results also suggested that the HepG2 cells enclosed in the GCAC microcapsules remained viable to a certain extent, though apparent decrease in metabolic activity was found for the cells within the GCAC microcapsules cross-linked for prolonged period of time. This study introduces a novel microcapsule formulation composed of naturally occurring alginate, chitosan and genipin, and demonstrates its feasibility for cell encapsulation. Further research, however, is needed before full potentials of this formulation for live cell encapsulation and therapy applications can be estimated.

#### **4.6 Acknowledgements**

This work was supported by Natural Science & Engineering Research Council (NSERC) of Canada and Canadian Institutes of Health Research (CIHR). Chen acknowledges the post graduate scholarships from NSERC and Fonds Québécois de la Recherche sur la Nature et les Technologies (FQRNT). We also thank J Laliberte for her help with the CLSM study.

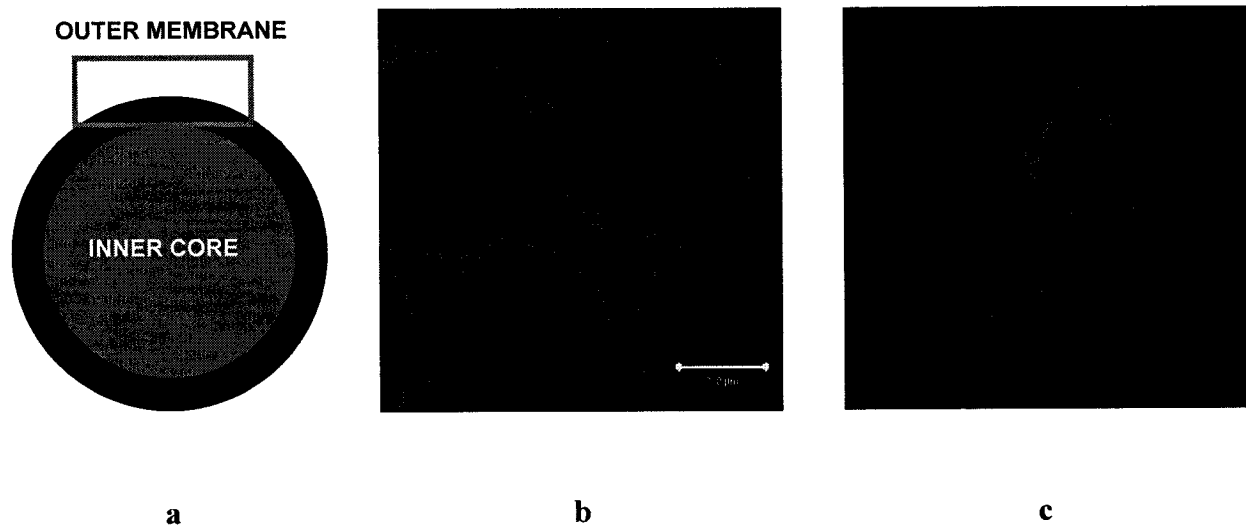


Figure 4.1. a, Schematic representation of the GCAC microcapsule structure; b-c, visualization of the GCAC microcapsule membrane by CLSM; b, Micrographs of an optical section taken through the equator of the microcapsules showing the fluorescent genipin cross-linked chitosan membrane; and c, 3D reconstruction of optical sections of the GCAC microcapsule showing the shell-like genipin cross-linked chitosan membrane. Bar represents 200  $\mu\text{m}$ .

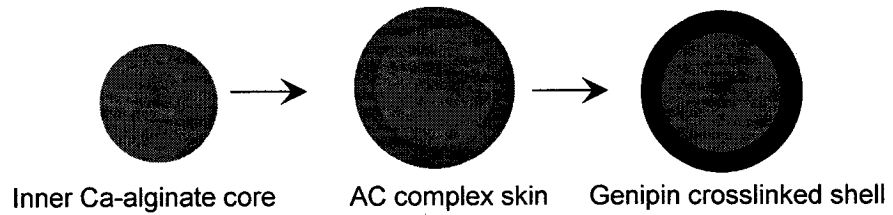
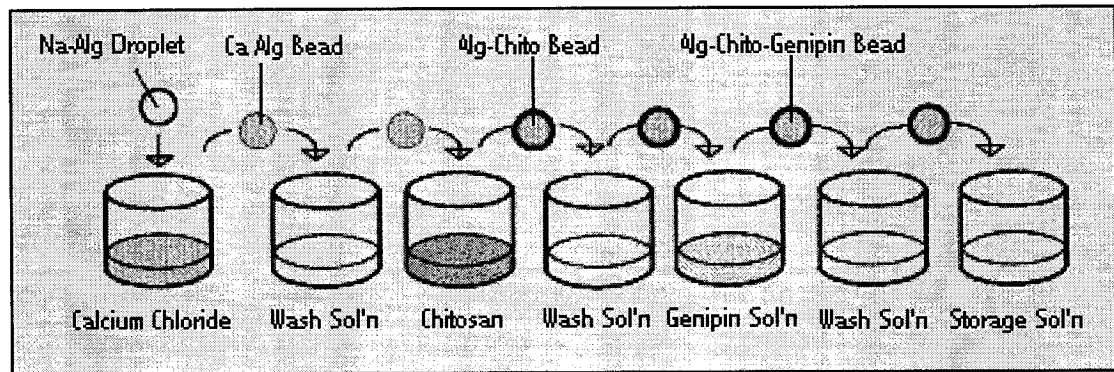


Figure 4.2. Preparation of the genipin crosslinked alginate-chitosan (GCAC) microcapsules.

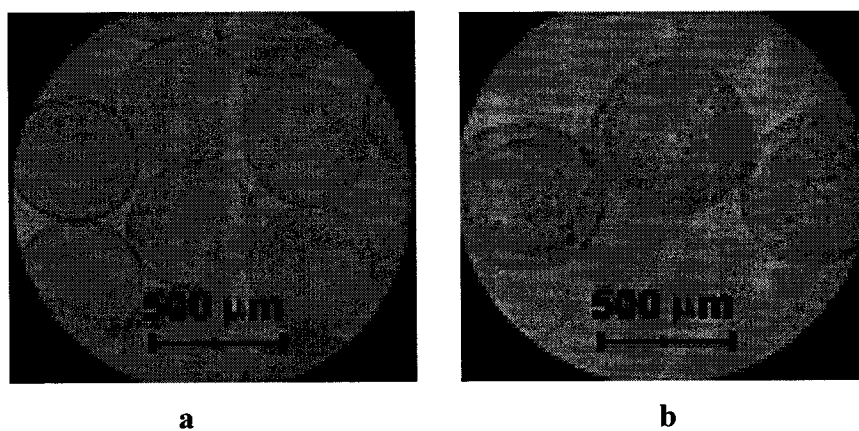
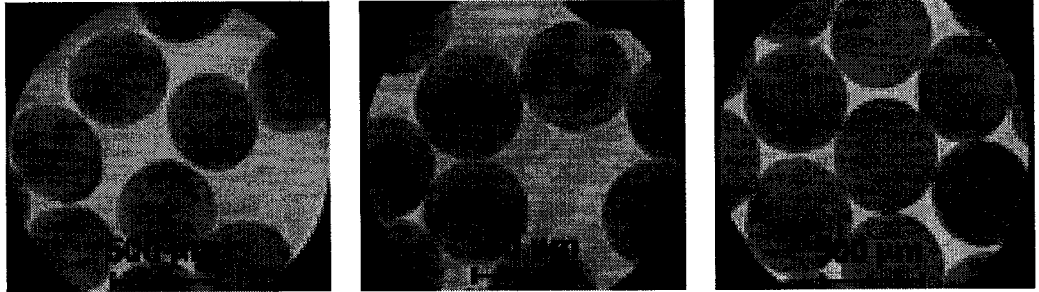


Figure 4.3. Optical photomicrographs of the GCAC microcapsules. a, freshly made; and b, after 1-week incubation in PBS.

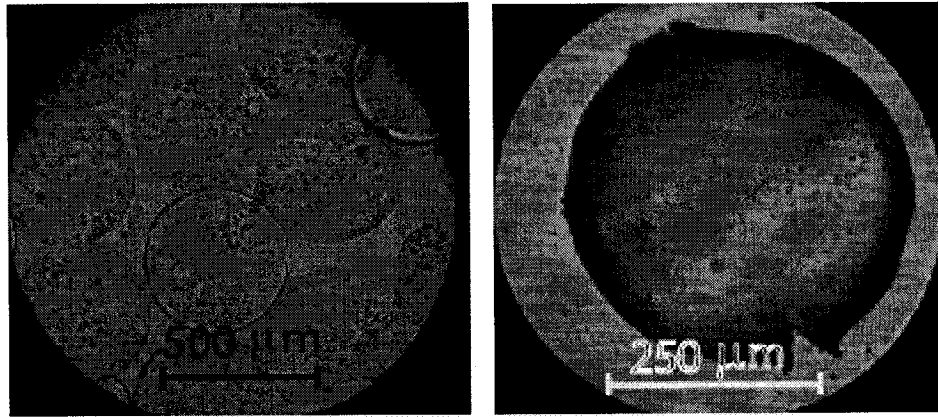


**a**

**b**

**c**

Figure 4.4. Optical photomicrographs of the GCAC microcapsules containing *LP80* bacterial cells. a, freshly made; b, after 1 month of storage in minimal broth media at 4 °C; and c, after 6 months of storage in minimal broth media at 4 °C.



**a**

**b**

Figure 4.5. a, optical photomicrographs of the GCAC microcapsules containing HepG2 cells; and b, a HepG2 encapsulated GCAC microcapsule being subjected to a trypan blue viability assay.

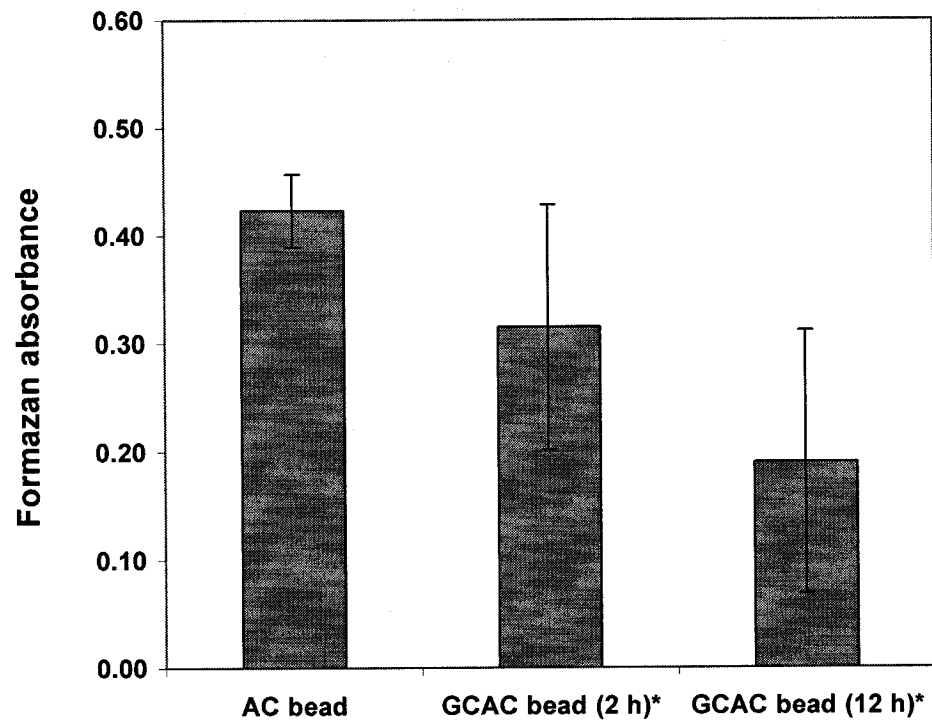


Figure 4.6. Metabolic activity of the encapsulated HepG2 cells after the process of capsule formation. \* indicates the time period that the genipin cross-linking reaction was performed.

**Reaction of chitosan with genipin and its fluorogenic attributes for potential  
microcapsule membrane characterization**

Hongmei Chen, Wei Ouyang, Bisi Lawuyi, Christopher Martoni and Satya Prakash \*

*Biomedical Technology and Cell Therapy Research Laboratory  
Department of Biomedical Engineering and Physiology, Artificial Cells and Organs Research  
Centre, Faculty of Medicine, McGill University, Montreal, Quebec, H3A 2B4 Canada.*

\*Corresponding author: Tel: 514 398-3676; Fax: 514 398-7461;  
Email: satya.prakash@mcgill.ca

---

**Preface:** This paper presents the findings of the fluorogenic characteristics of genipin, and elucidates the effects of chitosan-genipin reaction on the fluorescence generated. We further proposed that genipin can be used to characterize the chitosan membrane on the alginate-chitosan microcapsules.

Original paper published in *Journal of Biomedical Materials Research*. 75A (4): 917-927 (2005)

## 5.1 Abstract

This study investigates the fluorogenic characteristics of the chitosan-genipin reaction for applications in microencapsulation research. Results showed that the chitosan-genipin reaction generated a colored and fluorescent product, with the optimal excitation and emission wavelengths at 369 nm and 470 nm, respectively. Furthermore, it was found that reaction conditions affected the reaction efficiency as monitored by fluorescence intensity. Mixture at the ratio of 4:1 (chitosan: genipin by weight) fluoresced the most. It also fluoresced stronger if the reaction occurred at higher temperature, with the intensity of  $10.4 \times 10^5$  CPS at 37°C,  $5.9 \times 10^5$  CPS at 20°C and  $2.5 \times 10^5$  CPS at 4°C. As well, the fluorescence of the mixture developed gradually over time, attaining the emission maxima of  $2.9 \times 10^5$ ,  $7.6 \times 10^5$ , and  $10.0 \times 10^5$  CPS in 1, 6, and 18 h, respectively. Chitosan-coated alginate microcapsules were prepared without prior labeling, to which subsequent genipin treatment was applied in order to examine the potential of using genipin in microcapsule characterization. Chitosan bound to the alginate beads interacted with genipin, from which the resultant fluorescent signals allowed for clear visualization of the chitosan coating under confocal laser scanning microscopy. The relative fluorescence intensity across the chitosan membrane was found to be considerably higher than the controls (175 versus 50). The membrane thickness measured was  $29.2 \pm 7.3$   $\mu\text{m}$ . These findings demonstrate a convenient and effective way of characterizing chitosan-based microcapsules using genipin as a fluorogenic marker, a technique that will be useful in microcapsule research and other biomedical applications.

**Key words:** chitosan, genipin, fluorescence, microcapsule, CLSM, artificial cells

## 5.2 Introduction

Microencapsulation<sup>5</sup> describes the envelopment of a given substance in a coating for protection, isolation or controlled release of the enclosed material. It has attracted considerable attention over the past two decades and is currently employed in the food<sup>370</sup>, agriculture<sup>371</sup>, biotechnology<sup>372</sup> and biomedical industries<sup>55</sup>. Among its most important applications is the encapsulation of bioactive materials<sup>322,373</sup> for potential treatment of

diseases such as diabetes<sup>69</sup>, liver or kidney failure<sup>4,78</sup>, Parkinson's disease<sup>97</sup>, and cancer<sup>92</sup>. A number of natural polymers have been identified as suitable components for this microencapsulation strategy<sup>28</sup>. Chitosan, an abundantly available polysaccharide, is a copolymer of D-glucosamine and N-acetylglucosamine derived from naturally occurring chitin. Well-known for its biocompatibility and non-toxicity, chitosan has been extensively used in microcapsule formation<sup>374</sup>. In particular, the calcium-alginate microcapsule coated by chitosan via electrostatic interactions between carboxyl groups in alginate and amine groups in chitosan is widely studied. Many reports<sup>20,37,51,233,234</sup> demonstrate the effectiveness of chitosan-coated alginate microcapsules for sustained drug release and for live cell therapy. Several research groups have investigated the alginate-chitosan complexation<sup>35,234-238</sup> including the kinetic binding of chitosan to the alginate beads, the effects of chitosan characteristics and preparation parameters on microcapsule properties, as well as the diffusion mechanism of the enclosed drugs. However, few reports address the visualization and analysis of the chitosan-bound membrane on the alginate beads.

In earlier reports, synthetic bi-functional reagents such as glutaraldehyde or epoxy compounds were used in microcapsule preparation to enhance membrane resistance and delivery features<sup>40,51</sup>; but there remains problems of insufficient biocompatibility and potential cytotoxicity<sup>278,375</sup>. There is therefore a need to apply naturally derived reagents as an alternative. Genipin is an aglucone of geniposide extracted from gardenia fruits<sup>282</sup> and has been used as traditional herbal medicine. Genipin is known to react rapidly with amino acids to make blue pigments, which are currently used as a natural colorant in the food and fabric industries<sup>288</sup>. Genipin has been reported to bind with biological tissues and biopolymers such as chitosan and gelatin, leading to covalent coupling<sup>281,298,299</sup>. Recently, we described a novel genipin cross-linked alginate-chitosan microcapsule formulation that has potentials for cell encapsulation and delivery<sup>376</sup>. This study further explores the reaction between chitosan and genipin. Results show that this reaction created a new product with fluorescent characteristics that has potential in microcapsule research, a new approach that has not yet been investigated. This paper describes the details of these studies.

## 5.3 Materials and methods

### 5.3.1 Chemicals

Chitosan (low viscosity, 73.5 % deacetylation) and genipin were purchased from Wako BioProducts. Sodium alginate (low viscosity) was obtained from Sigma-Aldrich. All other reagents and solvents were of reagent grade.

### 5.3.2 Reaction of chitosan with genipin

The reaction of chitosan and genipin occurred after mixing an aqueous genipin solution (2.5 mg/mL) with a chitosan solution (10 mg/mL in 0.5 wt % acetic acid). Unless otherwise stated, a mixture of the above solutions at a ratio of 1:1 (v:v) was incubated at 4°C, 20°C, or 37°C for designated periods of time and tested before gelling occurred. Changes in the physical appearance of the mixture were also recorded.

### 5.3.3 Fluorometric studies

Aliquots of the chitosan-genipin mixture were diluted 10 times and scanned on a spectrofluorometer (FluoroMax-2). To investigate the fluorescent characteristics and determine the optimal excitation/emission wavelengths of the product, the absorption and fluorescence spectra were acquired. To study the effects of the reaction conditions, an optimized excitation wavelength at 369 nm was applied to acquire the emission spectra from 380 nm to 700 nm. The fluorescence intensities at the wavelength of maximum emission ( $\lambda_{em}^{max} = 470 \text{ nm}$ ) were plotted. The slit width was set at 3.5 nm for all the spectrum acquisition.

### 5.3.4 Chemical characterization

The solid state  $^{13}\text{C}$  nuclear magnetic resonance (NMR) spectra of chitosan before and after genipin treatment were obtained at 75.3 MHz using a Chemagnetics CMX-300 spectrometer. For this, 0.2 g chitosan was dissolved in 0.05N HCl and interacted with 0.02 g genipin at room temperature for 20 h. Chitosan without genipin treatment was prepared by a similar procedure and used as the control. Fourier transform infrared (FTIR) spectroscopy was also employed to investigate the chitosan-genipin reaction. The FTIR spectra of chitosan

before and after genipin treatment were recorded on a Perkin-Elmer Spectrometer equipped with a universal attenuated total reflection (ATR) sampling accessory.

### **5.3.5 Preparation of microcapsules**

The microcapsules used in this study were prepared as previously described<sup>376</sup>. Briefly, droplets of a sodium alginate solution (15 mg/mL) were generated by an encapsulator (Inotech. Corp.) and gelled in a stirred solution of 0.1M CaCl<sub>2</sub>. The Ca-alginate beads were then coated for 30 min in a chitosan solution of 10 mg/mL containing 0.1M CaCl<sub>2</sub>, producing alginate-chitosan (AC) microcapsules. Genipin treatment was performed by immersing the AC microcapsules in a genipin aqueous solution (1.0 mg/mL) at room temperature for 20 h resulting in the alginate-chitosan-genipin (ACG) microcapsules. The Ca-alginate beads with genipin treatment (AG) and the AC microcapsules without genipin treatment were also prepared and used as controls.

### **5.3.6 Confocal laser scanning microscopy**

A Zeiss LSM 510 Laser Scanning Confocal Imaging System (Carl Zeiss, Jena, Germany), equipped with a Titanium:Sapphire 2-photon laser (Coherent Inc., California) and a Zeiss Axiovert 100M microscope, was used to investigate the morphology of the microcapsules. For image acquisition, the microcapsules were placed in a chambered coverglass system (Lab-Tek) filled with deionized H<sub>2</sub>O. The focal planes were set at the equatorial sections of the microcapsules. All images were acquired at constant settings at an excitation wavelength of 370 nm and emission filter BP 435-485IR. The membrane thickness and the fluorescent intensity across the depicted microcapsule membrane were analyzed using LSM 510 software. Representative samples of at least 10 microcapsules were imaged and the measurements of membrane thickness were averaged.

## **5.4 Results**

### **5.4.1 Reaction between chitosan and genipin**

The reaction between chitosan and genipin occurred moderately after mixing the two solutions, and could be monitored by detecting the changes in the physical appearance of the

mixture. Table 5.1 summarizes the details of the chitosan-genipin reaction and the effect of temperature and reaction time. It was observed that the clear colorless solution turned into a dark blue gel gradually. The rate and extent of the reaction were found dependant on reaction temperature. At 37°C, the blue gel developed within 24 h, twice as fast as the reaction that occurred at room temperature. At 4 °C, the reaction occurred even slower; after 48 h, the mixture was still clear and non-gelled (Table 5.1).

#### **5.4.2 Absorption and fluorescence spectra**

To investigate the fluorogenic activity of the chitosan-genipin reaction, the fluorometric spectra of chitosan, genipin and their mixture were studied and compared. In the absorption spectra (Figure 5.1), two peaks appeared at the wavelengths of 267 nm and 369 nm for the mixture after a 12- h reaction at room temperature, which were otherwise absent or very weak in the spectra for genipin and chitosan. When using the wavelength of maximum absorption ( $\lambda_{ex}^{max}$ ) at 369 nm to excite the mixture, a strong fluorescence peak was found with the  $\lambda_{em}^{max}$  at 470 nm. In contrast, neither reactant individually showed this peak in its fluorescence spectrum (Figure 5.1).

#### **5.4.3 Effects of reaction conditions on the reaction efficiency as monitored by fluorescence intensity**

To further characterize the fluorogenic activity of the reaction product, more detailed experiments were carried out. Figure 5.2 demonstrates a linear relation ( $R^2=0.996$ ) between the fluorescence intensity and the concentration of the product. Figure 5.3-(a) shows the fluorescence spectra of the reaction mixture incubated at room temperature for 8 h and the maximum fluorescence intensities were plotted in Figure 5.3-(b) as a function of reactant ratios. Rapid increase in intensity with chitosan was found at the ratios from 0.5:1, 1:1, 2:1 to 4:1 (chitosan: genipin, by weight). Further increase in the amount of chitosan did not enhance the intensity as genipin had likely reached a saturated level. Consequently, the reactant ratio of 4:1 (chitosan: genipin, by weight) was considered optimal and used in performing subsequent experiments.

To examine the effect of the reaction temperature on the reaction efficiency of the chitosan-genipin mixture, samples were incubated at three different temperatures for 4 h and

their fluorescence profiles were shown in Figure 5.4. It was found that the reaction temperature significantly affected the fluorescence intensity of the product. The sample reacted at higher temperatures fluoresced much stronger than those at lower temperatures. As can be seen in Figure 5.4, the relative intensity of the samples incubated at 37°C was  $10.4 \times 10^5$ , in comparison to  $5.9 \times 10^5$  and  $2.5 \times 10^5$  for those at 20°C and 4°C, respectively.

As mentioned earlier, the reaction between chitosan and genipin was moderate and the blue gel developed gradually over time. To investigate it further, the fluorogenic process was monitored at room temperature as a function of time and the fluorescence spectra depicted in Figure 5.5. It was found that initially the fluorescence peak of the mixture at 470 nm was imperceptible and the Raman peak of H<sub>2</sub>O near 422 nm was detected<sup>377</sup>. The fluorescence in the mixture increased rapidly in the first 6 h of reaction, attaining the emission maxima of  $2.9 \times 10^5$ ,  $5.4 \times 10^5$  and  $7.6 \times 10^5$  CPS at 470 nm in 1, 3 and 6 h, respectively (Figure 5.5-b). Following this the intensity grew steadily, reaching the maximum intensity of  $10.0 \times 10^5$  CPS in 18 h, and then gradually decreased for the remainder of the experiment.

#### **5.4.4 Microcapsule formation and genipin treatment**

The preparation of alginate-chitosan (AC) microcapsules involved the formation of calcium-alginate beads followed by chitosan coating. Chitosan binded to the calcium-alginate gels through electrostatic interactions and formed a dense membrane on the microcapsules. Genipin treatment was achieved by immersing the AC microcapsules in an aqueous genipin solution. The chitosan bound to the beads, specifically the free amine groups in the chitosan chains, interacted with genipin and produced fluorescent derivatives within the membrane. Excess genipin could either be easily washed away after treatment or left with the samples during testing. This treatment did not noticeably affect the morphology of the microcapsules (Figure 5.6-a & c); they remained intact, spherical in shape and similar in size. However, genipin treatment resulted in a change in the shade of blue color in the microcapsules, which could be attributed to the formation of chitosan derivatives by the reaction with genipin<sup>289</sup>.

#### **5.4.5 Visual observation of chitosan coating on microcapsules**

Confocal laser scanning microscopy (CLSM) was employed to visualize the morphology of the microcapsules and verify the chitosan coating on the surface of the

alginate beads. Figure 5.6 represents the CLSM images of the microcapsules produced in this study. Under the regular transmission light channel, microcapsules with or without genipin treatment looked similar (Figure 5.6-a & c). When viewed under the fluorescent channel, the genipin-treated chitosan coating can be clearly identified by the appearance of distinguishing bright circles circumscribing the alginate beads (Figure 5.6-b). In contrast, the AC microcapsules without genipin treatment or the AG beads made of Ca-alginate with genipin treatment but without chitosan coating did not fluoresce under the same microscope settings (Figure 5.6-d & f). It was clear that the reaction between chitosan and genipin induced the formation of fluorophores. These results corroborated with the fluorometric observations described earlier and demonstrated the fluorescent features of the genipin-chitosan product. Figure 5.6 also illustrated the obvious advantage of CLSM over conventional light microscopy (Figure 5.6-left) in that CLSM allowed the visualization of the inner capsular structure without any destruction, extraction or chemical analysis.

#### **5.4.6 Fluorescence intensity and thickness of chitosan coating**

To better understand the chitosan coating formed on the microcapsules, the fluorescence intensity across the membrane was acquired by computational profile analysis. Figure 5.7 shows the intensity profiles along the randomly drawn lines across the microcapsule membrane. One can see that the relative emission intensity was drastically higher across the membrane of the ACG microcapsules (Figure 5.7-a) than those of the AC (Figure 5.7-b) and AG (Figure 5.7-c) microcapsules which were comparable to the background noise ( $< 50$ ). Furthermore, the fluorescence intensity was more pronounced at the border of the ACG membrane (as high as 175) and gradually decreased towards the interior of the microcapsules, where the fluorescence was as low as the background noise (Figure 5.7-a).

To characterize chitosan distribution, the membrane thickness of the coating was analyzed using the LSM 510 software. The averaged membrane thickness measured from CLSM images was  $29.2 \pm 7.3 \mu\text{m}$ , which corresponded with the results from atomic force microscopic (AFM) observations ( $32.1 \pm 5.0 \mu\text{m}$ ) for the cross-sectioned ACG samples (images not shown).

## 5.5 Discussion

Genipin is known to react exclusively with primary amines<sup>289</sup>. Therefore, the dark blue color that appeared in the chitosan-genipin mixture as well as on the genipin-treated AC microcapsules was presumably due to genipin reacting with chitosan's amino groups. While visibly evident, however, the detailed mechanism of blue gel transformation corresponding to the chitosan-genipin reaction remains under investigation<sup>245</sup>. The predicted reaction mechanism is shown in Figure 5.8. The amino groups at C-2 of the chitosan molecule initiate a nucleophilic attack at C-3 of genipin, resulting in the opening of the dihydropyran ring and the formation of a nitrogen-iridoid which undergoes dehydration to produce aromatic intermediates. Subsequent steps involve radical-induced polymerization, creating highly conjugated heterocyclic genipin derivatives. Additionally, secondary amide linkages can be established by the reaction of the ester group in genipin with the amino group in chitosan, leading to a polymeric network structure<sup>291</sup>. Solid state <sup>13</sup>C nuclear magnetic resonance (NMR) and fourier transform infrared (FTIR) spectra demonstrated the chemical changes of chitosan after reacting with genipin. In the NMR spectra (Figure 5.9-a), several changes were detected in the carbon signals of chitosan after genipin treatment, which included the up-field shift of C-1, the splitting of C-3, and the considerable decrease of overlapped C-4 and C-5 peaks for the chitosan molecule. One possible explanation is that the formation of secondary amide and heterocyclic amino linkages, as well as the conformational changes of chitosan linear chains produced considerable constriction on the polymer network<sup>291</sup>, involving significant carbon shifts on the glucopyranose repeating unit. FTIR spectrometry further confirmed the chemical reaction between chitosan and genipin. In Figure 5.9-b, the absorbance at 1570 cm<sup>-1</sup> corresponding to primary amine groups significantly decreased after genipin treatment, likely due to the consumption of these functional groups during the reaction<sup>291</sup>. Furthermore, an increase in the amide peak near 1640 cm<sup>-1</sup> was observed, indicating the formation of secondary amides as a result of the reaction between the ester groups on genipin with the amino groups on chitosan.

In the emission spectra of chitosan and genipin (Figure 5.1), the small sharp peak at 422 nm was due to the Raman scatter from the solvent H<sub>2</sub>O<sup>377</sup>. It was overwhelmed by the

broad and strong fluorescent peak at ~ 470 nm in the emission spectrum of the reaction mixture. The presence of this peak and its substantial increase in intensity reflect the chemical modifications of chitosan and genipin. From the presumed reaction mechanism (Figure 5.8), it appeared that a large conjugated system, possibly the  $\pi$ - $\pi^*$  conjugation, was formed by this reaction, thus explaining the fluorescent characteristics found in the reaction product. Furthermore, it was determined that the reaction parameters such as temperature and time affected the fluorescence intensity of the genipin-chitosan product. Specifically, the samples incubated at higher temperatures fluoresced stronger than those at lower temperatures (Figure 5.4). This result corresponded with the physical appearance changes of the chitosan-genipin mixture shown in Table 5.1, and could be explained by the higher level of molecular movement at 37 °C that accelerated the reaction than at lower temperatures. It should be noted that the samples incubated at different temperatures were equilibrated at room temperature for 15 min prior to the fluorometric testing so as to avoid the effects of temperature variations on fluorescence intensity. The reaction time was also found to influence the fluorogenic process of the chitosan-genipin mixture (Figure 5.5). The rapid increase in fluorescence during the first several hours may be due to the fact that genipin reacts spontaneously with primary amine producing conjugated compounds. The slight decrease in fluorescence after 24 h could possibly be induced from collisional quenching during a diffusive encounter with amines and the complex formation by further polymerization<sup>377</sup>.

One major advance of the present work is the potential exploitation of genipin's fluorogenic property in microcapsule characterization by CLSM. It is of interest to visualize the microcapsule membrane and analyze the distribution of the involved materials. While light microscopy limits the resolution and electron microscopy alters the samples, CLSM enables a non-destructive way to examine samples without compromising resolution<sup>321</sup>. Since non-fluorescent materials can not be detected under the fluorescent channel of CLSM, previous exploitation<sup>138,320-322</sup> of CLSM in microcapsule and coacervating system studies used fluorescent markers, such as fluoresceine isothiocyanate (FITC) or rhodamine B isothiocyanate (RITC), to label the polymers prior to coacervation or encapsulation, and thereafter identified their distribution under CLSM. The labeling approaches included covalently linking as well as basic blending of fluorescent markers with the polymers<sup>138,320</sup>. However, covalent linking presents a risk that some functional groups of the involved

polymers, an important prerequisite for polyelectrolyte complexation, may be blocked after the fluorescence-labeling step<sup>320</sup>. Alternatively, the markers may not bind firmly at the intended sites and may migrate into other sites leading to compromised results. In addition, other issues persist concerning the labeling efficiency and stability, as well as their influences on the coacervation or encapsulation process. In contrast, genipin treatment enabled the localization of chitosan coating in the alginate microcapsules easily and effectively under CLSM (Figure 5.6-b) with no prior fluorescence labeling required. The genipin treatment was readily performed after the microcapsules were made, and there was no interference from the free marker as genipin itself is non-fluorescent. This method overcomes many limitations of the current approaches found in literature.

Another distinct advantage of using genipin as a visualization reagent is its high selectivity. Primary amine groups represent the only targets for genipin reaction<sup>282,289</sup> with the potential to generate fluorescent products. The nucleophilic -OH groups did not react with genipin, as evidenced by the results from the control experiments with alginate, which contains -OH and -COOH but no -NH<sub>2</sub> groups. No physical appearance changes were detected in the alginate-genipin mixture (data not shown) and no bright images under the CLSM fluorescent channel were acquired for the control AG beads (Figure 5.6-f). Conversely, the activated isothiocyanate groups in many conventional fluorescence markers such as FITC or RITC interact with nucleophilic functional groups such as -NH<sub>2</sub> and -OH, commonly found in polypeptides and polysaccharides<sup>320</sup>, and hence may not be able to distinguish chitosan from alginate simultaneously in a microcapsule. Another possible application of this technology could be the measurement of drug release. In particular a drug that has a functional group that preferentially interacts with membranous chitosan could limit the sites available to genipin and in turn quench the fluorescence; the change in fluorescence could be a measurement of drug release.

Although several groups have studied chitosan coating on the alginate microcapsules, few reports addressed the visualization and thickness measurement of the chitosan in the microcapsule membrane. It is believed that a better understanding of chitosan binding in quantitative terms will provide improved control over the functional properties of microcapsules such as permeability and mechanical stability. This is now possible because CLSM allows for distinguishing the microcapsule wall from the interior core and the image

background, and enables non-destructive computational image analysis. As shown in Figure 5.7-a, a gradient distribution of the bound chitosan within the microcapsule wall was found with the highest concentration at the border, decreasing towards the interior core. For alginate-chitosan complexation, it is known that the initial chitosan binding may block further interaction of chitosan with alginate due to restricted diffusion<sup>35,236</sup>. This may explain the non-homogeneous deposition of chitosan across the membrane. Previous studies using radioactively labeled chitosan also indicated that chitosan penetrated into the alginate gel to a great extent and the binding occurred not only to the surface of the capsule but also the matrix<sup>235</sup>. This investigation agreed with our membrane thickness measurement, which was relatively thick (~30  $\mu\text{m}$ ) as compared to the commonly used alginate-poly-L-lysine-alginate membrane (below 10  $\mu\text{m}$ )<sup>241</sup>.

In summary, based on the above observations, it can be inferred that the fluorogenic characteristics of genipin has rendered it a promising candidate as a visualization reagent. After genipin treatment, the chitosan coating on the AC microcapsules was successfully visualized and analyzed under CLSM. This new method, simple, efficient and highly selective, may prove useful in microcapsule research and other biomedical applications.

## 5.6 Acknowledgements

This work was supported by research grants to Prakash from Canadian Institutes of Health Research (CIHR). The CIHR New Investigator Award to Prakash, postgraduate scholarships from Natural Sciences and Engineering Research Council (NSERC) of Canada to Chen and Martoni, postdoctoral fellowship from Fonds Québécois de la Recherche sur la Nature et les Technologies (FQRNT) to Ouyang are acknowledged. We also appreciate the constructive discussion with Z.Q. Chen and help from T. Halim in manuscript preparation.

Table 5.1. Effect of temperature and reaction time on the physical appearance of the chitosan-genipin reaction mixture\*

Incubation Temp.(°C)	Incubation Time (hr)							
	0	1	3	6	12	24	36	48
37	clear colorless	clear colorless	clear, light yellow	clear, green- blue	partly gelled dark blue	gel, dark blue	fully gelled dark blue	fully gelled dark blue
20	clear colorless	clear colorless	clear, faintly yellow	clear, slightly yellow	clear yellow	clear, blue-green	viscous, dark green-blue	gel, dark blue
4	clear colorless	clear colorless	clear colorless	clear colorless	clear colorless	clear, faintly yellow	clear, faintly yellow	clear, slightly yellow

\* An aqueous genipin solution (2.5 mg/mL) mixed with a chitosan solution (10 mg/mL) at a ratio of 1:1 (v/v) and incubated at varied temperatures for designated periods of time

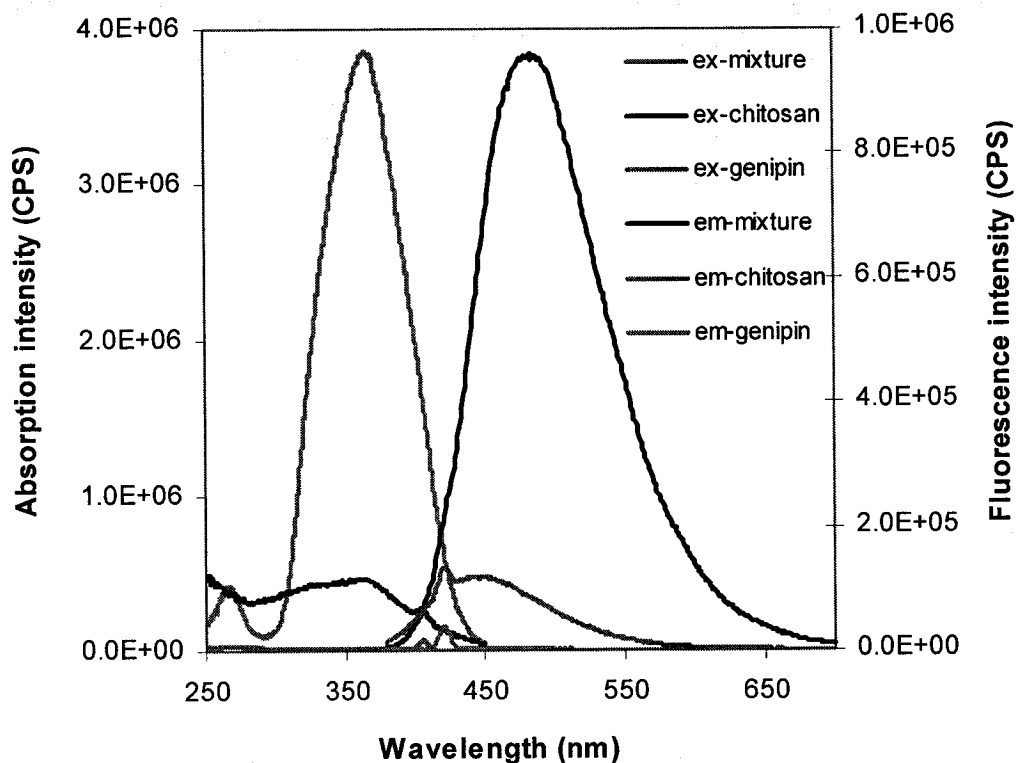


Figure 5.1. Absorption and fluorescence spectra of the chitosan-genipin mixture, chitosan and genipin solution acquired at excitation 369 nm and emission 469 nm, respectively. The chitosan-genipin mixture was composed of chitosan (10 mg/mL) and genipin (2.5 mg/mL) in a ratio of 1:1 (v/v) incubated for 12 h at room temperature. Aliquots of the mixture and reactants were diluted 10 times and 20 times, respectively, before scanning.

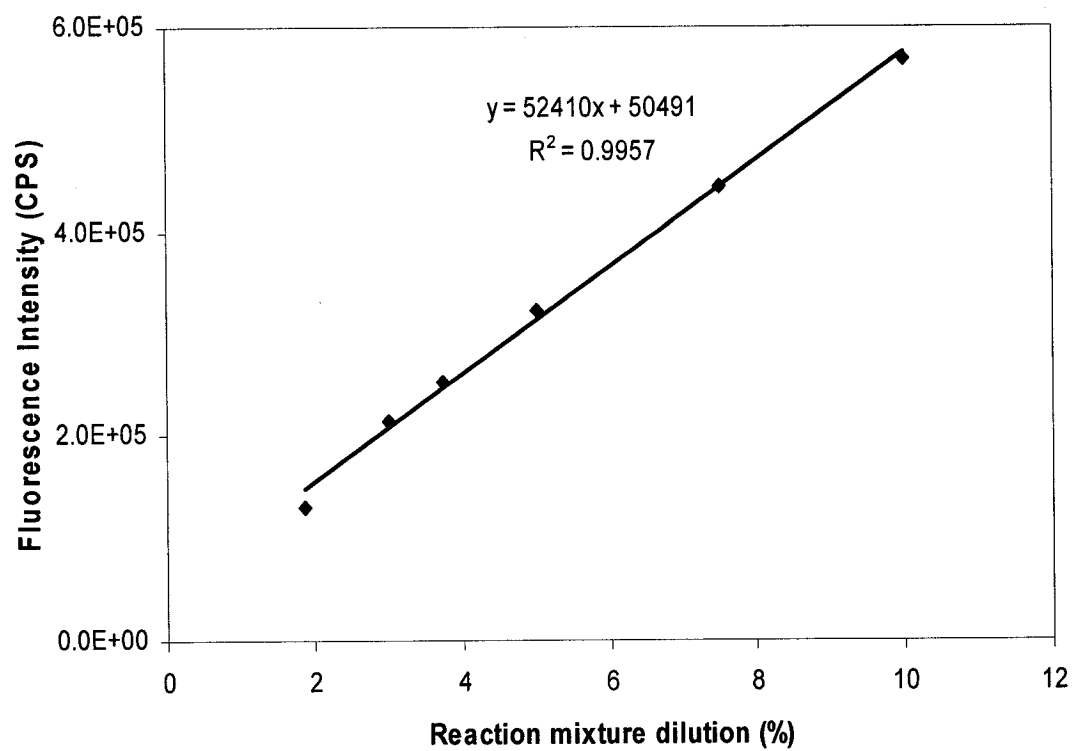


Figure 5.2. Linear relationship between fluorescence intensity and concentration of the chitosan-genipin reaction fluorescent product.

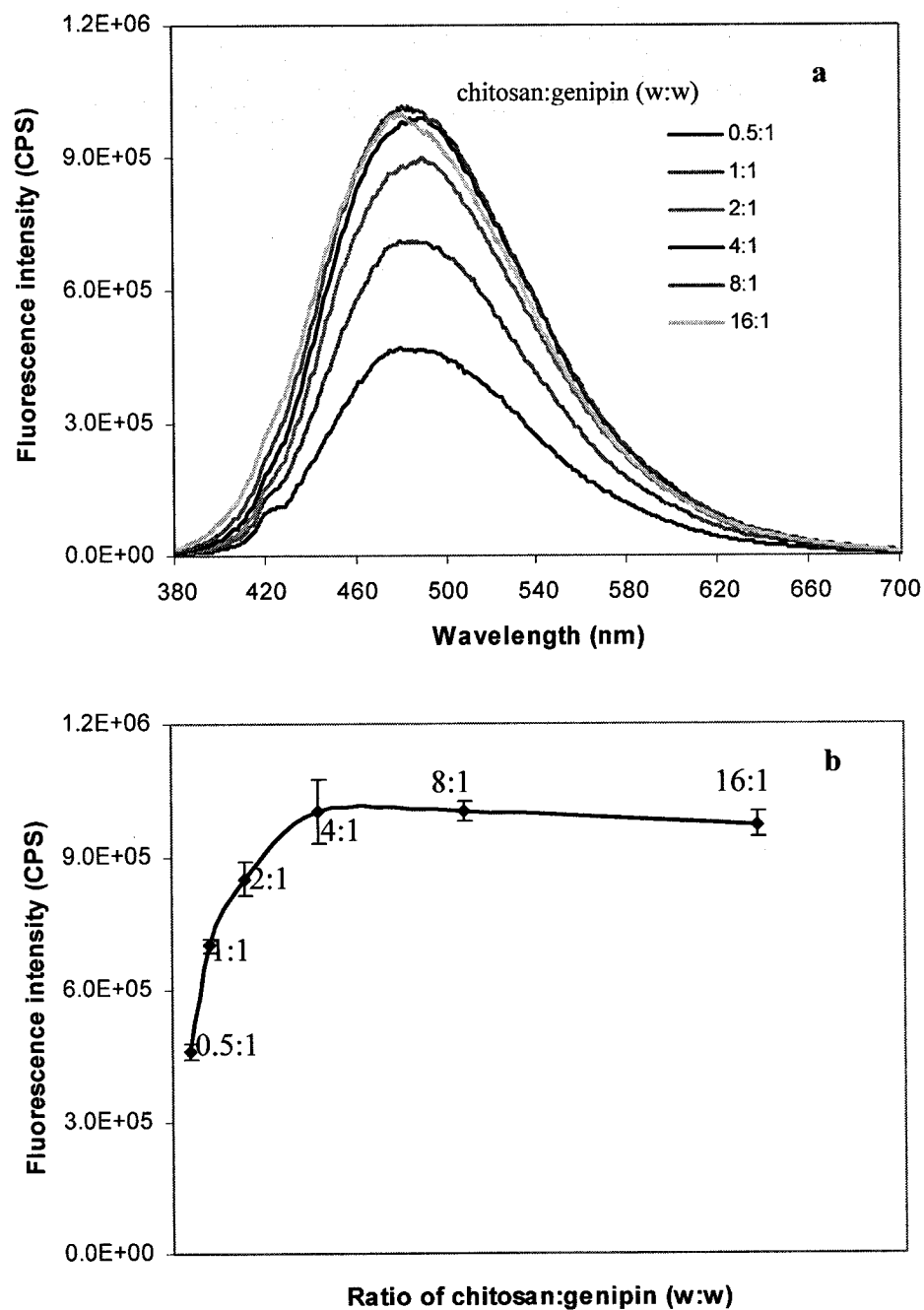


Figure 5.3. a, Fluorescence spectra of the chitosan-genipin mixture composed of varied reactant ratios; and b, Fluorescence intensities of the chitosan-genipin mixture at  $\lambda_{em}^{max}$  as a function of component ratios. For this study, mixture samples of chitosan (20 mg/mL) and genipin solution (2.5 mg/mL) at varied weight ratios were incubated at 20 °C for 8 h, diluted 10 times and scanned with the excitation wavelength set at 369 nm.

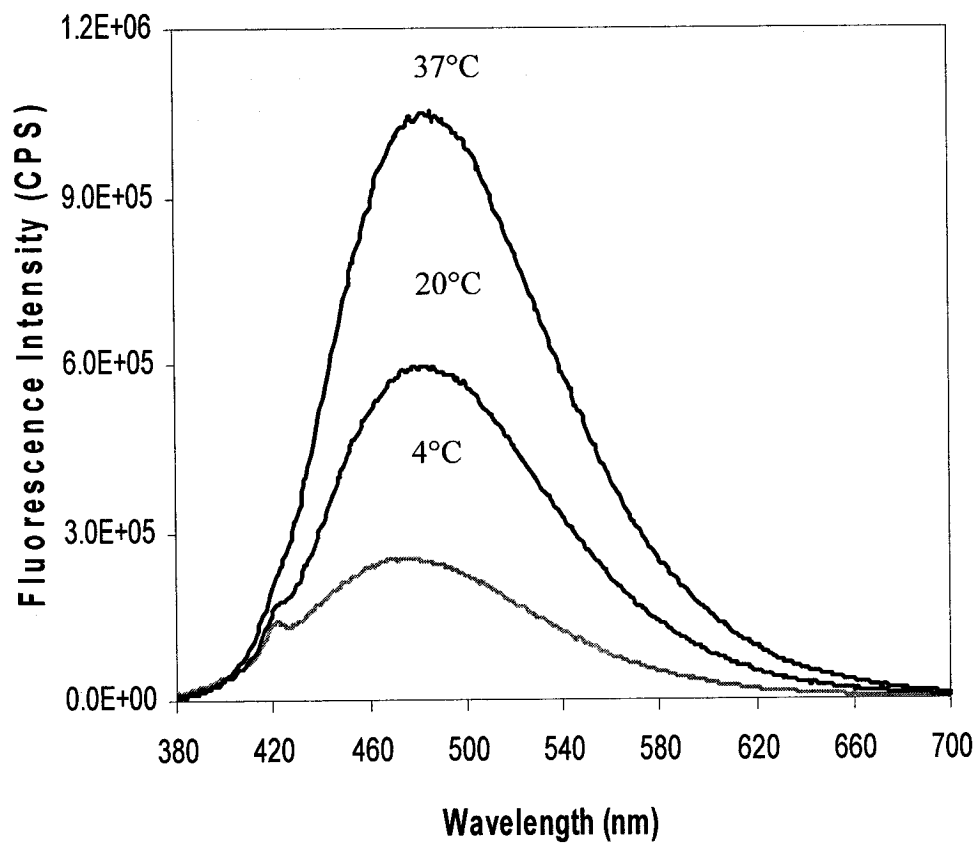


Figure 5.4. Effect of the reaction temperature on the fluorescence spectra of the chitosan-genipin mixture incubated for 4 h. Aliquots were diluted 10 times and scanned with the excitation wavelength set at 369 nm.

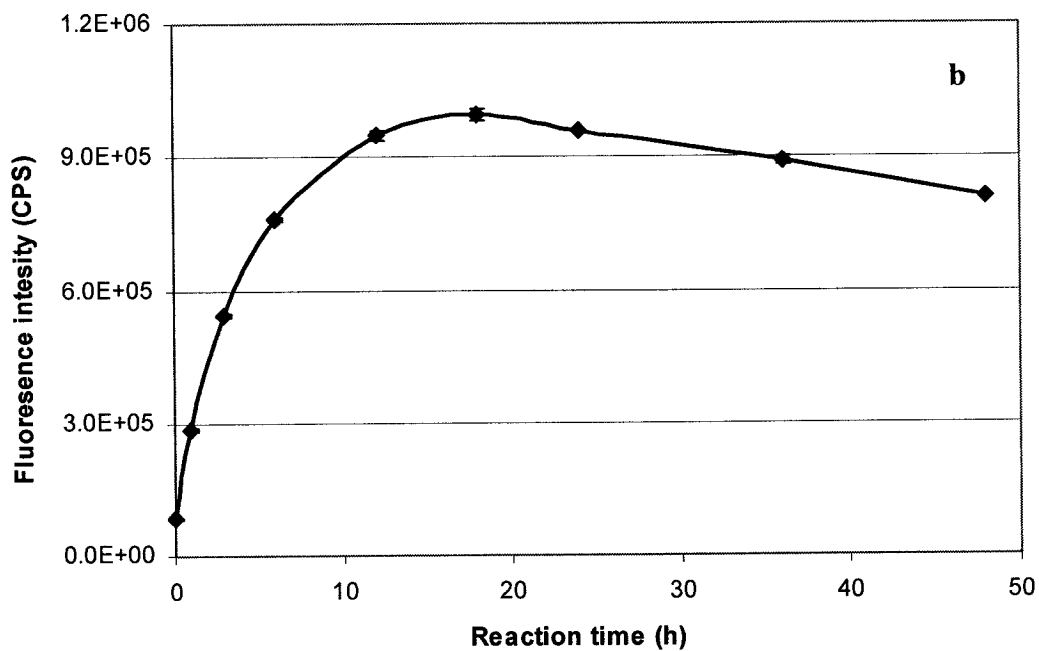
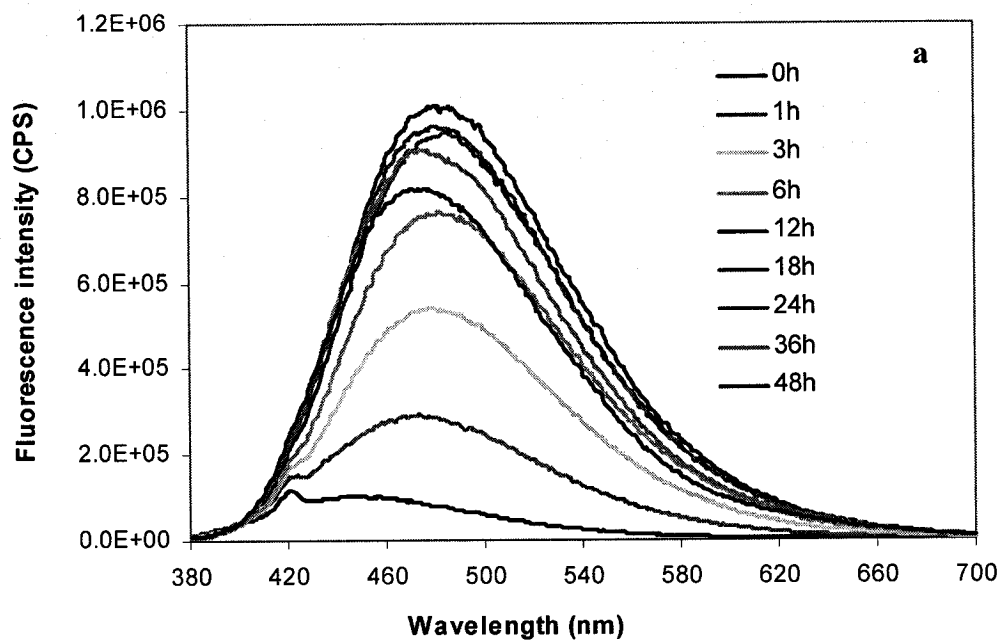


Figure 5.5. Fluorescence spectra (a) and intensity profile (b) of the chitosan-genipin mixture incubated at 20 °C. At designated time points, aliquots of the mixture were diluted 10 times and scanned with the excitation wavelength set at 369 nm. The fluorescence intensities at  $\lambda_{em}^{max}$  were plotted as a function of time.

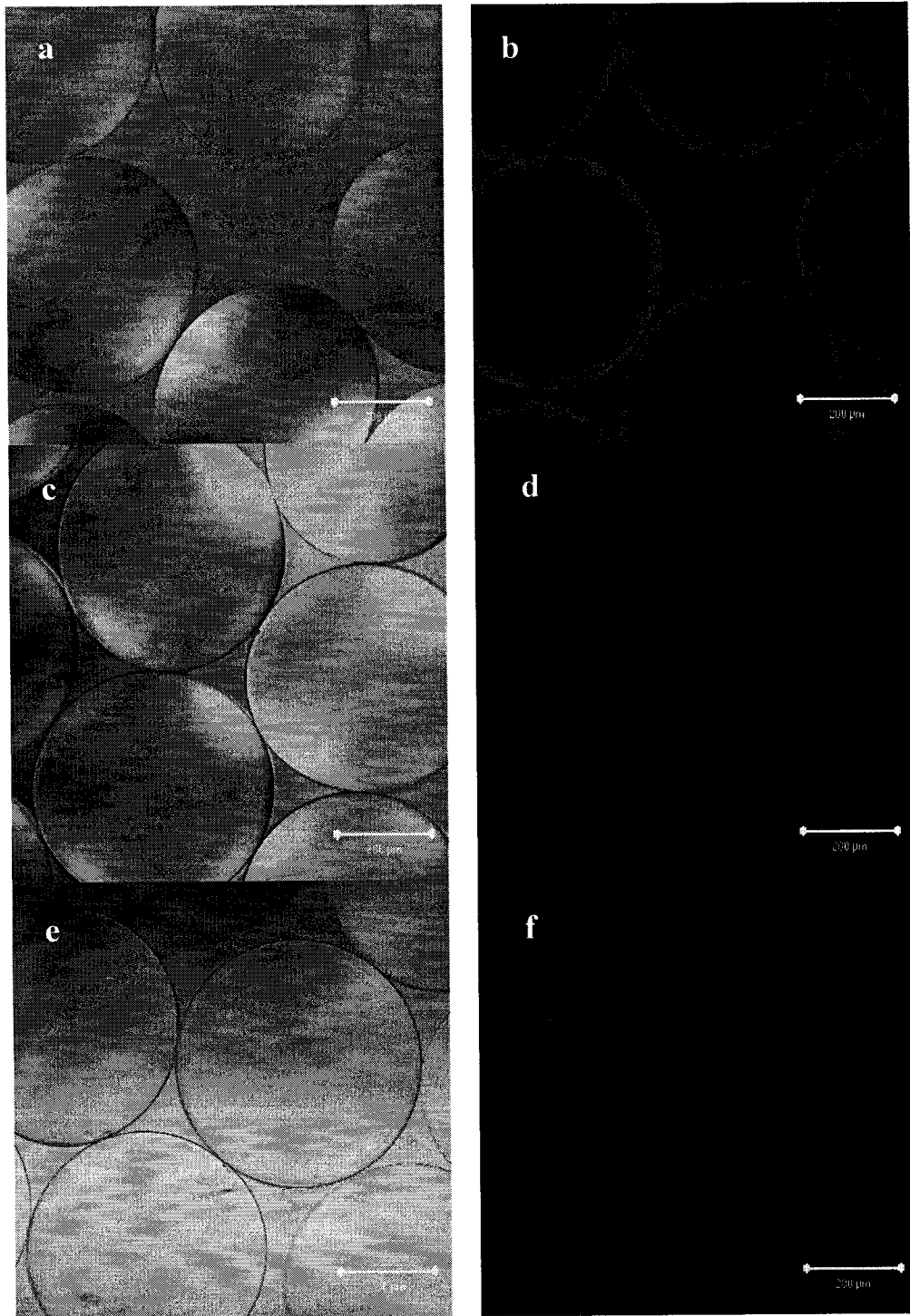


Figure 5.6. Confocal laser scanning microscopic (CLSM) images of the alginate-chitosan microcapsules after genipin treatment (ACG) (a & b); alginate-chitosan (AC) microcapsules (c & d); and alginate beads after genipin treatment (AG) (e & f) viewed at the transmission light channel (left) and at the fluorescence channel (right). The bars represent 200  $\mu\text{m}$ .

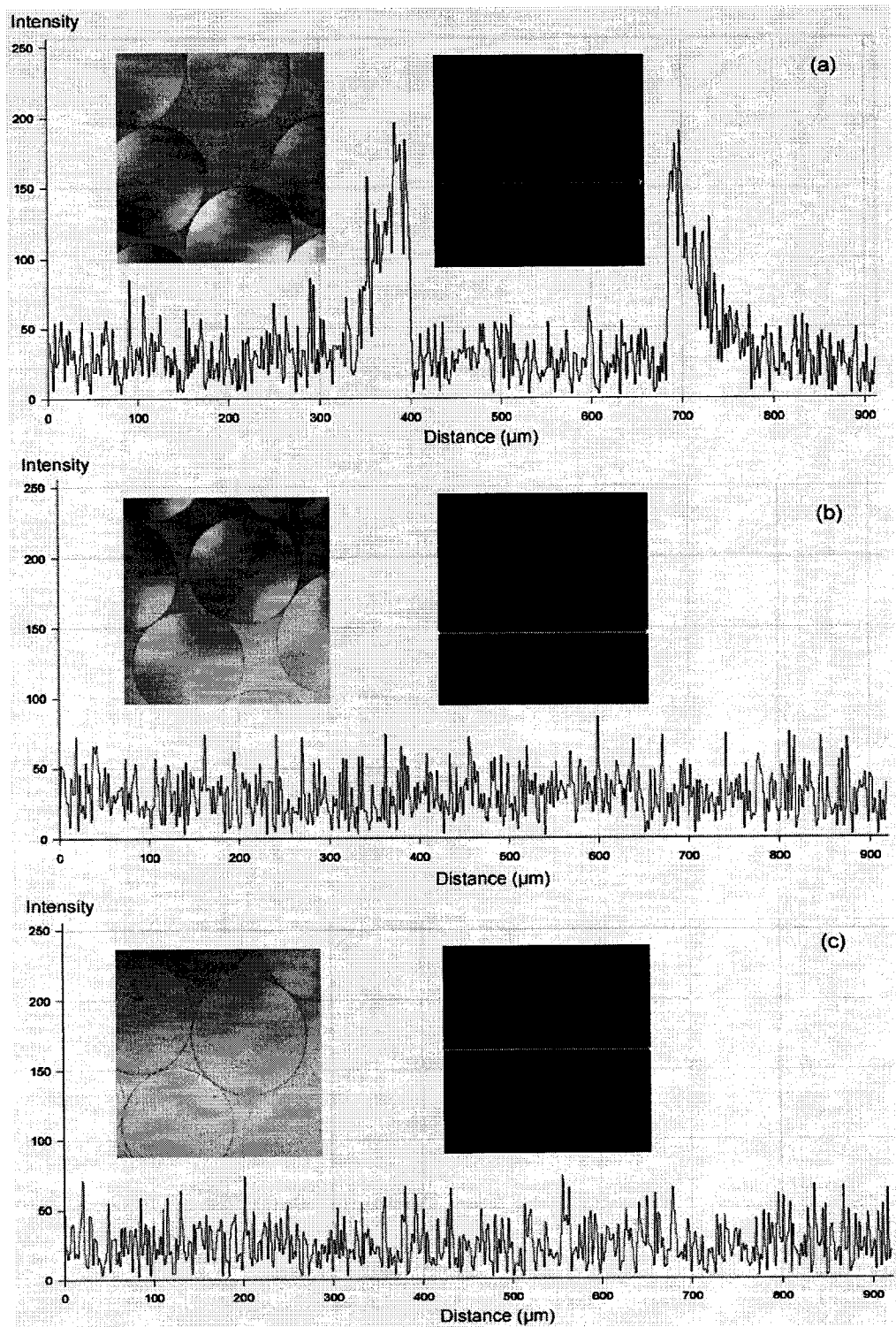


Figure 5.7. Fluorescence intensity profiles corresponding to the white lines across the microcapsule images at the focal planes. a, alginate-chitosan microcapsules after genipin treatment (ACG); b, alginate-chitosan microcapsules (AC); and c, alginate beads after genipin treatment (AG).

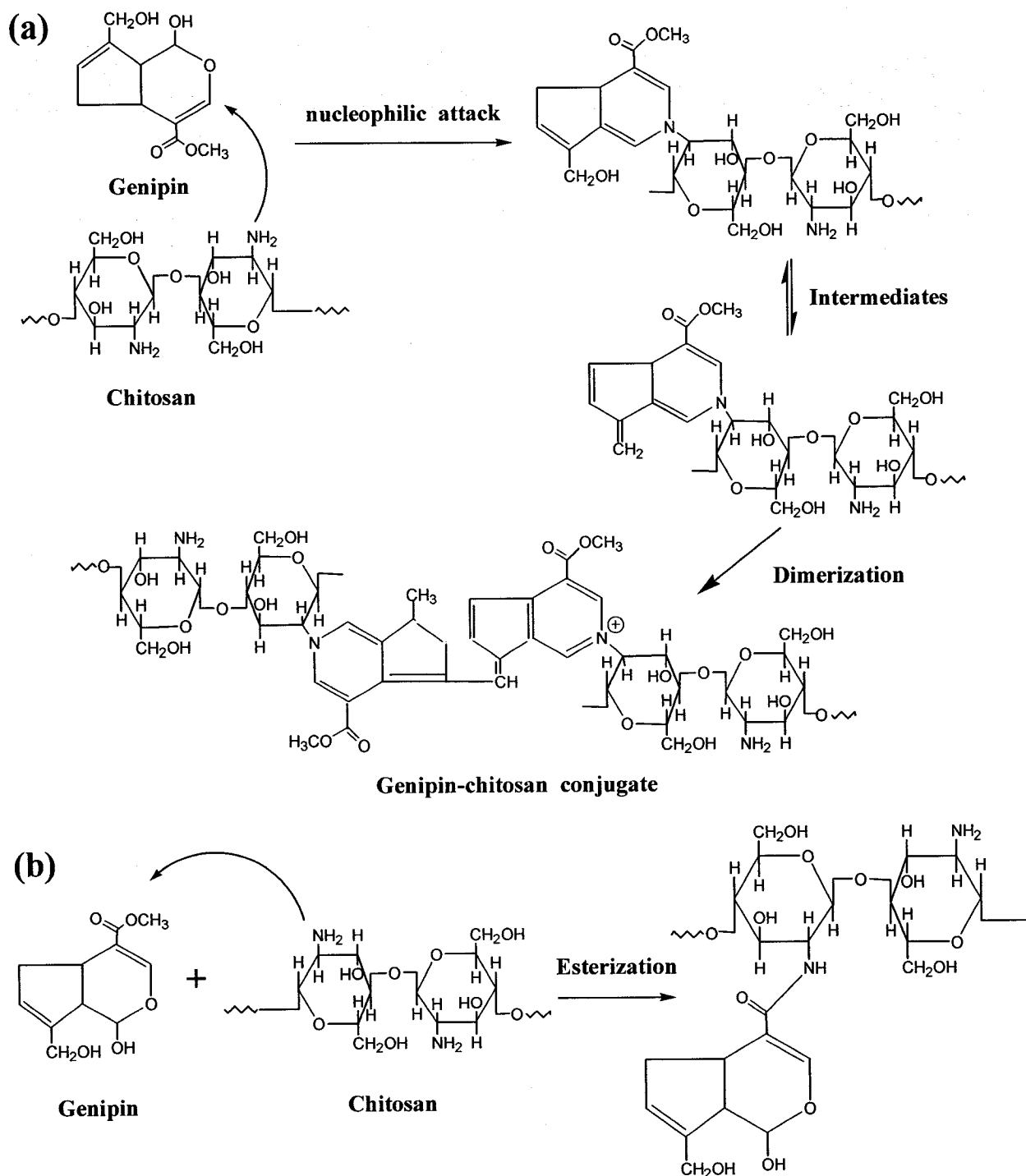


Figure 5.8. Predicted mechanism of the reaction between chitosan and genipin. (a): formation of highly conjugated genipin derivative; and (b): formation of secondary amide linkage.

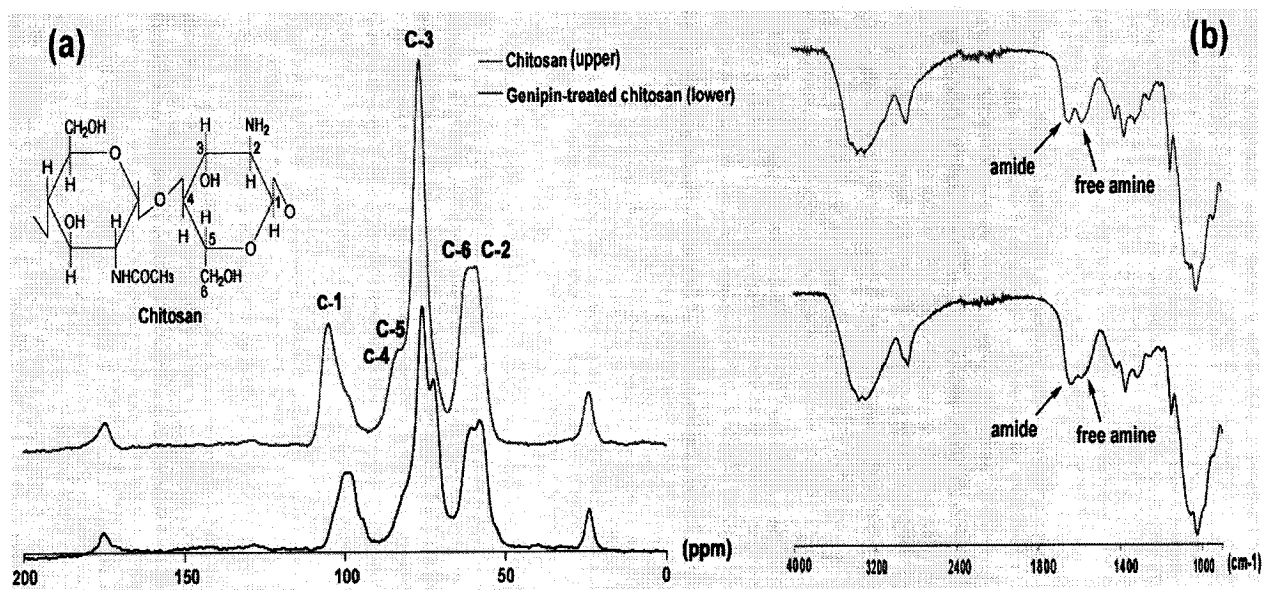


Figure 5.9. Solid state  $^{13}\text{C}$  NMR spectra (a) and FTIR spectra (b) of chitosan before and after genipin treatment.

**A new method for microcapsule characterization:  
Use of fluorogenic genipin to characterize polymeric microcapsule membranes**

Hongmei Chen, Wei Ouyang, Bisi Lawuyi, Trisna Lim and Satya Prakash \*

*Biomedical Technology and Cell Therapy Research Laboratory  
Department of Biomedical Engineering and Physiology, Artificial Cells and Organs Research  
Centre, Faculty of Medicine, McGill University, Montreal, Quebec, H3A 2B4 Canada.*

\*Corresponding author: Tel: 514 398-3676; Fax: 514 398-7461;  
Email: satya.prakash@mcgill.ca

---

**Preface:** As described in the last chapter, the reaction between genipin and the amino groups of chitosan led to the formation of fluorescence conjugates. Poly-L-lysine (PLL) is another widely used polycation that carries primary amino groups. The present chapter further studies the reaction between genipin and PLL, and profiles its fluorogenic characteristics. Based on these findings, a new, simple and highly selective method for microcapsule membrane characterization was developed.

Original article published in *Journal of Applied Biochemistry & Biotechnology* 134 (3):207-221 (2006)

## 6.1 Abstract

Numerous microcapsule systems have been developed for a wide range of applications including the sustained release of drugs, enzyme immobilization, cell transplantation for therapy, and other biotechnological applications. Despite the fact that the microcapsule membrane is a dominant factor governing overall microcapsule performance, its characterization is challenging. Herein we report a new method for characterizing microcapsule membranes, using the most common alginate-poly-L-lysine-alginate (APA) microcapsule as an example. Our data demonstrate that genipin, a natural-derived reagent extracted from gardenia fruits, interacts with poly-L-lysine (PLL) and generates fluorescence when excited. This fluorescence allows clear visualization and easy analysis of the PLL membrane in the APA microcapsules using confocal laser scanning microscopy. The results also show that the PLL binding correlates to the reaction variables during PLL coating such as PLL concentration and coating time. In addition, five other different microcapsule formulations consisting of PLL and/or chitosan membranes were examined, and the results imply that this method may be extended to characterize a variety of microcapsule membranes. These findings suggest that genipin may serve as a fluorogenic marker for rapid characterization of microcapsule membranes, a superior method that would have important implications for microcapsule research and great potential in many other applications.

**Keywords:** microcapsule, poly-L-lysine, alginate-poly-L-lysine-alginate, genipin, chitosan, fluorescence, confocal laser scanning microscopy

## 6.2 Introduction

Microencapsulation of bioactive materials such as drugs, vaccines, antibodies, enzymes and live cells provides a promising delivery tool for numerous applications including the treatment of a number of diseases<sup>9,19,55,68,70,78,83,89,97</sup>. Alginate based microcapsules are one of the most widely used owing to the superior biocompatibility and mild process suitable for both the host and the enclosed materials. For the preparation of microcapsules, generally, alginate droplets are gelled by multivalent ions (typically  $\text{Ca}^{2+}$ ). Additional polymers are used

to envelope the calcium-alginate beads, which create stable and semi-permeable membranes for applications such as immuno-isolation of live cells and sustained release of drugs. For example, positively charged polymers, also termed polycations, bind to the negatively charged alginate gel via electrostatic interactions and form strong polyelectrolyte complex membrane on the microcapsule surfaces<sup>34,69</sup>. The primary amine-containing poly-L-lysine (PLL) and chitosan, both simply named as polyamine in this paper, are widely used polycations for the construction of microcapsule membranes. The preparation and properties of alginate-poly-L-lysine-alginate (APA) and alginate-chitosan (AC) microcapsules have been studied extensively<sup>113,177,179,241-243</sup>.

Previous research show that microcapsule utility depends on its membrane properties. For example, the membrane thickness is known to correlate with permeability, resistance, mechanical strength, drug release capacity and biocompatibility<sup>113,133,162,235,241-243</sup>. A solid understanding of the structure-property of the microcapsule membranes, therefore, is essential for *in vitro* and *in vivo* applications. However, precise determination of the membrane thickness and polycation binding is challenging<sup>242</sup> owing to the small size, spherical shape and hydrogel nature of microcapsules along with the fragility of the membrane and other factors. Many techniques have been employed in previous studies; however they have had many limitations. For example, regular light or stereoscopic microscopy, though simple, may limit the resolution in measurement<sup>133,243,314</sup>. Electron microscopic methods, such as scanning electron microscopy and transmission electron microscope, are typically destructive<sup>49,125,138,315</sup> and require skilled knowledge for preparation of samples and interpretation of results. Gravimetric measurement, also being destructive and cumbersome, can not assess the distribution of the coating polymers<sup>241</sup>. Additionally, approaches using radio-labeled polymers and enzyme-linked sorption assays involve elaborate sample preparation<sup>235,242</sup>, while the availability of the particular materials needed may also impede the process. Other methods for assessing thin films and small particles, such as ellipsometry<sup>125</sup> and surface plasmon resonance spectroscopy<sup>319</sup>, may not be suitable for hydrogel microcapsule membrane systems. In recent years a non-destructive approach, confocal laser scanning microscopy (CLSM), has attracted much interest in microcapsule research<sup>179,317,321,322,378</sup>. In previous studies, the microcapsule core and/or membrane components must be labeled with fluorescent markers, such as fluoresceine isothiocyanate or rhodamine B isothiocyanate prior

to encapsulation<sup>113,138,179,188,320-322,379</sup>. This process, however, presents risks of blocking some of the functional groups in the involved polymers essential for polyelectrolyte complexation, leading to weak binding<sup>179,320</sup>. In addition, other issues pertaining to the stability and solubility of the labeled polymers, the control of labeling efficiency, the separation of free markers, as well as their influences on the encapsulation process still remain<sup>179,320</sup>. The characterization of microcapsule membranes is still plagued with persistent difficulties.

Genipin is an aglucone of geniposide extracted from gardenia fruits<sup>282</sup> and has been used traditionally as a herbal medicine<sup>380</sup>. It is known that genipin reacts rapidly with amino acids to make blue pigments, which are currently used as a natural colorant in the food and fabric industries<sup>288</sup>. The present study introduces a new and simple method of using genipin to characterize microcapsule membrane by CLSM without complicated prior labeling and sample treatment. Specifically, we characterized the commonly used PLL membrane in APA microcapsules using this novel method and evaluated the feasibility of characterizing polyamine microcapsule membranes using other five different microcapsule formulations.

## **6.3 Materials and methods**

### **6.3.1 Chemicals**

Sodium alginate (low viscosity), PLL ( $M_v$  27,400) and pectin (degree of esterification 25 %) were purchased from Sigma-Aldrich, USA. Polyethylene glycol (PEG) ( $M_w$  20,000) was obtained from Fluka BioChemika, Switzerland. Chitosan (low viscosity, 73.5 % degree of deacetylation and  $M_v=7.2 \times 10^4$ ) and genipin were obtained from Wako BioProducts, USA. All other reagents and solvents were of reagent grade and used as received without further purification.

### **6.3.2 Fluorometric study of reaction between genipin and PLL**

To investigate the fluorescent characteristics of the reaction between PLL and genipin, genipin and PLL were dissolved in physiological saline (PS) at a mass ratio of 2.5:1. The mixture was then incubated at 37°C for 4 h. The absorption and fluorescence spectra of the mixture were acquired using a spectrofluorometer (FluoroMax-2) with the slit width set at 3.5 nm, and compared with those of the reactants.

### **6.3.3 Preparation of microcapsules**

#### **a) Preparation of APA microcapsules**

Droplets of an Na-alginate solution (15 mg/mL) were generated by an encapsulator (Inotech. Corp.) and gelled in a stirred CaCl<sub>2</sub> solution (11 mg/mL) for 15 min. The obtained Ca-alginate beads, with a diameter of  $508.4 \pm 10.7 \mu\text{m}$  (n=10), were exposed to PLL solution (1 mg/mL) for 10 min to form AP beads; this was followed by washing with PS and a subsequent coating by Na-alginate solution (1 mg/mL) for 10 min. The obtained APA microcapsules were then washed and collected. To investigate the effects of PLL concentration and reaction time on the PLL binding in the APA microcapsule membrane, different microcapsules were prepared using PLL at a concentration of 0.5 mg/mL, 1.0 mg/mL, 2.5 mg/mL, or 5.0 mg/mL for varied incubation time (10, 60, and 120 min) during the coating process. To examine the effect of storage on the bound PLL layer, the APA microcapsules were made as described above using PLL at a concentration of 1.0 mg/mL for 10 min coating and stored in PS for 0, 5, 14, 20 days prior to genipin treatment and CLSM analysis.

#### **b) Preparation of other PLL-based microcapsules**

PEG was incorporated into APA microcapsules to form alginate-poly-L-lysine-PEG-alginate (AP-PEG-A) microcapsules by immersing the above AP beads in a PEG solution (5 mg/mL) following the PLL incubation. After washing with PS, a final layer of alginate was coated using 1 mg/mL alginate solution for 10 min. Multi-layer microcapsules composed of alginate-poly-L-lysine-pectin-poly-L-lysine-alginate (AP-PEC-PA) were also prepared by integrating pectin into the APA microcapsules. Briefly, the above AP microcapsules were incubated in a pectin solution (1 mg/mL), followed by another coating of PLL (1 mg/mL) and a final layer of alginate (1 mg/mL). All coating processes were carried out using the aforementioned method with an exposure time of 10 min and three PS washes after each coating step.

#### **c) Preparation of chitosan-based microcapsules**

To prepare the AC microcapsules, the above Ca-alginate beads were coated for 30 min in a chitosan solution (5 mg/mL, in dilute acetic acid with final pH=5.4). Multi-layer alginate-chitosan-PEG-alginate (AC-PEG-A) and alginate-chitosan-PEG-poly-L-lysine-alginate (AC-PEG-PA) microcapsules were prepared by immersing the AC microcapsules in the PEG solution (5 mg/mL) for 10 min and subsequently coating with either a layer of alginate (1 mg/mL) for 10 min, or a layer of PLL (1 mg/mL) followed by an alginate layer (1 mg/mL) for 10 min each. Three PS washes were applied after each coating to remove unbound polymers.

#### **6.3.4 Genipin treatment on microcapsules**

The microcapsules obtained as described in the above preparation section were immersed in a genipin solution (2.5 mg/mL in PS) for 20 h at 37 °C unless otherwise stated. The resulting microcapsules were washed and directly used for CLSM studies.

#### **6.3.5 Characterization of microcapsule membrane by CLSM**

The morphology and membrane structure/density of the microcapsules were examined using a Zeiss LSM 510 Laser Scanning Confocal Imaging System (Carl Zeiss, Jena, Germany), equipped with a Zeiss Axiovert 100M microscope and an argon-ion laser. For image acquisition, the microcapsules were directly placed in a chambered coverglass system (Lab-Tek). One channel of the CLSM was used in the single green fluorescence mode at an excitation of 488 nm and with the filter block BP500-550IR. The other channel was set to the transmitted light detector. The focal planes were set at the equatorial sections of the microcapsules. All images were acquired at constant microscopic settings under computer control in order to obtain comparable images and fluorescence intensity. An average of 8 consecutive scans of a single field was taken. The thickness of the fluorescent membrane in the microcapsules was analyzed using the equipped LSM 510 software and given as mean  $\pm$  SD of at least 10 measurements. The fluorescence intensity profile corresponding to a line across the microcapsule membrane at the focal plane was acquired by computational profile analysis (LSM 510 software). The relative fluorescence intensity of the membrane representing the PLL density on the APA membrane was plotted as a function of PLL reaction conditions.

## 6.4 Results

### 6.4.1 PLL-genipin reaction and fluorescent characteristics of its products

The reaction between PLL and genipin occurred gradually after mixing the two solutions, and could be observed by changes in the physical appearance of the mixture, from clear and colorless to a viscous and blue solution. To investigate the fluorogenic activity of this reaction, the fluorometric spectra of PLL, genipin, and the reaction mixture were studied. Results showed that two peaks appeared at the wavelengths of approx 267 nm and 370 nm in the absorption spectra of the mixture, which were otherwise absent or very weak in the spectra of the controls (genipin and PLL individually) (Fig. 6.1). After the genipin-PLL reaction, there is a large increase in fluorescence intensity of the emission spectrum with maximum emission at 453 nm. This increase reflects the chemical modifications of PLL and genipin. In contrast, other polymers used in this study including alginate, pectin and PEG did not show this fluorescence peak (data not shown).

### 6.4.2 Visualization of PLL membrane in genipin-treated APA microcapsules under CLSM

The APA microcapsules and their PLL membrane were visualized using CLSM. It was found that under the regular transmission light channel, the microcapsules before and after genipin treatment looked similar (Fig. 6.2 a, c). However, they differed when viewed under the fluorescent channel (Fig. 6.2 b, d). The genipin-treated PLL layer in the microcapsule wall was clearly identified by the appearance of a bright circle circumscribing each microcapsule core. Fluorescence from the non-genipin treated microcapsules, conversely, was barely detectable under the same CLSM settings. Moreover, Figure 6.2 e-f exemplifies the effects of the alginate/PLL interaction and the structural changes in the microcapsule membrane under varied reaction conditions. When a low concentration of PLL (0.5 mg/mL) and a short coating time (10 min) were used (Fig. 6.2 e), the fluorescent signals of the microcapsule membrane were weak. Increasing PLL concentration and exposure resulted in stronger fluorescence intensities of the membrane (Fig. 6.2 f, g). Figure 6.2 h shows the fluorescence profile corresponding to the line across the optical and equatorial section of the microcapsules shown in Figure 6.2 g. It was clear that the intensity of the inner alginate cores

was similarly low when compared to the background signals, whereas peaks corresponding to the fluorescence of the microcapsule membrane appeared, with the relative intensity attaining 150.

#### **6.4.3 Characterization of APA microcapsules using genipin**

To evaluate the influence of PLL coating variables on the APA microcapsule morphology, PLL membrane thickness and PLL binding density, APA microcapsules were prepared using different concentrations of PLL for varied periods of incubation time and examined by CLSM after genipin treatment. The results are described individually as follows for each characteristic of APA microcapsules: swelling behavior, PLL membrane thickness, and PLL binding density.

##### **a) Effects of PLL solution concentration and coating time on APA microcapsule swelling**

Results showed that the diameters of the microcapsules increased inversely with the concentration of PLL solution and incubation time (Fig. 6.3 a, c). When coated with PLL at a low concentration (0.5 mg/mL), the APA microcapsules swelled substantially, from  $508.4 \pm 10.7 \mu\text{m}$  of the original Ca-alginate beads to  $783.3 \pm 26.4 \mu\text{m}$ . For high PLL exposure (5.0 mg/mL, 10 min), shrunken and even collapsed microcapsules were observed (see Fig. 6.2 g), with the diameter reduced to  $482.1 \pm 15.6 \mu\text{m}$  (Fig. 6.3 a). Increasing incubation time in PLL solution did not drastically alter the morphology of the microcapsules, although a slight decrease in diameter was found (Fig. 6.3-c). These results implied that optimizing the PLL coating variables could limit the microcapsule swelling, which is indicative of the formation of dense alginate-PLL complex membrane<sup>162</sup>.

##### **b) Effects of PLL solution concentration and coating time on thickness of PLL layer**

Membrane thickness, a reflection of the distribution of PLL molecules along the microcapsule surface and their diffusion into the microcapsule cores, was found dependent on the PLL concentration and coating time during complexation. The thickness of the PLL layer increased linearly with the concentration of PLL solution used (Fig. 6.3 a), except for the highest level of PLL (5.0 mg/mL), at which the APA membrane became wrinkled and the

APA microcapsules tended to collapse. Extended time of interaction with PLL (1.0 mg/mL) from 10 to 120 min considerably increased the membrane thickness (9.4 versus 21.4  $\mu\text{m}$ ) (Fig. 6.3-c). A similar trend with respect to the influence of the alginate-PLL complex was previously reported by several groups using fluorescence labeling method, although the reported thickness of the similarly prepared PLL membrane was higher in the literature ( $>20 \mu\text{m}$ )<sup>113,179,188</sup>.

#### **c) Effects of PLL solution concentration and coating time on binding density of PLL layer**

We evaluated the effects of PLL solution concentration and coating time on PLL binding density in the membrane. Result shows that the fluorescence intensity of the membrane, representing the density of PLL deposition on the microcapsule wall, is directly proportional to the concentration of PLL solution used for coating ( $R^2 = 0.938$ ) (Fig. 6.3 b). Weak fluorescent signals were detected ( $43.6 \pm 10.2$ ) for the low PLL exposure (0.5 mg/mL, 10 min). When coated with concentrated PLL (5.0 mg/mL), the membrane exhibited strong fluorescence ( $163.0 \pm 17.0$ ), demonstrating denser PLL deposition in the microcapsule membrane. On the other hand, Figure 6.3 d shows that the membrane fluorescence intensified, however only moderately, under extended exposure to PLL solution, from  $64.8 \pm 9.0$  in 10 min to  $89.0 \pm 12.0$  in 120 min. These results corroborated with those of earlier investigations using prior labeled PLL<sup>113,179</sup>.

#### **6.4.4 Rearrangement of PLL layer in APA microcapsules during storage**

Using genipin we investigated the fate of the bound PLL in microcapsules during storage. For this, APA microcapsules were stored in physiological saline up to three weeks prior to genipin treatment and CLSM observation. It was found that the membrane thickness of the microcapsules made by 10 min of incubation in PLL solution (1.0 mg/mL) faintly changed over the 3-week storage (Fig. 6.3 e). For the APA microcapsules coated for 60 min, the PLL membrane doubled in thickness during the initial 5-day storage and further expanded to approx 18  $\mu\text{m}$  in the subsequent two weeks but did not increase further for the remainder of the experiment. Despite these shifts, the overall thickness of the PLL layer remained less than 20  $\mu\text{m}$  (Fig. 6.3 e), which was not consistent with previous reports<sup>113,188</sup>. Furthermore, the

relative fluorescence intensity of the PLL membrane slightly fluctuated among the microcapsules with different storing history (Fig. 6.3 f). An increase in the intensity occurred for those capsules with a storage history of no more than 5 days, after which the membrane intensity gradually declined in the subsequent two weeks.

#### **6.4.5 Evaluation of polyamine membrane in other microcapsules**

To assess the feasibility of using genipin to characterize other microcapsule membranes, different kinds of polyamine-based microcapsules were prepared. The subsequent genipin treatment and CLSM studies were performed using the above-described method. Figure 6.4 exemplifies the fluorescence intensity of the polyamine membrane in different microcapsule formulations after genipin treatment, in which the profiles correspond to the microcapsules shown in the inserts. Similar to the APA microcapsules, fluorescent and shell-like membranes were distinguished in the AP-PEC-PA, AP-PEG-A, AC, AC-PEG-A and AC-PEG-PA microcapsules. A sharp exterior delimitation and a slight inward spreading of the fluorescent membrane were observed. Table 6.1 summarizes the fluorescence intensity and the thickness of the polyamine membranes in six different microcapsule formulations. In contrast to the thin membrane in the PLL-based microcapsules ( $<9 \mu\text{m}$ ), chitosan formed a relatively thicker complex with alginate ( $>11 \mu\text{m}$ ), and the fluorescence intensity of the membrane was higher, attaining  $246.9 \pm 10.8$ ,  $167.6 \pm 12.0$  and  $253.9 \pm 2.3$  for the AC, AC-PEG-A and AC-PEG-PA microcapsules, respectively.

### **6.5 Discussion**

Genipin is known to react rapidly with primary amines<sup>289,381,382</sup>. Although visibly evident, the detailed mechanism of the polyamine-genipin reaction remains under investigation<sup>245,292</sup>. It has been suggested that the amino groups in the polycation molecules initiated a nucleophilic attack at C-3 of genipin, resulting in the opening of the dihydropyran ring and the formation of a nitrogen-iridoid as well as aromatic intermediates after dehydration. Radical-induced polymerization occurred in the subsequent steps, creating highly conjugated heterocyclic genipin derivatives<sup>245</sup>, which may thus explain the fluorescent characteristics exhibited after the PLL-genipin reaction.

Genipin treatment was performed by simply immersing the microcapsules in a genipin solution under mild conditions. The small genipin molecules can freely penetrate into the microcapsule membranes and interact with polyamines bound to the alginate gels. This treatment did not noticeably affect the morphology of the microcapsules (Fig. 6.2); they remained intact and spherical in shape, although gradual development of blue color in the microcapsules was observed.

Results from CLSM examination confirm the formation of new fluorescent conjugates and demonstrate the polyamine distribution within the microcapsule membrane. The thin PLL layer revealed that the PLL molecules were bound to the periphery of the alginate cores and that their diffusion was restricted to a small penetration depth ( $\sim 10 \mu\text{m}$ ) (Fig. 6.3 and Tab. 6.1). This was in accordance with investigations by Ma *et al*<sup>241</sup> and Ross *et al*<sup>144</sup>. Furthermore, it was clearly shown in our study that chitosan penetrated into the alginate gel to a larger extent and formed a relatively thicker membrane, which was consistent with previous reports using radio-labeling and indirect chromatographic methods<sup>235,243</sup>. Vandebossche *et al* proposed that the PLL membrane in the APA microcapsules would perpetually rearrange itself with time<sup>113,188</sup> due to the diffusion of the PLL molecules, leading to a thicker membrane ( $\sim 20 \mu\text{m}$  on day 1 to  $\sim 119 \mu\text{m}$  on day 7 of storage)<sup>188</sup>. Our results showed that this is not the case; the rearrangement of the bound PLL was very limited (Fig. 6.3-e). In the earlier method, PLL was fluorescence-labeled prior to coating<sup>188</sup>. This may reduce the functionalities ( $-\text{NH}_2$ ) of PLL<sup>179</sup>, leading to weak binding to alginate gels. Furthermore, there may be possible migration of non-firmly bound fluorescence markers liberating from PLL molecules<sup>320,379</sup>. In the present study, genipin, which is essentially non-fluorescent in its free form, was used to covalently and selectively couple with the PLL molecules already bound to the alginate beads. As such, the proposed characterization approach is highly likely to overcome the limitations found in the aforementioned method.

Although the membrane thickness and coating density substantially affect the properties and performance of the microcapsules, these parameters are difficult to quantify. Discrepant results were reported; for example, Ma *et al*<sup>241</sup> and Ross and Chang<sup>144</sup> found that APA microcapsules had a wall thickness of 11-13  $\mu\text{m}$ , whereas others reported a membrane thickness of 40–120  $\mu\text{m}$ <sup>113,179,188</sup> using prior labeling methods. Other destructive methods such as cross-sectioning or mass measurement are time and labor consuming<sup>241,315</sup>. Previous

attempts to visualize and assess microcapsule membranes have, therefore, had many shortcomings.

To overcome these limitations, our new method uses fluorogenic genipin treatment without prior labeling of polymers. It enables the visualization and quantification of polyamine microcapsule membrane rapidly, easily and effectively. Because genipin is highly selective for coupling with primary amines<sup>289,381</sup>, in the evaluated microcapsule systems, only PLL and chitosan bound to the alginate beads are likely candidates for this reaction; Specifically, the covalently coupled genipin-polyamine conjugates formed in situ within the microcapsule wall is the only fluorescent material in the system. Free genipin and other –OH and/or –COOH containing polymers used in this study, such as alginate, PEG and pectin, did not contribute to the fluorescent emission. Hence, the detected fluorescence revealed solely the distribution of these polyamines in the microcapsules and can be assessed without interference from other materials in the system. The dependence of the generated fluorescence on the polyamines presented provides a non-destructive and quantitative means of characterizing the microcapsule membranes. Furthermore, using this approach only little sample treatment is required; it is thus possible to quickly determine the membrane thickness and the density of polyamine membrane during the process of development and optimization on a routine basis, so as to facilitate the understanding and improvement of microcapsule performance.

The approach described in this paper may be used for a variety of other microcapsule formulations and biomaterials. For example, gelatin, a partially denatured protein containing primary amines, has been reported to interact with genipin<sup>304</sup>, which makes it a promising candidate for our approach in many applications in forms of capsules for sustained release<sup>383</sup>, scaffold for tissue repairing<sup>301</sup>, and nanoparticles for tumor targeted gene delivery<sup>384</sup>. Other polyamine candidates for the presented method include polyamido amide (PAMAM) dendrimers, which have recently become a subject of intense interdisciplinary research efforts as a new targeted drug delivery system<sup>385</sup>. Assuming that the –NH<sub>2</sub> terminals at the branches of PAMAM dendrimers interact with genipin, this fluorescence generation strategy may provide a valuable template for drug targeting purposes.

In summary, results of this research demonstrate a simple, sensitive and robust method of using fluorogenic genipin for the characterization of microcapsule membranes, a superior approach that overcomes the challenges of previous methods and has potential to be used for a variety of applications.

## **6.6 Acknowledgements**

We acknowledge the financial support from Canadian Institutes of Health Research (CIHR). Postdoctoral fellowship and postgraduate scholarships from Natural Sciences and Engineering Research Council (NSERC) of Canada and Fonds Québécois de la Recherche sur la Nature et les Technologies (FQRNT) are also appreciated. We wish to thank Z-Q Chen for his technical suggestions.

Table 6.1. Thickness and relative fluorescence intensity of polyamine coating on genipin-treated microcapsules †

Microcapsules	APA*	AP-PEC-PA*	AP-PEG-A	AC	AC-PEG-A	AC-PEG-PA
Thickness (μm)	4.5±0.6	6.3±0.6	8.6±1.4	11.6±1.7	15.3±1.4	16.5±1.1
Fluorescence intensity	111.4±15.5	160.3±17.4	110.6±11.8	246.9±10.8	167.6±12.0	253.9±2.3 #

† Data represent the mean ± s.d. ( $n=10$ )

\* Genipin treatment was carried out at room temperature. # Maximum detectable intensity attained

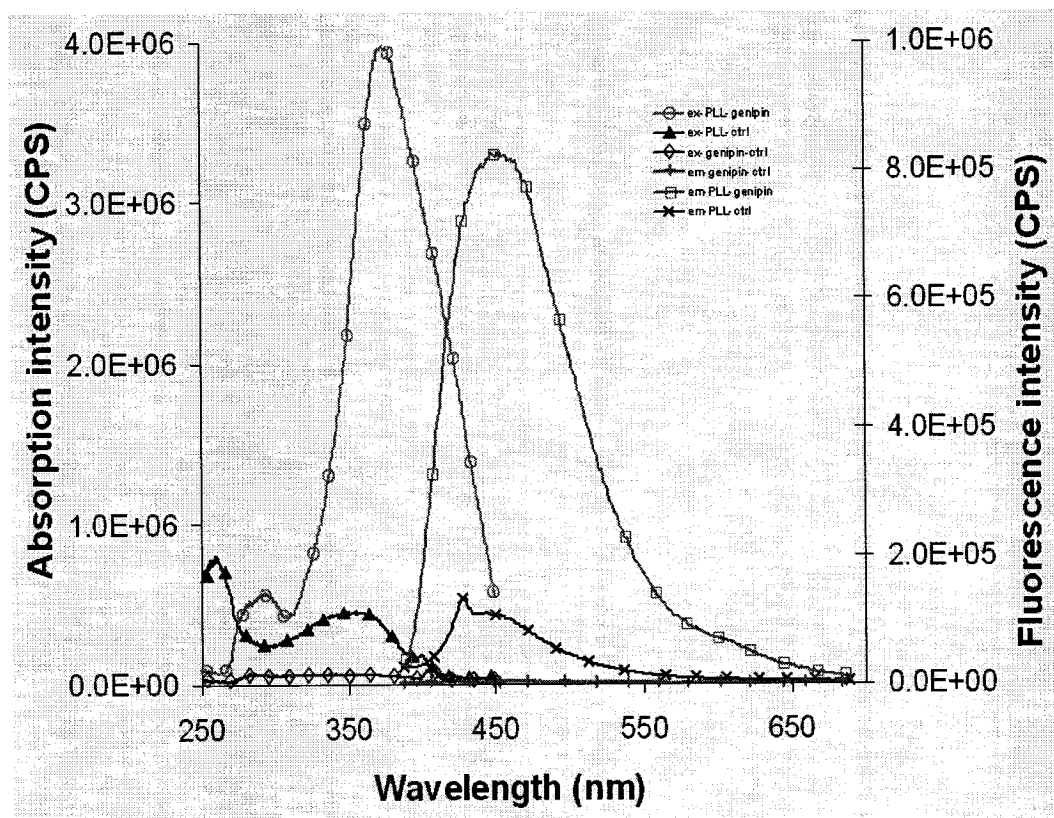


Figure 6.1. Absorption and fluorescence spectra of PLL, genipin, and their reaction mixture. The unit of CPS refers to as counts per second.

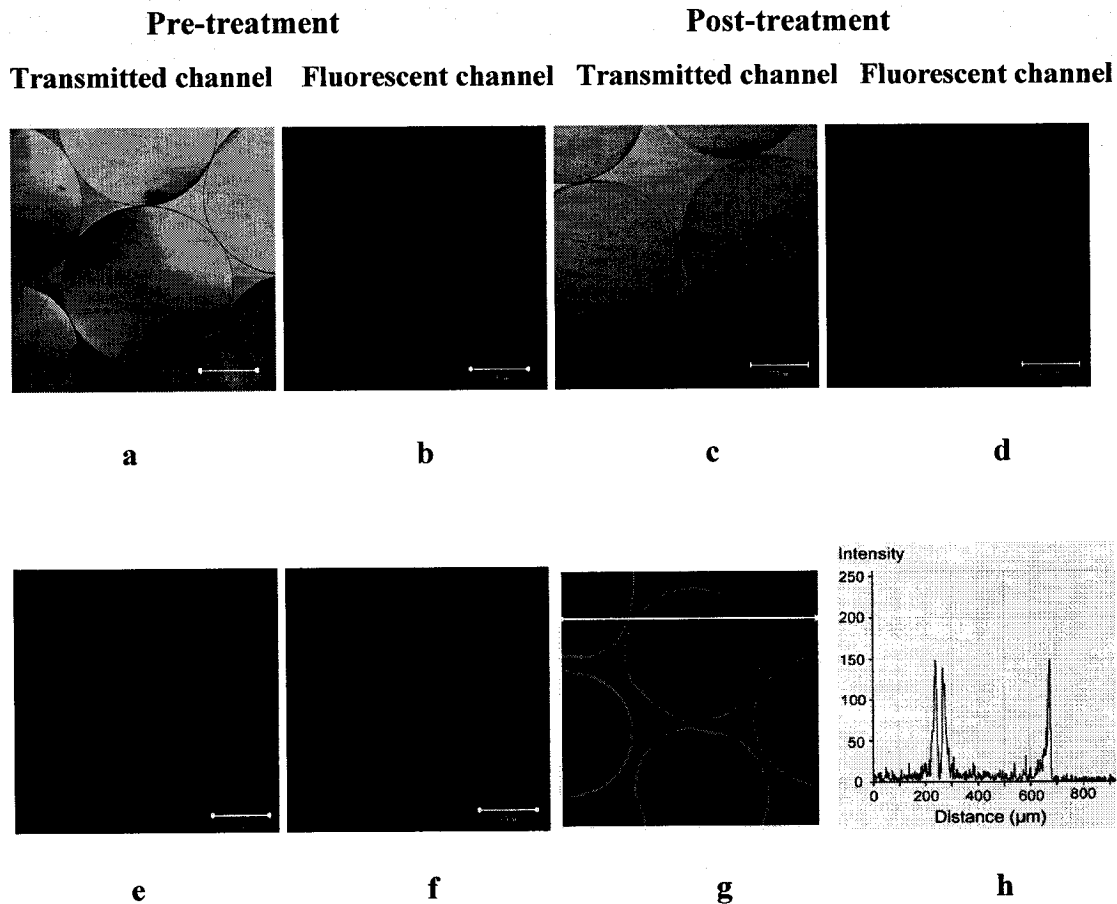


Figure 6.2. CLSM images of APA microcapsules and representative fluorescence intensity profile. a-d, microcapsules made by 2.5 mg/mL PLL x 10 min prior to and post genipin treatment viewed in the transmitted channel and the fluorescent channel. e-g, microcapsules with varied PLL binding viewed in fluorescence channel after genipin treatment. e, 0.5 mg/mL PLL x 10 min; f, 1.0 mg/mL PLL x 60 min; and g, 5.0 mg/mL PLL x 10 min. h depicts the fluorescence intensity profile corresponding to the white line in g. Note the presence of the green circles around the alginate beads that were PLL membranes. Bars represent 200  $\mu\text{m}$ .

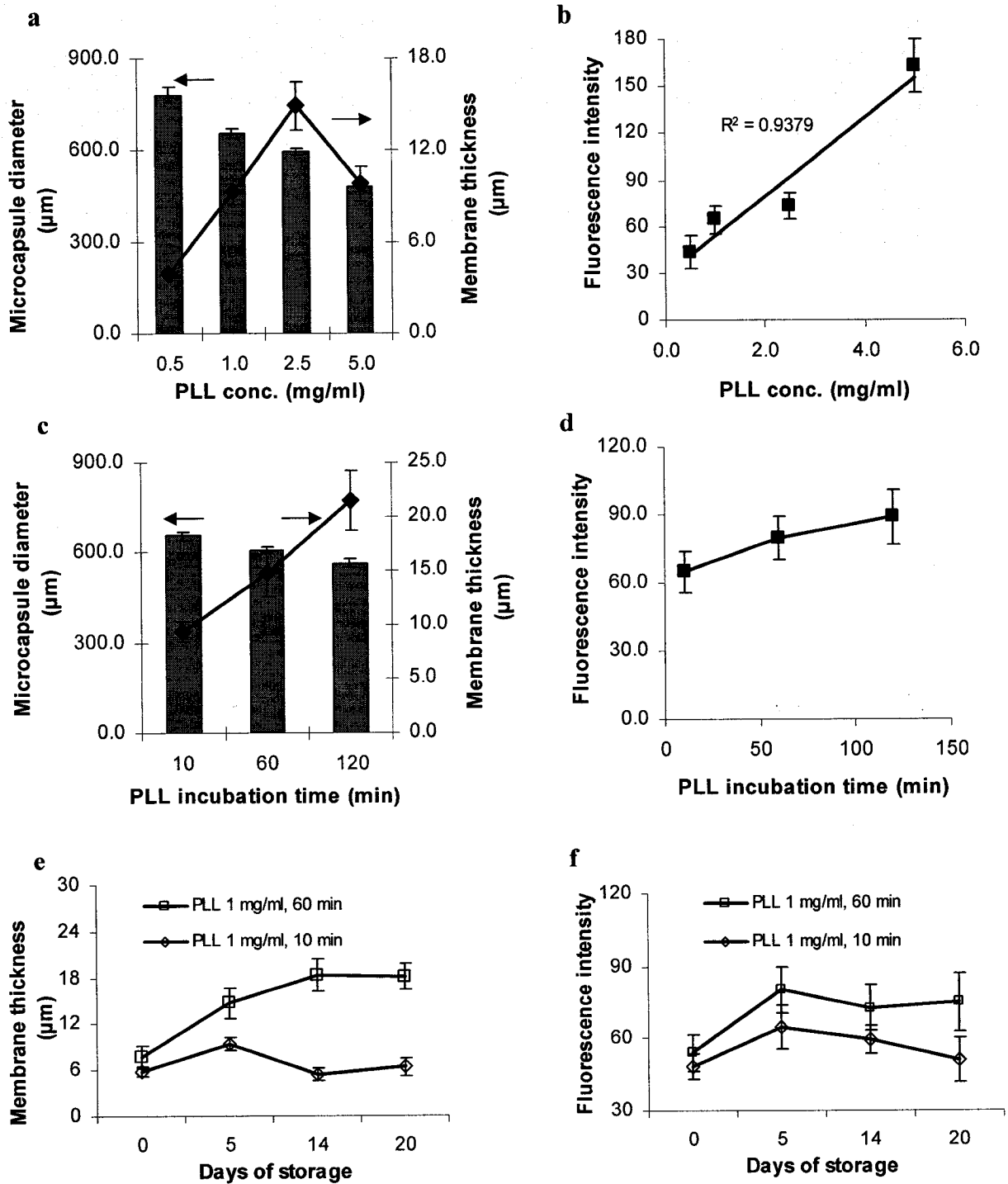
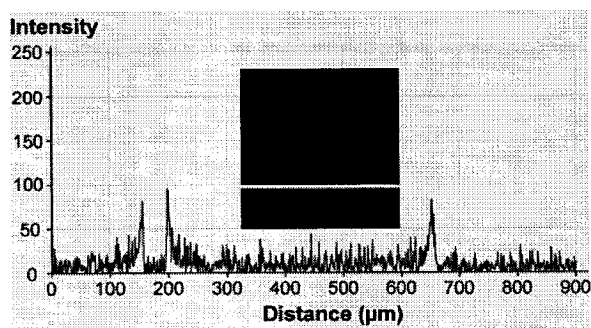
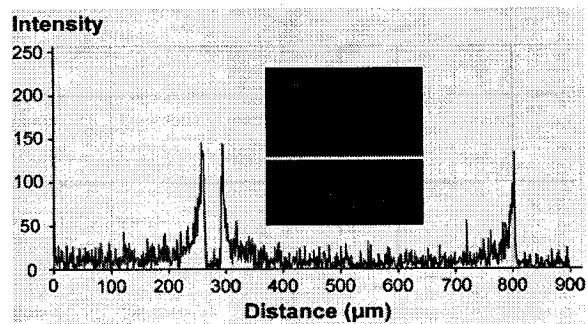


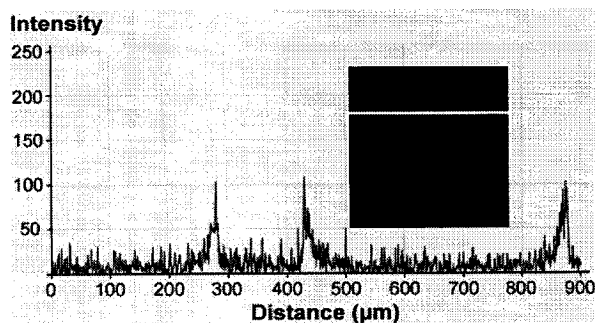
Figure 6.3. Quantification of PLL binding to APA microcapsules. (a, b) Dependence of PLL concentration on (a) APA microcapsule diameter and PLL membrane thickness, and (b) fluorescence intensity; (c, d) dependence of PLL incubation time on (c) APA microcapsule diameter and PLL membrane thickness, and (d) fluorescence intensity; and (e, f) effects of storage of APA microcapsules in PS on PLL membrane (e) thickness, and (f) fluorescence intensity. Data represent the mean  $\pm$  s. d. ( $n=10$ ).



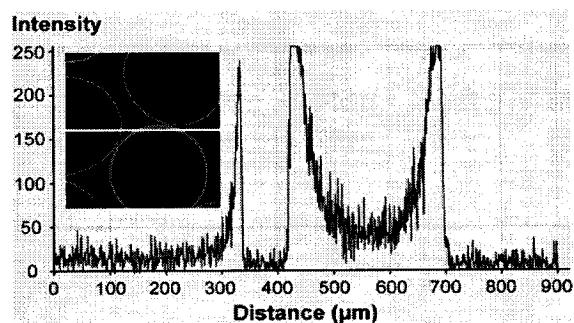
a



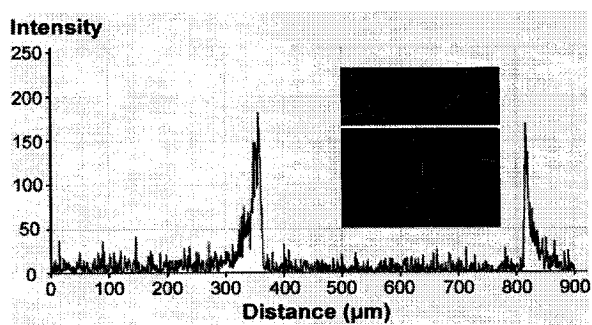
b



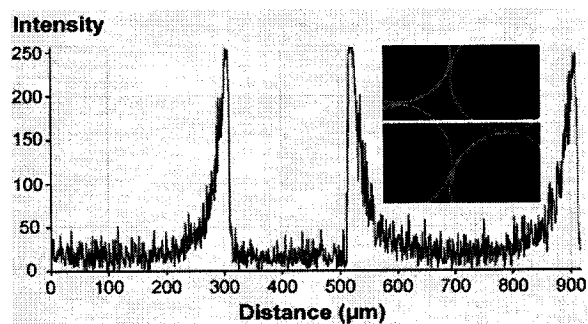
c



d



e



f

Figure 6.4. Fluorescence intensity profiles corresponding to a line across the optical equatorial sections of various polyamine-based microcapsules after genipin treatment. The tested microcapsules are: a, APA; b, AP-PEC-PA; c, AP-PEG-A; d, AC, e, AC-PEG-A; and f, AC-PEG-PA microcapsules.

**Genipin cross-linked alginate-chitosan microcapsules: Membrane characterization and optimization of cross-linking reaction**

Hongmei Chen, Wei Ouyang, Bisi Lawuyi and Satya Prakash\*

*Biomedical Technology and Cell Therapy Research Laboratory*

*Department of Biomedical Engineering and Physiology, Artificial Cells and Organs Research Centre, Faculty of Medicine, McGill University, Montreal, Quebec, H3A 2B4 Canada.*

\*Corresponding author: Tel: 514 398-3676; Fax: 514 398-7461;  
Email: satya.prakash@mcgill.ca

---

**Preface:** The noninvasive and *in situ* method, described in the past two chapters, was used in the present study to characterize details of the GCAC membrane without any physical or chemical modifications on the samples. The effects of reaction variables on the degree of cross-linking and the membrane thickness were elucidated, and the optimum cross-linking condition was disclosed.

Original article published in *Biomacromolecules*, 7: 2091-2098 (2006)

## 7.1 Abstract

The genipin cross-linked alginate-chitosan (GCAC) microcapsule, composed of an alginate core with a genipin cross-linked chitosan membrane, was recently proposed for live cell encapsulation and other delivery applications. This article for the first time describes the details of the microcapsule membrane characterization using a noninvasive and *in situ* method without any physical or chemical modifications on the samples. Results showed that the cross-linking reaction generated fluorescent chitosan-genipin conjugates. The cross-linked chitosan membrane was clearly visualized by confocal laser scanning microscopy (CLSM). A straightforward assessment on the membrane thickness and relative intensity was successfully achieved. CLSM studies showed that the shell-like cross-linked chitosan membranes of approx 37  $\mu\text{m}$  in thickness were formed surrounding the microcapsule. The reaction variables, including cross-linking temperature and time significantly affected the fluorescence intensity of the membranes. Elevating the cross-linking temperature from 4 to 37 °C drastically intensified the membrane fluorescence, suggesting the attainment of a high degree of cross-linking on the chitosan membranes. Extended cross-linking time altered the cross-linked membranes in modulation. Although genipin concentration and cross-linking time had little effects on the membrane thickness, cross-linking at higher temperatures tended to form relatively thinner membranes.

**Key Words:** microcapsule, chitosan, alginate, genipin, cross-linking, CLSM, AFM

## 7.2 Introduction

Microencapsulation has received increasing attention over the past two decades in various fields of both fundamental research and industrial applications<sup>19,103,372,386</sup>. Among others, cell encapsulation for therapy has generated considerable excitement as it enables the transplantation of live nonautologous cells in the absence of immuno-suppression by providing protection through a physical barrier. Potential applications include the treatment for enzyme deficiencies, diabetes, liver and kidney failure, cancers and many other diseases<sup>4,9,19,68,70,78,83,89</sup>. In all of the applications, the effectiveness of the immuno-protection

achieved by microencapsulation greatly depends on the integrity of the capsular membrane. The microcapsule membranes should exhibit sufficient structural stability to bear environmental constraints during processing, implantation, as well as both short-term and long-term *in vivo* utilization. The alginate-poly-L-lysine-alginate (APA) membrane<sup>69</sup> is widely investigated for cell encapsulation due to the gentle preparation process. These APA microcapsules have been used successfully to limit the major immuno-rejection problems related to the use of live cells and bacteria in some animal models<sup>4,64,83,170,387</sup>. However, problems regarding membrane instability arise over long-term *in vivo* conditions<sup>22,156,171,388,389</sup>. This mechanical insufficiency was associated with activation of the complement system, degradation of the poly-L-lysine coating, and destabilization of the alginate core matrix; accordingly, graft survival was usually limited<sup>156</sup>. Therefore, there is clearly a need for the development of stronger microcapsules that can protect the cells for a long time.

As an alternative to the APA system, we have proposed a novel alginate-chitosan complex microcapsule covalently cross-linked by naturally derived genipin<sup>390</sup>. Genipin is an aglucone of geniposide extracted from gardenia fruits<sup>282</sup>. It has been used as a traditional herbal medicine and natural colorant in the food and fabric industries<sup>288</sup>. Genipin has been reported to bind with biopolymers such as chitosan and gelatin, leading to covalent coupling<sup>291,295,298</sup>. Rather than the commonly used synthetic cross-linking reagents which have a recognized disadvantage of potential cytotoxic effects<sup>263,278,375,391</sup>, genipin is derived from herbal plant and has been reported 5,000 to 10,000 times less cytotoxic than glutaraldehyde<sup>295</sup>. This encouraged the use of genipin in cell encapsulation. Results from our earlier study suggested the suitability of the novel genipin cross-linked alginate-chitosan (GCAC) microcapsule for the encapsulation of live engineered bacteria<sup>390</sup>. Recent research on the fluorogenic characteristics of genipin showed the usefulness of genipin on the characterization of microcapsule membranes<sup>239,323</sup>. The objective of this paper is to characterize the cross-linked chitosan membrane on the GCAC microcapsules and optimize the cross-linking reaction using a novel, noninvasive, and *in situ* method by confocal laser scanning microscopy (CLSM).

### 7.3 Materials and methods

### **7.3.1 Chemicals**

Sodium alginate (low viscosity) was purchased from Sigma-Aldrich, USA. Chitosan (low viscosity, 73.5 % degree of deacetylation and  $M_v=7.2 \times 10^4$ ) and genipin were obtained from Wako BioProducts, USA. All other reagents and solvents were of reagent grade and used as received without further purification.

### **7.3.2 Preparation of Genipin Cross-linked Alginate-Chitosan (GCAC) Microcapsules**

The microcapsules were prepared as previously described<sup>390</sup>. Briefly, droplets of a sodium alginate solution (15 mg/mL) were generated by an encapsulator (Inotech. Corp.) and gelled in a stirred  $\text{CaCl}_2$  solution (11 mg/mL). The Ca-alginate beads were then coated for 30 min in a chitosan solution of 10 mg/mL containing  $\text{CaCl}_2$  (11 mg/mL), producing alginate-chitosan (AC) microcapsules, and subsequently cross-linked by immersing the AC microcapsules in an aqueous genipin solution. The resulting genipin cross-linked alginate-chitosan (GCAC) microcapsules were washed and collected. Ca-alginate beads with genipin treatment (AG) and AC microcapsules without genipin treatment were also prepared in a similar process and used as controls.

### **7.3.3 Characterization of Microcapsules by Confocal Laser Scanning Microscopy (CLSM)**

The morphology and internal structure of the microcapsules were investigated using a Laser Scanning Confocal Imaging System (Zeiss LSM 510, Carl Zeiss, Jena, Germany) equipped with a Zeiss Axiovert 100M microscope. For image acquisition, the microcapsules in storage solution (deionized  $\text{H}_2\text{O}$ ) were directly placed in a chambered coverglass system (Lab-Tek). A 488 nm argon laser was used in the single green fluorescence mode and the fluorescence was detected with the filter block BP500-550IR. The other channel was set to the transmitted light detector. The focal planes were set at the equatorial sections of the microcapsules. All images were acquired at constant microscopic settings under computer control in order to obtain comparable images. The fluorescent intensity profile corresponding to a line across the focal plane of the microcapsules was acquired by computational profile analysis (LSM 510 software).

#### **7.3.4 Atomic Force Microscopic (AFM) Observation**

The internal structure of the GCAC microcapsules was characterized by AFM (Digital Instrument, Veeco metrology Group, USA). The samples were cross-linked by genipin at the concentration of 5.0 mg/mL for 72 h at room temperature. After dehydration by gradient acetone, the microcapsules were embedded in epoxy resin and cross-sectioned by ultra microtome. The AFM topographic images were obtained by scanning the cross-sectioned microcapsules using a sharpened tip in contact mode at a rate of 1.0 Hz. The roughness profiles and the membrane thickness were analyzed using the equipped NanoScope Image software.

#### **7.3.5 Effects of Reaction Variables and Optimization of Cross-linking Process**

To evaluate the influences of cross-linking conditions on the microcapsule membrane, three control factors including the genipin concentration, cross-linking temperature, and time were selected to vary. For each factor, at least three levels were chosen to cover a wide range of variation. The factors and their levels were listed in Table 7.1. The microcapsules were prepared accordingly, and at least 10 beads per batch were assessed by CLSM. The relative fluorescence intensities along the microcapsule membranes (500  $\mu\text{m}$  in length) were analyzed, and the membrane thickness was measured using LSM 510 software. A statistical analysis using range tests<sup>392</sup> was performed to determine the relative magnitude of the control factors and estimate the optimum levels with regard to generating microcapsule membranes with highest cross-linking degree. The degree of confidence was set at 95 %.

### **7.4 Results**

#### **7.4.1 Formation of the GCAC Microcapsules and Cross-linking of Chitosan by Genipin**

The preparation of the GCAC microcapsules involved a three-step procedure, all under mild and aqueous conditions. The cross-linking was achieved by the interaction of genipin with the chitosan bound on the alginate beads, and the chitosan-genipin conjugates were formed within the membrane. Figure 7.1 displays the schematic diagrams for the structures of the materials used in microcapsule preparation and the predicted molecular

structure of the GCAC microcapsules. It was found that the cross-linking treatment did not noticeably affect the morphology of the microcapsules. They remained intact, spherical in shape, and similar in diameter ( $471.9 \pm 9.3 \mu\text{m}$  for the GCAC beads) and had high homogeneity (Fig. 7.2) though an apparent color change was observed. In particular, the GCAC microcapsules turned from white to dark blue in color if cross-linked at  $37^\circ\text{C}$ , to light blue at  $20^\circ\text{C}$ , and to faintly yellow-blue at  $4^\circ\text{C}$ .

#### 7.4.2 Characterization of GCAC Microcapsule Membranes by CLSM

To visualize the microcapsules and their membranes in the same imaging field, CLSM was employed with one channel set to the single green fluorescence mode and the other to the transmitted light detector. Figure 7.2 depicts the CLSM images of the GCAC microcapsules in comparison to the control AC and AG beads. Under the regular transmission light channel, microcapsules looked similar regardless of genipin cross-linking (Fig. 7.2, upper row), with the exception of considerable swelling of the AG beads (Fig. 7.2e). When viewed under the fluorescent channel, the alginate cores were shown as the black interior of the microcapsules, whereas the genipin cross-linked chitosan coating was clearly identified by the appearance of distinguishing bright circles, circumscribing the alginate cores (Fig. 7.2b). In contrast, neither the control AC microcapsules without genipin cross-linking (Fig. 7.2d) nor the control AG beads without chitosan coating (Fig. 7.2f) fluoresced under the same microscope settings. It was clear that the fluorescent signals were generated from the chitosan-genipin reaction products.

Figure 7.3 shows representative CLSM images of the GCAC microcapsules viewed in the fluorescence channel. Despite signals being weak or strong, the fluorescent cross-linked chitosan membranes were successfully imaged for all of the GCAC microcapsule samples prepared in this study. Deposited homogeneously around the microcapsules, the cross-linked chitosan formed a shell-like membrane near the surface of the microcapsule, with stronger fluorescence intensity at the external border of the membrane (Figure 7.4). Also clearly evidenced, the relative fluorescence intensity of the microcapsule membranes was correlated with the cross-linking conditions. For example, the fluorescence intensity of the membrane was high ( $\sim 250$ ) if cross-linked at  $37^\circ\text{C}$  (Fig. 7.4a); it decreased by roughly half ( $\sim 120$ ) when reacted at  $20^\circ\text{C}$  (Fig. 7.4b). If the cross-linking temperature dropped to  $4^\circ\text{C}$ , the

intensity was significantly lower ( $\sim 45$ ) (Fig. 7.4c). The 3-D diagrams shown in Figure 7.5 further illustrate this trend. The intensity of the interior alginate cores, shown in dark blue, was as low as the background signals ( $<10$ ), while the fluorescence of the membrane was strikingly higher. The higher the cross-linking temperature and the longer the reaction time, the greater level of the intensity exhibited by the microcapsule membranes, denoting stronger fluorescence (Fig. 7.5).

#### **7.4.3 Effects of Reaction Parameters on the Fluorescence Intensity of the Cross-linked Chitosan Membranes on the GCAC Microcapsules**

To assess the effects of the cross-linking process on the microcapsule membranes, three control factors including genipin concentration, cross-linking temperature and time were selected to vary (Table 7.1). The corresponding fluorescence intensities of the microcapsule membranes were analyzed semiquantitatively and plotted in Figure 7.6. It appeared that when cross-linked at 4 °C, the membranes displayed low fluorescence ( $<50$ ) which was hardly altered by the extended reaction time and the use of concentrated genipin (Fig. 7.6a). At 20 °C, extending the reaction time led to steady increase in the fluorescence intensity of the membranes, indicating more cross-linking points were formed after a longer reaction time (Fig. 7.6b). In addition, the membrane fluorescence increased rapidly at 37 °C and attained a saturated level after 24 h of cross-linking (Fig. 7.6c).

To further evaluate the effects of the cross-linking variables, statistical range tests<sup>392</sup> were performed to determine the relative effect of each control factor. Table 7.2 shows that the ranges of the cross-linking temperature and reaction time are higher than the corresponding confidence limits, suggesting that these two selected factors significantly affected the fluorescence intensity of the membranes ( $p < 0.05$ ), whereas the effect of genipin concentration was insignificant (range  $<$  confidence limit). Results also showed that the cross-linking temperature, with the highest range of 161, was the dominant factor affecting the extent of the reaction (Table 7.2). As can be seen in Figure 7.7a, elevating the cross-linking temperature from 4 to 37 °C intensified the membrane fluorescence at an exponential rate ( $r = 0.998$ ). The factor of reaction time changed the cross-linked membrane in modulation (Fig. 7.7b). The fluorescence intensity increased quickly during the initial 24 h of cross-linking and slowed thereafter until the end of the experiment, the trend of which well fit with a

logarithmic correlation at the confidence degree of 95 % ( $r = 0.946$ ). On the other hand, varying the genipin concentration within the experimental span had little effect on the fluorescence of the cross-linked membranes, though slightly stronger fluorescence could be attained by using 2.5 mg/mL genipin (Fig. 7.7c).

#### **7.4.4 Membrane Thickness of the GCAC Microcapsules**

Experiments were also designed to investigate the membrane thickness of the GCAC microcapsules and the results were summarized in Table 7.3. Results from statistical range tests (Table 7.4) showed that the range for the factor of cross-linking temperature was higher than the experimental confidence limit (14.4 versus 2.2), suggesting a significant effect of reaction temperature on the membrane thickness. At a low temperature (4 °C), the microcapsules tended to form relatively thicker cross-linked membranes (44.8  $\mu\text{m}$  in average); whereas slightly thinner GCAC membranes were formed at higher temperatures. Conversely, allowing for random experimental errors the other two factors including genipin concentration and reaction time did not significantly affect the membrane thickness (Table 7.4).

#### **7.4.5 AFM Observations on the GCAC microcapsules**

AFM studies were carried out to further characterize the inner structure of the GCAC microcapsules. The topography of the cross-sectioned GCAC microcapsule is shown in Figure 7.8. It was clear that the structure of the genipin cross-linked chitosan membrane was significantly different from the alginate core and the outer epoxy resin used for embedment; a distinctly rough structure was seen in the area of the microcapsule membrane, and an exceedingly smooth pattern was shown in the microcapsule core where the pores of the Ca-alginate gel were filled with epoxy. The thickness of the chitosan coating measured by AFM was  $32.1 \pm 5.0 \mu\text{m}$  ( $n=3$ ).

### **7.5 Discussion**

As described earlier, the success of live cell encapsulation and delivery is chiefly dependent on the ability of microcapsules to protect the enclosed cells. The microcapsule membranes are of importance for addressing the complex problems associated with *in vitro*

encapsulation and *in vivo* delivery for therapy. Earlier research showed that stronger microcapsules survived longer *in vivo*, which in turn would lead to a prolonged delivery of the therapeutic molecules and a greater efficiency of the cell encapsulation strategy<sup>389</sup>. Aiming to produce microcapsules with improved stability, covalent cross-linking was employed to strengthen the chitosan membrane using a naturally-derived cross-linker, genipin<sup>390</sup>. As shown in Figure 7.1-b, the hypothetical structure of this microcapsule includes the calcium-alginate core formed by ionotropic gelation, chitosan coating through complex coaervation, as well as the covalent cross-linking of chitosan by genipin. In the cross-linking reaction, genipin, a small molecule, can freely diffuse through the alginate-chitosan complex membrane and interact with the chitosan bound to the alginate gel. Specifically, the ester groups in genipin interact with the amino groups in chitosan leading to the formation of secondary amide linkages<sup>291</sup>. Additionally, the amino groups of chitosan initiate nucleophilic attacks at genipin, resulting in the opening of the dihydropyran ring followed by a number of reaction steps including the formation of nitrogen-iridoid, aromatic intermediates, as well as highly conjugated heterocyclic genipin-chitosan derivatives<sup>304</sup>. Eventually a three dimensional network structure is created within the microcapsule membranes.

The CLSM images of the GCAC microcapsules convincingly supported this hypothetical structure. Since genipin only interacts with primary amines<sup>382</sup> and alginate was not the target for genipin cross-linking (Fig. 7.2), the presence of bright rings validated the formation of new fluorophores and visually demonstrated the shell-like cross-linked membranes surrounding the microcapsule cores. The relatively stronger fluorescent signals at the external border of the membrane may be induced by (1) restricted further diffusion of chitosan into the alginate core blocked by initial chitosan binding<sup>35,236</sup>; (2) a higher degree of cross-linking at the external border of the membrane where more chitosan was deposited; and (3) different structure and optical characteristics of the chitosan-genipin derivatives formed at the surface of the microcapsules. The generation of fluorescence in the cross-linked products allowed for easy evaluation of the cross-linking reaction and the membrane distribution in the microcapsules.

The fluorescence intensity generated by exciting the genipin-chitosan fluorophores was in correlation with and indicative of the extent of cross-linking. The stronger the fluorescence, the more genipin-chitosan conjugates formed, and thus, the higher degree of

cross-linking on the chitosan coating was attained. As a result of this, more robusted microcapsules were likely generated. In the experiments, we investigated the influences of the cross-linking variables on the fluorophore formation on the membrane as monitored by the membrane fluorescence intensity, and optimized the genipin reaction process with regard to the highest fluorescent intensity generated. Results showed that the control factors of cross-linking temperature and reaction time significantly impacted the fluorescence intensity of the microcapsule membranes; the order of the effect' magnitude within tested ranges was: cross-linking temperature > cross-linking time > genipin concentration. It has to be noted that the tested genipin concentrations might have been saturated, which led to insignificant effect of genipin concentration detected (Fig. 7.7 c). The remarkable impact of temperature, also evidenced by the physical observation on the color change of the microcapsules, may be ascribed to the different levels of molecular collision during reaction. Sparse cross-linking at low temperature could be explained by the restricted molecular movement. At higher temperature, drastic molecular collision accelerated the reaction leading to denser cross-linking and rapid increase in membrane intensity. The decrease in fluorescence intensity of the membranes cross-linked by concentrated genipin at 37 °C may probably be due to collisional quenching and further complex formation<sup>377</sup>. On the whole, it could be inferred that the construction of the genipin cross-linked chitosan membranes could be varied by manipulation of the reaction conditions. The optimal reaction conditions for generating the microcapsules with most cross-linking included 2.5 mg/mL of genipin concentration, at 37 °C for 24 h. As well, the cross-linking reaction should be under careful temperature control to ensure consistent results.

Additionally, membrane thickness is a very important parameter controlling microcapsule property<sup>118,241</sup>. This paper explored a new and easy method to study the distribution of microcapsule membranes in original intact samples. By CLSM, the GCAC microcapsule membrane can be distinguished from the interior core and the image background. This enabled the noninvasive and *in situ* assessment of the microcapsule membrane including thickness measurement without any extraction, dehydration, or chemical modifications on the samples, which was otherwise difficult or impossible using other methods<sup>49,125,241</sup>. The effectiveness of this new method was validated by the atomic force microscopic (AFM) observations, from which the results on the membrane thickness of the

GCAC microcapsules were in close agreement with the CLSM measurements (32.1 versus 29.3  $\mu\text{m}$ ).

Previous research on alginate-chitosan complex by radio-labeling indicated that chitosan penetrated into the porous alginate gel matrix to a great extent<sup>35,236</sup> and the alginate-chitosan complex coaervation occurred not only at the surface of the capsule but also in the matrix<sup>236</sup>. Because genipin only interacted with the chitosan already bound to the alginate beads, the membrane thickness of the GCAC microcapsules would be mainly governed by the diffusion of chitosan and complexation with alginate. Our results corroborated with this hypothesis in that the GCAC microcapsules had relatively thick membranes which were largely independent of the cross-linking conditions (Tab. 7.3). One exception was that at higher cross-linking temperatures, slightly thinner membranes were formed, which could be attributed to the establishment of a denser membrane structure induced by the higher degree of cross-linking. Aside from this, it may be difficult to tailor the membrane thickness by varying the cross-linking conditions.

## **7.6 Conclusions**

In summary, the present work characterizes the genipin cross-linked alginate-chitosan microcapsule membranes using a novel CLSM method. Results showed that the construction of the genipin cross-linked chitosan membranes could be varied by manipulation of the genipin cross-linking conditions. The reaction factors of cross-linking temperature and reaction time significantly altered the fluorescence intensity of the membranes, whereas the tested genipin concentrations had little impact within the given ranges. Cross-linking by genipin at 37°C for 24 h may optimally yield the GCAC microcapsule membrane with strongest fluorescence and highest degree of cross-linking. These results will be useful in the future exploitation of the GCAC microcapsules for therapy.

## **7.7 Acknowledgements**

We acknowledge the research operating grant from Canadian Institutes of Health Research (CIHR). Scholarship supports from Natural Sciences and Engineering Research

Council (NSERC) of Canada (to H.C.) and Fonds Québécois de la Recherche sur la Nature et les Technologies (FQRNT) (to H.C. and W.O.) are also acknowledged. We also thank Prof. Z.Q. Chen for the constructive discussion, Prof. P. Deng for the suggestion on statistical analysis, and Mr. L. Bienenstock for the help with computational data analysis.

Table 7.1. Control factors and their levels for the cross-linking reaction

Factor	Level				
	1	2	3	4	5
A. Concentration (mg/mL)	1.0	2.5	5.0	-	-
B. Reaction temperature (°C)	4	20	37	-	-
C. Reaction time (h)	5	10	24	48	72

Table 7.2. Range tests on the fluorescence intensity of the GCAC microcapsule membranes

Factor	Fluorescence intensity <sup>a</sup>					Range <sup>c</sup>	Confidence limit <sup>d</sup>
	Level <sup>b</sup>						
	1	2	3	4	5		
A. Concentration	91	122	100	-	-	31	41
B. Temperature	33	86	194	-	-	161	22
C. Reaction time	66	78	123	128	127	62	52

<sup>a</sup> Mean of 15 (for factors A and B) or 9 (for factor C) fluorescence intensity data for microcapsules prepared under the same level of each factor; <sup>b</sup> See Table 7.1 for values corresponding to levels 1-5; <sup>c</sup> Range = maximum - minimum; <sup>d</sup> Degree of confidence was set at 95 %.

Table 7.3. Membrane thickness of GCAC microcapsules cross-linked under varied conditions

Genipin Conc. (mg/mL)	Reaction Time (h)	Membrane thickness ( $\mu\text{m}$ ) <sup>a</sup>		
		4 °C <sup>b</sup>	20 °C <sup>b</sup>	37 °C <sup>b</sup>
1.0	5	48.7 ± 7.6	45.9 ± 8.1	34.2 ± 7.0
	10	44.6 ± 3.9	37.1 ± 7.2	28.0 ± 7.3
	24	44.2 ± 7.0	33.8 ± 3.7	34.7 ± 4.2
	48	40.1 ± 8.6	28.8 ± 6.7	38.0 ± 7.7
	72	49.1 ± 5.5	29.2 ± 7.3	41.3 ± 7.9
2.5	5	43.7 ± 8.1	30.1 ± 3.2	35.0 ± 9.7
	10	47.2 ± 2.7	29.4 ± 4.7	33.1 ± 7.3
	24	46.8 ± 5.4	31.1 ± 5.5	35.7 ± 5.4
	48	45.4 ± 3.8	30.2 ± 4.6	38.8 ± 9.4
	72	37.0 ± 9.3	27.6 ± 6.3	43.0 ± 5.7
5.0	5	46 ± 10	24.1 ± 4.6	35.1 ± 6.8
	10	46.1 ± 9.2	25.2 ± 4.7	37.1 ± 7.5
	24	44.6 ± 4.5	27.2 ± 5.1	37.9 ± 8.6
	48	43.5 ± 6.4	27.3 ± 6.3	38.6 ± 5.4
	72	44.3 ± 3.6	29.3 ± 5.9	41.1 ± 4.8

<sup>a</sup> Expressed as mean ± s. d. ( $n = 10$ ); <sup>b</sup> Temperature at which the cross-linking reaction was performed.

Table 7.4. Range tests on membrane thickness of the GCAC microcapsule membranes

Factor	Membrane thickness ( $\mu\text{m}$ ) <sup>a</sup>					Range <sup>c</sup>	Confidence limit <sup>d</sup>
	Level <sup>b</sup>						
	1	2	3	4	5		
A. Concentration	38.5	36.9	36.5	-	-	2.0	3.8
B. Temperature	44.8	30.4	36.8	-	-	14.4	2.2
C. Reaction time	38.1	36.4	37.3	36.8	38.0	1.7	5.0

<sup>a</sup>Mean of 15 (for factors A and B) or 9 (for factor C) thickness data for microcapsules prepared under the same level of each factor; <sup>b</sup> See Table 7.1 for values corresponding to levels 1-5; <sup>c</sup> Range = maximum - minimum; <sup>d</sup> Degree of confidence was set at 95 %.

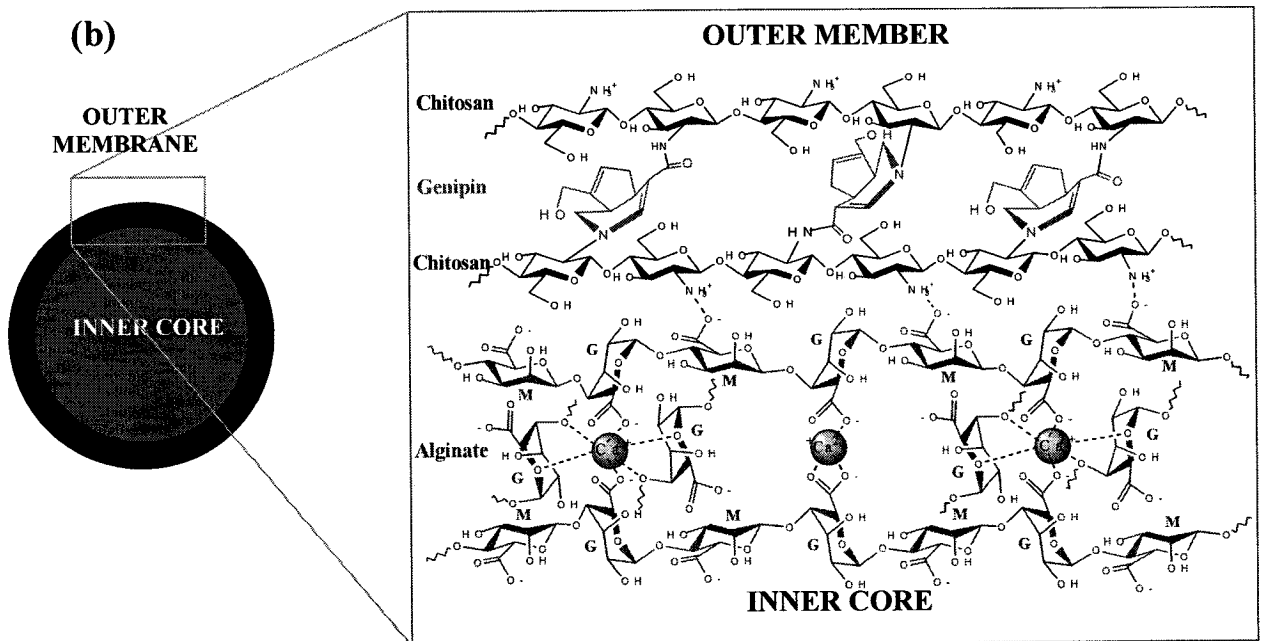
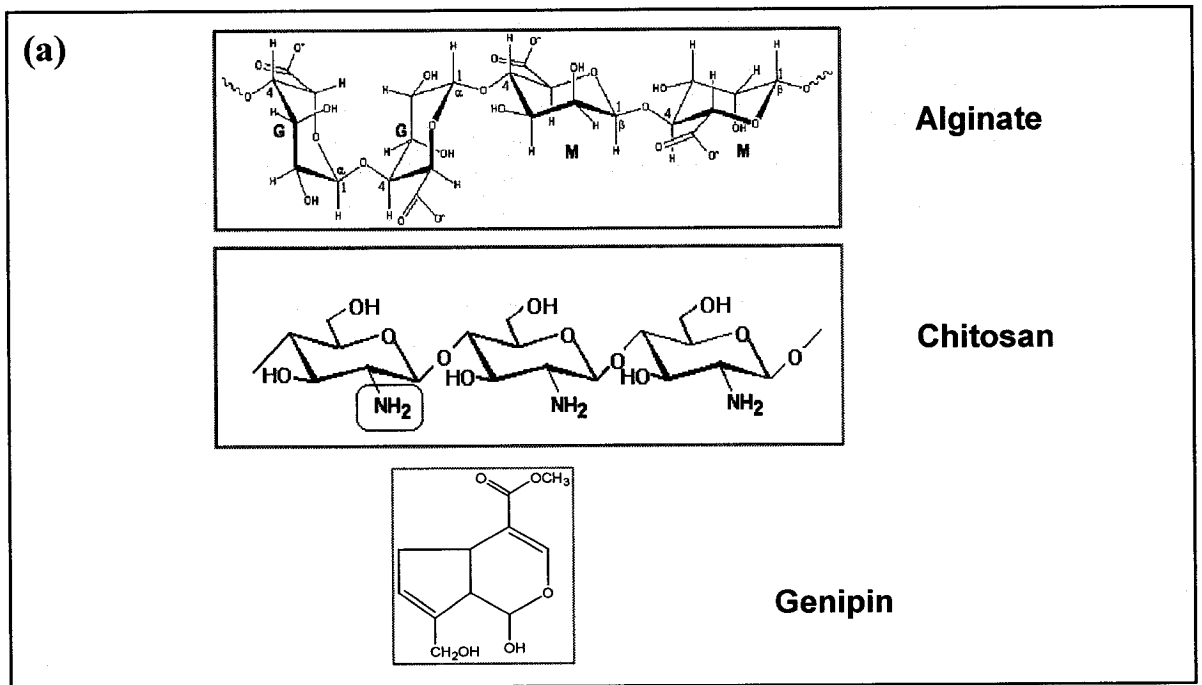


Figure 7.1. (a): Schematics of the chemical structures of alginate (top), chitosan (middle) and genipin (bottom) used in microcapsule preparation. (b): Schematic molecular structure of the genipin cross-linked alginate-chitosan (GCAC) microcapsules.

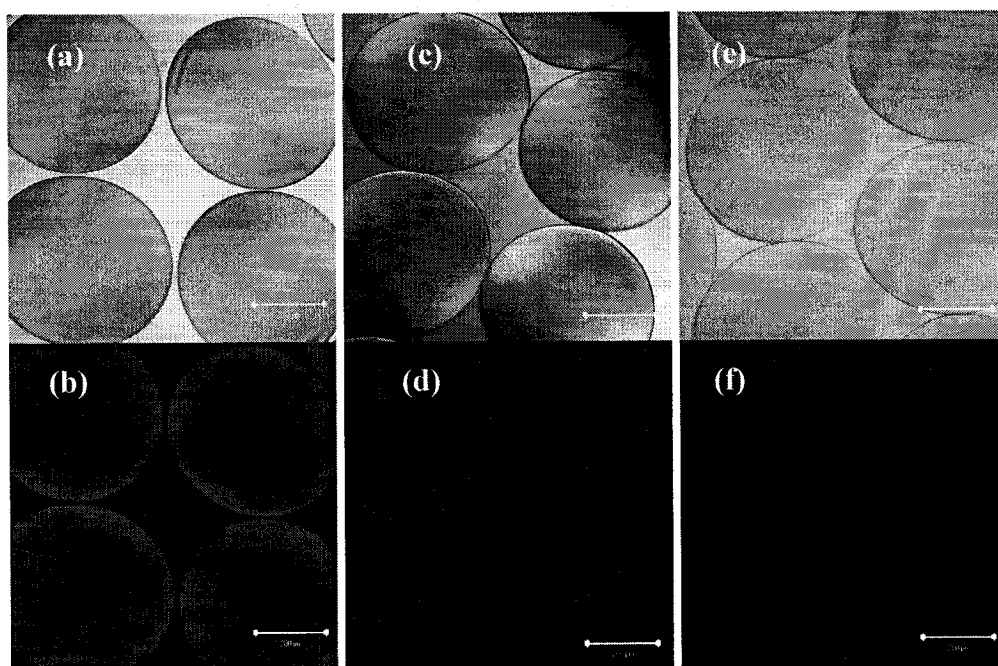


Figure 7.2. Photomicrographs of the GCAC (a-b), the control alginate-chitosan (c-d) and the control alginate-genipin (e-f) microcapsules viewed from the transmitted light channel (upper row) and the fluorescence channel (lower row) of CLSM. Genipin treatment (1.0 mg/mL) on microcapsules was performed at 37 °C for 24 h. Bars=200 μm.

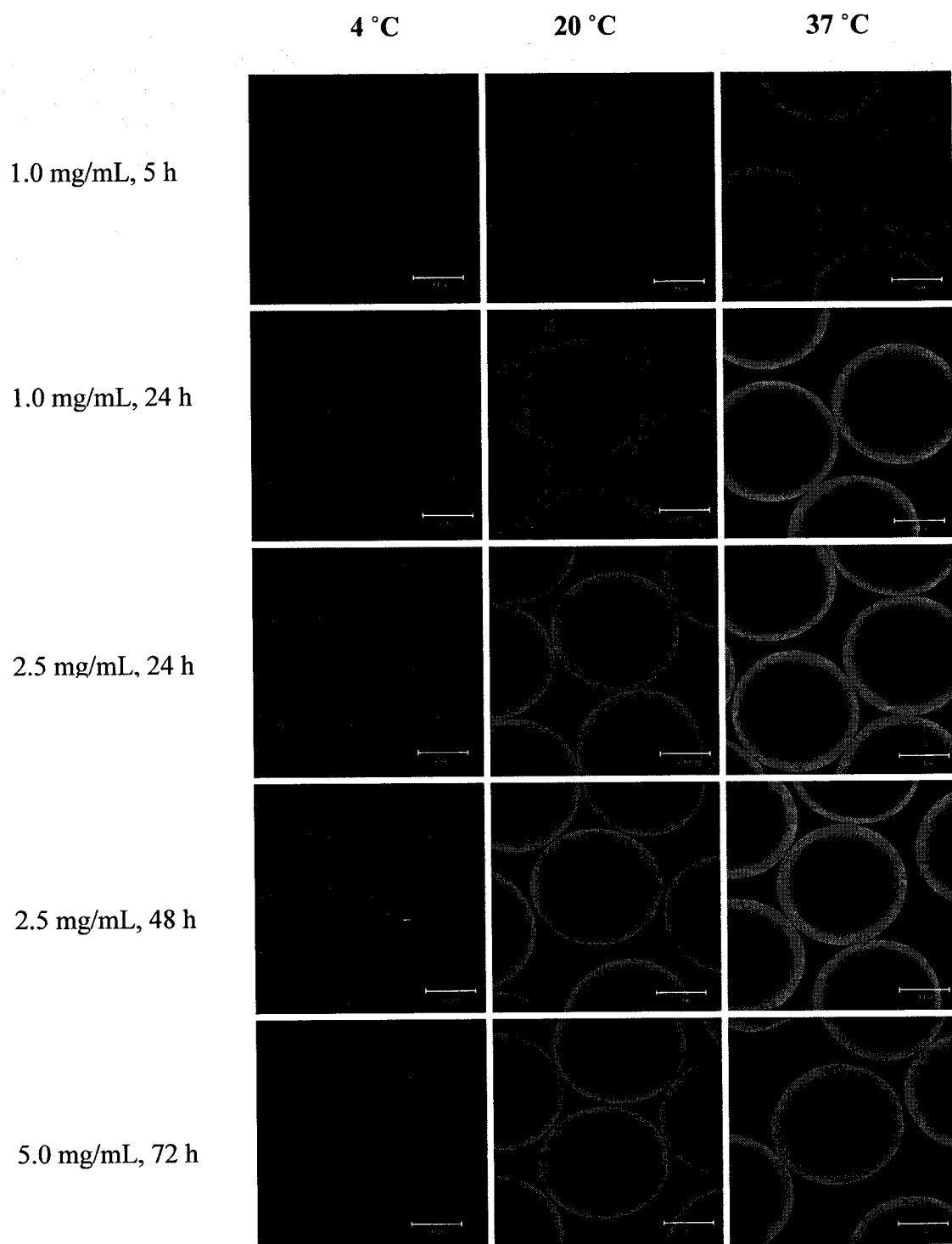


Figure 7.3. CLSM images of the GCAC microcapsules. The microcapsule membrane was cross-linked at varied genipin concentrations (1.0, 2.5, or 5.0 mg/mL) and temperatures (4, 20, or 37 °C) for different reaction time (5, 24, 48, or 72 h). Bars=200  $\mu$ m.

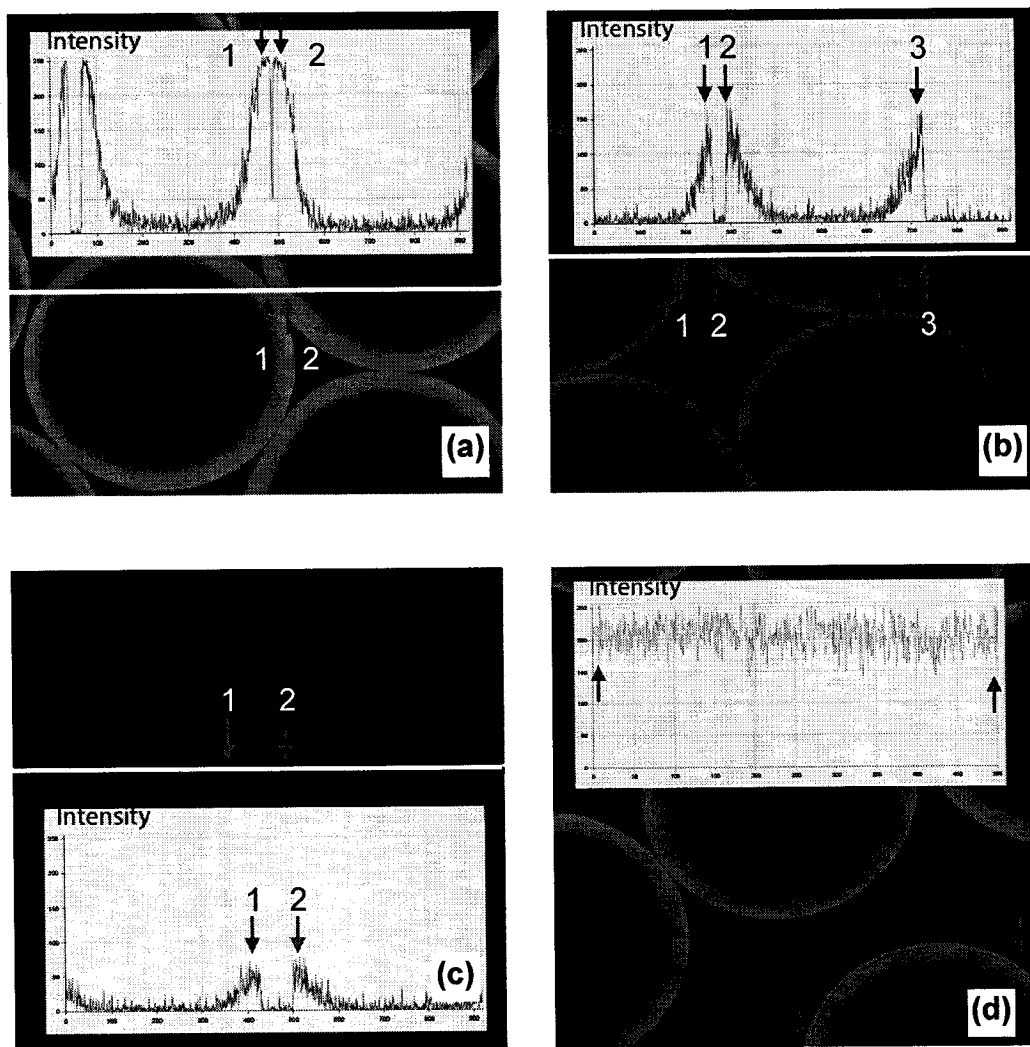


Figure 7.4. Fluorescence intensity profiles corresponding to the lines drawn across the focal plane of the GCAC microcapsules cross-linked by genipin at a concentration of 2.5 mg/mL for 24 h at (a) 37, (b) 20, and (c) 4 °C. (d) shows the fluorescence intensity of the membrane corresponding to a red line of 500  $\mu\text{m}$  in length indicating homogeneous distribution of the cross-linked chitosan in the microcapsule membrane.

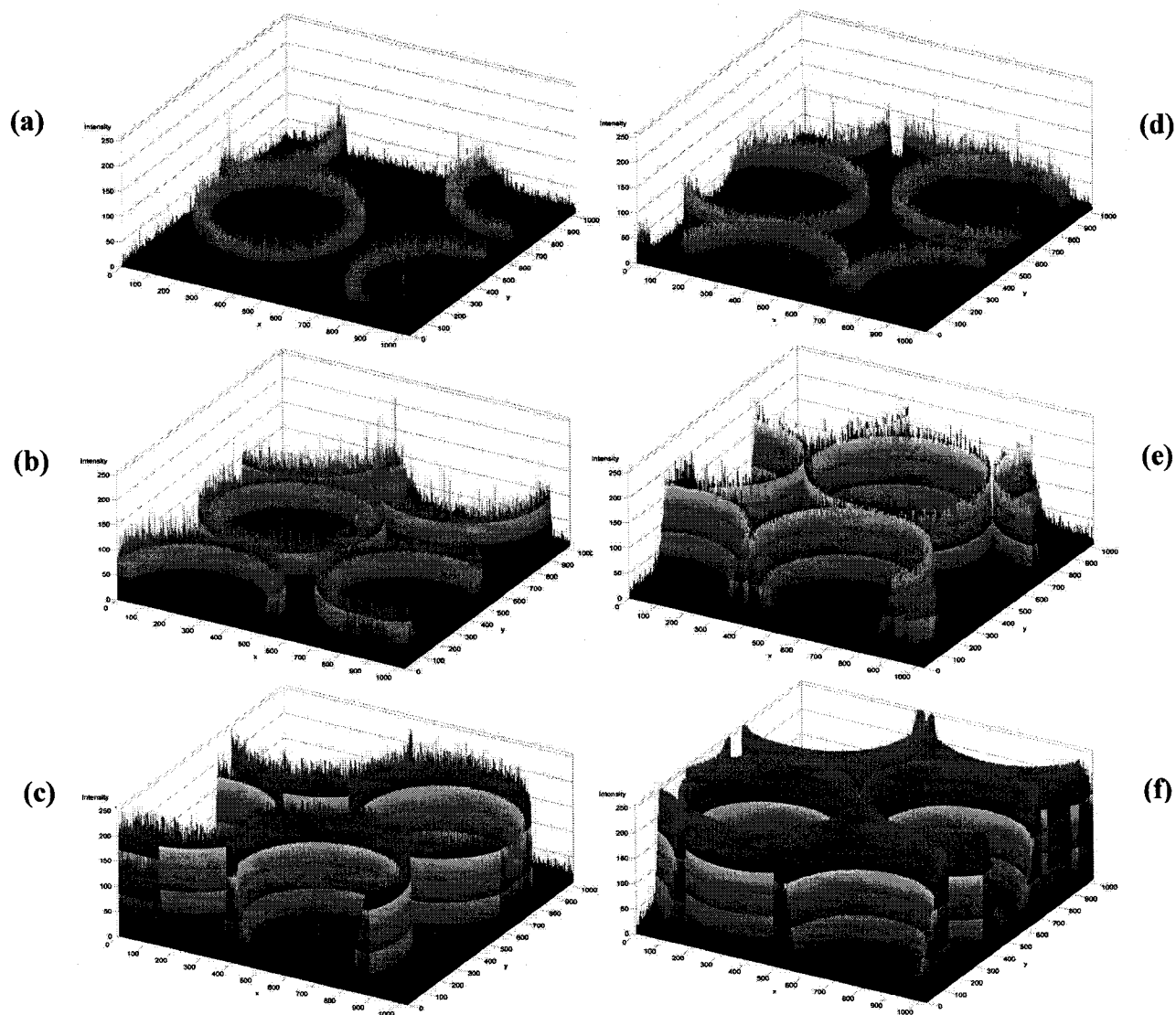


Figure 7.5. 3-D diagrams representing the intensity distribution over the scan areas and the relative fluorescence intensity of the GCAC microcapsule membranes. The GCAC microcapsules were cross-linked by genipin (2.5 mg/mL) at (a) 4 °C, 10 h; (b) 20 °C, 10 h; (c) 37 °C, 10 h; (d) 4 °C, 24 h; (e) 20 °C, 24 h; and (f) 37 °C, 24 h.

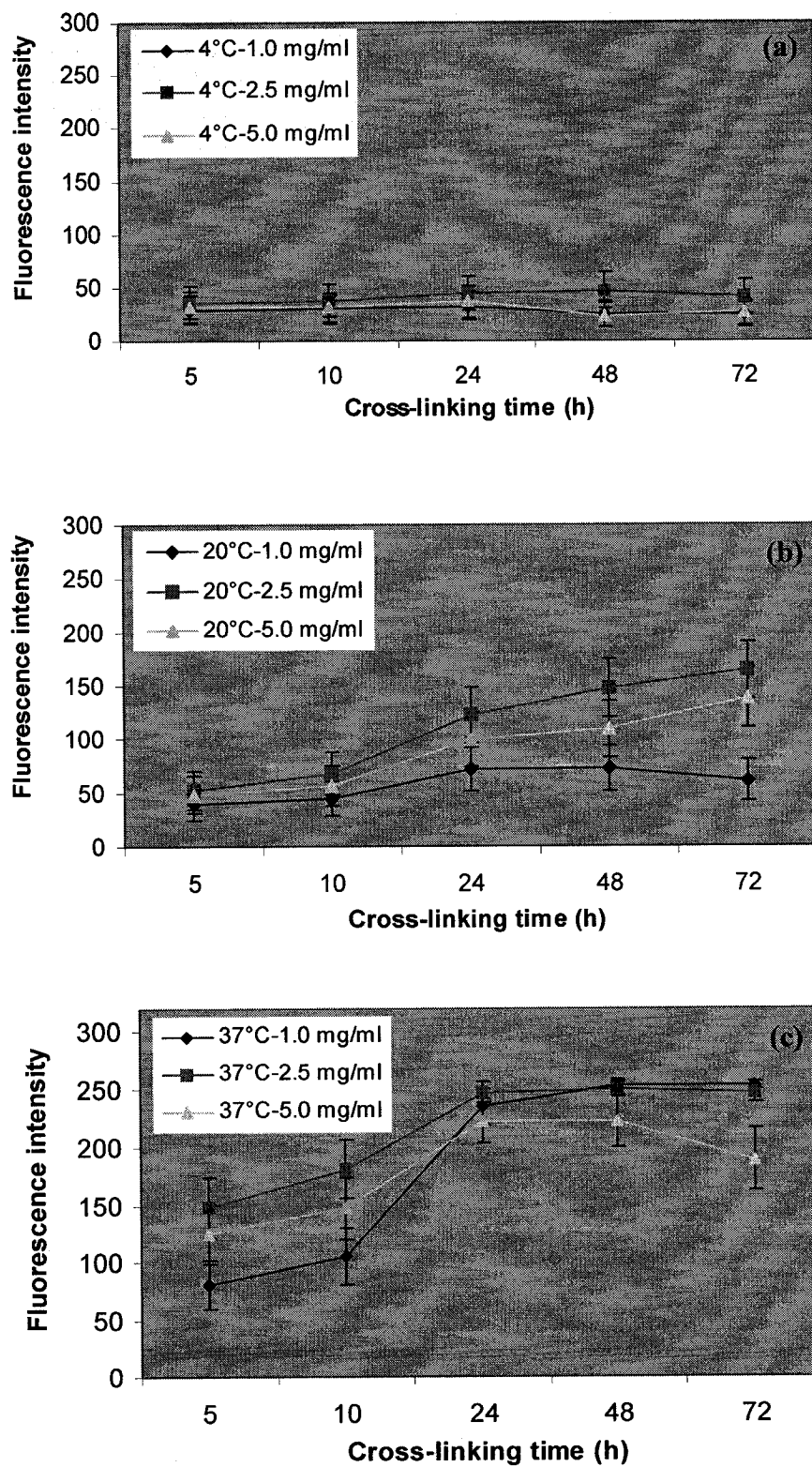


Figure 7.6. Fluorescence intensity of the GCAC microcapsules as a function of cross-linking time. The reaction temperatures used: (a) 4, (b) 20, and (c) 37 °C.

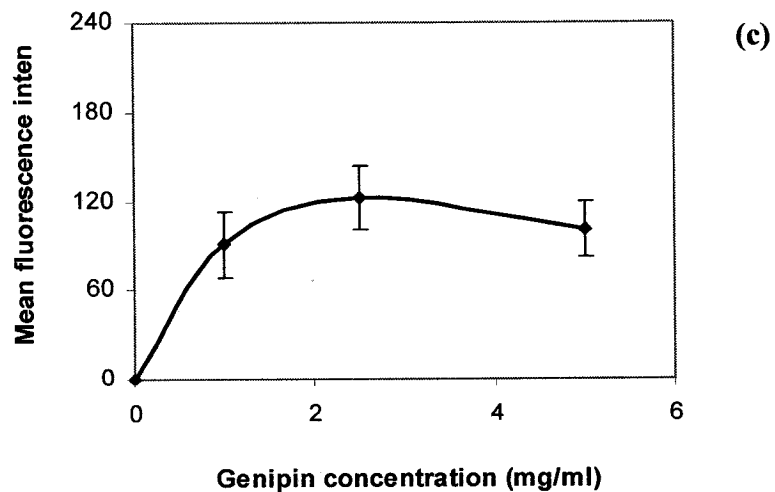
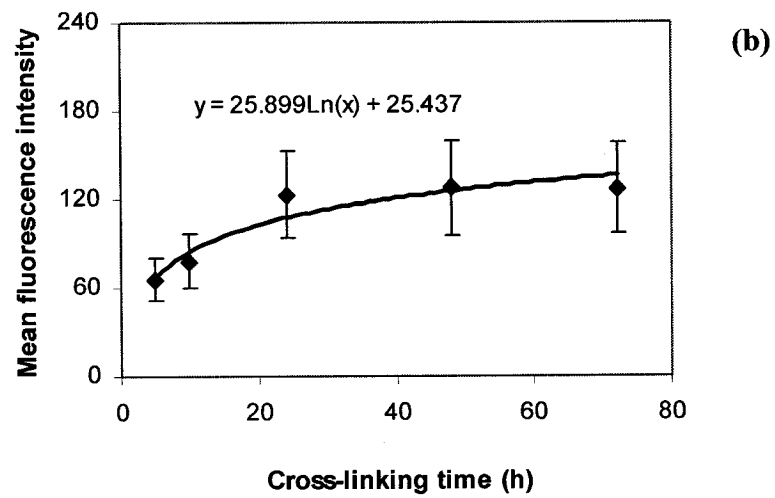
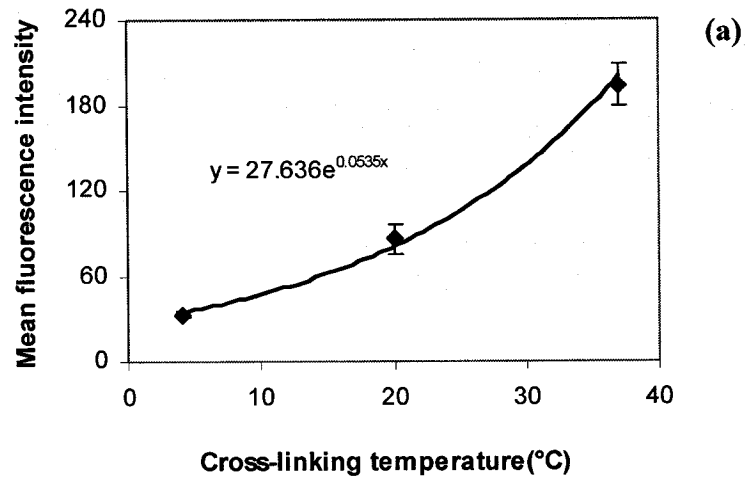


Figure 7.7. Effects of control factors on fluorescence intensity of the GCAC microcapsule membranes. Control factors: (a) cross-linking temperature; (b) cross-linking time; and (c) genipin concentration. Error bars indicate pooled s. d. of mean fluorescence at each level.

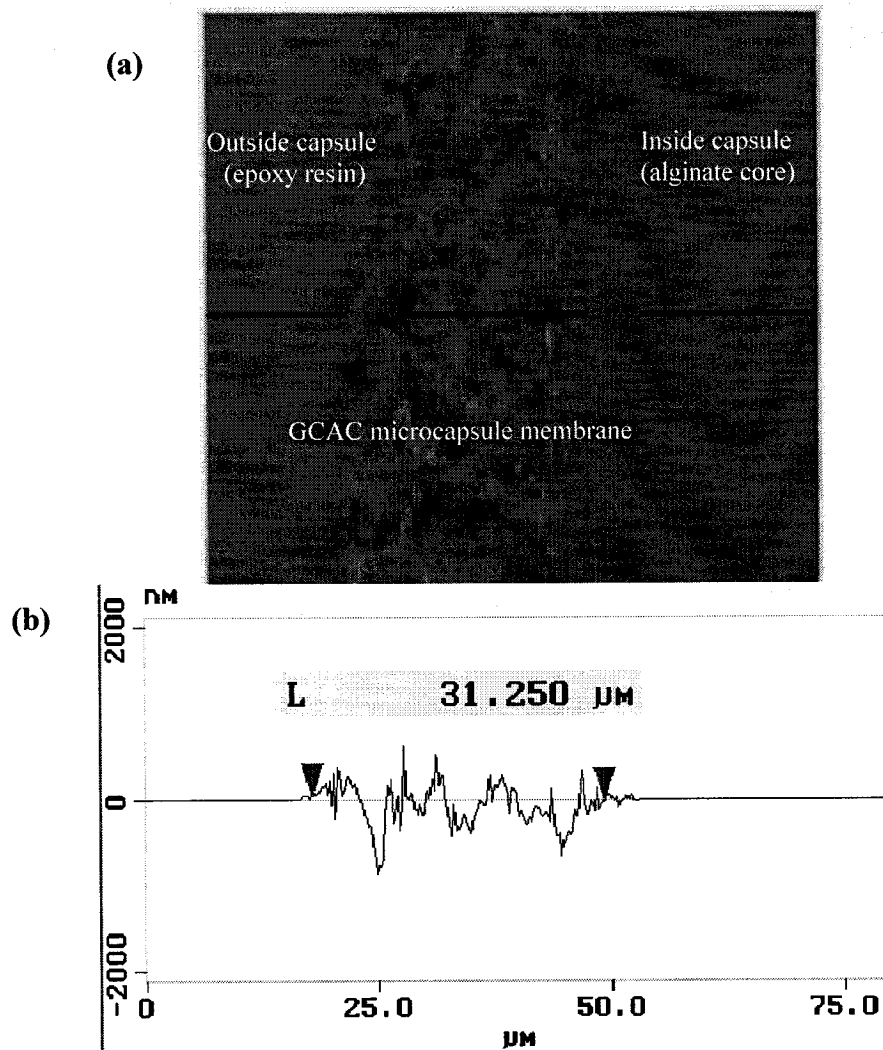


Figure 7.8. Topography (a) and roughness analysis (b) of the cross-sectioned GCAC microcapsule membrane obtained by AFM.

**Investigation of structure and relevant properties of the alginate-chitosan microcapsules covalently cross-linked by genipin**

Hongmei Chen, Wei Ouyang, Christopher Martoni, and Satya Prakash \*

*Biomedical Technology and Cell Therapy Research Laboratory  
Department of Biomedical Engineering and Physiology, Artificial Cells and Organs Research  
Centre, Faculty of Medicine, McGill University, Montreal, Quebec, H3A 2B4 Canada.*

\*Corresponding author: Tel: 514 398-3676; Fax: 514 398-7461;  
Email: satya.prakash@mcgill.ca

---

**Preface:** As a consecutive study to Chapters 4 and 7 on preparation and optimization of the GCAC microcapsule membranes, the present research characterizes the membrane structure and some key physical properties in regards to swelling behaviors, resistance to chelation and long term storage, mechanical stability, permeability, and tolerance to enzymatic degradation and the simulated gastrointestinal fluids. Results demonstrated the improvement on microcapsule stability and durability by genipin cross-linking, and warranted further studies on the membrane resistance to the human GI environment.

Original article is to be submitted to **Journal of Membrane Sciences**.

## 8.1 Abstract

We have previously reported the preparation of the genipin cross-linked alginate-chitosan (GCAC) microcapsules composed of an alginate core with a genipin cross-linked chitosan membrane. This study investigates their structural and physical characteristics. Results from SEM and TEM reveal that the GCAC microcapsules had a smooth and dense surface and a networked interior. Cross-linking by genipin substantially reduced capsular swelling and prevented physical disintegration in media containing non-gelling ions and calcium sequestrants. Strong membrane resistance to mechanical shear forces and enzymatic degradation was found. Furthermore, the GCAC membranes were permeable to bovine serum albumin (BSA, viscosity radius  $R_{\eta}=3.6$  nm) and maintained a MWCO of 70 KD for dextran ( $R_{\eta}=6.4$  nm), analogous to the alginate-chitosan (AC) and the widely studied alginate-poly-L-lysine-alginate (APA) microcapsules. The sustained release features and the tolerance of the GCAC microcapsules in the gastrointestinal tract were also investigated. This GCAC microcapsule formulation offers significant potential as a delivery vehicle for many biomedical applications.

**Key words:** membrane characterization, alginate-chitosan microcapsule, cross-linking, genipin

## 8.2 Introduction

Bioencapsulation describes a procedure where biologically active materials are enclosed within a semi-permeable membrane<sup>5</sup>. This technology has proven a valuable strategy to facilitate a wide range of pharmaceutical and biomedical processes in both fundamental research and industrial applications including drug delivery, artificial organs, and cell therapy<sup>19,21,55,70,80,352,362,393</sup>. The key required characteristics of microcapsules for such applications include biocompatibility, adequate resistance to environmental constraints, appropriate capsule stability, and selective membrane permeability<sup>28,29,76,104,108,324,394,395</sup>. In particular, preservation of the structural integrity of microcapsules is crucial in cell transplantation for the purpose of immunoisolation<sup>68</sup>. Previous research has suggested that

mechanically strong and durable capsules were less likely to rupture, thus prolonging *in vivo* functions of the encapsulated cells<sup>29,33,115,162,396</sup>.

Alginate, a polysaccharide isolated from brown algae, has been widely used in bioencapsulation due to its excellent biocompatibility and mild processing conditions. Addition of an outer poly-L-lysine (PLL)-alginate coating reduced the porosity of the Ca-alginate gel, rendering the resultant alginate-PLL-alginate (APA) capsules suitable as an immunoisolating device<sup>64,68,69,73</sup>. The major obstacle encountered by this encapsulation system, however, was the well known capsular fragility and short-term durability that may have contributed to the graft failure<sup>115,156,241,270,308</sup>. The loss of long-term stability of the APA microcapsules could be associated with activation of the complement system, proteolytic degradation of the polyamino acid coating, and destabilization of the alginate core matrix<sup>156</sup>. Chitosan, a naturally derived polycation, was employed as an alternative to PLL for microcapsule coating. Microencapsulation by alginate-chitosan (AC) complex, formed via electrostatic interactions between the two opposite charged polysaccharides, has been the topic of many investigations<sup>35,148</sup> for the delivery of drugs<sup>20,36,38,238,397</sup>, proteins<sup>39,245</sup>, enzymes<sup>40</sup>, growth factors<sup>37</sup>, DNA<sup>186,246</sup>, live microbes<sup>48,49,233,398</sup>, and cells<sup>46,47</sup>. However, the stability of the AC membrane remains limited<sup>43,49-52</sup>. Hence, the stability and durability of such devices require significant improvements in microcapsule chemistry to withstand long-term biological impediments.

To improve mechanical stability and resistance of microcapsules, exogeneous cross-linking in the membrane structure was utilized. Covalent cross-linking of microcapsules constitutes an effective way to generate polymeric networks giving rise to high gel strength and controllable resistance to chemical, proteolytic and mechanical stresses<sup>261,262</sup>. Although improvements in microcapsule stability using synthetic cross-linking reagents, such as bifunctional aldehydes<sup>40,263,265,268</sup>, carbodiimide (EDC)<sup>51</sup> and photo-sensitive molecules<sup>269,273,274</sup>, have been reported in the literature, concerns about their cytotoxicity persist<sup>210,278-281</sup>.

As an alternative cross-linker, genipin was reported to be much less cytotoxic, allowing for mild, but effective chemical cross-linking with a variety of biomaterials<sup>290-296</sup>. Genipin is an iridoid glucoside extracted from Gardenia fruits<sup>282</sup>. It has traditionally been used as a Chinese herbal medicine<sup>283-287</sup> as well as an edible colorant in the food industry<sup>399</sup>. In

recent years, due to its natural origin and low cytotoxicity, genipin has drawn considerable research interests in applications such as tissue fixation<sup>297</sup>, reinforcement of membranes<sup>299,400</sup> and hydrogels<sup>245,279,298,401</sup>, amino acids and proteins cross-linking<sup>382,402</sup>, tissue regeneration<sup>294,300,301,403</sup>, and cell immobilization<sup>305,390</sup>. We have earlier proposed the use of genipin to introduce covalent links into the microcapsule membrane for live cell encapsulation<sup>306,390</sup>. As a follow-up study, we present herein the characterization of the microcapsule structure and key physical characteristics including mechanical properties, permeability, resistance and durability.

### **8.3 Materials and methods**

#### **8.3.1 Materials**

Sodium alginate (low viscosity), bovine serum albumin (BSA,  $M_w$  66 KD), lysozyme (58,100 units/mg protein), poly (L-lysine) hydrobromide (molecular weight,  $M_v$  27.4 KD) and fluorescein isothiocyanate (FITC) labeled dextran ( $M_w$  4, 20, 40, 70, and 2,000 KD) were obtained from Sigma-Aldrich, USA. Chitosan (low viscosity,  $M_v=7.2 \times 10^4$  by viscometry, degree of deacetylation or DDA=73.5 % by titration) and genipin were purchased from Wako BioProducts, USA. All other reagents and solvents were of reagent grade and used as received without further purification.

#### **8.3.2 Preparation of GCAC microcapsules**

The GCACA microcapsules were prepared according to the protocol as earlier described<sup>390</sup>. Briefly, Ca-alginate beads were formed by extruding an alginate aqueous solution of 15 mg/mL into a gelling bath containing 11 mg/mL  $\text{CaCl}_2$ . Coating with chitosan was performed by immersing the Ca-alginate beads in a chitosan solution (10 mg/mL in 11 mg/mL  $\text{CaCl}_2$ ) for 30 min, resulting in the alginate-chitosan (AC) beads. Subsequently, the AC microcapsules were cross-linked by incubated in an aqueous solution of genipin (1.0 mg/mL) at 37 °C for 24 h. The resulting microcapsules were washed with deionized  $\text{H}_2\text{O}$  and subjected to testing.

### **8.3.3 Preparation of microcapsules containing blue dye or high molecular weight fluorescent labeled dextran (FITC-dextran)**

Microcapsules loaded with blue dye and FITC-dextran were prepared for studies on microcapsule long term stability and enzymatic degradation, respectively. For stability studies, a known amount of dye (Bleu ultramarine, Pb29, Kama Pigments) was mixed with an alginate solution (15 mg/mL). The preparation processes including alginate gelation, chitosan coating, and genipin cross-linking were performed using the aforementioned protocols. Similarly, microcapsules containing high molecular weight (HMW) fluorescent labeled dextran, used for degradation studies, were made from a mixture of alginate and FITC-dextran (FD2000, *M<sub>w</sub>* 2,000 KD, *R<sub>h</sub>*=34.2 nm, final dextran concentration of 2 mg/mL) with the preparation processes similar to those described above.

### **8.3.4 SEM and TEM observations**

The Ca-alginate beads (approximately 1mm in diameter) were prepared by extruding alginate solution into a CaCl<sub>2</sub> receiving bath using a 1 mL syringe and a 27 gauge needle. The AC and GCAC microcapsules were prepared as described above. For scanning electron microscopy (SEM) observation, the microcapsules were dehydrated by gradient ethanol and critical point drying (CPD, LADD Research Industries), and coated with Au-Pd using an Au-Pd sputtering coating unit (Hummer II Polaron Au Sputter Coater). A minimum of three beads randomly selected from each formulation batch were initially scanned to ensure batch homogeneity, and their microscopic structure was examined by SEM (FEG\_SEM, Hitachi model S-4700). To characterize the inner membrane structure, the microcapsules were dehydrated, embedded in Epon and cross-sectioned by ultramicrotome (Reichert Ultra Cut AV) prior to transmission electron microscopic (TEM) observations (Tecnai 12 120 kV TEM).

### **8.3.5 Swelling behavior, resistance to citrate chelation and long term stability**

To assess the swelling behavior and membrane resistance, aliquots of microcapsules were submerged in 2 mL of physiological solution (PS, 0.9 % NaCl) or phosphate buffered saline (PBS, pH 7.4). The solution was refreshed every 2 h in the first 8 h and then once a day for up to 1 week. The morphology and physical integrity of the microcapsules were examined under an inverted light microscope (LOMO PC). The microcapsule dimension was measured

with an eyepiece micro-meter equipped on the microscope at a magnification of 90x, and averaged from at least 8 beads per batch. The swelling ratio is expressed as percentage of diameter changed by the following equation:

$\% \text{ Swelling} = (D - D_0) / D_0 * 100$ , where  $D_0$  and  $D$  were microcapsule diameters before and after the treatment, respectively.

To examine the membrane resistance to citrate chelation, microcapsules were exposed to a sodium citrate solution (50 mg/mL) at room temperature for 24 h. The changes in morphology were studied by optical microscopy.

For the study of long term membrane stability, blue dye-entrapped microcapsules were incubated at room temperature in PS containing sodium azide (5 mM  $\text{Na}_3\text{N}$ ) to prevent microbial growth. The media were changed periodically. The morphology of the microcapsules was observed under the microscope, and images taken as records.

### **8.3.6 Osmotic pressure test and mechanical stability of microcapsules**

The mechanical stability of the microcapsules was examined by osmotic pressure and mechanical shear tests. Osmotic stress was applied to microcapsules using a modification of a previously described procedure<sup>332</sup>. Specifically, the GCAC microcapsules were equilibrated for 30 min in hypertonic solution (10x, 5x, 2x or 1x of 0.85 wt % aqueous NaCl) prior to transferal to a hypotonic medium (deionized  $\text{H}_2\text{O}$ ), which led to a high osmotic pressure inside the capsules. During the following 1 h, microcapsule breakage was analyzed under an inverted microscope. In the mechanical stress experiments, microcapsules (2 mL) suspended in 10 mL deionized  $\text{H}_2\text{O}$  were subjected to agitation (600 rpm for 3 h). The percentage of destroyed microcapsules in at least three randomly picked observation fields was estimated under an optical microscope, and images taken as records. The experiments were performed in triplicate.

### **8.3.7 Membrane permeability**

*In vitro* permeability studies were performed to determine the ingress ratio of macromolecular markers and the microcapsule membrane cutoffs (MWCO) using FITC-dextran (characteristics shown in Table 8.1) as fluorescent molecular weight standards and BSA ( $R_h = 3.6 \text{ nm}$ ) as a model protein permeant.

*Penetration of FITC-dextran into microcapsules:* microcapsules (approx 150 beads) were equilibrated overnight in PS at room temperature, followed by addition of a FITC-dextran solution (150  $\mu$ l, 0.5 mg/mL dissolved in PS, with an exception for FD-4 at 1.0 mg/mL in PS). The incubation continued for 24 h to reach equilibrium. Then, microcapsules along with the marker media were placed in a chambered coverglass system (Lab-TeK). The diffusion of FITC-dextran into the microcapsules was investigated by confocal laser scanning microscopy (Zeiss LSM 510, Jena, Germany) equipped with a Zeiss Axiovert 100M microscope. An argon-ion laser was used at an excitation of 488 nm and the fluorescence was detected with the filter block BP500-550IR. For quantitative evaluation, rectangles at an equatorial, optical section of microcapsules (0.05 mm<sup>2</sup> in area) were selected inside the microcapsules and in the surrounding media. Mean pixel grey values representing the relative fluorescence intensities were acquired using LSM 510 software command "Topography", and standard deviations of pixels within selected areas were maintained below 9. The diffusion of dextran into ten individual capsules per batch was assessed and expressed as percent of fluorescence intensity in the microcapsule confines relative to that in the marker solution (background reading). Microcapsule membranes with dextran diffusion less than 5 % were considered cutoff to the selected marker.

*Penetration of BSA into microcapsules:* immediately after BSA solution (1.5 mg/mL in 1.5 mL PS) was added to the vials containing the tested microcapsules ( $\sim 3.00 \pm 0.01$  g), the concentrations of BSA remaining in the supernatant was monitored for up to 8 h using the Bradford method. The absorbance at 595 nm was recorded using a  $\mu$ Quant Universal Microplate Spectrophotometer (Bio-Tek Instruments, Inc.) and the protein concentration was determined by comparison to a standard curve. The BSA diffusion profile was plotted as relative BSA remaining in the medium as a function of incubation time.

### **8.3.8 BSA encapsulation and sustained release *in vitro***

*BSA encapsulation:* To prepare the BSA encapsulated microcapsule, BSA was first dissolved in PS and mixed with alginate solution to give a final concentration of 15 mg/mL for both BSA and alginate. The mixture was extruded and droplets were gelled in a CaCl<sub>2</sub> receiving bath (11 mg/mL) for 15 min. The subsequent coating with chitosan and cross-linking by genipin were performed according to the aforementioned protocol. Prior to

assessment of protein release the microcapsules were equilibrated overnight in a physiological solution containing 15 mg/mL BSA to compensate for BSA loss during preparation.

*In vitro release of encapsulated BSA:* the BSA loaded microcapsules (0.20 g) were suspended in 2.0 mL 0.01M phosphate buffered saline (PBS, pH 7.4) with gentle rotation in an ENVIRON shaker at a speed of 125 rpm at 37 °C. At various time points, supernatant (1.0 mL) was withdrawn to determine the release of BSA by the Bradford assay as described above, and the medium was replaced with fresh PBS. Results of accumulated protein released from triplicate experiments were plotted as a function of incubation time.

*BSA stability assay:* to confirm the integrity and stability of the encapsulated BSA, freshly made BSA-containing microcapsules were immersed in a sodium citrate aqueous solution (10 wt %), followed by pressing the bead suspension through needles with gradually increasing gauge (from 18 to 27G) to break the capsules and liberate the entrapped BSA. Subsequently, the suspension was centrifuged at 5 000 g for 5 min and the supernatant was pressed through a 0.22 µm syringe filter. The clear filtrate was analyzed on a column (Biosep-SEC3000, Phenomenex) by a high-performance liquid chromatographic system (HPLC, Varian Inc. Canada). The mobile phase was 50 mM phosphate buffer solution (pH 6.8, K) pre-filtered through 0.22 µm vacuum-driven filter unit (Millipore, Japan), and used at a flow rate of 0.5 mL/min at room temperature. The injection loop was set at 20 µl and UV detection at 280 nm. A standard BSA solution was used as reference.

### **8.3.9 *In vitro* degradation by lysozyme**

A known amount ( $0.50 \pm 0.01$  g) of the microcapsules containing high molecular weight fluorescent-labeled dextran (2,000 KD,  $R\eta=34.2$  nm) were washed and incubated at 37 °C in lysozyme solutions (2.0 mL) of different concentrations (15 µg/mL, 150 µg/mL, and 15 mg/mL dissolved in PBS) with gentle mixing of 100 rpm in a platform shaker for either 7 or 30 d. The leakage of fluorescent marker from the microcapsules was assessed as indicative of membrane defects induced by lysozyme activity (erosion and degradation). To evaluate the anti-degradability of the microcapsule membranes, supernatant (0.2 mL) was withdrawn at different intervals to determine the leaking fluorescence spectrofluorometrically using a Microplate Fluorescence Reader (FLx800, Bio-Tek Instruments, Inc.) with the absorption and emission wavelengths at 485 and 528 nm, respectively. The volume of the media was kept

constant by adding fresh lysozyme solution after sampling. Data are presented as mean  $\pm$  s. d. from triplicate experiments.

#### **8.3.10 Membrane resistance to simulated gastrointestinal fluids**

To examine the potential of microcapsules for gastrointestinal applications, the simulated gastric fluid (SGF, pH 1.2) and the simulated intestinal fluid (SIF, pH 7.5) were prepared according to United States Pharmacopoeia XXII protocol, and used to test the microcapsule resistance. The morphological changes of the tested microcapsules were studied by optical microscopy (LOMO PC), and microphotographs were recorded using a digital camera (Canon Power shot G2).

### **8.4 Results and discussion**

#### **8.4.1 Surface and internal structure of microcapsules**

The morphology of microcapsules is known to affect their general *in vitro* and *in vivo* performance. Smooth surface may result in good biocompatibility<sup>203</sup>. The surface and internal structure of the microcapsules under investigation were examined by electron microscopy and are shown in Figures 8.1-8.4. It was found that these microcapsules were essentially spherical in geometry, possessing a homogenous, smooth and compact structure on the surface in the presence of sporadic small nubs (Fig. 8.1). Preliminary energy-dispersive x-ray (EDX) analysis on these small nubs did not reveal differences in chemical compositions from the other parts of the capsule surface. It appeared that the GCAC microcapsule had a denser and smoother surface than the AC membrane (Fig. 8.1d). At higher magnifications, the presence of clusters and small spheres on the cross-linked surface was clearly evident (Figures 8.1f & 8.3c). Moreover, porous structure was found inside the membranes, though no distinguished differences in porosity and density of the network were detected between the AC and GCAC capsules (Figures 8.2 & 8.3). The internal morphology of the microcapsule membranes at the boundary regions assessed by TEM also revealed a smoother and denser structure for the GCAC membranes (Fig. 8.4f) and, a more granular pattern for the alginate beads (Fig. 8.4 b) in comparison to the AC capsules (Fig. 8.4d). These differences between the three types of capsules were most likely caused by different membrane chemistries.

#### **8.4.2 Effect of genipin cross-linking on microcapsule swelling and resistance**

Alginate is highly hydrophilic, due to the presence of –OH and –COOH groups in its chain. At neutral pH, the water of the environment penetrates into the chains of alginate to form hydrogen bridges through their available –OH and COO<sup>-</sup> groups, and fills up the space among the chains and/or the centre of wide pores or voids<sup>32</sup>. As a consequence, the beads tend to swell substantially. Additional swelling and eventual destabilization are promoted by the presence of non-gelling ions and chelators, such as sodium, magnesium, phosphate, lactate, and citrate, owing to the ions exchange with the non-cooperatively bound calcium ions and loss of the egg-box structure in the alginate matrix<sup>404</sup>. A substantial quantity of sodium and phosphate ions in physiological conditions induce osmotic swelling, which presents one of the main causes of alginate polycation capsule breakage<sup>162</sup>. Previous studies suggested that microcapsules can be stabilized by creating a strong membrane and keeping a low swelling gel network<sup>156,162,164,165</sup>. In our study, resistance of the microcapsules to PS, PBS and citrate chelation was investigated. Results showed that the GCAC microcapsules remained intact and swelled  $2.7 \pm 1.8$  and  $11.7 \pm 1.4$  % in PS and PBS, respectively. During the study, both AC and APA microcapsules experienced substantial swelling in PBS, increasing in size by approximately 46 and 80 %, respectively (data not shown). With respect to the calcium sequestration, the citrate treatment provokes chelation of the bound cross-linking calcium ions, giving a result of dissolution of the alginate core and generally a rapid swelling of the capsules. Results showed after 24 h of citrate treatment, the AC membrane, although resistant against complete dissolution in the challenging medium, appeared worn out and thinner, and showed significant capsular swelling (Fig. 8.5d); where the GCAC microcapsules underwent limited swelling and remained stable (Fig. 8.5c). In addition, the cross-linked microcapsules retained their structural integrity for at least 6 months in PS, while membrane defection was found for the AC capsules (Fig. 8.6). These observations demonstrate the enhancement of microcapsule resistance and durability by the generation of covalent links.

#### **8.4.3 Mechanical stability of GCAC microcapsule membrane**

Mechanical properties of microcapsule membranes are of key importance for their integrity preservation and *in vivo* performance. It was previously reported that microcapsules

with strong membranes were more durable and less likely to rupture, providing with prolonged functions of the encapsulated cells<sup>115,156,396</sup>. Despite being crucial, precise determination of microcapsule mechanical strength is difficult because of the size (generally 100  $\mu\text{m}$  to 2 mm in diameters<sup>144</sup>) and fragile nature of the microcapsule. A number of assessment techniques have been explored, but standard testing methods have yet to be established<sup>28,164,241,324,332,405</sup>. In this study, the membrane strength was evaluated by subjecting the microcapsules to osmotic pressure and mechanical agitation. It was found that after exposure to an osmotic shock (which was much stronger than suggested in literature<sup>332</sup>), none of the GCAC microcapsules burst, while there was complete fracture of the APA capsules (data not shown). In the mechanical shear test, the vigorous agitation accelerated the breakage of the capsules. After 3 h of continuous mechanical agitation, the APA microcapsules became totally fragmented; 70 - 80 % of the AC beads had been destroyed; whereas only ~ 30 % of the cross-linked microcapsules ruptured (Fig. 8.7). Noticeably, some of the GCAC microcapsules had changed into an elliptical shape under mechanical force, indicating the elasticity of the cross-linked capsules (Fig. 8.7c). The improvement in mechanical stability correlated with the reduction in swelling capacity of the GCAC capsules, suggesting that covalent cross-linking by genipin considerably stabilized the microcapsules.

#### **8.4.4 Permeability of microcapsules**

In cell microencapsulation, live cells are isolated from the external environment by an artificial, semi-permeable membrane, which should allow for ingress of oxygen and nutrients, and egress of waste products and therapeutic molecules. Proper encapsulated cell functions require strict control over permeability of the microcapsule membrane. The current research characterized the capsule permeability by ingress experiments using dextran and BSA as the permeate markers. Dextran is a linear and neutral polysaccharide, whereas globular BSA bears negative charges at  $\text{pH} > 5.0$  ( $\text{pI} = 4.8$ ) and hydrophobic character. In capsule permeability research, using neutral polysaccharide molecular weight standards precludes the problems of absorption, aggregation and other charge/hydrophobic interactions, while proteins are thought to be more appropriate in determining the permeability of capsules designed for biological systems<sup>190,335</sup>. Furthermore, since the volume to mass ratios of dextrans and proteins vary largely, it is suggested to use a universal viscosity radius ( $R\eta$ ) to

estimate the molecular dimension of the markers; otherwise permeability results expressed in terms of molecular weight will be misleading<sup>190,406</sup>. In our study, permeability measurements were carried out with individual capsules using confocal laser scanning microscopy (CLSM) for the diffusion of fluorescent dextran markers, and by batch experiments detecting the decrease in concentration of the incubating protein marker.

Figure 8.8 depicts a normal distribution of the pixels with a particular light intensity within tested rectangles. The significant difference in grey values of the two red rectangles (mean pixels 125 versus 242) was clearly displayed, suggesting the non-homogeneous dissemination of FITC-dextran (20 KD,  $R\eta=3.6$ ) inside and outside the microcapsule. The representative CLSM images in Figure 8.9 demonstrate that the dextran ingress was significantly reduced with the increasing molecular weights of fluorescent markers. Irrespective of microcapsules, dextran with  $R\eta=1.7$  nm (FD-4, 4 KD, see Table 8.1) infiltrated to the interior of the microcapsules by a great extent (diffusion ratio > 70 %), whereas permeation of larger dextrans (40 and 70 KD) was greatly restricted, with the inflow ratios of around 20 % and below 5 %, respectively (Fig. 8.10). These investigations yielded the cut-off values for the GCAC membrane on the order of 70 KD FITC-dextran ( $R\eta=6.4$  nm), and the same as for the APA and AC capsules. It has to be noted that Based on this membrane cutoff and the dependence of  $R\eta$  on molecular weight under “ideal” conditions<sup>190</sup>, the corresponding limit presumably excluded by the tested membranes was estimated to be 360 KD for proteins. According to this conversion, the microcapsule membranes were supposedly permeable to immunoglobulins of IgG class ( $R\eta=5.2$  nm) and enzymes such as murine  $\beta$ -glucuronidase, which corroborated with the published results for the APA capsules<sup>114,155,187,189,190,334</sup>. Nevertheless, it should be pointed out that the conversion provides an estimated value since a direct comparison of linear and globular polymers as markers of permeability is still a matter of discussion.

As the diameter of BSA ( $R\eta = 3.6$  nm) may correspond to dextran with molecular weight of ~ 20 KD, which is below the above-described exclusion limit, BSA should theoretically penetrate the studied capsule membranes. Our observations on BSA diffusion confirmed this postulation. As shown in Figure 8.11, a rapid influx of BSA into the calcium alginate, APA and AC microcapsules occurred in the first 30 min of incubation, during which, little decrease in BSA concentration was detected in the media containing the GCAC

microcapsules. Despite initial retardation, BSA was able to diffuse into the GCAC capsules, as seen by a gradual decline of BSA remaining in the media (Fig. 8.11). After 4 h, the BSA infiltration reached a similar level to that for the APA capsules, with ~ 55 % of BSA remaining in the media. Figure 8.11 also showed the slower BSA diffusion into the GCAC microcapsules in comparison to the AC capsules. It is known that the structural characteristics of the microcapsule membrane influenced the diffusion kinetics of the permeants and the molecular weight cutoff of the membranes. In the GCAC and AC systems, the membrane thickness was mainly governed by the binding of chitosan<sup>306</sup>. This may account for their similar permeability for dextran diffusion (Fig. 8.10). The retardation of protein infiltration to the GCAC microcapsules shown in Figure 8.11 may be ascribed to the transport hindrance caused by the denser network structure of the genipin cross-linked membrane. The effects of chitosan-genipin reaction variables on the permeability of the GCAC microcapsules were also investigated, and no statistically significant differences on the membrane cutoffs were detected within the tested ranges (data not shown). The above findings indicated that the covalent cross-linking treatment by genipin modulated the diffusion kinetics of the permeants but did not alter the membrane MWCO cutoffs.

#### **8.4.5 Sustained release of encapsulated BSA**

The above permeability characteristics of the chitosan-based microcapsules were further confirmed by the release profiles of the encapsulated BSA. As shown in Figure 8.12, prolonged release of BSA from both the AC and GCAC microcapsules was evidenced. As well, the genipin cross-linked membrane delayed the release of BSA for an appreciable period of time. Specifically, the cumulative percentage of BSA released from the GCAC and AC capsules was 38.1 and 55.5 % in the first 1 h, respectively. Thereafter, these numbers increased to 46.8 versus 69.5 % in 2 h, and 70.4 versus 76.7 % in 4 h, and both above 95 % after 12 h (Fig. 8.12). This delay in BSA release, which was consistent with the results obtained from the BSA ingress experiments, could be a result of transport obstruction in the GCAC membranes generated by the genipin-chitosan cross-links.

Additionally, the loss of stability of the encapsulated protein is one of the concerns regarding protein immobilization and drug delivery. In the present research, the stability of microencapsulated BSA was further examined by the integrity change reflected in their

chromatographs. One can see in Figure 8.13 that the entrapped BSA in both AC and GCAC capsules showed a peak equivalent to the standard protein in terms of retention time and peak shape. The presence of some large molecules with molecular weights higher than the BSA standard was also detected at earlier elution time in the chromatographs of both AC-BSA and GCAC-BSA microcapsules, and a higher amount of these unknown molecules was found inside the GCAC capsules. These large molecules, present in the GCAC capsules in a greater quantity, may likely arise from the BSA-chitosan complex, the genipin cross-linked BSA, or other impurities. Although the integrity of the encapsulated BSA was confirmed by HPLC, whether the genipin treatment will affect the enclosed proteins needs further investigation.

#### **8.4.6 *In vitro* degradation by lysozyme**

For this study, HMW FITC-dextran (2,000 KD,  $R\eta= 34.2$  nm) was encapsulated as a tracer. Being a large polymer in this size, this fluorescent probe is indefinitely withheld inside the intact microcapsules and could not spread out unless the membranes became defected. In the human gastrointestinal (GI) tract, lysozyme is synthesized and secreted by specialized granular epithelial Paneth cells in the small intestine. A universal enzyme lysozyme was used to decompose microcapsule membranes constituted of polysaccharides and/or polyamino acid, and the leaching of encapsulated dextran induced by corrosion and degradation of capsular membranes was examined. Results showed that the APA membranes were susceptible to enzymatic actions. Exposure to lysozyme of 15  $\mu\text{g}/\text{mL}$  resulted in an increase in the media's fluorescence proportional with incubation time ( $R^2=0.9775$ , see Fig. 8.14a), reaching the intensity of 243 and 503 at day 3 and 7, respectively. With 10 times more concentrated lysozyme, the leaking of FITC-dextran occurred more rapidly, from 9, 272, to 513 at time 0, day 1 and day 3, respectively (Fig. 8.14b). At the end of the experiment, the APA capsules became too fragile to withstand handling for retrieval (data not shown). This gave an idea of inferior resistance to enzymatic degradation offered by the capsules with an APA membrane. Conversely, leaking of encapsulated dextran from the AC and GCAC microcapsules was negligible (Fig. 8.14 a-b) under the same challenging condition, and the membrane integrity was preserved over the 7-d experimental period (data not shown). We further extended the test period to 30 d. Apparent deterioration of microcapsule membranes began from the third week when using 150  $\mu\text{g}/\text{mL}$  lysozyme. As shown in Figure 8.14c, fluorescence leakage from

the AC capsules intensified from 31, 68 to 136 on days 7, 14 and 21, respectively. The enzyme actions on the GCAC capsules, on the other hand, limited liberation of the enclosed FITC-dextran, with the fluorescence maintained below 40 for the first 2 weeks and reaching a plateau of ~ 66 from day 19. This indicated the integrity of the GCAC membranes were preserved to a large extent. Conversely, exposure to highly concentrated lysozyme (15 mg/mL) caused considerable leaking of FITC-dextran. High FITC-dextran liberation from the AC capsules was found, with the intensity escalating from 207, 440 to 582 at the end of the 2<sup>nd</sup>, 3<sup>rd</sup> and 4<sup>th</sup> week, respectively. In comparison, the leaking of the fluorescent marker from the GCAC microcapsules remained insignificant for the first 24 d (intensity <100). Pronounced leaking was detected from day 28, but the intensity in the challenging media remained less than half of the AC capsules (Fig. 8.14d). Based on the above findings, we deduced that (1) the APA microcapsules were vulnerable to enzymatic degradation; (2) the deterioration of the AC and GCAC membranes occurs at higher lysozyme concentrations and extended time periods; and (3) the covalently cross-linked membranes showed stronger resistance to enzyme degradation as compared to the non-cross-linked AC membrane. Further structural investigations on the degraded membranes by SEM would provide supporting information.

#### **8.4.7 Resistance of microcapsules to simulated gastrointestinal fluids**

The preferred route of administration for pharmaceutical products has been oral ingestion. However, most macromolecules are susceptible to rapid degradation by the gastric stresses, digestive enzymes and the natural microflora in the gastrointestinal tract<sup>3</sup>, where the pH fluctuates from below 2 in the stomach to higher than 7 in the intestine, and the proteolytic enzyme activity is highest in the stomach and duodenum, and significantly reduced in the ileum and colon<sup>407</sup>. Various encapsulation systems have been proposed in order to target therapeutics absorption from the colon and ileum<sup>102,247,378,408-410</sup>. In particular, covalent cross-linking gives rise to sufficient improvement in membrane stability and chemical, proteolytic resistance to the GI environments<sup>42,121,265,266,273,411,412</sup>. To investigate the potential of the GCAC systems in oral applications, the microcapsule resistance to the simulated GI conditions was tested by sequential incubation in the simulated gastric fluid (SGF, pH 1.2) and the intestinal fluid (SIF, pH 7.5). Results show that the microcapsules remained physically intact in the SGF. After subjected to the SIF, microcapsules with high

degree of cross-linking (genipin treatment at 20 °C) appeared robust and remained in a relatively good condition after 1 week of interaction (Fig. 8.15 upper row). In contrast, despite the fact that some of the capsules with low cross-linking extent (cross-linked at 4 °C) retained spherical morphology, substantial membrane deterioration occurred, implying the impaired tolerance to the GI impediments (Fig. 8.15 middle row). These indicated that the microcapsule resistance and anti-degradation capacity could be regulated to suit different oral applications, for instance sustained release of drugs, by controlling the extent of cross-linking, which could be achieved by manipulating the chitosan-genipin reaction variables<sup>306</sup>. On the other hand, images in the lower row of Figure 8.15 demonstrated that a large percentage of the APA capsules ruptured with the remaining showing significant swelling after exposure to SIF. As time elapsed, these capsules continued to degrade until they were no longer visible after 12 h. This could be explained by the instability of the APA membrane, and was consistent with the literature reports<sup>27,115,156,308</sup>.

## 8.5 Conclusions

This paper characterizes the structure and physical properties of the genipin cross-linked alginate-chitosan (GCAC) microcapsules. Results showed that by creating the covalent links on the chitosan membrane, the microcapsules possessed strong membrane stability and potent resistance to a number of constraints including mechanical stress, calcium sequestration, enzyme degradation, and GI impediments. Results also demonstrated that the GCAC membranes excluded the infiltration of 70 KD FITC-dextran ( $R_n = 6.4$  nm), while allowing the permeation of bovine serum albumin (BSA,  $R_n = 3.6$  nm). The above findings suggested that covalent cross-linking by genipin provides considerable improvement in the microcapsule strength and resistance while maintaining the permeability characteristics comparable to the AC and APA membranes. Further development of this preparation may permit its use in various biomedical applications.

## 8.6 Acknowledgements

We acknowledge the financial support from Canadian Institutes of Health Research (CIHR). Postgraduate scholarships from Natural Sciences and Engineering Research Council (NSERC) of Canada, Fonds Québécois de la Recherche sur la Nature et les Technologies (FQRNT), and Greville Smith McGill Major to Chen are appreciated. The authors want to thank L. Mongeon, J Laliberte, and H. Vali for the experimental assistance, as well as T. Haque for proofread of the manuscript.

Table 8.1. Characteristics of FITC-dextran used for the measurement of microcapsule permeability

FITC-dextran	FD-4	FD-20	FD-40	FD-70
$M_w$ (KD) <sup>a</sup>	4.4	21.2	38.2	68.1
$M_w/M_n$ <sup>a, b</sup>	1.30	1.32	1.30	1.20
Degree of substitution (mol FITC/mol) <sup>a</sup>	0.003	0.008	0.008	0.008
$R\eta$ (nm) <sup>c</sup>	1.7	3.6	4.8	6.4

<sup>a</sup> Provided by supplier; <sup>b</sup> Polydispersity index; <sup>c</sup> Relative viscosity radius as described by Brissova *et al*<sup>190</sup>.

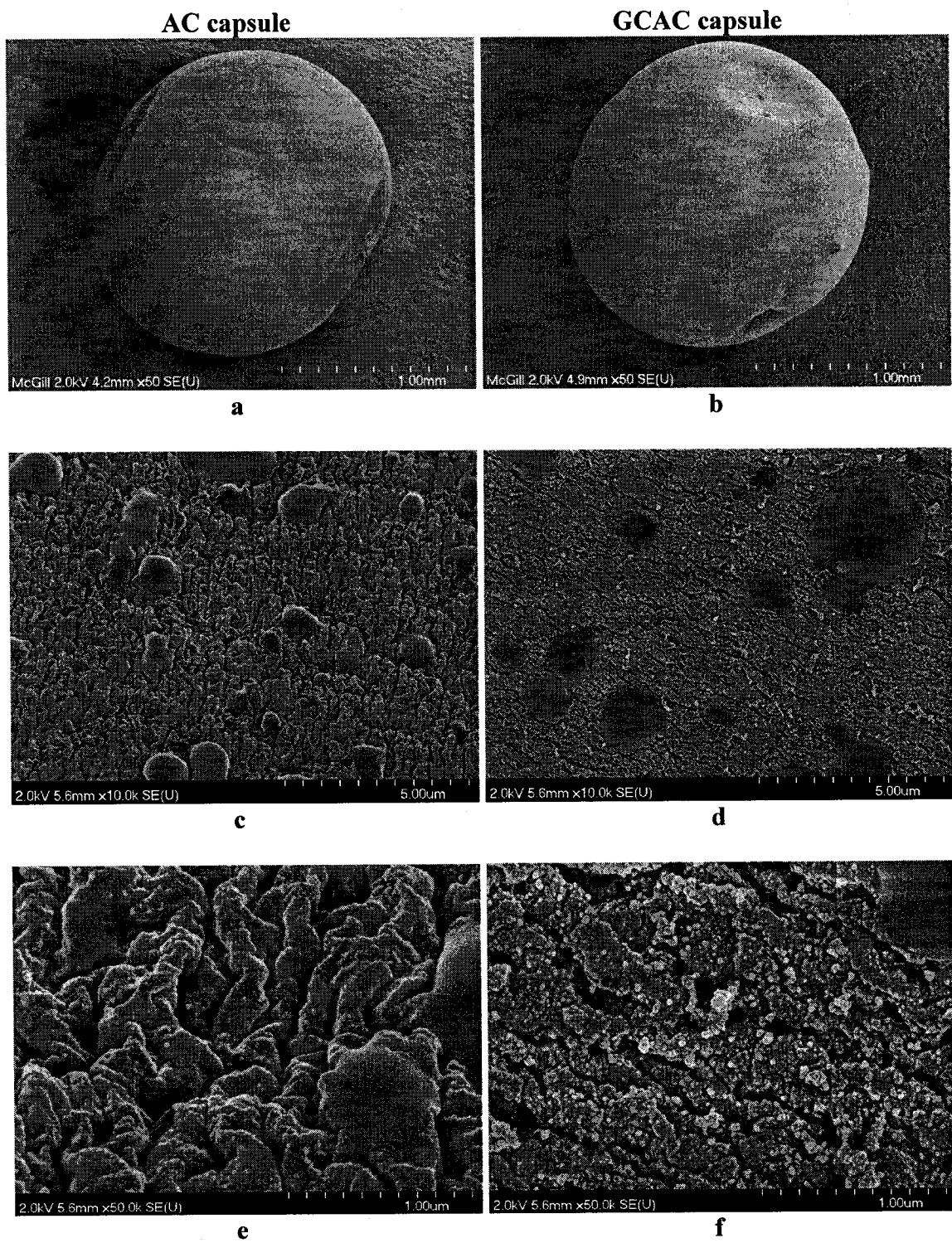
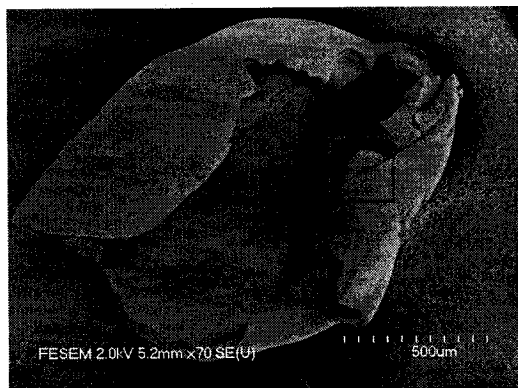
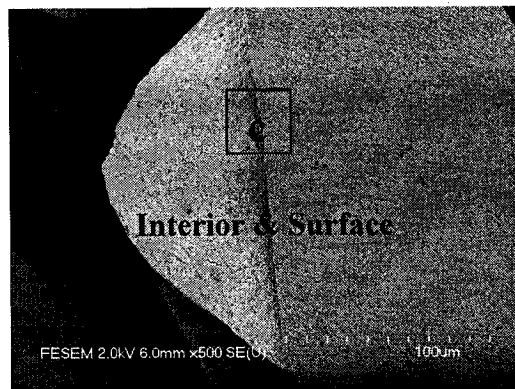


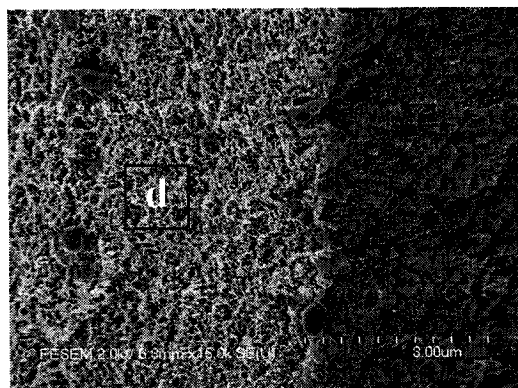
Figure 8.1. SEM images show the general appearance (a-b) and surface structure (c-f) of the AC (left) and GCAC (right) microcapsules. Original magnifications: a-b, 50x; c-d, 10kx; and e-f, 50kx.



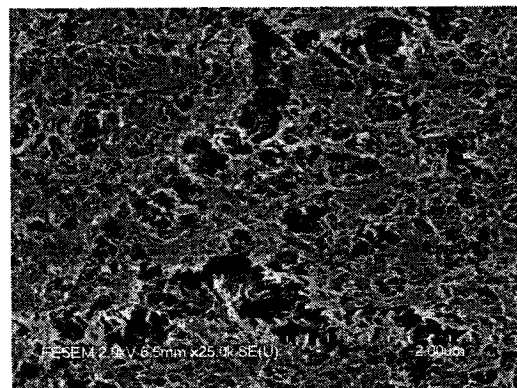
**a**



**b**

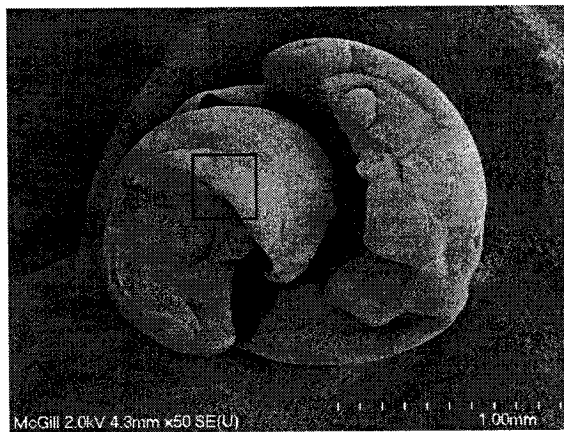


**c**

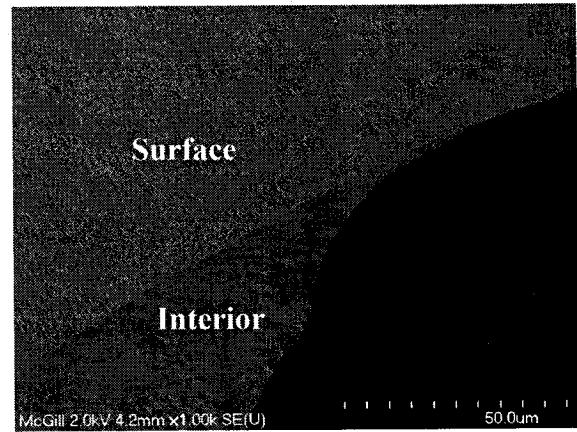


**d**

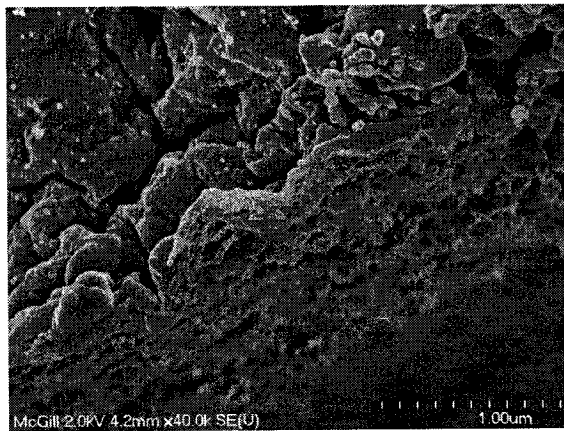
Figure 8.2. SEM images show different structure of the surface and interior of the AC microcapsules. Red boxes indicate selected areas for detailed investigation. Original magnifications: a, 70x; b, 500x; c, 15kx; and d, 25kx.



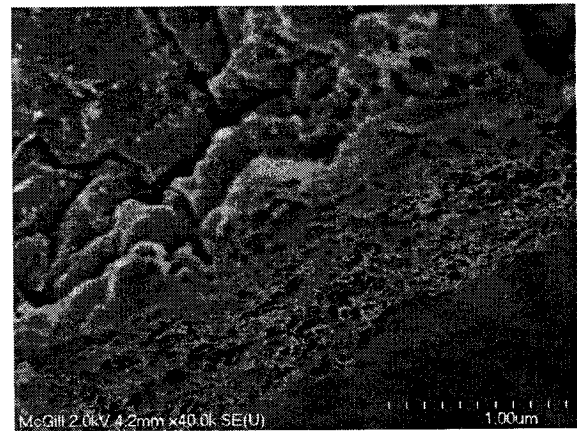
**a**



**b**



**c**



**d**

Figure 8.3. SEM images show the different structure of the surface and interior of the GCAC microcapsules. a, a full view; and b-d, border focused at varied regions. Original magnifications: a, 50x; b, 1kx; and c-d, 40kx.

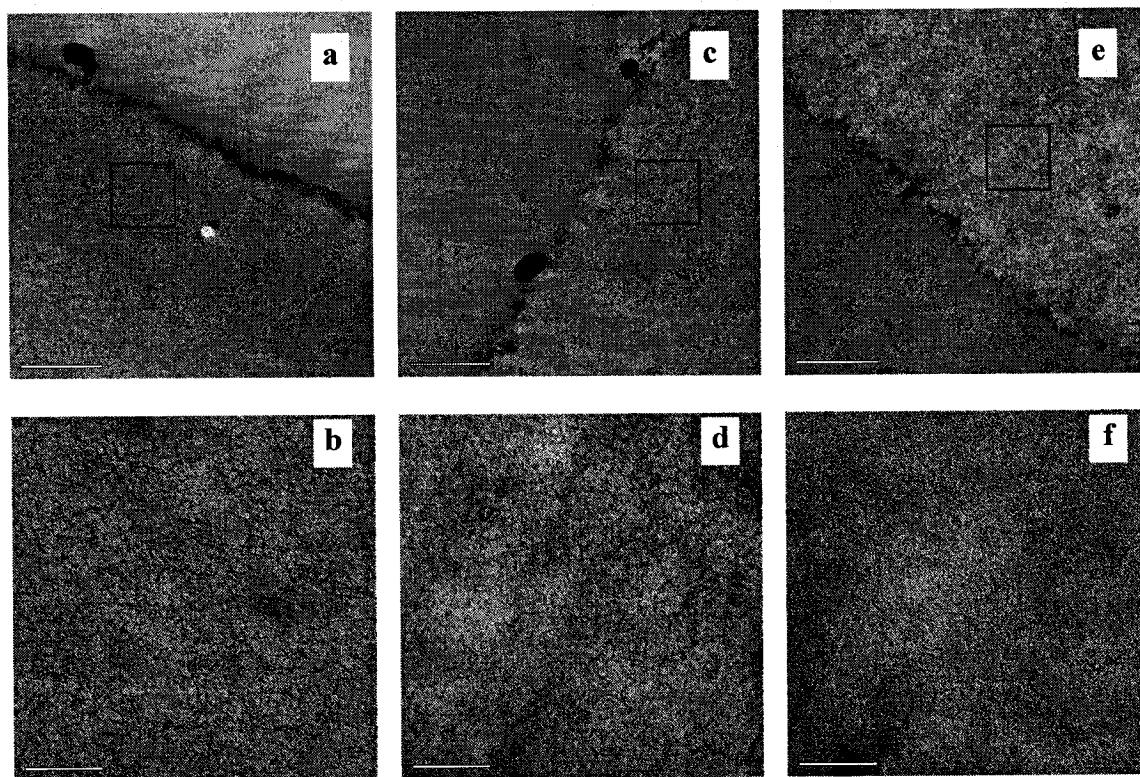


Figure 8.4. TEM images of the microcapsules. a-b, alginate bead; c-d, AC microcapsule; e-f, GCAC microcapsule. Upper row shows the boundary regions of the microcapsule membrane (10Kx, bars=2  $\mu\text{m}$ ), and the structural details of selected regions (shown in red boxes) were depicted in the lower row (100Kx, bars=0.2  $\mu\text{m}$ ).

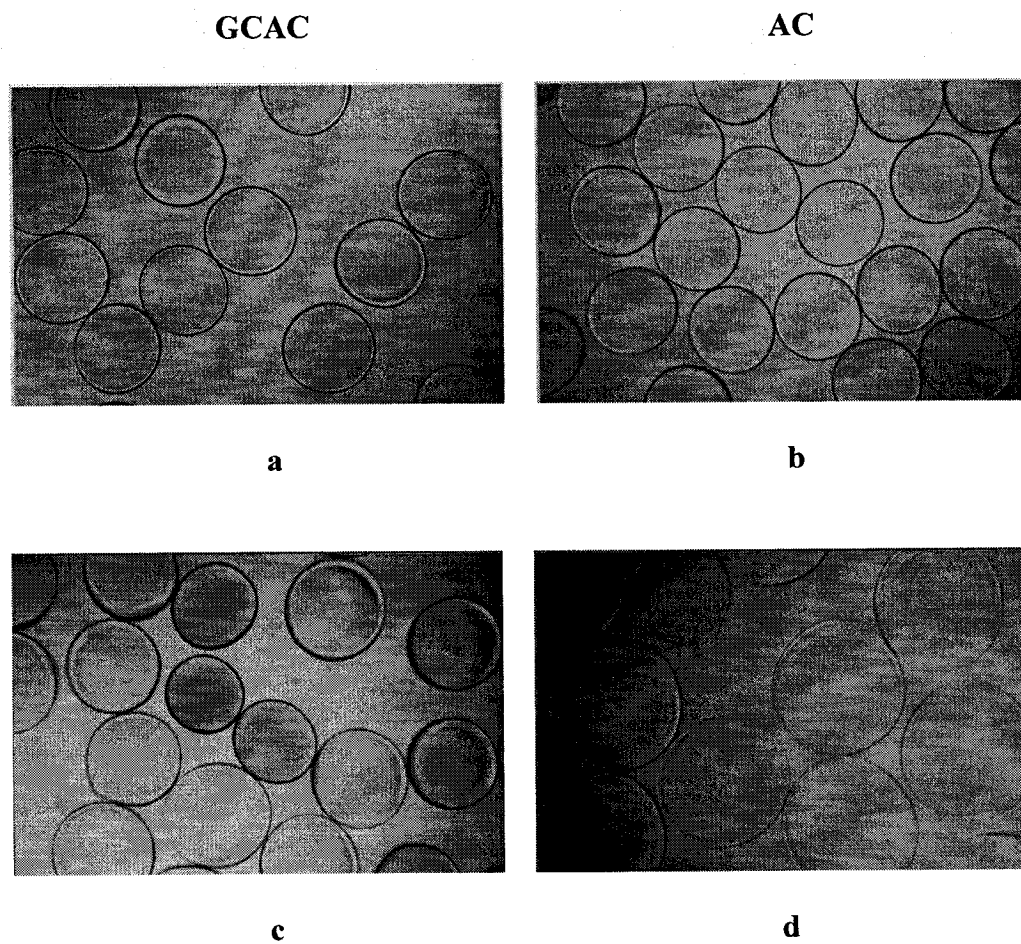
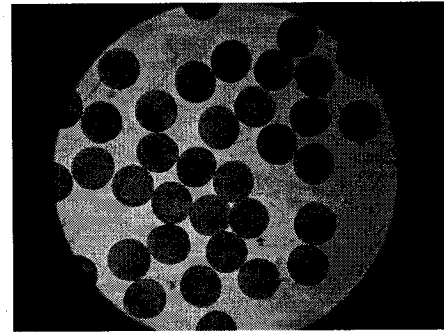
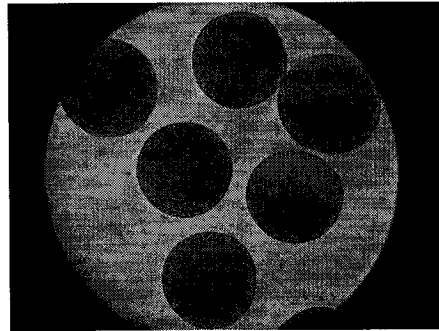


Figure 8.5. Microphotographs of the GCAC (a, c) and AC (b, d) microcapsules before (a- b) and after (c- d) chelation by sodium citrate (50 mg/mL) for 24 h. Original magnifications: 35x.

**GCAC microcapsules**



**AC microcapsules**

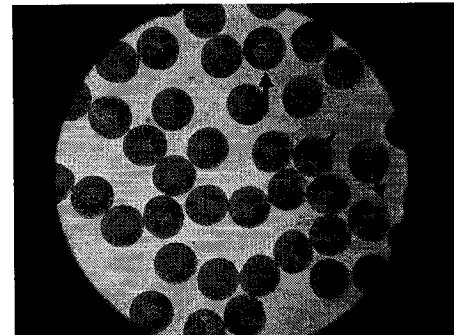
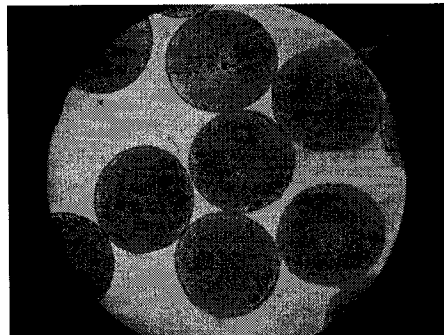


Figure 8.6. Morphological stability of the GCAC (upper row) and AC (lower row) microcapsules containing blue dye after incubation in saline for 6 months. Red arrows indicate defects of the capsules. Original magnifications are either 90x (left) or 35x (right).

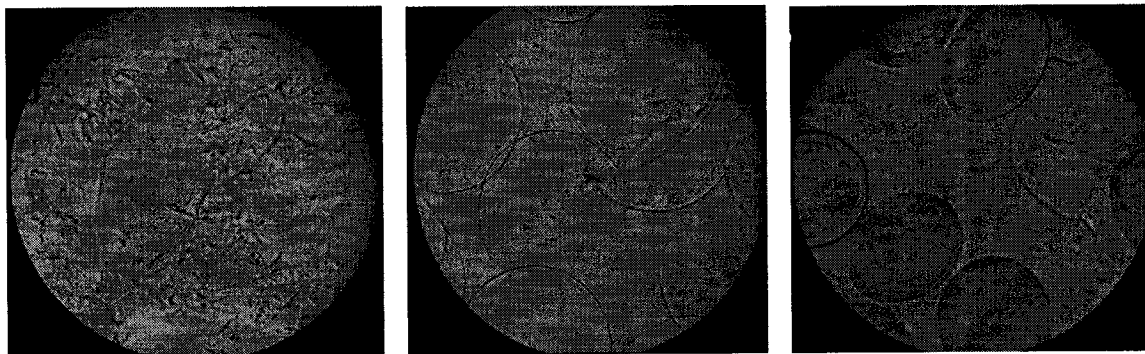


Figure 8.7. Microphotographs of microcapsules after being subjected to continuous mechanical agitation (600 rpm for 3 h). a, APA; b, AC; and c, GCAC (original magnifications: 90x).

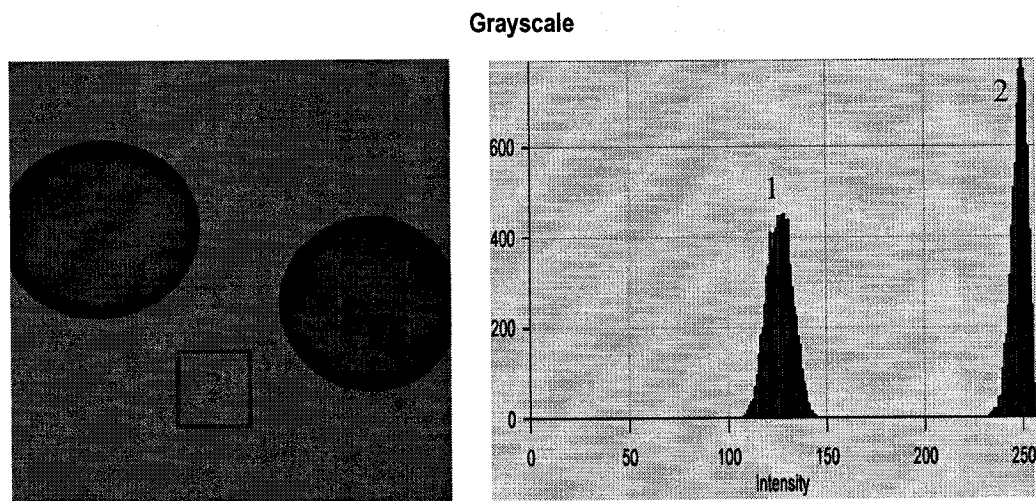


Figure 8.8. Analysis of fluorescence intensity inside and outside the microcapsule. The GCAC microcapsules were cross-linked by genipin (2.5 mg/mL, at 20 °C for 5 h) and incubated in a FITC-dextran solution (20 KD, 250  $\mu\text{g}/\text{mL}$ ) at room temperature overnight.

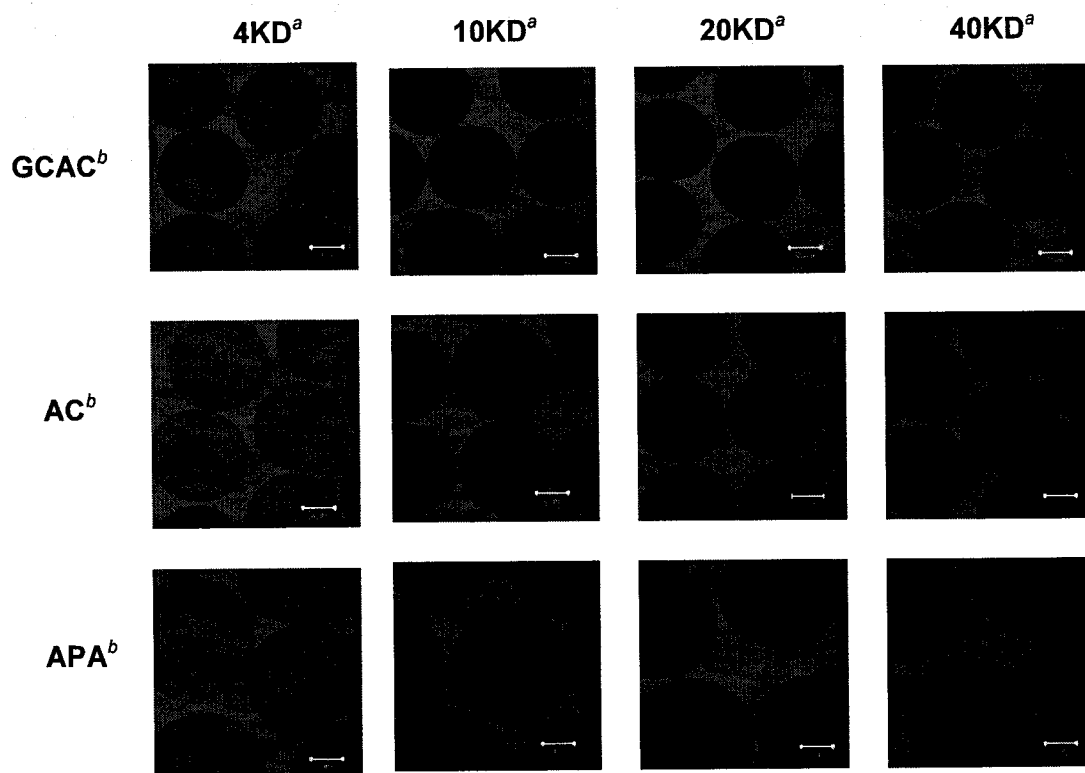


Figure 8.9. Visualization of FITC-dextran permeation into microcapsules by CLSM. <sup>a</sup> Molecular weight of FITC-dextran; <sup>b</sup> Type of microcapsules. Bars= 200  $\mu$ m.

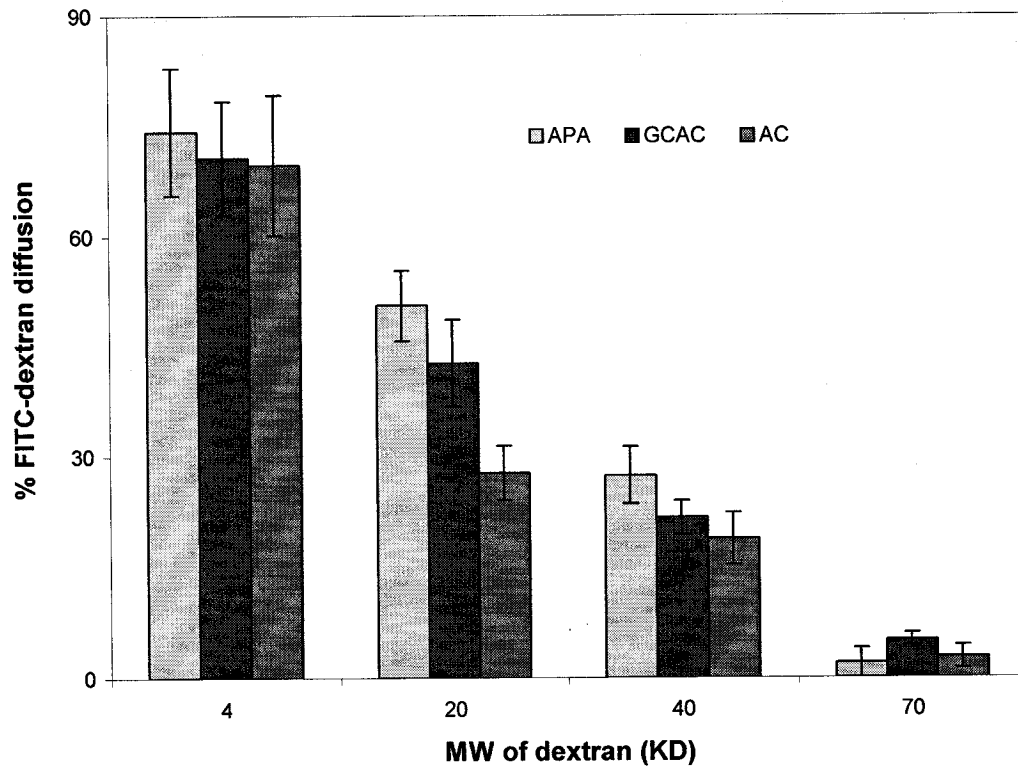


Figure 8.10. Diffusion of FITC-dextran into microcapsules as a function of dextran molecular weight.

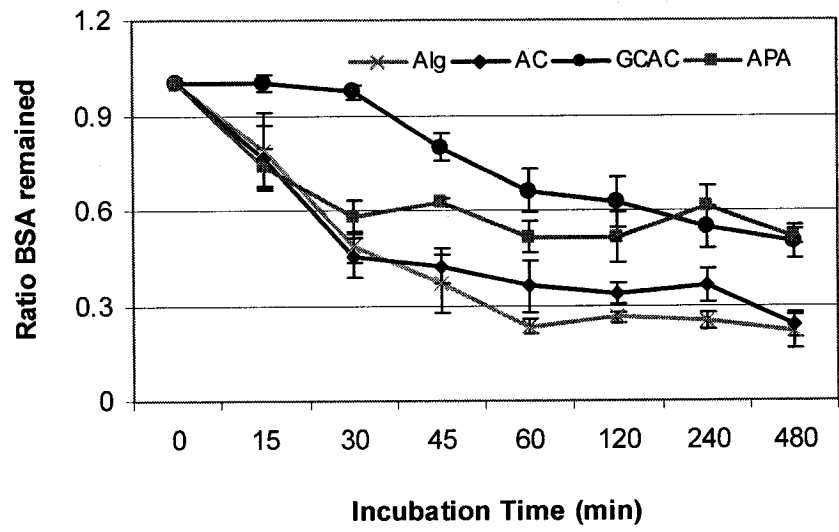


Figure 8.11. Penetration of BSA into microcapsules as a function of incubation time.

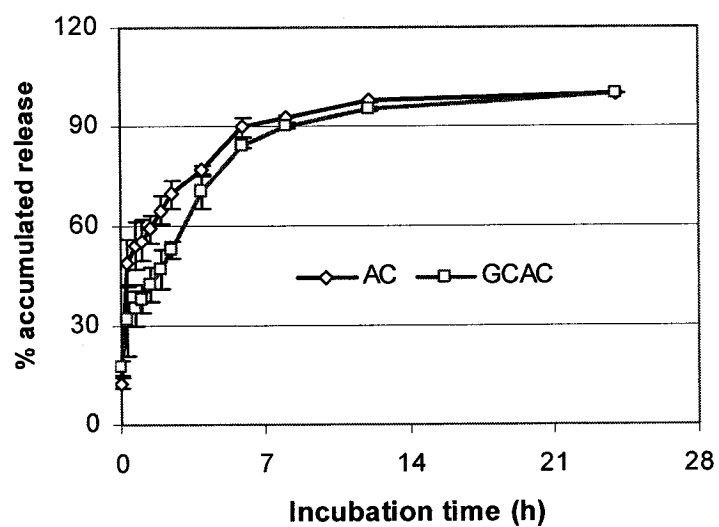


Figure 8.12. Cumulative release of encapsulated BSA from microcapsules as a function of incubation time

**Detector signals  
(mVolts)**

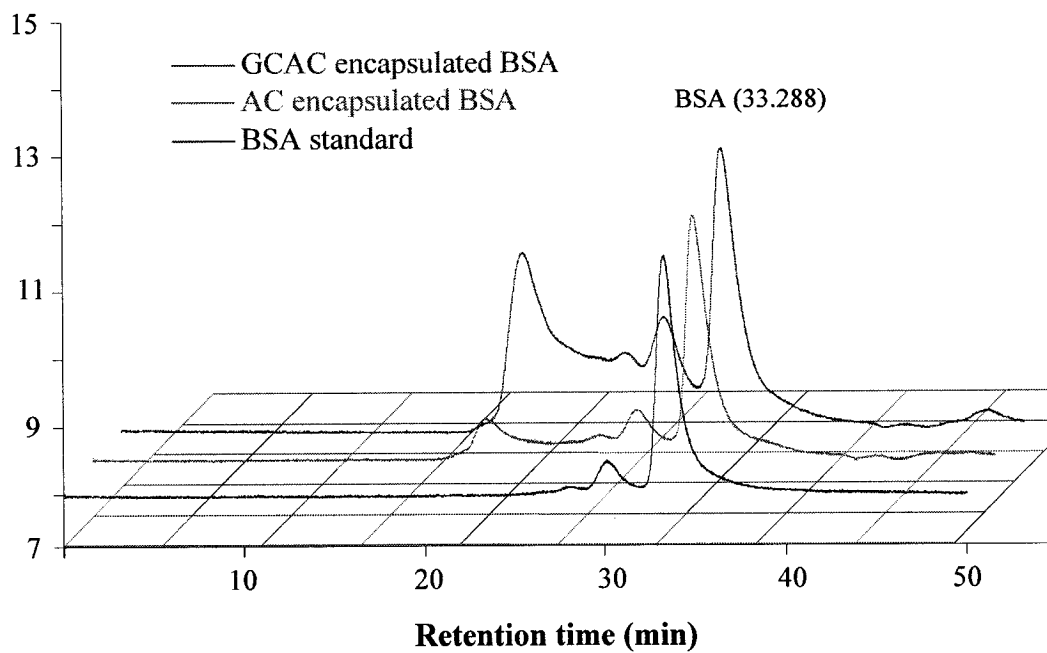
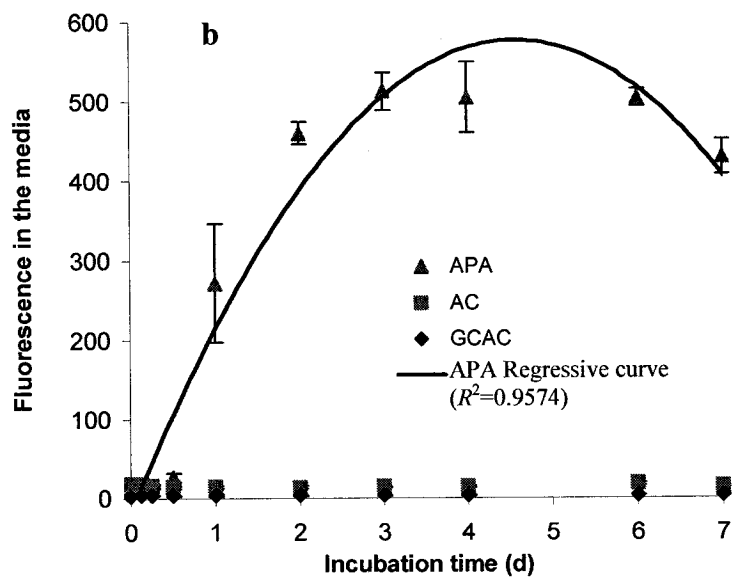
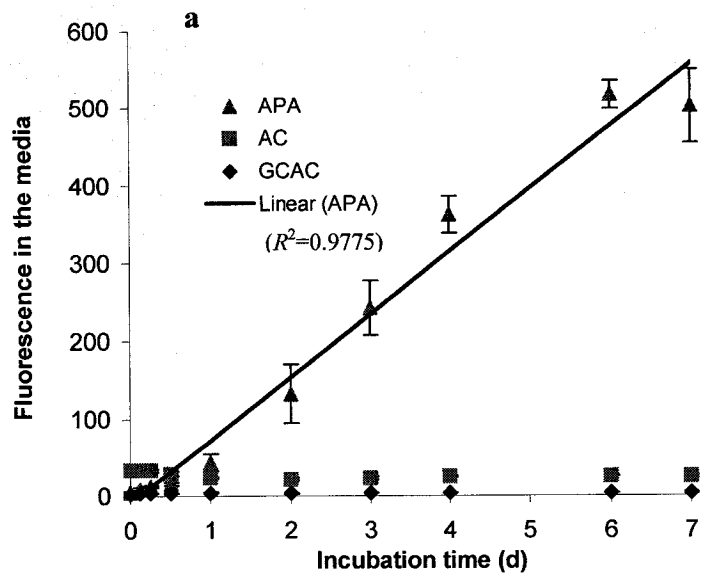


Figure 8.13. HPLC chromatographs of the encapsulated BSA in the GCAC and AC microcapsules as compared to BSA standard.



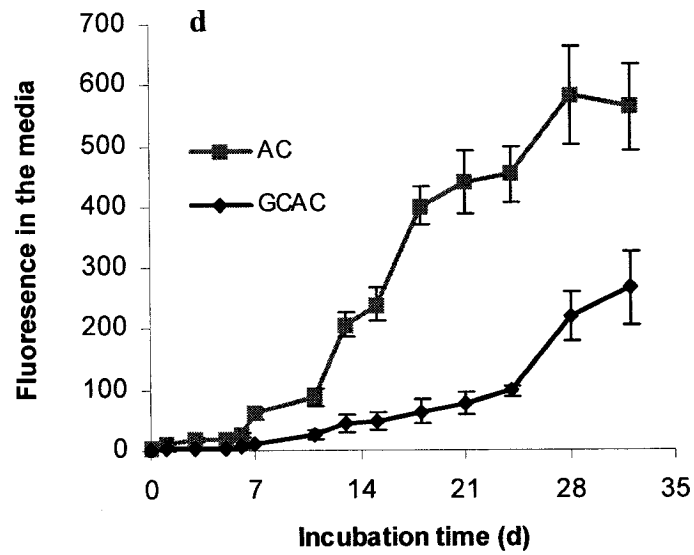
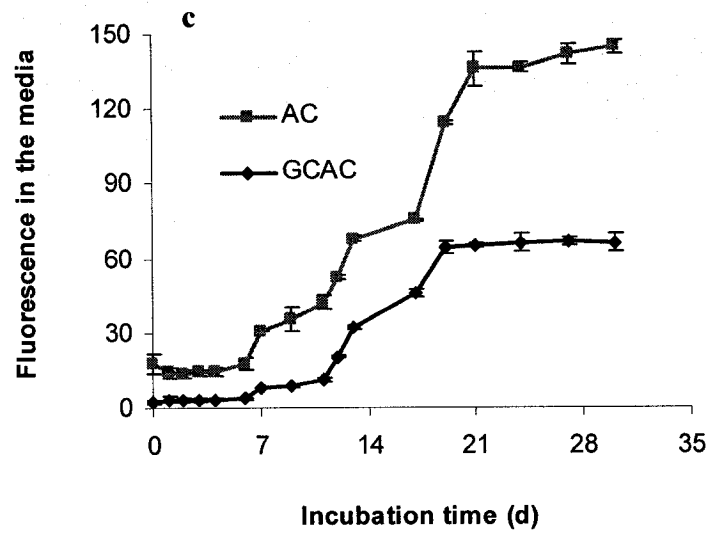


Figure 8.14. Leaking of the entrapped FITC-dextran (MW 2000 KD) from microcapsules incubated in lysozyme solution at the concentrations of a, 15  $\mu\text{g/mL}$ ; b-c, 0.15 mg/mL; and d, 15 mg/mL.

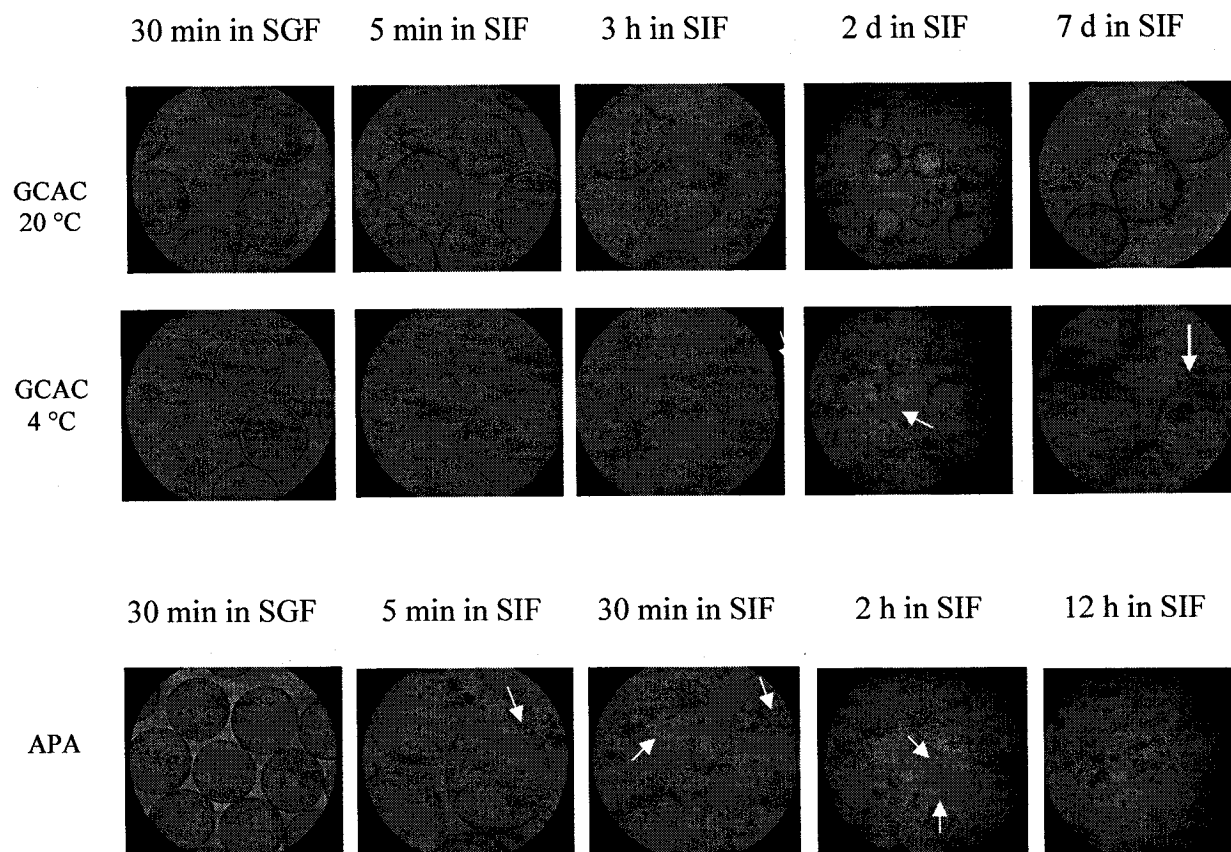


Figure 8.15. Microphotographs of microcapsules after sequential incubation in the simulated gastric fluid and the simulated intestinal fluid. Upper row: GCAC microcapsules cross-linked at 20 °C; middle row: GCAC microcapsules cross-linked at 4 °C; and lower row: APA microcapsules. Arrows indicate the presence of ruptured microcapsules. (Original magnifications were 90x except for the images on the 4<sup>th</sup> column at 35x)

**Investigation of microcapsules for potential gastrointestinal applications using a dynamic simulated human gastrointestinal model**

Hongmei Chen, Wei Ouyang, Christopher Martoni, Fatemeh Afkhami, Trisna Lim and Satya Prakash\*

*Biomedical Technology and Cell Therapy Research Laboratory*

*Department of Biomedical Engineering and Physiology, Artificial Cells and Organs Research Centre, Faculty of Medicine, McGill University, Montreal, Quebec, H3A 2B4 Canada.*

\*Corresponding author: Tel: 514 398-3676; Fax: 514 398-7461;  
Email: satya.prakash@mcgill.ca

---

**Preface:** The pertinent microcapsule performance in the gut lumen requires prudent examination as it largely influences the extent of delivery of therapeutic biologics to the intestine and may be of relevance for assessing risks regarding the use of live and genetically-engineered cells. This paper examines the membrane resistance of the GCAC microcapsules during the simulated human GI transit using a dynamic computer-controlled simulated gastrointestinal (GI) model which is a more accurate representation of the human GI environment. Results for the GCAC membrane were compared with other non-cross-linked control capsules. This work demonstrates the potential of the GCAC microcapsule system for oral applications.

This paper has been submitted to *Journal of pharmaceutical sciences*. Part of the results was published in *IFMBE proceeding series 12, 2005*.

## 9.1 Abstract

Oral administration of live genetically engineered microorganisms requires protection by microencapsulation and complete retention of the encapsulated cells, preventing leakage into the host's gastrointestinal (GI) system, to assuage safety concerns. It is thus imperative that microcapsules be able to tolerate the harsh environment in the human gut and uphold their structural integrity throughout the GI transit. The present research examines the suitability of a novel covalently cross-linked microcapsule system as a potential oral delivery device using a computer-controlled dynamic simulated human GI model. This *in vitro* apparatus mimics the gradual transit of ingested materials through the human digestive tract and enables the study under physiologically-pertinent conditions. After a 3-day simulated GI transit, a well-preserved morphology of the genipin cross-linked alginate-chitosan (GCAC) microcapsules and a high retrieval were attained. Results also showed negligible leaking of encapsulated high molecular weight dextran from the GCAC microcapsules. This signified the preservation of membrane integrity and the improvement in membrane stability of the microcapsules by covalent genipin cross-links, in comparison to the conventional ionically linked alginate-chitosan (AC) and the alginate-poly-L-lysine-alginate (APA) microcapsules. Furthermore, the effects of the microcapsules on the micro-flora and the enzymatic activities of the simulated human colonic media were investigated. Results of this paper suggested the superior resistance of the GCAC microcapsules to the simulated human GI environment and their potential for oral cell therapy.

**Key words:** microcapsule, GI, integrity, resistance, genipin, cross-linking, alginate, chitosan

## 9.2 Introduction

Advances in molecular biology research have introduced a wide range of genetically engineered cells with a superior capacity to produce disease modifying substrates, such as cytokines, enzymes, vaccines, hormones, antibodies, growth factors and other therapeutic products<sup>1,2</sup>. The use of these materials opens up new hopes of treating a wide array of human diseases. However, these biologics are generally fragile and easily degraded or denatured<sup>3</sup>.

The combination of cell therapy and encapsulation technology offers significant advantages over conventional biotechnological production methods using engineered cells<sup>22</sup>. The functional cells can be protected by microencapsulation and delivered proximally to the target site *in vivo*. This strategy eliminates the complex isolation processes, and also benefits from the continuous secretion and delivery of therapeutic products to the host at a more physiological and effective concentration. Also, the semi-permeable membrane of the microcapsule provides a physical barrier and isolates the engineered cells from the host system, which potentially allows the use of xenogeneic cells or tissues without the need for immuno-suppression. Recent research on the microencapsulation of genetically engineered cells has shown promise in the treatment of a number of diseases<sup>9,19,68,82,83,85,93,94</sup>. Nevertheless, the greatest concern is that of cell leakage, in particular for oral administration of genetically modified bacteria.

Oral ingestion is the preferred route of administration for therapy; however, microcapsules containing genetically engineered bacteria can be disrupted by a number of means during exposure to the harsh gastrointestinal (GI) environment. The eruption of microcapsules and the subsequent release of engineered bacteria could induce many adverse effects on the body. For instance, there have been concerns about potential provocation of host immune responses, propagation of foreign bacteria in the GI tract, disturbance of the gut natural flora balance and possible gene transfer<sup>2,12-17</sup>. Translocation of orally administered viable microorganisms into Peyer's patches and mesenteric lymph nodes has been reported<sup>413</sup>. Other risks include systemic infections, deleterious metabolic activities and adjuvant side-effects<sup>13</sup>. Thus it is likely that the FDA will require absolutely no leaking of GE bacteria from orally administered microcapsules into the host's GI system, even though they are classified as non-pathogenic<sup>19</sup>. In other words, live engineered microorganisms, unlike conventional probiotics such as in dietary supplements, must be encased in the microcapsules throughout the entire GI transit and be excreted in the feces along with the intact microcapsules after executing their therapeutic functions such as the secretion of needed biologics and the absorption of undesirable metabolites. Therefore, it is essential to preserve the structural integrity of the microcapsules in relevant oral applications.

Although numerous microcapsule systems have been studied for oral delivery, such devices are mostly used for the controlled release of curative agents, for instance drugs and

probiotics to the intestine<sup>20-25</sup>. Scanty research is available on microcapsules intended to retain the live cells throughout the GI transit. Towards this goal, we have recently developed a novel covalently cross-linked microcapsule system, composed of a calcium alginate core with a genipin cross-linked chitosan membrane<sup>306,390</sup>. Genipin and its derivatives, extracted from gardenia fruits<sup>282</sup>, have traditionally been used as a herbal medicine as well as a natural colorant in the food and fabric industries<sup>288</sup>. While previous research has demonstrated its low cytotoxicity and its potential in live cell encapsulation and membrane reinforcement<sup>299,390,414</sup>, the present work investigates the suitability of the genipin cross-linked alginate-chitosan (GCAC) microcapsule system for GI applications. An *in vitro* dynamic human GI model was used to examine the microcapsule behaviors in relation to the capsular integrity and retention of encapsulated materials. For comparison, the frequently used and ionically linked alginate-chitosan (AC) and alginate-poly-L-lysine-alginate (APA) microcapsules were also tested. The results obtained highlight the potential of the novel GCAC microcapsules in relevant GI applications.

### **9.3 Experimental**

#### **9.3.1 Chemicals**

Sodium alginate (low viscosity), poly-L-lysine hydrobromide ( $M_v$  27,400) and fluorescein isothiocyanate (FITC) labeled dextran ( $M_w$  2,000 KD) were supplied by Sigma-Aldrich, USA. Chitosan (low viscosity,  $M_v=7.2 \times 10^4$ , degree of deacetylation or DDA=73.5 %) and genipin were purchased from Wako BioProducts, USA. 4-nitrophenyl- $\alpha$ -D galactopyranoside, 4-nitrophenyl- $\alpha$ -D glucopyranoside and 4-nitrophenyl- $\beta$ -D galactopyranoside were obtained from Acros Organics, USA. 4-nitrophenol, 4-nitrophenyl- $\beta$ -D glucopyranoside and 4-nitrophenyl- $\beta$ -D glucuronide were also purchased from Sigma-Aldrich, USA. All other reagents and solvents were of reagent grade and used as received without further purification.

#### **9.3.2 Preparation of microcapsules**

To prepare the alginate microcapsules, droplets of a sodium alginate solution (15 mg/mL) were generated by an encapsulator (Inotech. Corp.), extruded through a 300  $\mu$ m

nozzle and gelled for 15 min in a stirred  $\text{CaCl}_2$  solution (11 mg/mL). The resulting microcapsules were approximately 560  $\mu\text{m}$  in diameter. The rigid Ca-alginate beads were then coated with chitosan by immersion in a chitosan solution (10 mg/mL in  $\text{CaCl}_2$  solution) for 30 min followed by washing three times with deionized  $\text{H}_2\text{O}$ , resulting in the formation of alginate-chitosan (AC) microcapsules. The subsequent cross-linking reaction was performed by suspending the AC microcapsules in a genipin solution (2.5 mg/mL) at room temperature, unless otherwise stated. The resulting GCAC microcapsules were washed and collected. The APA microcapsules, initially developed by Lim and Sun<sup>69</sup>, were also prepared as previously described and used in our laboratory for cell encapsulation and oral delivery<sup>27</sup>. Sterile microcapsules were prepared using similar methods with the exception that the entire encapsulation procedure was carried out in a biological containment hood and all solutions used were either 0.22  $\mu\text{m}$  filtered or autoclaved to ensure sterility.

### **9.3.3 Preparation of microcapsules containing FITC-labeled dextran**

Microcapsules containing high molecular weight FITC-labeled dextran ( $M_w$  2,000 KD) were prepared by mixing FITC-dextran with an alginate solution, making the final concentrations of alginate and FITC-dextran at 15 mg/mL and 2 mg/mL, respectively. The subsequent processes, including the formation of alginate beads, coating and cross-linking were performed using aforementioned procedures.

### **9.3.4 Simulation of the human gastrointestinal (GI) environment**

The human GI conditions used in this study were simulated *in vitro* by means of a series of bioreactors consisting of five vessels in series with each compartment simulating a different stage of human GI transit, which includes the stomach, the small intestine, the ascending colon, the transverse colon, and the descending colon. Human fecal slurries containing normal human GI bacterial cells were inoculated into the simulated colon (the last three vessels). The whole system was maintained under anaerobic conditions by flushing the headspace of each vessel with  $\text{N}_2$  and the temperature was kept constant at 37 °C. A carbohydrate-based diet suspension was fed to the first vessel three times a day. After feeding, acidification of the stomach ( $\text{pH} \leq 2$ ) occurred, followed by neutralization ( $\text{pH} \geq 6.8$ ) in the second vessel and addition of simulated pancreatic juice, composed of  $\text{NaHCO}_3$ , oxgall and

pancreatin, to the simulated small intestine. Afterwards, the suspension was transferred to the simulated ascending colon, the transverse colon, and the descending colon, and finally excreted as effluent. The entire process, including pH conditions, fluid volume and retention time at each stage was simulated and under computer control.

### **9.3.5 Resistance of microcapsules to the simulated human GI transit**

To study the microcapsule resistance to the simulated human GI transit, microcapsules (0.80 g) were exposed to the simulated human GI fluids for the estimated maximum period of time for the human GI transit (Table 9.1)<sup>415</sup>. Microcapsule samples were withdrawn at varied stages for morphological examination under an inverted microscope (LOMO, PC).

Microphotographs were taken as records using a digital camera (Canon Power shot G2).

To assess the recovery of microcapsules after the simulated human GI transit, microcapsules of known weight were retained in a sealed teabag-like container and exposed to the simulated GI media as described above. At the end of the transit, the microcapsules retrieved were washed and weighed. The percent recovered was defined as:

$$\% \text{ recovery} = (W_0 - W) / W_0 * 100$$

where  $W_0$  and  $W$  are the weights of the microcapsules before and after the exposure to the simulated GI transit, respectively.

### **9.3.6 Retention of encapsulated FITC-dextran against leaching into the simulated GI tract**

To evaluate the capacity of the GCAC microcapsules to retain enclosed materials, high molecular weight FITC-dextran was encapsulated as model macromolecules. FITC-dextran encapsulated beads ( $0.60 \pm 0.01$  g) were exposed to 2 mL of the simulated human gastric fluid and incubated in an Environ shaker at 37 °C, 100 rpm for 1 h, followed by a 72 h incubation in 2 mL of the simulated human intestinal fluid (37 °C, 100 rpm). Samples of the media were periodically withdrawn during incubation and the leaking of the encapsulated FITC-dextran was assessed spectrofluorometrically using a Microplate Fluorescence Reader (FLx800, Bio-Tek Instruments, Inc.) at absorption and emission wavelengths of 485 and 528 nm, respectively. The volume of the media was kept constant by adding fresh medium after sampling. Data are presented as mean  $\pm$  s.d. from triplicate experiments.

### **9.3.7 Effect of oral administration of microcapsules on the simulated gut microflora**

To investigate the influence of oral administration of microcapsules on gut microflora, sterile microcapsules (1.0 g) were mixed with the suspension from the simulated transverse colon (10 mL). After pre-designated periods of anaerobic incubation at 37 °C, samples of the incubation medium were aseptically withdrawn and serially diluted by physiological saline. Bacterial enumeration for specific fecal marker microorganisms, total aerobes, total anaerobes, *Escherichia coli*, *Staphylococcus* sp., and *Lactobacillus* sp. was performed in triplicate using an agar-plate-count assay. The plating media and incubation conditions used are listed in Table 9.2. The simulated colonic suspension without microcapsules was used as control.

### **9.3.8 Effect of oral administration of microcapsules on the enzymatic activities in the simulated GI model**

To assess the effect of oral administration of microcapsules on the extra-cellular intestinal enzyme activities, the suspension from the simulated transverse colon (20 mL) was incubated anaerobically at 37 °C in the presence of sterile microcapsules (2.0 g) for up to 24 h. At intervals, the enzymatic activities of  $\beta$ -galactosidase,  $\beta$ -glucosidase,  $\beta$ -glucuronidase,  $\alpha$ -galactosidase and  $\alpha$ -glucosidase in the incubation medium were analyzed spectrometrically using the method described earlier<sup>27,416</sup>. The absorbance at 405 nm was recorded by a  $\mu$ Quant multi-plate reader (Bio-Tek Instruments). The simulated colonic fluid free of microcapsules was used as control. Results are expressed as percentage of enzymatic activities relative to the control at each time point. Control values at each time point were normalized to 100%.

## **9.4 Results**

### **9.4.1 Resistance of microcapsule to the simulated human GI transit**

To assess the capsular resistance to the GI environment, the genipin cross-linked alginate-chitosan (GCAC) microcapsules were exposed to the simulated GI media representing different phases of digestion for a length of time based on the estimated

maximum retention in the human GI tract (Table 9.1). Figure 9.1 depicts the photomicrographs of the microcapsules cross-linked at two different temperatures and exposed to the simulated human GI fluids. During the 2 h incubation in the simulated stomach ( $\text{pH} \leq 2.0$ ), the tested microcapsules were found morphologically stable (Fig. 9.1-a, d, g, and j). In the subsequent simulated GI transit, the performance of the GCAC microcapsules with different degree of cross-linking varied. For those cross-linked at 4 °C, although the structural integrity was largely retained in the transverse colon (microphotographs not shown), appreciable capsular swelling and slight membrane thinning occurred in the simulated small intestine ( $\text{pH} 7.2-7.4$ ) (Fig. 9.1-b and e). At the final stage of GI transit, these capsules became weak and adhesive; some even shriveled or partially dissolved, with nearly 30-40 % of the capsules losing their structural integrity when leaving the simulated descending colon (Fig. 9.1-c and f). In contrast, the majority of the GCAC microcapsules cross-linked at 20 °C maintained their physical stability during the entire simulated human GI transit, as evidenced by well-preserved morphology (Fig. 9.1 g-l). No obviously ruptured or disintegrated microcapsules were detected. In addition, more than 80 % of these cross-linked microcapsules were recovered after the 72-h simulated human GI transit (Fig. 9.2). In comparison, the recovery of those cross-linked at 4 °C was lower (61.4 %), and less than 17 % of the APA microcapsules were retrieved after a 3-day exposure to the simulated GI environment (Fig. 9.2).

#### **9.4.2 Retention of encapsulated HMW dextran during the simulated GI transit**

To examine the capacity of the GCAC microcapsules to retain the enclosed materials in the harsh GI environment, high molecular weight FITC-labeled dextran was selected as a model material to be protected by microencapsulation. Being a large polymer of 2,000 KD, this fluorescent probe was indefinitely withheld inside the intact microcapsules and could not leak out unless the microcapsule membranes became defective or damaged<sup>331</sup>. When the microcapsules containing FITC-dextran were exposed for 1 h in the simulated gastric fluid, no FITC-dextran was detected in the incubation medium (data not shown). In the subsequent exposure to the simulated intestinal medium, considerable liberation of FITC-dextran from the conventional APA microcapsules was found. The fluorescence intensity of the medium augmented quickly from nominal at time 0 to 73, 205 and 283 at 3, 24 and 72 h, respectively

(Fig. 9.3). For the non-cross-linked AC beads, the leakage of the encapsulated FITC-dextran increased gradually with the incubation time, attaining the fluorescence intensity of 70, 100 and 115 at 24, 48 and 72 h, respectively. In contrast, negligible amounts of FITC-dextran escaped from the GCAC microcapsules, with very low fluorescence intensity of the medium detected (not exceeding 50) throughout the experiment (Fig. 9.3), which significantly outran those of the APA and AC microcapsules.

#### **9.4.3 Oral administration of microcapsules on gut microflora and enzymatic activities**

Another important prerequisite of encapsulated cell oral therapy is that the administration of microcapsules should not disturb the natural colonic flora, particularly when prolonged and repeated oral intake of a rather large quantity of microcapsules is required as a therapy for patients. To address this, the representative microbe populations and enzyme activities in the simulated human colonic media, in the presence of and in the absence of microcapsules, were investigated. Since the simulated GI model is a dynamic system, in this study, static experiments were performed in order to maximize the effects. Table 9.3 shows no marked differences, as compared to the control, in the population of tested microbes including total aerobes, total anaerobes, *Escherichia coli*, *Staphylococcus sp.* and *Lactobacillus sp.*, in the media containing microcapsules, except for slightly lower log units of *E. coli* in the media containing microcapsules than that in the control after 24 h of incubation.

Figure 9.4 shows the influence of the microcapsules on the activities of five tested enzymes in the suspension of the simulated transverse colon. As time elapsed, a slight decline in the tested enzymatic activities was found in the simulated colonic fluids in the presence of microcapsules. As an exception, a decrease of more than 20 % in the activity of  $\beta$ -glucuronidase was detected after 12 h of contact with microcapsules, but the loss of the activity remained at a similar level with extended interaction time for up to 24 h (Fig. 9.4-c). Furthermore, no apparent differences in the alteration of enzymatic activities were found among different microcapsule samples.

### **9.5 Discussion**

For the successful exploitation of microcapsules as an oral delivery device, knowledge of microcapsule performance under physiologically pertinent conditions that represent the human GI conditions is required. With respect to the simulation of the human GI system, buffered solutions, such as hydrochloric solution at pH 1-2 and phosphate buffered saline served as the simulated gastric and intestinal conditions, respectively, are simple and widely used<sup>49,417,418</sup>; however they only correspond to the pH in the stomach and in the intestine, and do not represent the complex human GI environment. Other *ex vivo* and *in vitro* simulated models were also reported, but have yet to give satisfying results<sup>419</sup>. Although there has been *in vivo* research in animals and humans that progressively tracked the microcapsules in the GI tract using histological sectioning<sup>247</sup>, radiography<sup>420</sup> and gamma scintigraphy<sup>421,422</sup>, it remained difficult to follow the orally administered microcapsule at every stage of digestion on its passage through the complex GI environment. Additionally, these *in vivo* practice methods may be affected by ethical constraints, which make in-depth mechanistic studies difficult. In the current research, we used a dynamic computer-controlled simulated human gastrointestinal model to evaluate the GCAC microcapsules. This apparatus, which is different from the above models, mimics the gradual transit of ingested food through the human digestive tract and simulates the complex intestinal microbial ecosystem composed of hundreds of different bacterial species<sup>423</sup>. It allows for examining the fate of administered microcapsules under physiologically-pertinent conditions that are relatively close to the human GI environment. Moreover, this computer controlled *in vitro* model is easier to operate, which is especially preferable for screening and examining a variety of samples.

As has been noted earlier, to prevent the leaking of genetically engineered cells to the GI tract, it is imperative that microcapsules maintain physical integrity during the GI transit. This capacity is strongly dependent on the capsule robustness and stability. So far relevant studies addressing this issue are scarce<sup>27</sup>. The present study investigated the behaviour of the recently developed GCAC microcapsules in the simulated human GI environment. Specifically, the microcapsules were exposed in the simulated GI media in an attempt to mimic the experience along the GI course including pH fluctuation, enzymatic degradation, microorganism actions, mechanical stresses as well as other related chemical and physiological constraints. After being subjected to the simulated GI environment for 3 days, better-preserved morphology and higher retrieval rate were found for the GCAC

microcapsules cross-linked at a higher temperature (Fig. 9.1 & 9.2), indicating the improvement in membrane stability by a higher degree of cross-linking. Moreover, it was found that negligible amounts of encapsulated fluorescent probe were released into the incubation GI media from the GCAC capsules (Fig. 9.3), signifying that the integrity of the microcapsule membrane was retained. In comparison, the non-cross-linked AC and the conventional APA microcapsules were less resistant to structural disruption in the harsh GI condition<sup>27</sup>. It is clear that microcapsules prepared via ionic complexation of polyelectrolytes, such as alginate, chitosan and poly-L-lysine (PLL), are prone to structural disintegration by gastric and proteolytic degradation, which corroborated the results reported previously<sup>27</sup>. Other impediments also included the cleavage of the complex coating, which may have caused disintegration of the microcapsules<sup>29,33,184</sup>. The present research demonstrated that covalent cross-linking of microcapsule membranes by genipin substantially improved the resistance of the microcapsules to degradation in the hostile simulated human GI environment. Another key property for microcapsules as an oral delivery vehicle for live cells is the maintenance of the cell viability in the gut lumen, which will be addressed in future studies.

It is known that a well-balanced gut microbiota plays an important role on human health<sup>424</sup>; upsetting the intestinal flora can lead to many health problems<sup>425</sup>. It is thus important to ensure that oral administration of microcapsules does not disturb the natural colonic flora. Taking into consideration the static nature and rather large dosage (1.0 g of microcapsules in 10 mL of intestinal fluid) of the experiments, the results from the present *in vitro* study may suggest that the materials used to construct the microcapsules did not evoke appreciable adverse effects on the human intestinal flora and that genipin cross-linked chitosan membranes did not compromise the biocompatibility of the microcapsules with respect to the effect on the human intestinal flora in comparison with the control subjects. The decrease in the activities of tested enzymes in the simulated colonic media containing the microcapsules could be the results of some effects of the membrane materials, such as binding of proteins to the microcapsule surfaces, penetration of small enzymes into the microcapsule interiors, as well as possible denature actions, though further research may continue to elucidate the consequence.

In summary, the present research evaluates the suitability of the genipin cross-linked alginate-chitosan (GCAC) microcapsules *in vitro* for potential live cell oral applications using a dynamic simulated human GI model. Results showed that the GCAC microcapsules possessed superior resistance against disintegration in the simulated GI environment and did not appreciably affect the normal gut flora. This novel microcapsule formulation is promising in fulfilling the essential requirements for oral delivery of recombinant cells; however, further *in vivo* investigations are needed before its full potential can be realized. Additionally this *in vitro* study may advance the understanding of microcapsule performance in conditions pertinent to the human GI physiology by using the dynamic simulated human GI model.

## **9.6 Acknowledgements**

This work was supported by research grants to Prakash from Canadian Institutes of Health Research (CIHR). The postgraduate fellowships from NSERC (to H.C. and C.M.) and Fonds Québécois de la Recherche sur la Nature et les Technologies (FQRNT) (to H.C. and W.O.) are greatly acknowledged. We also thank M. Jones for his help with the GI model set-up, M Shafiei and H Wightman for their help with the experiments.

Table 9.1. Exposure of GCAC microcapsules to the simulated human GI transit (72 h in total) and the corresponding morphological changes

Part in GI model	Stomach (V1 <sup>a</sup> )	Small intestine (V2 <sup>a</sup> )	Ascend. Colon (V3 <sup>a</sup> )	Transvers colon (V4 <sup>a</sup> )	Descend. Colon (V5 <sup>a</sup> )
pH	≤2	7.2-7.4	5.6-5.8	6.2-6.4	6.6-6.8
Exposure time (h)	2	4	18	24	24
Microcapsule morphology <sup>b</sup>	Intact	Swelled, ~15% deformed	Some collapsed	Some collapsed or dissolved	Adhesive, ~30% ruptured
Microcapsule morphology <sup>c</sup>	Intact	Slightly swelled, < 1 % burst	Spherical, < 2 % broken	Spherical Most intact	Spherical Most intact

<sup>a</sup> Vessel (V) of bioreactors in the GI model representing the human GI components

<sup>b</sup> Microcapsules cross-linked by genipin at 4 °C.

<sup>c</sup> Microcapsules cross-linked by genipin at 20 °C.

Table 9.2. Media and incubation conditions used for enumeration of representative microbes in the simulated human colon

Microbial group	Medium	Incubation conditions and time	Colonies formed
Total aerobes	Brain heart infusion agar	Aerobic, 37°C, 24 h	White
Total anaerobes	Brain heart infusion agar	Anaerobic, 37°C, 72 h	White
<i>Escherichia coli</i>	Mc Conkey agar	Aerobic, 43 °C, 24 h	Red-purple
<i>Staphylococcus</i> sp.	Mannitol Salt agar	Aerobic, 37 °C, 48 h	White with yellow/purple zone
<i>Lactobacillus</i> sp.	Rogosa agar	Anaerobic, 37°C, 72 h	White

Table 9.3. Effects of microcapsules on selected microbes in the simulated transverse colonic medium

Microbes	Incubation time (h)	Log CFU/mL medium <sup>a</sup>			
		GCAC <sup>b</sup>	AC <sup>b</sup>	APA <sup>b</sup>	Control <sup>c</sup>
Total aerobes	0	8.41	8.41	8.41	8.41
	6	8.37	8.32	8.33	8.36
	12	8.36	8.37	8.41	8.39
	24	8.22	8.17	8.00	8.04
Total anaerobes	0	8.44	8.44	8.44	8.44
	6	8.37	8.33	8.34	8.41
	12	8.37	8.43	8.49	8.40
	24	8.41	8.30	8.20	8.03
<i>Escherichia coli</i>	0	8.31	8.31	8.31	8.31
	6	8.18	7.97	8.23	8.18
	12	8.20	8.02	8.41	8.41
	24	8.10	8.03	8.11	8.68
<i>Staphylococcus sp.</i>	0	6.96	6.96	6.96	6.96
	6	6.52	6.60	6.77	6.81
	12	6.61	6.72	7.02	6.77
	24	6.57	6.62	6.82	6.54
<i>Lactobacillus sp.</i>	0	5.48	5.48	5.48	5.48
	6	5.45	5.52	5.43	5.51
	12	5.35	5.40	5.53	5.32
	24	5.50	5.46	5.49	5.37

<sup>a</sup>  $n=3$ , standard deviation < 0.20.

<sup>b</sup> Colonic suspension in the presence of microcapsules;

<sup>c</sup> Colonic suspension in the absence of microcapsules.

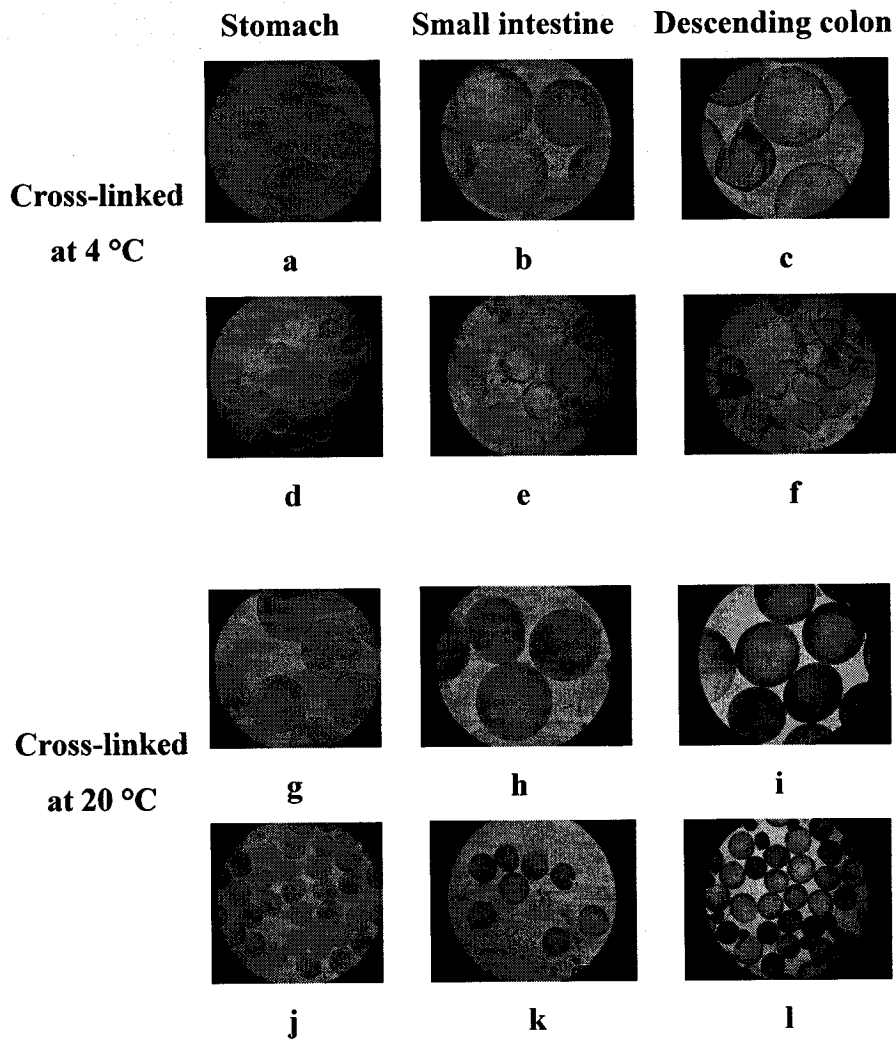


Figure 9.1. Microphotographs of the GCAC microcapsules cross-linked at 4 (a-f) and 20 °C (g-l) during the simulated human GI transit through the simulated stomach, small intestine, and descending colons. Original magnifications were either 90x (a-c and g-i) or 35x (d-f and j-l).

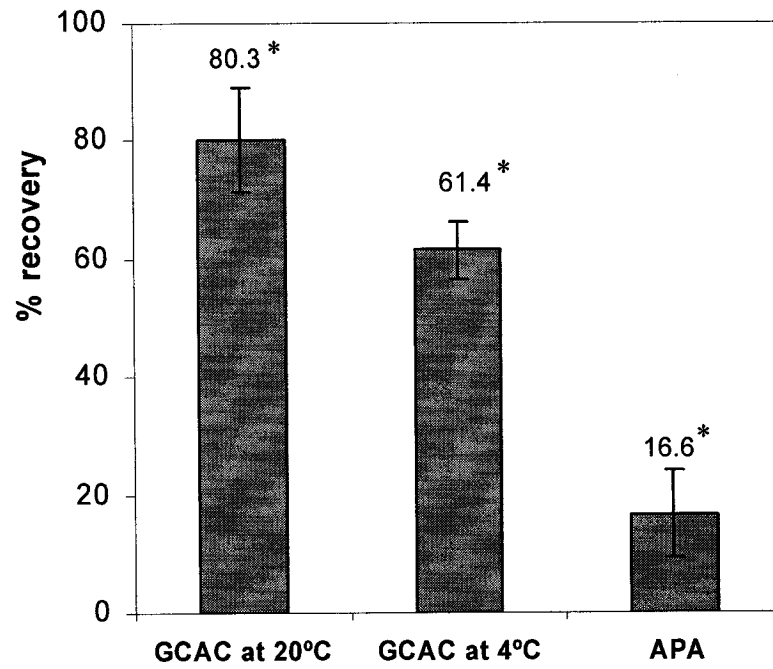


Figure 9.2. Recovery of microcapsules after 72 h of simulated human GI transit.  
\* indicates significant difference at  $p < 0.05$ .

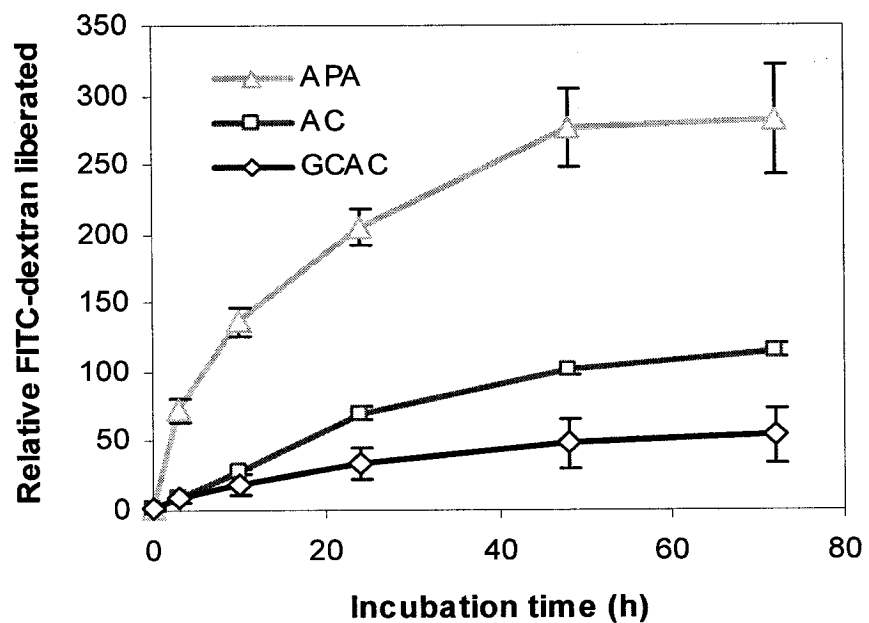
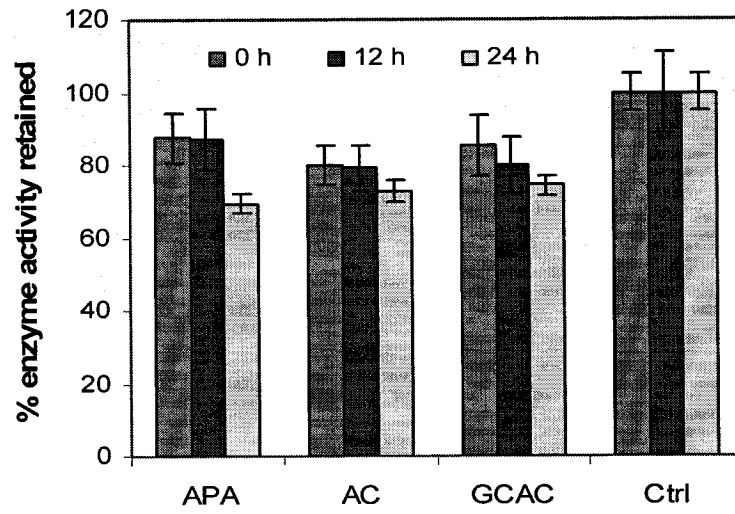
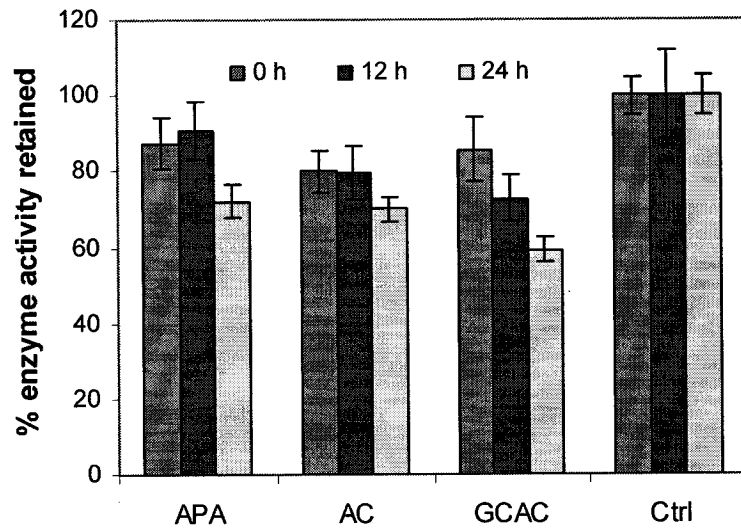


Figure 9.3. Leaching of the encapsulated FITC-dextran into the simulated intestinal medium following 1-h simulated gastric exposure. Error bars indicate standard deviation of mean ( $n=3$ ).

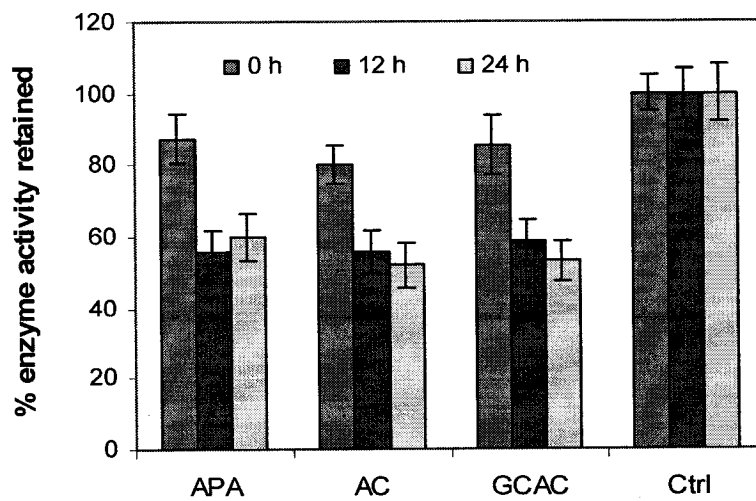
(a)



(b)



(c)



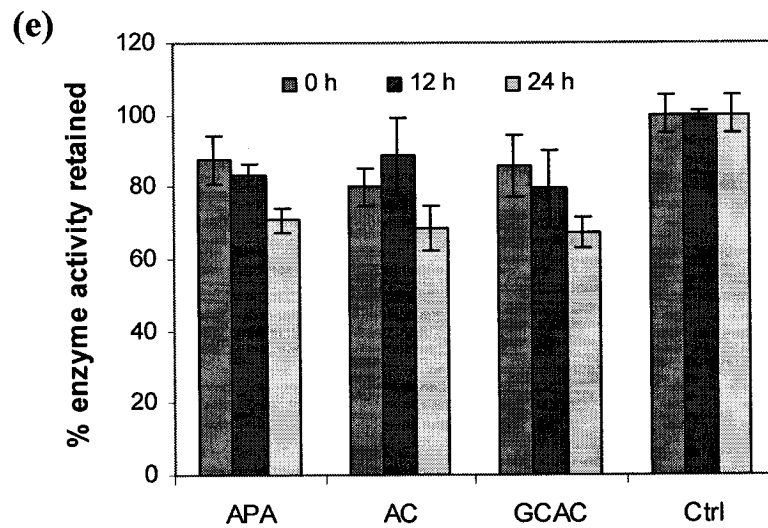
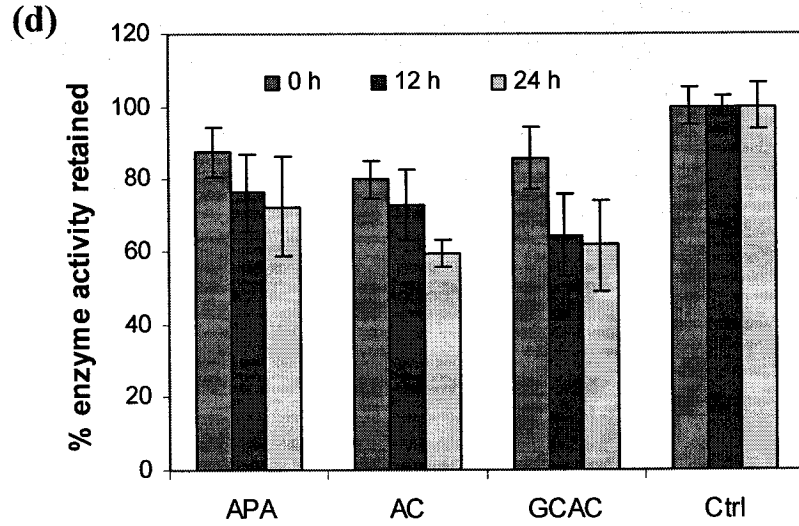


Figure 9.4. Enzymatic activities retained in the suspension of the simulated human transverse colon in the presence of microcapsules relative to those in the absence of microcapsules (control). Control values at each time point were normalized to 100% and used in comparison to the microcapsule containing media at the corresponding time points. a,  $\beta$ -galactosidase; b,  $\beta$ -glucosidase; c,  $\beta$ -glucuronidase; d,  $\alpha$ -galactosidase; and e,  $\alpha$ -glucosidase.

**Microencapsulation of *Lactobacillus plantarum* 80 in covalently cross-linked microcapsules for potential gastrointestinal applications**

Hongmei Chen, Wei Ouyang, Bisi Lawuyi, Christopher Martoni and Satya Prakash \*

*Biomedical Technology and Cell Therapy Research Laboratory*

*Department of Biomedical Engineering and Physiology, Artificial Cells and Organs Research*

*Centre, Faculty of Medicine, McGill University, Montreal, Quebec, H3A 2B4 Canada.*

\*Corresponding author: Tel. 514 398-3676; Fax. 514 398-7461; Email:  
satya.prakash@mcgill.ca

---

**Preface:** The results obtained from previous chapters warrant further investigations on the GCAC microcapsule system for oral livery of live cells. In this paper, genetically engineered live *Lactobacillus plantarum* 80 (LP80) were encapsulated. The viability and growth of the cells within the GCAC microcapsules were investigated. The capacity of these microcapsules to protect LP80 from the adverse gastrointestinal (GI) conditions was evaluated. Results highlight the usefulness of this GCAC preparation for oral delivery of live microbial cells.

This paper is to be submitted to *Pharmaceutical Research*.

## 10.1 Abstract

**Purpose.** Oral administration of microencapsulated non-pathogenic and genetically engineered (GE) microorganisms has shown important therapeutic potential. This study investigates microencapsulation of genetically engineered *Lactobacillus plantarum* 80 (*LP80*) using a covalently cross-linked microcapsule system and evaluates their suitability for oral delivery applications.

**Methods.** The novel genipin cross-linked alginate-chitosan (GCAC) microcapsules containing *LP80* were prepared. The stability of the microcapsule membrane was examined. A multi-compartment human GI model was used to assess the behaviors of the *LP80*-loaded GCAC microcapsules in the simulated human GI environment in relation to the preservation of cell viability and microcapsule integrity.

**Results.** The GCAC microcapsules were highly resistant to mechanical shear forces and degradation in physiologically pertinent media. They supported the growth and survival of the encapsulated cells. When being subjected to the simulated gastric conditions, the viable cells decreased proportionally with time, with a loss of 1.3 log units for the GCAC microcapsules versus 3.6 log units for the free cultures after 1 h, indicating the protective benefits of microencapsulation. Exposure to the simulated human intestinal media had no deleterious effect on the survival of the encapsulated cells. The long term viability of the encapsulated *LP80* cells was achieved over a 12-month course during refrigerated storage in physiological solution.

**Conclusions.** This *in vitro* study provides a basis for future research on the therapeutic potential using the GCAC preparations as a platform for oral delivery of live GE bacteria.

**Key Words:** encapsulation, genipin, alginate, chitosan, cross-linking, microorganisms, survival

## 10.2 Introduction

With the development of molecular biology, it is now possible to engineer nonpathogenic cells to bear a desired metabolic capacity and synthesize a wide array of

disease modifying substrates<sup>1,6,65,68,426</sup>. The positive aspects of using these GE bacteria for therapeutic purposes have attracted considerable research interest over the past two decades. To overcome the obstacles in delivering these cells and products to the body in an active form, Prakash and Chang proposed the concept of artificial cell oral therapy<sup>4</sup>, wherein live functional cells encapsulated in the confines of a semi-permeable membrane were administered orally. The polymeric membrane isolates the encased cells from the host system, allows the bi-directional exchange of small molecules, such as nutrients, wastes, selected substrates and products, and simultaneously prevent the passage of large substances, for instance cells, immunocytes and antibodies<sup>5</sup>. When given orally, a large controlled number of viable microbes, being protected by microencapsulation, can reach the intestine. They can be designed to secrete small biologics (peptides, enzymes, growth factors, etc.), which can be diffused through the membrane into the gut lumen for therapy. Alternatively, artificial cells can act as bioreactors during their GI transit by metabolizing undesirable small substances (amino acids, bile acids, ammonia, etc.) presented in the gut and eventually eliminating them from the body<sup>6</sup>. Previous research has demonstrated the potential of oral delivery of microencapsulated GE cells as an alternative oral therapy. Examples include microencapsulated *Escherichia coli* DH5 cells over-expressing the *Klebsiella aerogenes* urease gene for urea removal in renal failure<sup>4</sup>, *Oxalobacter formigenes* producing oxalate-degrading enzymes for removal of accumulated oxalate in urolithiasis<sup>7,8</sup>, and bile salt hydrolase-overproducing *Lactobacillus plantarum* 80 (*pCBH1*) BSH<sup>+</sup> to promote elevated bile salt deconjugation and serum cholesterol lowering<sup>9</sup>, as well as others<sup>10</sup>.

It is known that any orally administered material is subjected to breakdown by mechanical stress/motion, gastric acidity, digestive enzymes, bile and microbes in the human GI system. Effective oral therapy utilizing live microorganisms requires the cells to remain viable and functional during GI transit. Furthermore, GE microorganisms should be retained in the microcapsules and not leak into the GI tract. It has been shown that novel cells may, if prolonged and repeated large doses are taken, stimulate a host immune response, systematically propagate in the intestine, disrupt the indigenous microflora, and have risks of immuno-modulation, translocation and gene transfer<sup>2,12-18</sup>. Consequently, the regulatory agencies may likely require exclusively no leaking of the GE cells from ingested

microcapsules into the host's GI system, even though they are classified as nonpathogenic<sup>19</sup>. Therefore, it is imperative that GE bacteria be encased in the microcapsules, performing their therapeutic functions during the GI transit, and be excreted along with the intact microcapsules in the feces without being retained in the body. To fulfill these requirements, it is essential to maintain the structural integrity of the microcapsules, in which the membrane stability is of great importance.

Designing an appropriate microcapsule membrane for oral delivery of GE cells is challenging. On one hand, there is a need for creating a robust isolating barrier between the cells and the host gut. On the other hand, cell viability, metabolism, and functions should be sustained during processing and GI transit. In addition, targeted substrates and products should be able to freely pass through the microcapsule membrane for therapy. Although numerous microcapsule systems have been studied for oral delivery, such devices are mostly used for the controlled release of curative agents, for instance drugs and probiotics into the intestine<sup>20-26</sup>. Scanty research is available on microcapsules intended to support cell functions while retaining cells throughout the GI transit.

Alginate has been prevalently used for cell encapsulation because of its excellent cell-compatibility, status as an FDA approved food additive, and mild process conditions. The incorporation of other polymers, by enveloping the alginate beads, is necessary to create a stable and semi-permeable membrane. Alginate polycation complexes, such as the alginate-poly-L-lysine-alginate (APA)<sup>427</sup> and the alginate-chitosan (AC)<sup>398</sup> capsules, have been reported to reduce the gel porosity and enhance the microcapsule stability<sup>34,44,235</sup>. They have been extensively studied for cell encapsulation<sup>4,9,69,76,78</sup>. However, problems persist, pertaining to inadequate membrane stability, susceptibility to gastric and enzymatic degradation, as well as substantial cell release in the GI environments<sup>22,27,53,76,115,156,427,427</sup>. Therefore, such cell delivery devices require significant improvements in microcapsule chemistry to withstand GI impediments and fulfill the requirements for oral applications of GE bacteria<sup>12</sup>.

To address this matter, a novel microcapsule system with a covalently cross-linked membrane was recently proposed<sup>306,390</sup>. While previous studies have demonstrated the superior membrane strength and high resistance of these genipin cross-linked alginate-chitosan (GCAC) microcapsules to the simulated human GI environment, this article investigates the microencapsulation of live genetically engineered *Lactobacillus plantarum* 80 (LP80), with respect to the microcapsule stability, cell viability and proliferation, and their tolerance in the harsh GI environment. Results obtained suggest the potential of using GCAC microcapsules in relevant oral applications of GE bacteria.

### 10.3 Materials and methods

#### 10.3.1 Materials

Sodium alginate (low viscosity), poly-L-lysine hydrobromide ( $M_v$  27,400), pepsin and pancreatin were supplied by Sigma-Aldrich, USA. Chitosan (low viscosity, degree of deacetylation or DDA=73.5 %, and  $M_v=7.2 \times 10^4$ ) and genipin were purchased from Wako BioProducts, USA. De Man Rogosa Sharpe (MRS) broth, MRS agar and erythromycin were obtained from Fisher Scientific, USA. All other reagents and solvents were of reagent grade and used as received without further purification.

#### 10.3.2 Bacterial strain and culture conditions

The bacterial strain used in this study was bile salt hydrolytic (BSH) isogenic *Lactobacillus plantarum* 80 (pCBH1) BSH<sup>+</sup> (LP80) obtained from LabMET, Belgium. This genetically engineered strain carries the multicopy plasmid pCBH1 containing the *L. plantarum* 80 chromosomal bsh gene and an erythromycin resistance gene, able to overproduce bile salt hydrolase (BSH) enzymes. The stock cultures of LP80 were kept in MRS broth containing 20 % (v/v) glycerol at -86 °C. The microorganisms were revived twice in MRS broth, followed by sub-culture of 1 % inoculum anaerobically in MRS broth supplemented with 100 µg/mL of erythromycin in a multi-gas incubator (Sanyo MCO-18M) at 37 °C. Cultures were harvested, as estimated by the growth curve, after 20 h of incubation at the end of the exponential phase of growth.

### 10.3.3 Preparation of microcapsules containing *Lactobacillus plantarum* 80

Cultures of *L. plantarum* 80 (*LP80*) were isolated by centrifugation at 10 000 g, 4 °C, for 12 min. The collected cell pellets (1.3 g, cell wet mass) were suspended in sterile physiological saline (PS), 0.9 % NaCl, pooled and mixed carefully with pre-filtered sterile alginate solution by gentle stirring to form a uniform mixture (50 mL) with a final alginate concentration of 15 mg/mL. Droplets of an alginate-cell suspension were generated by an Encapsulator (IER-20, Inotech. Corp.), extruded through a 300 µm nozzle using a syringe driven pump and gelled for 15 min in a stirred CaCl<sub>2</sub> solution (11 mg/mL). The resulting *LP80* entrapped alginate beads, approximately 560 µm in diameter, were then coated with chitosan by immersing in a chitosan solution (10 mg/mL) containing 11 mg/mL CaCl<sub>2</sub> for 30 min followed by three washes, forming the *LP80*-encapsulated alginate-chitosan (AC) beads. The subsequent cross-linking reaction was performed by suspending the above AC microcapsules in a genipin solution (2.5 mg/mL) at room temperature for 48 h. The resulting GCAC-*LP80* microcapsules were washed and collected. Non-bacteria containing GCAC microcapsules were prepared analogously to/by the aforementioned procedures except for using a pure alginate solution rather than the cell-alginate suspension. The APA microcapsules containing *LP80* cells were also produced based on the protocol initially developed by Lim and Sun<sup>69</sup> with a few modifications as previously described<sup>27</sup>. The entire preparation procedure was carried out in a biological containment hood, and all solutions used were either 0.22 µm filtered or autoclaved to ensure sterility. At the end, the obtained microcapsules were stored at 4 °C in either minimal broth media (MRS broth:PS = 1:1, by volume) or in PS.

### 10.3.4 Microcapsule integrity and membrane stability

To assess the membrane stability, the *LP80*-containing microcapsules (1 mL) were submerged in 15 mL model medium including MRS broth, PS, phosphate buffered saline (PBS), and the sequential media of simulated gastric fluid (SGF), pH 1.2 and simulated intestinal fluid (SIF), pH 7.5, and then subjected to mechanical stress by agitation at 175 rpm, 37 °C in a Lab Line Environ Shaker for 3 days. The SGF and SIF were prepared in accordance with United States Pharmacopoeia XXII, in which SGF consisted of 3.2 mg/mL pepsin in 0.03 M NaCl, at pH 1.2, and SIF of 10 mg/mL pancreatin in 0.05 M KH<sub>2</sub>PO<sub>4</sub>, at pH

7.5. The morphology and physical integrity of the microcapsules were examined under an inverted light microscope (LOMO PC). And the microcapsule diameters were measured with an eyepiece micro-meter equipped on the microscope at a magnification of 90x. The swelling ratio of the microcapsules was defined as:

% Swelling =  $(D-D_0)/D_0*100$ , where  $D_0$  and  $D$  were diameters of the microcapsules before and after incubated in model media, respectively.

### **10.3.5 Determination of mechanical stability of microcapsules**

A modified osmotic pressure test, originally developed by Van Raamsdonk and Chang<sup>332</sup> was used to examine the mechanical stability of the microcapsules containing *LP80* cells. For this, microcapsule samples (0.2 mL) were first washed with and equilibrated for 1 h in isotonic PS (0.9 % NaCl), after which the media were sucked out by careful pipeting, and a hypotonic solution of decreased osmotic pressure (15 % PS diluted with deionized H<sub>2</sub>O) was added. The percentage of burst microcapsules was scored under an optical microscope in three randomly picked observation fields. The experiment was performed in triplicate.

### **10.3.6 Enumeration of encapsulated *LP80***

To determine the viability of the encapsulated cells, the *LP80* containing microcapsules (0.1 mL) were mechanically crushed using a sterile tissue pestle. The samples of bacteria suspensions from 10-fold serial dilutions with PS were plated on selective MRS agar supplemented with 100 µg/mL of erythromycin. Viable counts were determined after 72 h of anaerobical incubation at 37 °C in a multi-gas incubator (Sanyo MCO-18M).

### **10.3.7 Growth profiles of encapsulated *LP80***

To analyze the growth profiles of the encapsulated cells, microcapsules with a cell load of approximately log 4 CFU/ml were made and used. The subsequent encapsulation, coating and cross-linking processes were performed as above-mentioned. The *LP80* containing microcapsules (0.1 mL) were incubated anaerobically in 1.0 mL MRS broth supplemented with erythromycin at 37 °C for up to 72 h. At different intervals, the culture medium was discarded and the viable *LP80* inside the capsules were determined by spread

plate as aforementioned. Free *LP80* was also incubated and its growth profile determined for comparison. Data in log CFU/mL were plotted as a function of incubation time.

### **10.3.8 Survival of encapsulated *LP80* in the simulated human GI environment**

To assess the cell survival for potential GI applications, a computer controlled dynamic multi-compartment human GI model was used. The *LP80* loaded GCAC, AC microcapsules (0.1 mL), and free cells with similar *LP80* concentration were incubated separately for 1 h in the simulated gastric medium (1.0 mL) taken from Vessel 1 (V1) of the GI model, representing the stomach that contains the food content of a human western diet suspension at pH 2.0. The tolerance of the cells entrapped in the GCAC microcapsules to a combination of constraints of both the simulated GI barriers and mechanical forces was also examined. For this, *LP80*-GCAC microcapsules (0.1 mL) were placed in micro-vials containing 1.0 mL of the simulated human GI media taken from different compartments of the GI model, V1 (the simulated stomach, pH 2.0), V2 (the simulated small intestine, contains the human diet suspension and pancreatin juice, pH 7.4), V3 (the simulated ascending colon, contains the V2 suspension and normal human microflora, pH 5.6), V4 (the simulated transverse colon, contains the V3 suspension and normal human microflora, pH 6.2), and V5 (the simulated descending colon, contains the V4 suspension and normal human microflora, pH 6.8), and incubated anaerobically under mechanical agitation (175 rpm) at 37 °C. After pre-designated periods of time (up to 2, 4, 24, 24 and 24 h in V1, V2, V3, V4, and V5 medium, respectively), the medium was discarded. The microcapsules were washed by PS and crushed. The viable counts of *LP80* were determined using the above-described procedure.

### **10.3.9 *LP80* encapsulated beads during Long-term storage**

Microcapsules containing *LP80* were stored in PS at 4 °C after preparation. Physical observations of microcapsule integrity and enumeration of the viable cells inside microcapsules were performed periodically using the aforementioned method.

## **10.4 Results**

#### 10.4.1 Microencapsulation of live bacteria

*Lactobacillus plantarum* 80 (*pCBHI*) BSH<sup>+</sup> (*LP80*) was chosen as a model microbe to evaluate the suitability of the GCAC microcapsule formulation for live cell encapsulation. The encapsulator settings (Table 10.1) were optimized in order to obtain well-formed spherical alginate-*LP80* beads. Reaction parameters for chitosan coating and genipin cross-linking were selected based on previous experimentation<sup>306,428</sup> in order to form strong GCAC microcapsules, with the exception of cross-linking at room temperature instead of 37 °C to moderate bacterial metabolism. Morphologically, microcapsules containing *LP80* bacterial cells were not different from the cell-free beads, exclusive of the opaque appearance (Fig. 10.1 a-b). A color change was observed after genipin treatment, from milky white to slightly gray and bluish. The diameters of the obtained GCAC beads were determined to be  $560.3 \pm 20.1 \mu\text{m}$ , similar to that of the alginate beads. The cell load in all the three microcapsules achieved  $10^8$  CFU/mL beads, though a slight loss of viability was detected during the cross-linking process (Table 10.2).

#### 10.4.2 Mechanical stability of microcapsules containing *LP80*

Mechanical stability of the microcapsules was assessed by an osmotic pressure test. Figure 10.2 shows that after being subjected to the hypotonic solution, more than 95 % of the APA-*LP80* capsules became ruptured within 10 min. The burst of the AC-*LP80* beads increased from  $7.3 \pm 1.5 \%$  at 10 min to  $33.6 \pm 4.5 \%$  at 30 min after the hypotonic incubation, and maintained the similar burst percent ( $38.2 \pm 5.9 \%$ ) for the remaining 24 h. The percent of defected GCAC microcapsules was  $11.3 \pm 2.4 \%$  at 10 min, and chiefly unaltered for the next 24 h ( $10.0 \pm 1.6 \%$ ).

#### 10.4.3 Resistance of *LP80* loaded microcapsules to mechanical stress and simulated media

To assess the membrane stability and microcapsules integrity, the *LP80*-containing microcapsules were subjected to mechanical stress in various *in vitro* and *in vivo* model media. Our results confirmed the well-preserved morphology of the GCAC microcapsules after 3 days of agitation in MRS broth (Fig. 10.3 c&f), PBS (Fig. 10.4d) and saline (data not shown), where they swelled  $23.7 \pm 6.4 \%$ ,  $17.5 \pm 4.3 \%$  and  $7.8 \pm 3.4 \%$ , respectively. In contrast, a

large percent of the APA capsules became ruptured or burst under the same experimental conditions (Fig. 10.3 a&d and Fig. 10.4 a-b). Although the *LP80*-containing AC microcapsules remained morphologically unaltered after exposure to MRS broth (Fig. 10.3 b&e), the capsular membrane began to peel off or bulge in some of AC beads after 3 days of constant agitation in PBS (Fig. 10.4c). Figure 10.5 exemplifies the behaviors of the GCAC-*LP80* microcapsules after sequential incubation in the simulated gastric fluid (SGF, pH=1.2, x 1 h) and the simulated intestinal fluid (SIF, pH=7.5, up to 3 days). These microcapsules maintained physical integrity and shrank to a small extent when being exposed to mechanical stress in SGF. They swelled drastically ( $44.7 \pm 15.7\%$ ) soon after being transferred to the SIF. Nearly 10-15 % of the GCAC microcapsules burst or became defective within half an hour and this number did not change during the remainder of the experiment. A majority of the GCAC microcapsules were able to uphold the integrity until the end of the experiment and the microcapsule cores became slightly translucent and less dense (Fig. 10.5e). It is noteworthy that the cross-linked microcapsule membrane was clearly visualized, encircling the core of alginate and *LP80*.

#### **10.4.4 Growth profile of encapsulated *LP80***

To investigate the effects of microcapsule environments and membrane materials on the cell proliferation, microcapsules containing approximately  $\log 4$  CFU/ml *LP80* were incubated in culture medium and the viable counts inside the microcapsules were examined periodically. Compared to the *LP80* cultures under the same conditions, the encapsulated cells began to proliferate soon after incubated in broth (Fig. 10.6). The *LP80* cells in the AC beads grew from 4.4 log CFU at time 0 to 7.0 and 10.1 log CFU after 24 and 48 h of incubation, respectively, and reached a plateau phase thereafter. The *LP80* inside the GCAC microcapsules demonstrated a similar growth trend to that of the AC capsules; the viable counts increased from 4.2 log CFU at time 0 to 5.8, 8.8, and 9.1 log CFU after 24, 48, and 72 h, respectively; the ultimate counts in the GCAC microcapsules were comparable to the free cells (9.4 log CFU in 72 h) but approximately 1 log cycle lower than that in the AC beads.

#### **10.4.5 Tolerance of encapsulated cells in simulated human GI suspension**

To evaluate microcapsule tolerance and cell survival in a more representative manner, the simulated gastric and small intestinal suspension from a dynamic human GI model were used to represent the human GI conditions. We found that the microcapsules remained intact during the tests (data not shown). Figure 10.7 illustrates a linear reduction in the logs of the surviving *LP80* with time of exposure to the simulated gastric suspension (pH 2.0). Cell death in microcapsules was constrained to a large extent in comparison to the free cultures, noting the slope of the linear trend being 0.02 versus 0.06. In particular, the decreases in viable cells inside the GCAC beads were 0.4 and 1.5 log cycles after 0.5 and 1 h of gastric exposure, respectively (Fig. 10.7a). On the other hand, free *LP80* underwent drastic cell death, with a loss of 2.0 and 3.6 log cycles in survival for the same periods of time (Fig. 10.7c). Microencapsulation by the AC capsules also provided substantial protection for the cells within the experimental period of time (Fig. 10.7b). When being subjected to added mechanical stress, the encapsulated *LP80* in GCAC beads survived the gastric exposure similarly; a loss of 2.4 log units in cell counts was found after 2 h of incubation with the gastric medium (Fig. 10.8a). Moreover, when being exposed to the simulated small intestinal suspension (pH 7.4) that contained physiological concentrations of pancreatin (0.18 g/L), a slight increase in surviving cell numbers from 6.7 to 7.0 log CFU was found during the first 2 h, followed by a moderate decline to 6.5 log CFU in the succeeding 2 h (Fig. 10.8b). In the simulated human colonic conditions, the viable *LP80* numbers in the GCAC microcapsules increased about 0.5 – 0.7 log units in the first 12 h-incubation and thereafter slightly declined (Fig. 10.8c). The viability of the encapsulated cells appeared similar when exposed to the suspensions of V4 (the simulated transverse colon, pH 6.2) and V5 (the simulated descending colon, pH 6.8), which were slightly higher than that to V3 (the simulated ascending colon, pH 5.6).

#### **10.4.6 Effect of long term storage on microcapsules containing *LP80* cells**

Morphologically, a small percentage of the GCAC-*LP80* microcapsules ( $9.4 \pm 0.5$  %) were found burst after 2 years of storage in PS at 4 °C, and some became lighter in color and less dense than when initially prepared, while the plain microcapsules remained intact (Fig. 10.1). Despite this, the GCAC microcapsule membranes were deemed as strong and durable. Figure 10.9 shows that, irrespective of microcapsule types, the encapsulated *LP80* cells

remained viable after 12 months of refrigerated storage, with the cell counts decreasing proportionally with storage time ( $r > 0.972$ ). However, the viable cells inside the GCAC microcapsules seemed more susceptible to the storage environment. The survival of GCAC encapsulated *LP80* decreased from 8.1 log CFU/mL beads right after preparation to 7.8, 6.3, 5.6, 4.8, and 3.1 log CFU/mL beads after 1, 2, 6, 9, and 12 months of storage, displaying a relatively faster rate of cell death when compared to the other two types of microcapsules.

## 10.5 Discussion

Alginate-based microcapsules have long been studied for encapsulation of live cells and probiotics<sup>48,49,69,102,103,427,429-431</sup>. Previous research on oral delivery of bacteria suggested fast degradation and release of live cells from inadequately stable microcapsule membrane<sup>12,13,15,27,102,373,427</sup>. This is particularly unfavourable when novel microorganisms are used<sup>12</sup>. This paper described an improved method of cell microencapsulation and evaluated its capacity to protect the GE *Lactobacillus plantarum* 80 (*pCBH1*) BSH<sup>+</sup> (*LP80*) cells from the GI environment. *Lactobacillus plantarum* is a well characterized bacterial strain with published probiotic potential. *LP80* is genetically engineered, able to overproduce bile salt hydrolase that effectively increases intraluminal bile salt deconjugation making them less likely to be reabsorbed into the enterohepatic circulation, and thus causing *de novo* synthesis of bile acids in the liver from serum cholesterol<sup>365</sup>. Recent research has demonstrated the therapeutic potential of oral delivery of *LP80* for serum cholesterol lowering<sup>9,432</sup>. For effective and safe oral therapy, *LP80* cells need both increased protection from GI and limited contact with the GI tract due to potential gene transfer and immune issues. To circumvent the problems with the conventional APA system, genipin, a naturally derived cross-linker, was used in our GCAC preparation to form a covalently cross-linked chitosan membrane around the *LP80* entrapped alginate core. The gray-bluish color in the obtained microcapsules was previously postulated to develop from the reaction between genipin with the amino group of chitosan<sup>245,296</sup> and probably involves oxidation<sup>302</sup>. Although the relationship between cross-linking and color formation is not fully understood, the blue color is not a problem for cell encapsulation as its generation did not adversely affect the viability and growth of the encapsulated cells using our established preparation procedure (see Table 10.2 and Fig. 10.6).

In addition, genipin cross-linking substantially improved the membrane stability of the GCAC microcapsules (Fig. 10.2), and strong resistance to disintegration in various physiologically pertinent media was validated (Figures 10.3-10.5).

As has been noted, chitosan coating and genipin treatment had few deleterious effects on the viability of the enclosed bacterial cells; the initial cell loading reached  $10^8$  CFU/mL in all of the APA, AC and GCAC microcapsules, a level comparable to the cell concentration in alginate suspension (Table 10.2) indicating a high encapsulation yield. Moreover, the GCAC encapsulated *LP80* cells had a similar growth trend as in the AC capsules and free cultures (Fig. 10.6), suggesting the suitability of the GCAC system for the encapsulation of these biological substances. The slightly lower cell load in the GCAC microcapsules (Table 10.2) may likely be due to the prolonged reaction time (2 d), and could be the reason for lower cell metabolism in comparison to the AC microcapsules (Fig. 10.6). This reduction could be compensated for either by increasing the initial cell concentration during encapsulation<sup>49,102</sup>, or by regulating the degree of cross-linking<sup>306</sup>. Figure 10.6 also indicated a short delay in the growth of free cultures. This might be attributed to cell-cell communication through the production of extra-cellular signals, which has been suggested as playing a role in the growth of *lactic acid* bacteria<sup>367</sup> and may be different in the confines of a microcapsule from in free bacteria suspension. Free cells need time to migrate and communicate, which might delay multiplication, while the encapsulated cells accumulated at higher local concentration that might facilitate cell signaling and intensify the initial cell proliferation.

Since therapeutic microorganisms are usually required at the sites of destination in the intestine, the entrapped cells must be able to pass the stomach-duodenum barrier in a viable state and in sufficient numbers to elicit the potential benefits. To address this crucial issue objectively, the simulated GI model, a more accurate representation of human GI conditions, were utilized in this study. It is known that the acidity of the stomach forms a major barrier when applying live bacteria by oral administration. Our results showed that the survival of *LP80* was highly dependent on the pH of exposing media. At low pH (1.2) in the media of 0.2 N HCl, SGF, and the highly acidified feed for the GI model, drastic cell death occurred (data not shown). In the simulated human stomach medium (pH 2.0), the viable cells decreased in moderation and proportionally to the exposure time (Fig. 10.7), which concurred with the studies by Krasaekoopt *et al*<sup>49</sup> and Lee and Heo<sup>433</sup>. On the other hand, cell viability was

preserved when incubated in non-acidified food for the GI model (pH 4.6), physiological solution at pH 6.8 (data not shown), and in the simulated human small intestinal medium at pH 7.4 (Fig. 10.8b). No obvious morphological defects in the GCAC membrane were found after exposure to mechanical stress along with the gastric actions, in which the GCAC encasing *LP80* showed a similar death rate as evidenced by the equivalent slopes in Figures 10.7a and 10.8a. These results confirmed the membrane stability of the GCAC microcapsules and their resistance to gastric digestion and destruction. In comparison to free *LP80* cultures, microencapsulation by the GCAC preparations improved the survival in the adverse gastric conditions (see Fig. 10.7). The AC membrane also provided considerable protection against cell death, which was in agreement with previous investigations<sup>48,49</sup>. The protective mechanisms may likely include: (1) the GCAC microcapsules being highly resistant to gastric degradation; (2) the cross-linked membrane provided physical barriers against the entry of the harmful components found in the GI tract; (3) the possible buffering capacity of the alginate core in the microcapsule may limit the hostile effect induced by the low pH in the stomach. Furthermore, the viability of the encapsulated cells was not considerably affected by constraints in the simulated human intestinal environments such as microflora actions and enzymatic degradation, indicating the activity of the encapsulated *LP80* cells was sustained. Future research on their metabolism and therapeutic functions will provide additional evidences.

Regarding the cell concentration needed for GI applications, it is accepted that in probiotic products, viable microbes should be immobilized in a high density, allowing for surviving the stomach-duodenal digestion in sufficient quantities (suggested therapeutic dose of  $10^8 - 10^9$  CFU/day)<sup>434</sup>. This facilitates their colonization in the intestine needed to gain health-promoting benefits<sup>102,103,373,429</sup>. In the case of GE bacteria, cell leaking and propagation of foreign bacteria in the intestine are undesirable. It has also been found that a bulky cell load weakened the beads<sup>431</sup> and resulted in fast and substantial cell release<sup>373</sup>. We speculated that to maximize the therapeutic benefits, the cell loading should be optimized on a strain-by-strain basis<sup>415,430</sup>, dependent on the functional capacity of GE microorganisms and patients' need. Our previous research has suggested the effectiveness of bile salt hydrolase overproduced by encapsulated *LP80* to breakdown conjugated bile acids *in vitro*<sup>9</sup>, and a

dosage study on serum cholesterol lowering in animal models is currently under investigation in our laboratory.

In this study, we were not able to follow the cell leaking to the simulated human colonic environment by the plating assay since the large intestine of our GI model (Vessels 3-5) represents a complex microbial environment and some *Lactic acid* bacteria may be intrinsically resistant to many antibiotics<sup>15</sup>. To address this end, a working method for selective enumeration is needed. The use of modified organisms with distinctive characteristics, for example, being highly resistant to concentrated antibiotics or fluorescent-labeled<sup>413,435</sup>, and alternative viability testing techniques<sup>413,436-438</sup> would be explored in future research.

## 10.6 Conclusions

This study demonstrated that genetically engineered *Lactobacillus plantarum* 80 (*pCBHI*) BSH<sup>+</sup> (*LP80*) cells can be encapsulated by the established GCAC preparation method. Results showed that genipin cross-linking improved the resistance of the GCAC microcapsules to osmotic pressure shock, mechanical shear forces and other disintegrative impediments in physiologically pertinent media. The GCAC microcapsules provided with suitable microenvironment for the viability and proliferation of encapsulated *LP80*. In addition, microencapsulation by the GCAC preparations gave rise to better cell tolerance to the gastrointestinal barriers, and the microbial viability during long term refrigerated storage was confirmed. Results of this *in vitro* study warrant further *in vivo* investigations into the potential of using the GCAC preparation in oral delivery of GE microorganisms for therapy.

## 10.7 Acknowledgements

This work was supported by Canadian Institutes of Health Research (CIHR) and Natural Sciences and Engineering Research Council (NSERC) of Canada. Postgraduate scholarships from NSERC and Fonds Québécois de la Recherche sur la Nature et les Technologies (FQRNT) to Chen are greatly appreciated. We also acknowledge M. Jones for

initiating the research on *LP80* bacteria in our lab, and H Wightman for experimental assistance and proofread of the manuscript.

Table 10.1. Summary of the optimized encapsulator settings for *Lactobacillus plantarum* 80 encapsulation

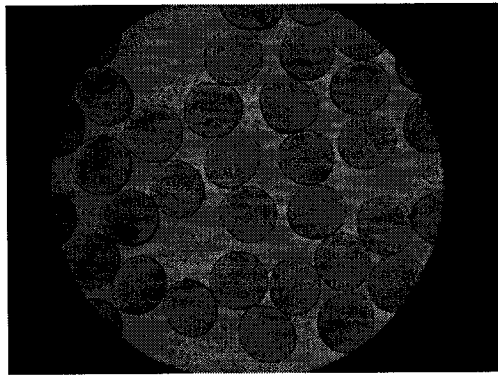
Nozzle diameter ( $\mu\text{m}$ )	Flow rate (mL/min)	Vibration frequency (Hz)	Voltage (Kv)	Current amplitude	Drop height (cm) <sup>a</sup>	Capsule diameter ( $\mu\text{m}$ )
300	8.6	918	1.400	2	18.5	560.3 $\pm$ 20.1

<sup>a</sup> Distance from the extruder (nozzle tip) to the surface of CaCl<sub>2</sub> receiving bath.

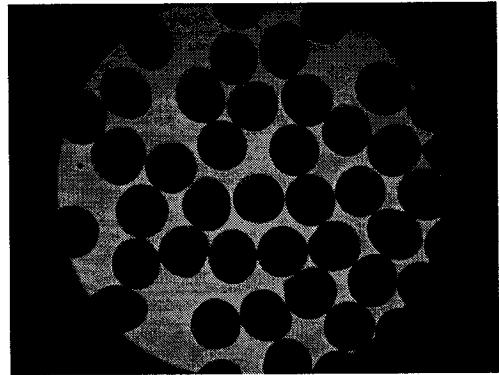
Table 10.2. Initial loading of *Lactobacillus plantarum* 80 in microcapsules

Sample	APA microcapsules	AC microcapsules	GCAC microcapsules	Alginate- <i>LP80</i> Suspension
Cell load <sup>a</sup>	8.20	8.39	8.09	8.51

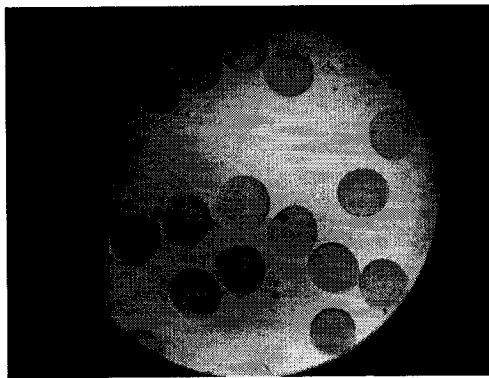
<sup>a</sup> Log CFU/mL microcapsules or suspension.



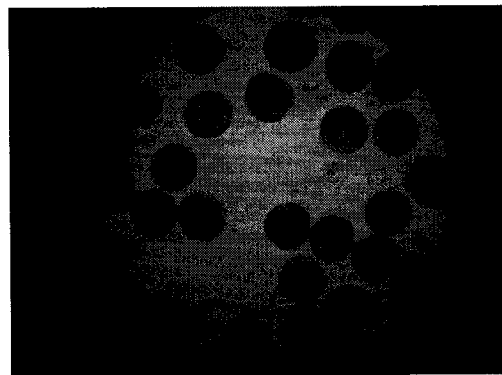
**a**



**b**



**c**



**d**

Figure 10.1. Microphotographs of the GCAC microcapsules: a, plain and freshly made; b, containing *LP80* cells and freshly made; c, plain and after 2 yr of storage in deionized H<sub>2</sub>O at 4 °C; and d, containing *LP80* cells and after 2 yr of refrigerated storage in minimum medium (1: 1 = broth: PS) at 4 °C (original magnification: 35x).

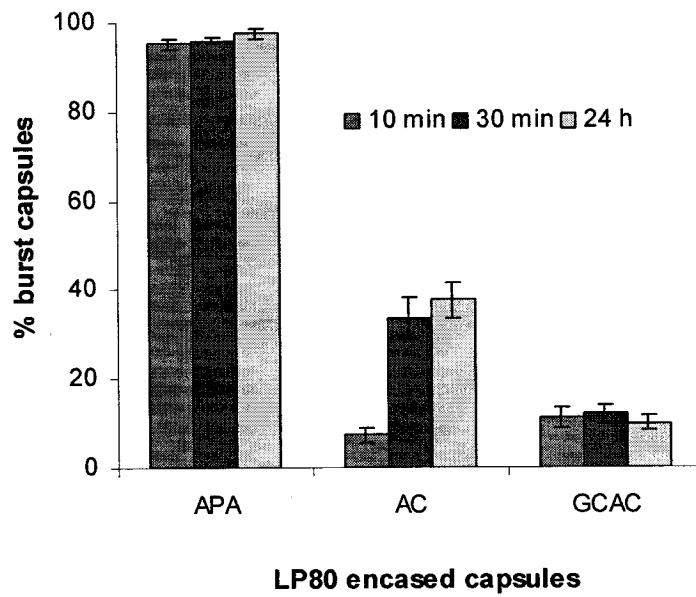


Figure 10.2. Resistance of *LP80* enclosed microcapsules to osmotic pressure shock.

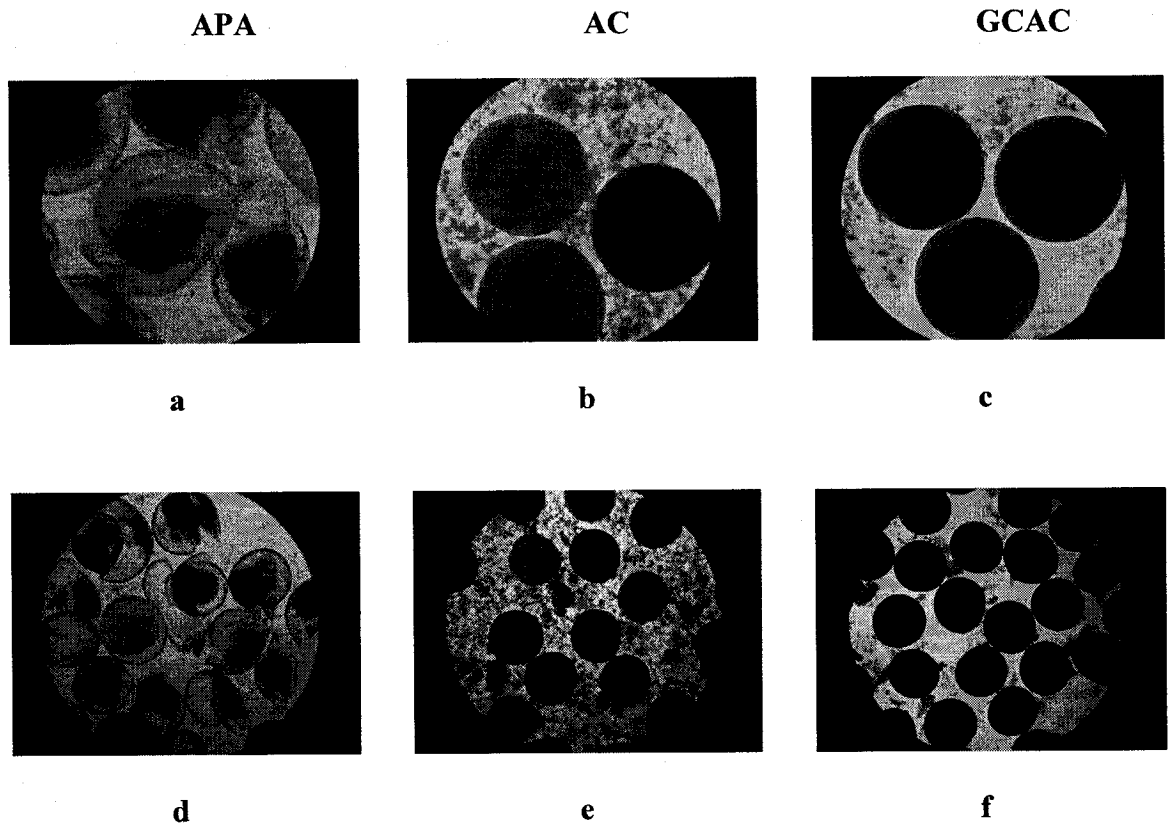


Figure 10.3. Microphotographs of microcapsules containing *L. plantanrum 80* (pC BH1) post exposure to mechanical stress in MRS broth (175 rpm, 37 °C) for 3 days. Microcapsules tested were APA (a, d), AC (b, e) and GCAC (c, f). Original magnifications: a-c, 90x; and d-f, 35x.

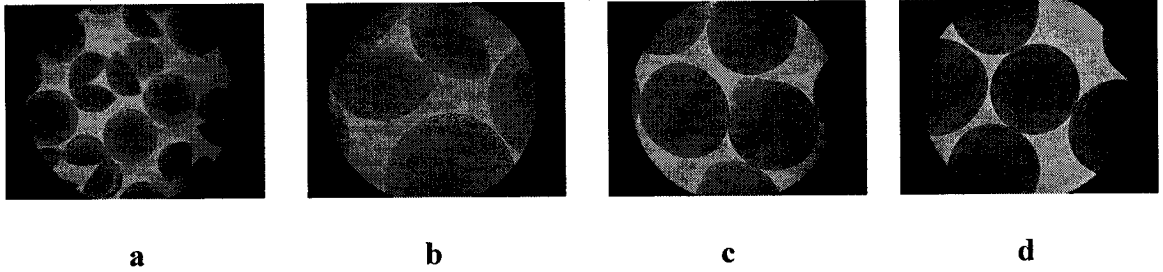
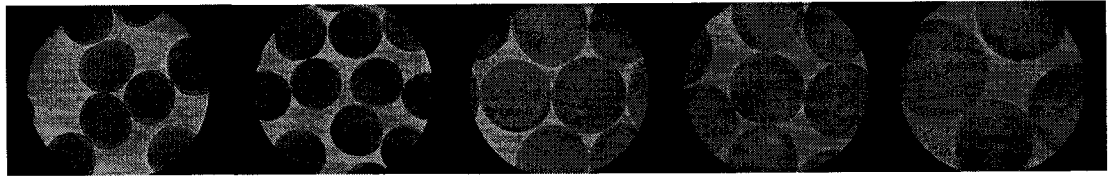


Figure 10.4. Microphotographs of microcapsules containing *L. plantanrum* (pC BH1) post exposure to mechanical stress in PS (175 rpm, 37 °C) for 3 days. a-b, APA microcapsules; c, AC microcapsules; and d, GCAC microcapsules (original magnifications: a, 35x; and b-d, 90x).



**a**

**b**

**c**

**d**

**e**

Figure 10.5. Microphotographs of the GCAC microcapsules containing *L. plantanrum* (pC BH1) after exposure to mechanical stress and sequential incubation in SGF (pH 1.2) and SIF (pH 7.5) at 175 rpm, 37°C. a, freshly made; b, 1 h in SGF; c, 1 h in SGF and 0.5 h SIF; d, 1 h in SGF and 1 d in SIF; and e, 1 h in SGF and 3 d in SIF (original magnifications: 90x).

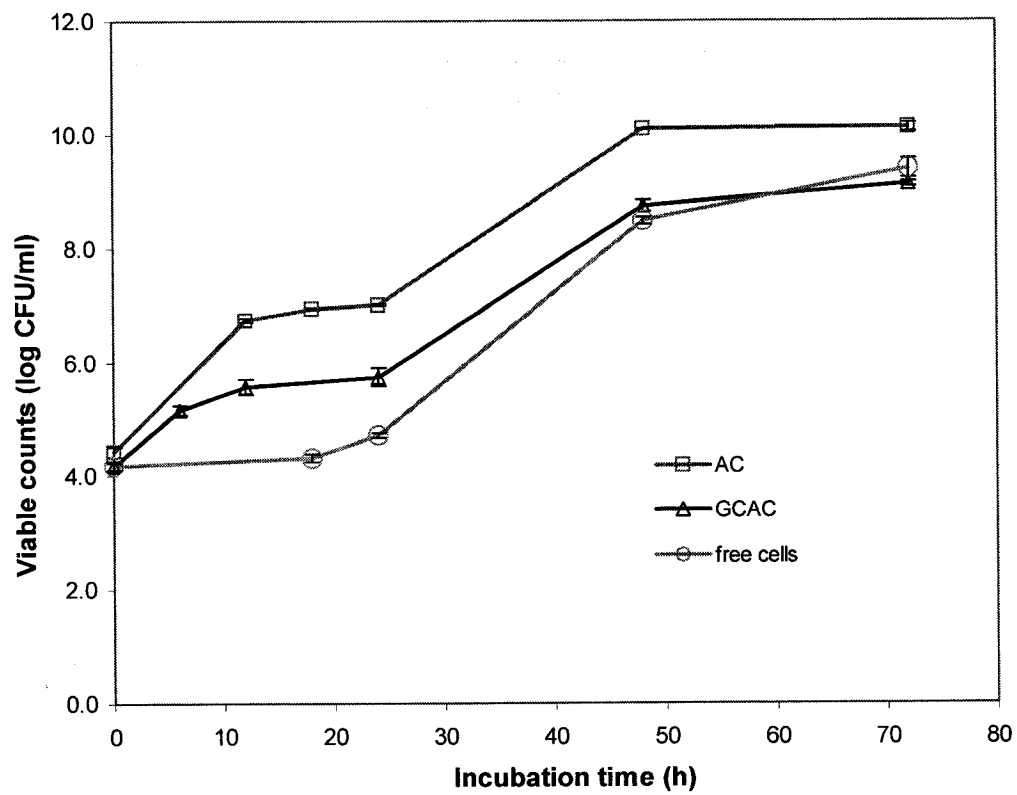
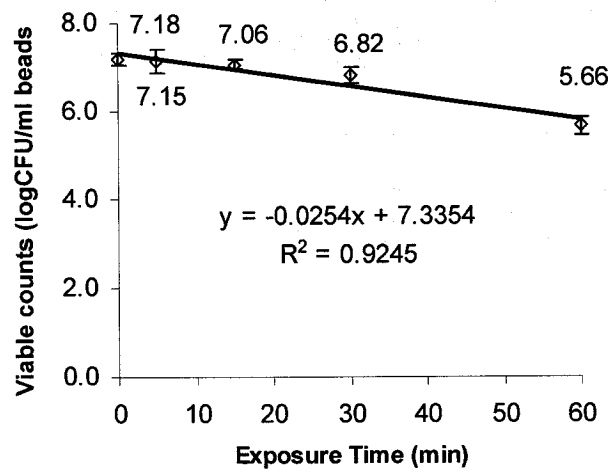
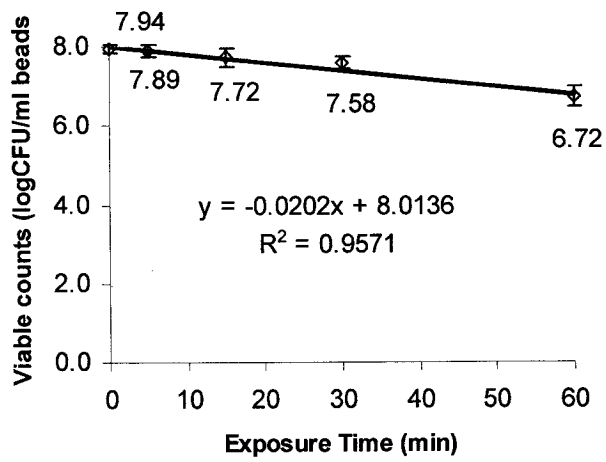


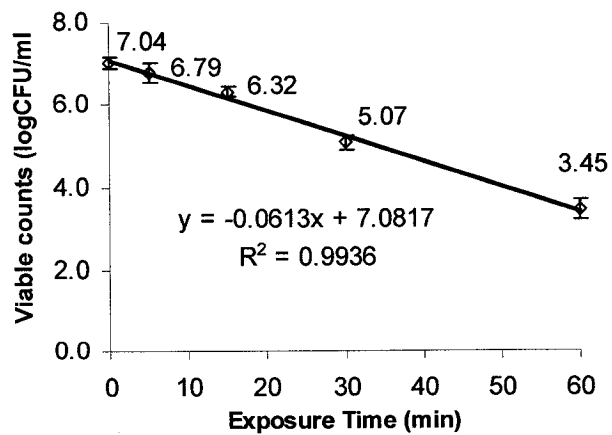
Figure 10.6. Growth profiles of encapsulated and free *Lactobacillus plantarum* 80 incubated in MRS broth, 37 °C.



a

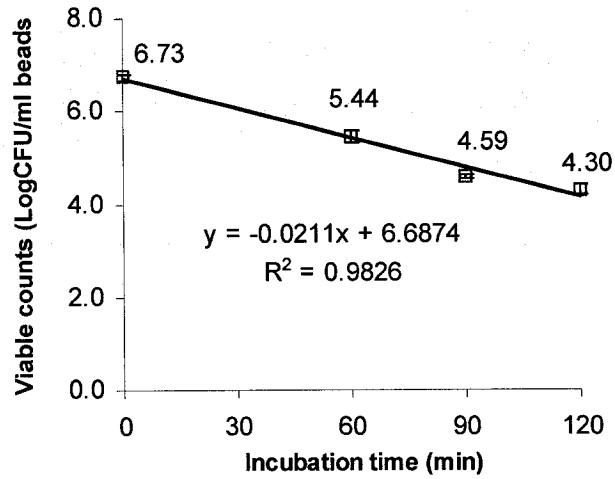


b

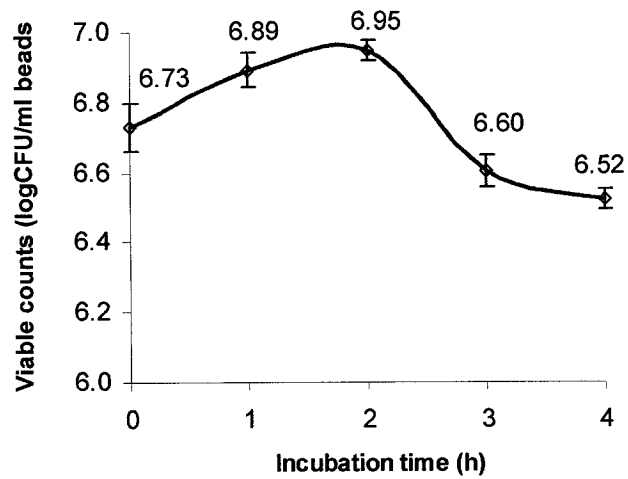


c

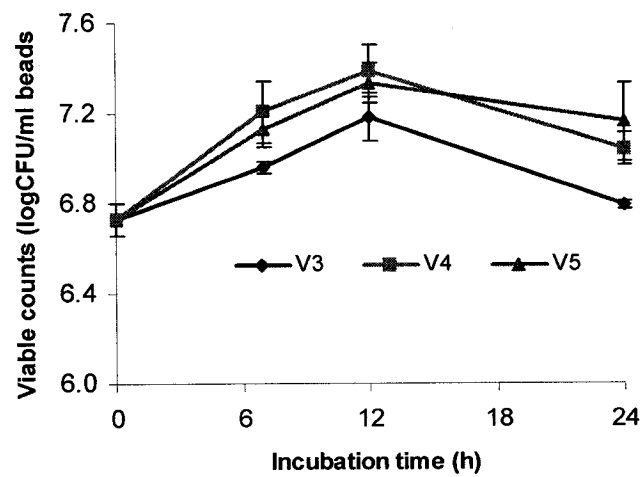
Figure 10.7. Survival of *LP80* cells as a function of exposure time in the simulated human gastric medium (pH 2.0, 37 °C). a, in GCAC capsules; b, in AC capsules; and c, free cells.



a



b



c

Figure 10.8. Tolerance of the GCAC encapsulated *LP80* cells to the simulated human GI media taken from the simulated a, stomach (V1, pH 2.0); b, small intestine (V2, pH 7.4); and c, large intestine (V 3: ascending colon, pH 5.6; V 4: transverse colon, pH 6.2; and V5: descending colon, pH 6.8) under mechanical agitation (175 rpm) and in anaerobic conditions at 37 °C.

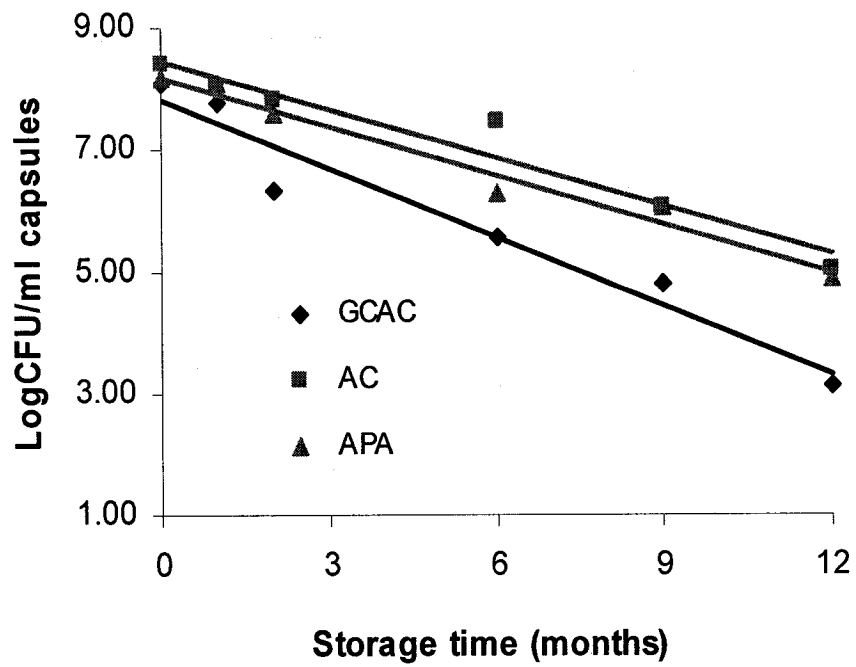


Figure 10.9. Survival of microencapsulated *Lactobacillus plantarum* 80 during long term storage in physiological solution at 4 °C.

**Summary of Observations, Conclusions and Claims to Original Contributions**

---

**11.1 Summary of observations**

In this thesis research, a novel microcapsule formulation consisting of a Ca-alginate core with a genipin covalently cross-linked chitosan membrane was designed, prepared and characterized. The potential of using this microcapsule system for oral delivery of live cells was investigated. Furthermore, the fluorogenic characteristics of genipin were studied. Lastly, a simple and effective genipin-CLSM approach was developed for microcapsule membrane characterization.

The following is a summary of the observations and results:

**1) Formation of Ca-alginate beads**

The formation of Ca-alginate beads was optimized by controlling the operation conditions applied to an Inotech Encapsulator. Investigated facets include complete sterile settings, microcapsule diameter and geometric control. By employing the optimized settings, we were able to reproducibly manufacture spherical alginate microbeads ranging from 0.3 to 1.5 mm in diameter with a narrow size distribution. Alginate beads of ~ 450  $\mu\text{m}$  in diameter were used in this thesis research. The optimum settings are proven suitable for regular microencapsulation practice in our Biomedical Technology and Cell Therapy Research Laboratory.

**2) Design and preparation of the GCAC microcapsules**

A novel GCAC microcapsule formulation composed of a gel core made of cell-compatible alginate and a covalently cross-linked chitosan membrane was proposed. A three-

step preparation procedure, involving ionotropic gelation of the calcium-alginate core, coating with chitosan through polyelectrolyte complex coacervation, and covalent cross-linking of chitosan by naturally derived genipin, was established. The obtained GCAC microcapsules were spherical, bluish,  $471.9 \pm 9.3 \mu\text{m}$  in diameter and had high homogeneity. Genipin reaction variables affected the fluorescence intensity and the degree of cross-linking on the membranes; within the investigated ranges, the order of the effect's magnitude was: cross-linking temperature > cross-linking time > genipin concentration. Elevating the cross-linking temperature from 4 to 37 °C drastically intensified the membrane fluorescence from below 50 to nearly 250. Extended cross-linking time (up to 72 h) altered the cross-linked membranes in modulation, whereas genipin concentrations within the tested range had little impact. Cross-linking by genipin at 37 °C for 24 h may optimally yield the GCAC microcapsule membrane with the strongest fluorescence and highest degree of cross-linking.

### **3) Characterization of the GCAC microcapsule structure**

CLSM studies demonstrated that the cross-linked chitosan deposited homogeneously around the microcapsules and formed a shell-like membrane ( $\sim 37 \mu\text{m}$  in thickness). Electron microscopic studies revealed that the GCAC microcapsules had a smooth and dense surface, and a porous interior structure.

### **4) Characterization of key physical properties of the GCAC microcapsules**

The genipin cross-linked microcapsules possessed strong membrane stability and potent resistance. Genipin cross-links substantially reduced capsular swelling and prevented physical disintegration in media containing non-gelling ions and calcium sequestrants. The GCAC membrane was highly resistant to mechanical shear forces, osmotic pressure, and degradation by lysozyme. In addition, this membrane excluded the infiltration of 70 KD FITC-dextran ( $R\eta=6.4 \text{ nm}$ ) while allowing the permeation of bovine serum albumin (BSA,  $R\eta=3.6 \text{ nm}$ ), indicating a comparable permeability to AC and APA microcapsules. Furthermore, sustained release of BSA from the GCAC microcapsules was observed at a slower rate than in the AC microcapsules.

## 5) Resistance of the GCAC membrane to the simulated human GI environment

A dynamic simulated human gastrointestinal model was employed to evaluate the suitability of microcapsule membranes for oral delivery. In comparison to the APA microcapsules, well-preserved morphology and high retrieval ( $80.3 \pm 8.8 \%$ ) of the GCAC microcapsules were attained after a 3-day simulated human GI transit. The leaking of the encapsulated high molar mass FITC-dextran from the GCAC microcapsules was negligible, indicating the membrane integrity and the retention of the encapsulated macromolecules. In comparison, substantial fluorescence leakage was found from the AC and APA membranes. The presence of microcapsules (either GCAC, AC, or APA) did not evoke appreciable adverse effects on the human intestinal flora.

## 6) Microencapsulation of live cells utilizing the GCAC membrane

To facilitate our research on microencapsulation of living microorganisms, a practical protocol for enumeration of microbial cells inside microcapsules was elaborated, and has been routinely utilized in the Biomedical Technology and Cell Therapy Research Laboratory.

Live *Lactobacillus plantarum* 80 (*pCBHI*) (*LP80*) bacterial cells were encapsulated in the GCAC microcapsules. Cell viability and growth were preserved within this membrane. *LP80* load in the GCAC capsules ( $8.1 \log \text{CFU/mL}$  beads) remained similar to those in the AC and APA capsules. In culture broth, the viable cells inside the GCAC capsules grew from  $4.2 \log \text{CFU/mL}$  beads at time 0 to 5.8, 8.8, and  $9.1 \log \text{CFU}$  after 24, 48, and 72 h, respectively. The GCAC microencapsulated cells were still viable after 12 months of refrigerated storage in PS, with the viable counts decreasing proportionally with storage time. Genipin cross-linking improved the resistance of the *LP80* containing GCAC microcapsules to osmotic pressure shock and other disintegrative impediments in physiologically pertinent media. In addition, mammalian HepG2 cells were encapsulated, but an apparent decrease in cell metabolism was found for HepG2 within the GCAC microcapsules when cross-linked for 12 h.

## **7) Survival of microencapsulated cells in simulated human GI conditions**

A simulated human GI model was used in the study. In the simulated stomach medium (pH 2.0), the viability of *LP80* cells decreased proportionally with exposure time. Microencapsulation by the GCAC preparations improved cell survival, with the loss of 1.5 log units after 1 h incubation in the gastric medium, in contrast to a decrease of 3.6 log units for free cells. The AC microcapsules also provided substantial protection against cell death. Exposure to the simulated human intestinal media did not have obvious deleterious effects on the survival of the GCAC encapsulated cells during the tested periods.

## **8) Fluorogenic characteristics of genipin reactions with chitosan and with PLL**

The chitosan-genipin reaction formed fluorophores, with the optimal excitation and emission wavelengths at 369 nm and 470 nm, respectively. The reaction conditions affected the reaction efficiency as monitored by the fluorescence intensity, with a mixture at the ratio of 4:1 (chitosan: genipin by weight) fluorescing the most. The detected fluorescence was stronger for those fluorophores reacted at higher temperatures, with an intensity of  $10.4 \times 10^5$  CPS at 37°C,  $5.9 \times 10^5$  CPS at 20°C and  $2.5 \times 10^5$  CPS at 4°C. Furthermore, the fluorophores developed gradually over reaction time. Solid state  $^{13}\text{C}$  nuclear magnetic resonance (NMR) and fourier transform infrared (FTIR) spectra demonstrated the chemical changes of chitosan after reacting with genipin.

In addition, the maximum absorption for the genipin-PLL mixture occurred at 370 nm, similar to that of the genipin-chitosan reaction. A large increase in fluorescence intensity of the emission peak with maximum emission at 453 nm was found after the reaction occurred, reflecting the chemical modifications of PLL and genipin. In contrast, other polymers including alginate, pectin and PEG did not show this fluorescence peak.

## **9) Exploitation of fluorogenic genipin in microcapsule membrane characterization**

Genipin, essentially non-fluorescent in its free form, was used to covalently and selectively couple with polyamines, such as chitosan and poly-L-lysine (PLL), and in turn

generate fluorescence. This allows clear visualization and easy analysis of the polymers on the microcapsule membranes using confocal laser scanning microscopy (CLSM). A simple, *in situ*, efficient, and non-destructive method was developed. This genipin-CLSM approach precluded the need for prior labeling of membrane materials, sample dehydration and extraction. Furthermore, it did not affect the functionality of materials or the encapsulation process, was easy to perform on a routine basis, and can be extended to characterize many other polyamine-based formulations. Microcapsule samples can be observed in either dried or wet state. In the present work, this new approach was used to examine the chitosan coating on the AC capsules, the PLL coating on the APA capsules, and the genipin cross-linked chitosan membrane on the GCAC microcapsules. The membrane characteristics with regard to polymer deposition, membrane distribution and thickness were found to correlate with the reaction variables. In addition, five other different microcapsule formulations consisting of PLL and/or chitosan membranes were investigated.

## **11.2 Conclusions**

There is excellent potential for using live cells to treat diseases. However, available technologies to orally deliver live cells are not sufficient. In this thesis, a new class of genipin-cross-linked alginate-chitosan (GCAC) microcapsule system was designed and developed. The suitability of GCAC microcapsules for oral delivery of live cells was investigated. The results obtained show that the GCAC microcapsule has strong membrane stability, highly resists structural degradation and GI impediments, and provides a favorable microenvironment for cell proliferation and survival in harsh GI conditions. Results also demonstrate the effectiveness of the newly developed method for the characterization of microcapsule membranes, which is otherwise difficult using other approaches. This work highlights the immense potential of the GCAC microcapsules for the oral delivery of live cells and other applications. Future studies will investigate its full potential.

### 11.3 Claims to original contributions

1. A novel GCAC microcapsule system was developed using natural occurring materials.
2. Reaction factors affecting the formation of GCAC microcapsule membrane were identified and optimized. The encapsulation, delivery and other features of the novel GCAC microcapsule system were comprehensively investigated.
3. The GCAC microcapsule membrane was characterized for the first time using a noninvasive and *in situ* method without any physical or chemical modifications.
4. The potential for using GCAC microcapsules for oral delivery were successfully investigated. A new formulation for the oral delivery of live *Lactobacillus plantarum* 80 (*pC* BH1) cells was developed using GCAC microcapsules.
5. Details of the APA and GCAC microcapsule oral delivery features were analyzed in a dynamic computer-controlled simulated human GI model. These studies should contribute significantly to the research and development of microencapsulation-based oral-therapy procedures.
6. A new, simple, *in situ*, and non-destructive CLSM approach was developed for the characterization of polyamine microcapsule membranes. This approach is rapid, effective, and highly selective, and overcomes many limitations associated with the conventional methodologies. A number of polyamine-based microcapsule membranes can be characterized easily using the method developed.
7. The novel GCAC microcapsule system offers several advantages over the available microcapsule systems for oral delivery reported in the literature.

Oral administration of microencapsulated live therapeutic cells has shown significant therapeutic potential. Developing suitable microcapsule systems for this application will open up new avenues for the treatment of many human diseases. In this thesis, we have developed a novel covalently cross-linked GCAC microcapsule system and demonstrated its potential for live *LP80* cell oral delivery. Further investigations on microcapsule biocompatibility and metabolic functions of the microencapsulated therapeutic *LP80* cells (BSH secretion and serum cholesterol lowering) in animal models will test the efficiency and advance the development of this preparation. To go forward, a variety of other therapeutic cells could be encapsulated into the GCAC membrane to further exploit the artificial cell oral delivery strategy.

Incorporation of genipin cross-linking into other microcapsule structures, for example, the widely used APA membrane and gelatin-based delivery system, is expected to improve the membrane stability and functional performance. Our preliminary investigations have shown that genipin considerably increased the mechanical strength of the APA microcapsules, suggesting that the genipin treatment may likely overcome the recognized limitation of fragility associated with this membrane.

In this thesis work, a novel approach using genipin as a fluorogenic reagent was developed for the characterization of microcapsule membranes. This method may be extended to characterize a variety of other microcapsule formulations and biomaterials. For example, after coupling with genipin, gelatin could be assessed in the form of capsules for sustained release, scaffolds for tissue repairing, and nanoparticles for targeted gene delivery. Other polyamine candidates for the presented method include polyamido amide (PAMAM) dendrimers, which have recently become a subject of intense interdisciplinary research efforts as a new targeted drug delivery system. The  $-NH_2$  terminals at the branches of PAMAM dendrimers may interact with genipin, by which the fluorescence generation strategy would provide a valuable tool for assessing drug targeting.

The potential of the GCAC microcapsule system is widespread as there is an urgent need for a safe and effective delivery system for targeted delivery of therapeutic products. In addition, this new class of microcapsule system can be further investigated for other biomedical, biotechnological and pharmaceutical applications.

## References

1. Chang,P. Somatic gene therapy. (CRC Press Inc., Bova Raton; 1995).
2. Steidler,L. Genetically engineered probiotics. *Best Practice & Research Clinical Gastroenterology* **17**, 861-876 (2003).
3. Goldberg,M. Challenges for the oral delivery of macromolecules. *Nature reviews. Drug discovery* **2**, 289-295 (2003).
4. Prakash,S. & Chang,T.M. Microencapsulated genetically engineered live E. coli DH5 cells administered orally to maintain normal plasma urea level in uremic rats. *Nature Medicine* **2**, 883-887 (1996).
5. Chang,T.M.S. Semipermeable microcapsules. *Science* **146**, 524-525 (1964).
6. Chang,T.M.S. & Prakash,S. Therapeutic uses of microencapsulated genetically engineered cells. *Molecular Medicine Today* **4**, 221-227 (1998).
7. Batich, Chris, Vaghefi, and Farid. Process for microencapsulating cells. 442925[6,242,230]. 6-5-2001. USA.

Ref Type: Patent

8. Hoppe,B., von Unruh,G., Laube,N., Hesse,A., & Sidhu,H. Oxalate degrading bacteria: new treatment option for patients with primary and secondary hyperoxaluria? *Urological Research* **33**, 372-375 (2005).
9. Jones,M.L., Chen,H.M., Ouyang,W., Metz,T., & Prakash,S. Microencapsulated genetically engineered *Lactobacillus plantarum* 80 (pCBH1) for bile acid deconjugation and its implication in lowering cholesterol. *Journal of Biomedicine and Biotechnology* **1**, 61-69 (2004).
10. Garofalo,F.A. & Chang,T.M.S. Effects of Mass-Transfer and Reaction-Kinetics on Serum-Cholesterol Depletion Rates of Free and Immobilized *Pseudomonas-Pictorum*. *Applied Biochemistry and Biotechnology* **27**, 75-91 (1991).
11. Johnson,L.R. Physiology of the gastrointestinal tract. (Elsevier Academic Press, Burlington, MA; 2006).
12. Chin,J. Immune response to orally consumed antigens and probiotic bacteria. *Immunology and Cell Biology* **78**, 55-66 (2000).
13. Ishibashi,N. Probiotics and safety. *The American journal of clinical nutrition* **73**, 465S-470S (2001).

14. Reuter,G. Probiotics - Possibilities and limitations of their application in food, animal feed, and in pharmaceutical preparations for man and animals. *Berliner und Mu?nchener tiera?rztliche Wochenschrift* **114**, 410-419 (2001).
15. Salminen,S., von Wright,A., Morelli,L., Marteau,P., Brassart,D., de Vos,W.M., Fonden,R., Saxelin,M., Collins,K., Mogensen,G., Birkeland,S.E., & Mattila-Sandholm,T. Demonstration of safety of probiotics - a review. *International Journal of Food Microbiology* **44**, 93-106 (1998).
16. Rihova,B. Immunocompatibility and biocompatibility of cell delivery systems. *Advanced Drug Delivery Reviews* **42**, 65-80 (2000).
17. Champagne,C.P. Challenges in the addition of probiotic cultures to foods. *Critical reviews in food science & nutrition* **45**, 61-84 (2005).
18. Donohue,D.C. & Salminen,S. Safety assessment of probiotic bacteria. *Asia Pacific Journal of Clinical Nutrition* **5**, 25-28 (1996).
19. Chang,T.M.S. Therapeutic applications of polymeric artificial cells. *Nature Reviews Drug Discovery* **4**, 221-235 (2005).
20. Moses,L.R., Dileep,K.J., & Sharma,C.P. Beta cyclodextrin-insulin-encapsulated chitosan/alginate matrix: Oral delivery system. *Journal of Applied Polymer Science* **75**, 1089-1096 (2000).
21. Freiberg,S. & Zhu,X.X. Polymer microspheres for controlled drug release. *International Journal of Pharmaceutics* **282**, 1-18 (2004).
22. Orive,G., Hernandez,R.M., Gascon,A.R., Calafiore,R., Chang,T.M.S., De Vos,P., Hortelano,G., Hunkeler,D., Lacik,I., & Pedraz,J.L. History, challenges and perspectives of cell microencapsulation. *Trends in Biotechnology* **22**, 87-92 (2004).
23. Orive,G., Gascon,A.R., Hernandez,R.M., Dominguez-Gil,A., & Pedraz,J.L. Techniques: New approaches to the delivery of biopharmaceuticals. *Trends in Pharmacological Sciences* **25**, 382-387 (2004).
24. Sinha,V.R. & Trehan,A. Biodegradable microspheres for protein delivery. *Journal of Controlled Release* **90**, 261-280 (2003).
25. Nechaeva,E. Development of oral microencapsulated forms for delivering viral vaccines. *Expert Review of Vaccines* **1**, 385-397 (2002).
26. Chow,K.M., Liu,Z.C., Prakash,S., & Chang,T.M.S. Free and microencapsulated Lactobacillus and effects of metabolic induction on urea removal. *Artificial Cells Blood Substitutes and Immobilization Biotechnology* **31**, 425-434 (2003).

27. Chen,H., Ouyang,W., Jones,M., Haque,T., Lawuyi,B., & Prakash,S. *In-vitro* analysis of APA microcapsules for oral delivery of live bacterial cells. *Journal of Microencapsulation* **22**, 539-547 (2005).
28. Prokop,A., Hunkeler,D., Powers,A.C., Whitesell,R.R., & Wang,T.G. Water soluble polymers for immunoisolation II: Evaluation of multicomponent microencapsulation systems. *Adv. Polym. Sci.* **136**, 53-73 (1998).
29. Bhatia,S.R., Khattak,S.F., & Roberts,S.C. Polyelectrolytes for cell encapsulation. *Current Opinion in Colloid & Interface Science* **10**, 45-51 (2005).
30. Prokop,A., Hunkeler,D., DiMari,S., Haralson,M.A., & Wang,T.G. Water soluble polymers for immunoisolation I: Complex coacervation and cytotoxicity. *Adv. Polym. Sci.* **136**, 1-51 (1998).
31. Saburova,E.A., Bobreshova,M.E., Elphimova,L.I., & Sukhorukov,B.I. Inhibitory effect of polyelectrolytes on oligomeric enzymes. *Biochemistry-Moscow* **65**, 976-985 (2000).
32. Martinsen,A., Skjakbraek,G., & Smidsrod,O. Alginate As Immobilization Material .1. Correlation Between Chemical and Physical-Properties of Alginate Gel Beads. *Biotechnology and Bioengineering* **33**, 79-89 (1989).
33. Zimmermann,H., Zimmermann,D., Reuss,R., Feilen,P.J., Manz,B., Katsen,A., Weber,M., Ihmig,F.R., Ehrhart,F., Gessner,P., Behringer,M., Steinbach,A., Wegner,L.H., Sukhorukov,V.L., Vasquez,J.A., Schneider,S., Weber,M.M., Volke,F., Wolf,R., & Zimmermann,U. Towards a medically approved technology for alginate-based microcapsules allowing long-term immunoisolated transplantation. *Journal of Materials Science-Materials in Medicine* **16**, 491-501 (2005).
34. Lee,K.Y., Park,W.H., & Ha,W.S. Polyelectrolyte complexes of sodium alginate with chitosan or its derivatives for microcapsules. *Journal of Applied Polymer Science* **63**, 425-432 (1997).
35. Gaserod,O., Smidsrod,O., & Skjak-Braek,G. Microcapsules of alginate-chitosan - I - A quantitative study of the interaction between alginate and chitosan. *Biomaterials* **19**, 1815-1825 (1998).
36. Li,S. Studies on alginate-chitosan microcapsules and renal arterial embolization in rabbits. *Journal of Controlled Release* **84**, 87-98 (2002).
37. Lee,K.W., Yoon,J.J., Lee,J.H., Kim,S.Y., Jung,H.J., Kim,S.J., Joh,J.W., Lee,H.H., Lee,D.S., & Lee,S.K. Sustained release of vascular endothelial growth factor from calcium-induced alginate hydrogels reinforced by heparin and chitosan. *Transplantation Proceedings* **36**, 2464-2465 (2004).

38. Metz, T., Jones, M.L., Chen, H.M., Halim, T., Mirzaei, M., Haque, T., Amre, D., Das, S.K., & Prakash, S. A new method for targeted drug delivery using polymeric microcapsules. *Cell Biochemistry and Biophysics* **43**, 77-85 (2005).
39. Coppi, G., Iannuccelli, V., Leo, E., Bernabei, M.T., & Cameroni, R. Protein immobilization in crosslinked alginate microparticles. *Journal of Microencapsulation* **19**, 37-44 (2002).
40. Boadi, D.K. & Neufeld, R.J. Encapsulation of tannase for the hydrolysis of tea tannins. *Enzyme and Microbial Technology* **28**, 590-595 (2001).
41. DeGroot, A.R. & Neufeld, R.J. Encapsulation of urease in alginate beads and protection from alpha-chymotrypsin with chitosan membranes. *Enzyme and Microbial Technology* **29**, 321-327 (2001).
42. Taqieddin, E. & Amiji, M. Enzyme immobilization in novel alginate-chitosan core-shell microcapsules. *Biomaterials* **25**, 1937-1945 (2004).
43. Maysinger, D., Berezovskaya, O., & Fedoroff, S. The hematopoietic cytokine colony stimulating factor 1 is also a growth factor in the CNS.2. Microencapsulated CSF-I and LM-10 cells as delivery systems. *Experimental Neurology* **141**, 47-56 (1996).
44. Bartkowiak, A. Optimal conditions of transplantable binary polyelectrolyte microcapsules. *Bioartificial Organs Iii: Tissue Sourcing, Immunoisolation, and Clinical Trials* **944**, 120-134 (2001).
45. Maysinger, D., Kriegelstein, K., FilipovicGrcic, J., Sendtner, M., Unsicker, K., & Richardson, P. Microencapsulated ciliary neurotrophic factor: Physical properties and biological activities. *Experimental Neurology* **138**, 177-188 (1996).
46. Green, D.W., Leveque, I., Walsh, D., Howard, D., Yang, X.B., Partridge, K., Mann, S., & Oreffo, R.O.C. Biom mineralized polysaccharide capsules for encapsulation, organization, and delivery of human cell types and growth factors. *Advanced functional materials* **15**, 917-923 (2005).
47. Haque, T. In vitro study of alginate-chitosan microcapsules: an alternative to liver cell transplants for the treatment of liver failure. *Biotechnology Letters* **27**, 317-322 (2005).
48. Iyer, C. Effect of co-encapsulation of probiotics with prebiotics on increasing the viability of encapsulated bacteria under in vitro acidic and bile salt conditions and in yogurt. *Journal of food science* **70**, M18-M23 (2005).
49. Krasaekoopt, W., Bhandari, B., & Deeth, H. The influence of coating materials on some properties of alginate beads and survivability of microencapsulated probiotic bacteria. *International dairy journal* **14**, 737-743 (2004).

50. Zanina,A., Vilesov,A., & Budtova,T. Shear-induced solvent release from gel particles: application to drug-delivery systems. *International Journal of Pharmaceutics* **242**, 137-146 (2002).
51. Chandy,T., Mooradian,D.L., & Rao,G.H. Evaluation of modified alginate-chitosan-polyethylene glycol microcapsules for cell encapsulation. *Artif. Organs* **23**, 894-903 (1999).
52. Orive,G., Bartkowiak,A., Lisiecki,S., De Castro,M., Hernandez,R.M., Gascon,A.R., & Pedraz,J.L. Biocompatible oligochitosans as cationic modifiers of alginate/Ca microcapsules. *Journal of Biomedical Materials Research Part B-Applied Biomaterials* **74B**, 429-439 (2005).
53. Klinkenberg,G., Lystad,K.Q., Levine,D.W., & Dyrset,N. Cell release from alginate immobilized *Lactococcus lactis* ssp *lactis* in chitosan and alginate coated beads. *Journal of Dairy Science* **84**, 1118-1127 (2001).
54. Chang,T.M.S. Artificial cells, encapsulation, and immobilization. *Bioartificial Organs II: Technology, Medicine, and Materials* **875**, 71-83 (1999).
55. Orive,G., Hernandez,R.M., Gascon,A.R., Calafiore,R., Chang,T.M., Vos,P.D., Hortelano,G., Hunkeler,D., Lacik,I., Shapiro,A.M., & Pedraz,J.L. Cell encapsulation: Promise and progress. *Nature Medicine* **9**, 104-107 (2003).
56. Orive,G. Cell microencapsulation technology for biomedical purposes: novel insights and challenges. *Trends in Pharmacological Sciences* **24**, 207-210 (2003).
57. Chang,T.M.S. Artificial cells for replacement of metabolic organ functions. *Artificial cells, blood substitutes, and immobilization biotechnology* **31**, 151-161 (2003).
58. Orive,G., Hernandez,R.M., Gascon,A.R., Igartua,M., & Pedraz,J.L. Encapsulated cell technology: from research to market. *Trends in Biotechnology* **20**, 382-387 (2002).
59. Senior,K. Encapsulated cell technology provides new treatment options. *Drug discovery today* **6**, 6-7 (2001).
60. Chang,P.L. Encapsulation for somatic gene therapy. *Bioartificial Organs II: Technology, Medicine, and Materials* **875**, 146-158 (1999).
61. Chang,T.M.S. Artificial cells for cell and organ replacements. *Artificial Organs* **28**, 265-270 (2004).
62. Prakash,S. Artificial cell therapy: New strategies for the therapeutic delivery of live bacteria. *Journal of Biomedicine and Biotechnology* 44-56 (2005).

63. Chang, T.M.S. Artificial cell bioencapsulation in macro, micro, nano, and molecular dimensions: Keynote lecture. *Artificial Cells Blood Substitutes and Immobilization Biotechnology* **32**, 1-23 (2004).
64. Soonshiong, P., Heintz, R.E., Merideth, N., Yao, Q.X., Yao, Z.W., Zheng, T.L., Murphy, M., Moloney, M.K., Schmehl, M., Harris, M., Mendez, R., Mendez, R., & Sandford, P.A. Insulin Independence in A Type-I Diabetic Patient After Encapsulated Islet Transplantation. *Lancet* **343**, 950-951 (1994).
65. Lohr, M., Hoffmeyer, A., Kroger, J.C., Freund, M., Hain, J., Holle, A., Karle, P., Knofel, W.T., Liebe, S., & Muller, P. Microencapsulated cell-mediated treatment of inoperable pancreatic carcinoma. *The Lancet* **357**, 1591-1592 (2001).
66. Hasse, C., Klock, G., Schlosser, A., Zimmermann, U., & Rothmund, M. Parathyroid allotransplantation without immunosuppression. *Lancet* **350**, 1296-1297 (1997).
67. Aebischer, P., Schlupe, M., Deglon, N., Joseph, J.M., Hirt, L., Heyd, B., Goddard, M., Hammang, J.P., Zurn, A.D., Kato, A.C., Regli, F., & Baetge, E.E. Intrathecal delivery of CNTF using encapsulated genetically modified xenogeneic cells in amyotrophic lateral sclerosis patients. *Nature Medicine* **2**, 696-699 (1996).
68. Bloch, J., Bachoud-Levi, A.C., Deglon, N., Lefaucheur, J.P., Winkel, L., Palfi, S., Nguyen, J.P., Bourdet, C., Gaura, V., Remy, P., Brugieres, P., Boisse, M.F., Baudic, S., Cesaro, P., Hantraye, P., Aebischer, P., & Peschanski, M. Neuroprotective gene therapy for Huntington's disease, using polymer-encapsulated cells engineered to secrete human ciliary neurotrophic factor: Results of a phase I study. *Human Gene Therapy* **15**, 968-975 (2004).
69. Lim, F. & Sun, A.M. Microencapsulated islets as bioartificial endocrine pancreas. *Science* **210**, 908-910 (1980).
70. de Vos, P. & Marchetti, P. Encapsulation of pancreatic islets for transplantation in diabetes: the untouchable islets. *Trends in Molecular Medicine* **8**, 363-366 (2002).
71. Soonshiong, P., Feldman, E., Nelson, R., Komtebedde, J., Smidsrod, O., Skjakbraek, G., Espevik, T., Heintz, R., & Lee, M. Successful Reversal of Spontaneous Diabetes in Dogs by Intraperitoneal Microencapsulated Islets. *Transplantation* **54**, 769-774 (1992).
72. Sun, Y.L., Ma, X.J., Zhou, D.B., Vacek, I., & Sun, A.M. Normalization of diabetes in spontaneously diabetic cynomolgous monkeys by xenografts of microencapsulated porcine islets without immunosuppression. *The Journal of clinical investigation* **98**, 1417-1422 (1996).
73. Zhou, M., Chen, D., Yao, Q., Xia, Z., Wang, C., & Zhu, H. Microencapsulation of rat islets prolongs xenograft survival in diabetic mice. *Chin Med. J. (Engl.)* **111**, 394-397 (1998).

74. De Vos,P., Hamel,A.F., & Tatariewicz,K. Considerations for successful transplantation of encapsulated pancreatic islets. *Diabetologia* **45**, 159-173 (2002).
75. De Vos,P. Long-term biocompatibility, chemistry, and function of microencapsulated pancreatic islets. *Biomaterials* **24**, 305-312 (2003).
76. de Groot,M., Schuurs,T.A., & van Schilfgaarde,R. Causes of limited survival of microencapsulated pancreatic islet grafts. *Journal of Surgical Research* **121**, 141-150 (2004).
77. Ranganathan, Natarajan, Dickstein, and Jack. Composition for alleviating symptoms of uremia in patients. 557011[6,706,263]. 3-16-2004. PA/USA.

Ref Type: Patent

78. Umehara,Y., Hakamada,K., Seino,K., Aoki,K., Toyoki,Y., & Sasaki,M. Improved survival and ammonia metabolism by intraperitoneal transplantation of microencapsulated hepatocytes in totally hepatectomized rats. *Surgery* **130**, 513-520 (2001).
79. Wang,L.S., Sun,J.H., Li,L., Harbour,C., Mears,D., Koutalistras,N., & Sheil,A.G.R. Factors affecting hepatocyte viability and CYP1A1 activity during encapsulation. *Artificial Cells Blood Substitutes and Immobilization Biotechnology* **28**, 215-227 (2000).
80. Chang,T.M. The role of artificial cells in cell and organ transplantation in regenerative medicine. *Panminerva Med.* **47**, 1-9 (2005).
81. Hortelano,G. & Chang,P.L. Gene therapy for hemophilia. *Artificial Cells Blood Substitutes and Immobilization Biotechnology* **28**, 1-24 (2000).
82. Van Raamsdonk,J.M., Ross,C.J.D., Potter,M.A., Kurachi,S., Kurachi,K., Stafford,D.W., & Chang,P.L. Treatment of hemophilia B in mice with nonautologous somatic gene therapeutics. *Journal of Laboratory and Clinical Medicine* **139**, 35-42 (2002).
83. Tagalakis,A.D. Apolipoprotein E delivery by peritoneal implantation of encapsulated recombinant cells improves the hyperlipidaemic profile in apoE-deficient mice. *Biochimica et biophysica acta-Molecular and cell biology of lipids* **1686**, 190-199 (2005).
84. AlHendy,A., Hortelano,G., Tannenbaum,G.S., & Chang,P.L. Correction of the Growth Defect in Dwarf Mice with Nonautologous Microencapsulated Myoblasts - An Alternate Approach to Somatic Gene-Therapy. *Human Gene Therapy* **6**, 165-175 (1995).
85. Ross,C.J.D., Bastedo,L., Maier,S.A., Sands,M.S., & Chang,P.L. Treatment of a lysosomal storage disease, mucopolysaccharidosis VII, with microencapsulated recombinant cells. *Human Gene Therapy* **11**, 2117-2127 (2000).

86. Chang,P.L., Van Raamsdonk,J.M., Hortelano,G., Barsoum,S.C., MacDonald,N.C., & Stockley,T.L. The in vivo delivery of heterologous proteins by microencapsulated recombinant cells. *Trends in Biotechnology* **17**, 78-83 (1999).
87. Hann,E., Reinartz,S., Clare,S.E., Passow,S., Kissel,T., & Wagner,U. Development of a delivery system for the continuous endogenous release of an anti-idiotypic antibody against ovarian carcinoma. *Hybridoma* **24**, 133-140 (2005).
88. Hao,S.G., Su,L.P., Gu,X.L., Moyana,T., & Xiang,J. A novel approach to tumor suppression using microencapsulated engineered J558/TNF-alpha cells. *Experimental Oncology* **27**, 56-60 (2005).
89. Visted,T. Progress and challenges for cell encapsulation in brain tumour therapy. *Expert opinion on biological therapy* **3**, 551-561 (2003).
90. Thorsen,F., Read,T.A., Lund-Johansen,M., Tysnes,B.B., & Bjerkvig,R. Alginate-encapsulated producer cells: A potential new approach for the treatment of malignant brain tumors. *Cell Transplantation* **9**, 773-783 (2000).
91. Read,T.A., Farhadi,M., Bjerkvig,R., Olsen,B.R., Rokstad,A.M., Huszthy,P.C., & Vajkoczy,P. Intravital microscopy reveals novel antivascular and antitumor effects of endostatin delivered locally by alginate-encapsulated cells. *Cancer Research* **61**, 6830-6837 (2001).
92. Cirone,P., Bourgeois,J.M., Austin,R.C., & Chang,P.L. A novel approach to tumor suppression with microencapsulated recombinant cells. *Human Gene Therapy* **13**, 1157-1166 (2002).
93. Bergers,G. & Hanahan,D. Cell factories for fighting cancer. *Nature Biotechnology* **19**, 20-21 (2001).
94. Read,T.A., Sorensen,D.R., Mahesparan,R., Enger,P.O., Timpl,R., Olsen,B.R., Hjelstuen,M.H.B., Haraldseth,O., & Bjerkvig,R. Local endostatin treatment of gliomas administered by microencapsulated producer cells. *Nature Biotechnology* **19**, 29-34 (2001).
95. Ponce,S., Orive,G., Gascon,A.R., Hernandez,R.M., & Pedraz,J.L. Microcapsules prepared with different biomaterials to immobilize GDNF secreting 3T3 fibroblasts. *International Journal of Pharmaceutics* **293**, 1-10 (2005).
96. Visted,T., Bjerkvig,R., & Enger,P.O. Cell encapsulation technology as a therapeutic strategy for CNS malignancies. *Neuro-Oncology* **3**, 201-210 (2001).
97. Vallbacka,J.J., Nobrega,J.N., & Sefton,M.V. Tissue engineering as a platform for controlled release of therapeutic agents: implantation of microencapsulated dopamine producing cells in the brains of rats. *Journal of Controlled Release* **72**, 93-100 (2001).

98. Bachoud-Levi,A.C., Deglon,N., Nguyen,J.P., Bloch,J., Bourdet,C., Winkel,L., Remy,P., Goddard,M., Lefaucheur,J.P., Brugieres,P., Baudic,S., Cesaro,P., Peschanski,M., & Aebischer,P. Neuroprotective gene therapy for Huntington's disease using a polymer encapsulated BHK cell line engineered to secrete human CNTF. *Human Gene Therapy* **11**, 1723-1729 (2000).
99. Winn,S.R. & Emerich,D.F. Managing chronic pain with encapsulated cell implants releasing catecholamines and endogenous opioids. *Frontiers in Bioscience* **10**, 367-378 (2005).
100. Benoit,J.P., Faisant,N., Venier-Julienne,M.C., & Menei,P. Development of microspheres for neurological disorders: From basics to clinical applications. *Journal of Controlled Release* **65**, 285-296 (2000).
101. Hagihara,Y., Saitoh,Y., Iwata,H., Taki,T., Hirano,S., Arita,N., & Hayakawa,T. Transplantation of xenogeneic cells secreting beta-endorphin for pain treatment: Analysis of the ability of components of complement to penetrate through polymer capsules. *Cell Transplantation* **6**, 527-530 (1997).
102. Chandramouli,V., Kailasapathy,K., Peiris,P., & Jones,M. An improved method of microencapsulation and its evaluation to protect *Lactobacillus* spp. in simulated gastric conditions. *Journal of Microbiological Methods* **56**, 27-35 (2004).
103. Krasaekoopt,W. Evaluation of encapsulation techniques of probiotics for yoghurt. *International dairy journal* **13**, 3-13 (2003).
104. Colton,C.K. Engineering challenges in cell-encapsulation technology. *Trends in Biotechnology* **14**, 158-162 (1996).
105. Sefton,M.V., May,M.H., Lahooti,S., & Babensee,J.E. Making microencapsulation work: conformal coating, immobilization gels and in vivo performance. *Journal of Controlled Release* **65**, 173-186 (2000).
106. Winder,R.S., Wheeler,J.J., Conder,N., Otvos,I.S., Nevill,R., & Duan,L. Microencapsulation: a strategy for formulation of inoculum. *Biocontrol Science and Technology* **13**, 155-169 (2003).
107. Goosen,M.F.A., Oshea,G.M., Gharapetian,H.M., Chou,S., & Sun,A.M. Optimization of Microencapsulation Parameters - Semipermeable Microcapsules As A Bioartificial Pancreas. *Biotechnology and Bioengineering* **27**, 146-150 (1985).
108. Uludag,H. Technology of mammalian cell encapsulation. *Advanced Drug Delivery Reviews* **42**, 29-64 (2000).
109. Kidchob,T., Kimura,S., & Imanishi,Y. Degradation and release profile of microcapsules made of poly[L-lactic acid-co-L-lysine(Z)]. *Journal of Controlled Release* **54**, 283-292 (1998).

110. Freitas,S., Merkle,H.P., & Gander,B. Microencapsulation by solvent extraction/evaporation: reviewing the state of the art of microsphere preparation process technology. *Journal of Controlled Release* **102**, 313-332 (2005).
111. Chang,T.M.S. & Prakash,S. Procedures for microencapsulation of enzymes, cells and genetically engineered microorganisms. *Molecular Biotechnology* **17**, 249-260 (2001).
112. De Vos,P., Hoogmoed,C.G., & Busscher,H.J. Chemistry and biocompatibility of alginate-PLL capsules for immunoprotection of mammalian cells. *Journal of Biomedical Materials Research* **60**, 252-259 (2002).
113. Gugerli,R. Quantitative study of the production and properties of alginate/poly-L-lysine microcapsules. *Journal of Microencapsulation* **19**, 571-590 (2002).
114. Okada,N., Miyamoto,H., Yoshioka,T., Sakamoto,K., Katsume,A., Saito,H., Nakagawa,S., Ohsugi,Y., & Mayumi,T. Immunological studies of SK2 hybridoma cells microencapsulated with alginate-poly(L)lysine-alginate (APA) membrane following allogeneic transplantation. *Biochemical and Biophysical Research Communications* **230**, 524-527 (1997).
115. Rokstad,A.M., Holtan,S., Strand,B., Steinkjer,B., Ryan,L., Kulseng,B., Skjak-Braek,G., & Espevik,T. Microencapsulation of cells producing therapeutic proteins: Optimizing cell growth and secretion. *Cell Transplantation* **11**, 313-324 (2002).
116. Peyratout,C.S. Tailor-made polyelectrolyte microcapsules: From multilayers to smart containers. *Angewandte Chemie* **43**, 3762-3783 (2004).
117. Sukhorukov,G.B., Donath,E., Moya,S., Susha,A.S., Voigt,A., Hartmann,J., & Mohwald,H. Microencapsulation by means of step-wise adsorption of polyelectrolytes. *Journal of Microencapsulation* **17**, 177-185 (2000).
118. Dong,W.F., Ferri,J.K., Adalsteinsson,T., Schonhoff,M., Sukhorukov,G.B., & Mohwald,H. Influence of shell structure on stability, integrity, and mesh size of polyelectrolyte capsules: Mechanism and strategy for improved preparation. *Chemistry of Materials* **17**, 2603-2611 (2005).
119. Krishna,G., Shutava,T., & Lvov,Y. Lipid modified polyelectrolyte microcapsules with controlled diffusion. *Chemical Communications* 2796-2798 (2005).
120. Germain,M., Balaguer,P., Nicolas,J.C., Lopez,F., Esteve,J.P., Sukhorukov,G.B., Winterhalter,M., Richard-Foy,H., & Fournier,D. Protection of mammalian cell used in biosensors by coating with a polyelectrolyte shell. *Biosensors & Bioelectronics* **21**, 1566-1573 (2006).
121. Park,M.K., Deng,S.X., & Advincula,R.C. Sustained release control via photo-cross-linking of polyelectrolyte layer-by-layer hollow capsules. *Langmuir* **21**, 5272-5277 (2005).

122. Vinogradova,O.I., Lebedeva,O.V., Vasilev,K., Gong,H.F., Garcia-Turiel,J., & Kim,B.S. Multilayer DNA/poly(allylamine hydrochloride) microcapsules: Assembly and mechanical properties. *Biomacromolecules* **6**, 1495-1502 (2005).
123. Heuberger,R., Sukhorukov,G., Voros,J., Textor,M., & Mohwald,H. Biofunctional polyelectrolyte multilayers and microcapsules: Control of non-specific and bio-specific protein adsorption. *Advanced functional materials* **15**, 357-366 (2005).
124. Bhadra,D., Gupta,G., Bhadra,S., Umamaheshwari,R.B., & Jain,N.K. Multicomposite ultrathin capsules for sustained ocular delivery of ciprofloxacin hydrochloride. *Journal of Pharmacy and Pharmaceutical Sciences* **7**, 241-251 (2004).
125. Schneider,S., Feilen,P.J., Slotty,V., Kampfner,D., Preuss,S., Berger,S., Beyer,J., & Pommersheim,R. Multilayer capsules: a promising microencapsulation system for transplantation of pancreatic islets. *Biomaterials* **22**, 1961-1970 (2001).
126. Srivastava,R. & McShane,M.J. Application of self-assembled ultra-thin film coatings to stabilize macromolecule encapsulation in alginate microspheres. *Journal of Microencapsulation* **22**, 397-411 (2005).
127. Zhu,H.G., Srivastava,R., & McShane,M.J. Spontaneous loading of positively charged macromolecules into alginate-templated polyelectrolyte multilayer microcapsules. *Biomacromolecules* **6**, 2221-2228 (2005).
128. Amsden,B. The production of uniformly sized polymer microspheres. *Pharmaceutical research* **16**, 1140-1143 (1999).
129. Strand,B.L., Gaserod,O., Kulseng,B., Espevik,T., & Skjak-Braek,G. Alginate-polylysine-alginate microcapsules: effect of size reduction on capsule properties. *Journal of Microencapsulation* **19**, 615-630 (2002).
130. Koch,S., Schwinger,C., Kressler,J., Heinzen,C., & Rainov,N.G. Alginate encapsulation of genetically engineered mammalian cells: comparison of production devices, methods and microcapsule characteristics. *Journal of Microencapsulation* **20**, 303-316 (2003).
131. Senuma,Y., Franceschin,S., Hilborn,J.G., Tissieres,P., Bisson,I., & Frey,P. Bioresorbable microspheres by spinning disk atomization as injectable cell carrier: from preparation to in vitro evaluation. *Biomaterials* **21**, 1135-1144 (2000).
132. Senuma,Y., Lowe,C., Zweifel,Y., Hilborn,J.G., & Marison,I. Alginate hydrogel microspheres and microcapsules prepared by spinning disk atomization. *Biotechnology and Bioengineering* **67**, 616-622 (2000).
133. Rehor,A., Canaple,L., Zhang,Z.B., & Hunkeler,D. The compressive deformation of multicomponent microcapsules: Influence of size, membrane thickness, and compression speed. *Journal of Biomaterials Science-Polymer Edition* **12**, 157-170 (2001).

134. Desai, T.A. Microfabricated immunoisolating biocapsules. *Biotechnology and Bioengineering* **57**, 118-120 (1998).
135. Tao, S.L. & Desai, T.A. Microfabricated drug delivery systems: from particles to pores. *Advanced Drug Delivery Reviews* **55**, 315-328 (2003).
136. Esquisabel, A., Hernandez, R.M., Igartua, M., Gascon, A.R., Calvo, B., & Pedraz, J.L. Preparation and stability of agarose microcapsules containing BCG. *Journal of Microencapsulation* **19**, 237-244 (2002).
137. Vladisavljevic, G.T. Recent developments in manufacturing emulsions and particulate products using membranes. *Advances in colloid and interface science* **113**, 1-20 (2005).
138. Nakagawa, K., Iwamoto, S., Nakajima, M., Shono, A., & Satoh, K. Microchannel emulsification using gelatin and surfactant-free coacervate microencapsulation. *Journal of Colloid and Interface Science* **278**, 198-205 (2004).
139. Anilkumar, A.V., Lacik, I., & Wang, T.G. A novel reactor for making uniform capsules. *Biotechnology and Bioengineering* **75**, 581-589 (2001).
140. Schwinger, C., Koch, S., Jahnz, U., Wittlich, P., Rainov, N.G., & Kressler, J. High throughput encapsulation of murine fibroblasts in alginate using the JetCutter technology. *Journal of Microencapsulation* **19**, 273-280 (2002).
141. Serp, D., Cantana, E., Heinzen, C., von Stockar, U., & Marison, I.W. Characterization of an encapsulation device for the production of monodisperse alginate beads for cell immobilization. *Biotechnology and Bioengineering* **70**, 41-53 (2000).
142. Canaple, L., Rehor, A., & Hunkeler, D. Improving cell encapsulation through size control. *Journal of Biomaterials Science-Polymer Edition* **13**, 783-796 (2002).
143. De Vos, P., De Haan, B.J., & Van Schilfgaarde, R. Is it possible to use the standard alginate-PLL procedure for production of small capsules? *Transplantation Proceedings* **30**, 492-493 (1998).
144. Ross, C.J.D. & Chang, P.L. Development of small alginate microcapsules for recombinant gene product delivery to the rodent brain. *Journal of Biomaterials Science-Polymer Edition* **13**, 953-962 (2002).
145. Coppi, G., Iannuccelli, V., Bernabei, M.T., & Cameroni, R. Alginate microparticles for enzyme peroral administration. *International Journal of Pharmaceutics* **242**, 263-266 (2002).
146. Schrezenmeir, J., Kirchgessner, J., Gero, L., Kunz, L.A., Beyer, J., & Muellerklieser, W. Effect of Microencapsulation on Oxygen Distribution in Islets Organs. *Transplantation* **57**, 1308-1314 (1994).

147. Devos,P., DeHaan,B., Pater,J., & VanSchilfgaarde,R. Association between capsule diameter, adequacy of encapsulation, and survival of microencapsulated rat islet allografts. *Transplantation* **62**, 893-899 (1996).
148. Li,R.H. Materials for immunoisolated cell transplantation. *Advanced Drug Delivery Reviews* **33**, 87-109 (1998).
149. Lekka,M. Hydrogel microspheres: Influence of chemical composition on surface morphology, local elastic properties, and bulk mechanical characteristics. *Langmuir* **20**, 9968-9977 (2004).
150. Hoffman,A.S. Hydrogels for biomedical applications. *Advanced Drug Delivery Reviews* **54**, 3-12 (2002).
151. Peppas N.A. Hydrogels in medicine and pharmacy. (CPC Press,1987).
152. Risbud,M.V. Islet immunoisolation: experience with biopolymers. *Journal of biomaterials science. Polymer edition* **12**, 1243-1252 (2001).
153. Germain,M., Balaguer,P., Nicolas,J.C., Lopez,F., Esteve,J.P., Sukhorukov,G.B., Winterhalter,M., Richard-Foy,H., & Fournier,D. Protection of mammalian cell used in biosensors by coating with a polyelectrolyte shell. *Biosensors and Bioelectronics* **21**, 1566-1573 (2006).
154. Smidsrod,O. & Skjakbraek,G. Alginate as immobilization matrix for cells. *Trends in Biotechnology* **8**, 71-78 (1990).
155. Peirone,M., Ross,C.J.D., Hortelano,G., Brash,J.L., & Chang,P.L. Encapsulation of various recombinant mammalian cell types in different alginate microcapsules. *Journal of Biomedical Materials Research* **42**, 587-596 (1998).
156. Van Raamsdonk,J.M., Cornelius,R.M., Brash,J.L., & Chang,P.L. Deterioration of polyamino acid-coated alginate microcapsules in vivo. *Journal of Biomaterials Science-Polymer Edition* **13**, 863-884 (2002).
157. Jork,A., Thurmer,F., Cramer,H., Zimmermann,G., Gessner,P., Hamel,K., Hofmann,G., Kuttler,B., Hahn,H.J., Josimovic-Alasevic,O., Fritsch,K.G., & Zimmermann,U. Biocompatible alginate from freshly collected *Laminaria pallida* for implantation. *Applied Microbiology and Biotechnology* **53**, 224-229 (2000).
158. Drury,J.L., Dennis,R.G., & Mooney,D.J. The tensile properties of alginate hydrogels. *Biomaterials* **25**, 3187-3199 (2004).
159. Wandrey,C., Espinosa,D., Rehor,A., & Hunkeler,D. Influence of alginate characteristics on the properties of multi-component microcapsules. *Journal of Microencapsulation* **20**, 597-611 (2003).

160. Quong,D., Neufeld,R.J., Skjak-Braek,G., & Poncelet,D. External versus internal source of calcium during the gelation of alginate beads for DNA encapsulation. *Biotechnology and Bioengineering* **57**, 438-446 (1998).
161. Strand,B.L., Morch,Y.A., & Skjak-Braek,G. Alginate as immobilization matrix for cells. *Minerva Biotechnologica* **12**, 223-233 (2000).
162. Thu,B., Bruheim,P., Espevik,T., Smidsrod,O., Soonshiong,P., & Skjakbraek,G. Alginate polycation microcapsules .2. Some functional properties. *Biomaterials* **17**, 1069-1079 (1996).
163. Smidsrod,O. & Skjakbraek,G. Alginate As Immobilization Matrix for Cells. *Trends in Biotechnology* **8**, 71-78 (1990).
164. Dusseault,J., Leblond,F.A., Robitaille,R., Jourdan,G., Tessier,J., Menard,M., Henley,N., & Halle,J.P. Microencapsulation of living cells in semi-permeable membranes with covalently cross-linked layers. *Biomaterials* **26**, 1515-1522 (2005).
165. Darrabie,M., Freeman,B.K., Kendall,W.F., Hobbs,H.A., & Opara,E.C. Durability of sodium sulfate-treated polylysine-alginate microcapsules. *Journal of Biomedical Materials Research* **54**, 396-399 (2001).
166. O Shea,G.M. & Sun,A.M. Encapsulation of Rat Islets of Langerhans Prolongs Xenograft Survival in Diabetic Mice. *Diabetes* **35**, 943-946 (1986).
167. Haque,T., Chen,H., Ouyang,W., Martoni,C., Lawuyi,B., Urbanska,A., & Prakash,S. Investigation of a new microcapsule membrane combining alginate, chitosan, polyethylene glycol and poly-L-lysine for cell transplantation applications. *International Journal of Artificial Organs* **28**, 631-637 (2005).
168. Silva,A.I., de Matos,A.N., Brons,I.G., & Mateus,M. An overview on the development of a bio-artificial pancreas as a treatment of insulin-dependent diabetes mellitus. *Medicinal Research Reviews* **26**, 181-222 (2006).
169. Lee,C.H., Wang,Y.J., Kuo,S.M., & Chang,S.J. Microencapsulation of parathyroid tissue with photosensitive poly(L-lysine) and short chain alginate-co-MPEG. *Artificial Organs* **28**, 537-542 (2004).
170. Okada,N., Miyamoto,H., Yoshioka,T., Katsume,A., Saito,H., Yorozu,K., Ueda,O., Itoh,N., Mizuguchi,H., Nakagawa,S., Ohsugi,Y., & Mayumi,T. Cytomedical therapy for IgG1 plasmacytosis in human interleukin-6 transgenic mice using hybridoma cells microencapsulated in alginate-poly(L)lysine-alginate membrane. *Biochimica et Biophysica Acta-Molecular Basis of Disease* **1360**, 53-63 (1997).
171. Strand,B.L., Ryan,L., Veld,P.I., Kulseng,B., Rokstad,A.M., Skjak-Braek,G., & Espevik,T. Poly-L-lysine induces fibrosis on alginate microcapsules via the induction of cytokines. *Cell Transplantation* **10**, 263-275 (2001).

172. Toso,C. Effect of microcapsule composition and short-term immunosuppression on intraportal biocompatibility. *Cell Transplantation* **14**, 159-167 (2005).
173. King,A., Sandler,S., & Andersson,A. The effect of host factors and capsule composition on the cellular overgrowth on implanted alginate capsules. *Journal of Biomedical Materials Research* **57**, 374-383 (2001).
174. Robitaille,R., Dusseault,J., Henley,N., Desbiens,K., Labrecque,N., & Halle,J.P. Inflammatory response to peritoneal implantation of alginate-poly-L-lysine microcapsules. *Biomaterials* **26**, 4119-4127 (2005).
175. Shimi,S.M., Newman,E.L., Hopwood,D., & Cushieri,A. Semi-Permeable Microcapsules for Cell-Culture - Ultra-Structural Characterization. *Journal of Microencapsulation* **8**, 307-316 (1991).
176. Wang,X.H., Li,D.P., Wang,W.J., Feng,Q.L., Cui,F.Z., Xu,Y.X., & Song,X.H. Covalent immobilization of chitosan and heparin on PLGA surface. *International Journal of Biological Macromolecules* **33**, 95-100 (2003).
177. Juste,S. Effect of poly-L-lysine coating on macrophage activation by alginate-based microcapsules: Assessment using a new in vitro method. *Journal of biomedical materials research. Part A* **72A**, 389-398 (2005).
178. Tam,S.K., Dusseault,J., Polizu,S., Menard,M., Halle,J.P., & Yahia,L. Physicochemical model of alginate-poly-L-lysine microcapsules defined at the micrometric/nanometric scale using ATR-FTIR, XPS, and ToF-SIMS. *Biomaterials* **26**, 6950-6961 (2005).
179. Strand,B.L., Morch,Y.A., Espevik,T., & Skjak-Braek,G. Visualization of alginate-poly-L-lysine-alginate microcapsules by confocal laser scanning microscopy. *Biotechnology and Bioengineering* **82**, 386-394 (2003).
180. Germain,M., Balaguer,P., Nicolas,J.C., Lopez,F., Esteve,J.P., Sukhorukov,G.B., Winterhalter,M., Richard-Foy,H., & Fournier,D. Protection of mammalian cell used in biosensors by coating with a polyelectrolyte shell. *Biosensors and Bioelectronics* **In Press, Corrected Proof**, (2005).
181. De Vos,P., van Hoogmoed,C.G., De Haan,B.J., & Busscher,H.J. Tissue responses against immunisolating alginate-PLL capsules in the immediate posttransplant period. *Journal of Biomedical Materials Research* **62**, 430-437 (2002).
182. De Vos,P., De Haan,B., & Van Schilfgaarde,R. Effect of the alginate composition on the biocompatibility of alginate-polylysine microcapsules. *Biomaterials* **18**, 273-278 (1997).
183. Godlewska,E., Sitarek,E., Iwanska,M., & Orłowski,T. In vitro activation of mice splenocytes by free and encapsulated rat islets and by components of capsular wall. *Transplantation Proceedings* **34**, 659-660 (2002).

184. Hsu,B.R.S., Fu,S.H., Tsai,J.S., Huang,Y.Y., Huang,H.S., & Chang,K.S.S. The plasminogen-plasmin fibrinolytic system accelerates degradation of alginate-poly-L-lysine-alginate microcapsules in vitro. *Transplantation Proceedings* **29**, 1877-1880 (1997).
185. Kobayashi,T., Harb,G., & Rayat,G.R. Prolonged survival of microencapsulated neonatal porcine islets in mice treated with a combination of anti-CD154 and anti-LFA-1 monoclonal antibodies. *Transplantation* **80**, 821-827 (2005).
186. Quong,D. DNA encapsulation within co-guanidine membrane coated alginate beads and protection from extracapsular nuclease. *Journal of Microencapsulation* **16**, 573-585 (1999).
187. Goosen,M.F.A., King,G.A., Mcknight,C.A., & Marcotte,N. Animal-Cell Culture Engineering Using Alginate Polycation Microcapsules of Controlled Membrane Molecular-Weight Cutoffs. *Journal of Membrane Science* **41**, 323-343 (1989).
188. Vandebossche,G.M.R., Vanoostveldt,P., Demeester,J., & Remon,J.P. The Molecular-Weight Cutoff of Microcapsules Is Determined by the Reaction Between Alginate and Polylysine. *Biotechnology and Bioengineering* **42**, 381-386 (1993).
189. Awrey,D.E., Tse,M., Hortelano,G., & Chang,P.L. Permeability of alginate microcapsules to secretory recombinant gene products. *Biotechnology and Bioengineering* **52**, 472-484 (1996).
190. Brissova,M., Petro,M., Lacik,I., Powers,A.C., & Wang,T. Evaluation of microcapsule permeability via inverse size exclusion chromatography. *Analytical Biochemistry* **242**, 104-111 (1996).
191. Qi,W., Ma,J., Liu,Y., Liu,X., Xiong,Y., Xie,Y., & Ma,X. Insight into permeability of protein through microcapsule membranes. *Journal of Membrane Science* **269**, 126-132 (2006).
192. Rokstad,A.M., Kulseng,B., Strand,B.L., Skjak-Braek,G., & Espevik,T. Transplantation of alginate microcapsules with proliferating cells in mice - Capsular overgrowth and survival of encapsulated cells of mice and human origin. *Bioartificial Organs Iii: Tissue Sourcing, Immunoisolation, and Clinical Trials* **944**, 216-225 (2001).
193. Sakai,S., Ono,T., Ijima,I., & Kawakami,K. Alginate/aminopropyl-silicate/alginate membrane immunoisolatability and insulin secretion of encapsulated islets. *Biotechnology progress* **18**, 401-403 (2002).
194. Sakai,S., Ono,T., Ijima,H., & Kawakami,K. In vitro and in vivo evaluation of alginate/sol-gel synthesized aminopropyl-silicate/alginate membrane for bioartificial pancreas. *Biomaterials* **23**, 4177-4183 (2002).

195. Coradin, T., Mercey, E., Lisnard, L., & Livage, J. Design of silica-coated microcapsules for bioencapsulation. *Chemical Communications* 2496-2497 (2001).
196. Sawhney, A.S. & Hubbell, J.A. Poly(ethylene oxide)-graft-poly(L-lysine) copolymers to enhance the biocompatibility of poly(L-lysine)-alginate microcapsule membranes. *Biomaterials* **13**, 863-870 (1992).
197. Sawhney, A.S., Pathak, C.P., & Hubbell, J.A. Interfacial photopolymerization of poly(ethylene glycol)-based hydrogels upon alginate-poly(L-lysine) microcapsules for enhanced biocompatibility. *Biomaterials* **14**, 1008-1016 (1993).
198. Chen, J.P., Chu, I.M., Shiao, M.Y., Hsu, B.R.S., & Fu, S.H. Microencapsulation of islets in PEG-amine modified alginate-poly(L-lysine)-alginate microcapsules for constructing bioartificial pancreas. *Journal of Fermentation and Bioengineering* **86**, 185-190 (1998).
199. Wang, S.B. Effect of the molecular weights of poly-L-arginine on membrane strength and permeability of poly-L-arginine group microcapsules. *Macromolecular bioscience* **3**, 347-350 (2003).
200. Wang, S.B. Novel alginate-poly(L-histidine) microcapsules as drug carriers: In vitro protein release and short term stability. *Macromolecular bioscience* **5**, 408-414 (2005).
201. Thanos, C.G., Bintz, B.E., Bell, W.J., Qian, H., Schneider, P.A., MacArthur, D.H., & Emerich, D.F. Intraperitoneal stability of alginate-polyornithine microcapsules in rats: An FTIR and SEM analysis. *Biomaterials* **27**, 3570-3579 (2006).
202. De Vos, P., De Haan, B.J., Wolters, G.H., Strubbe, J.H., & Van Schilfgaarde, R. Improved biocompatibility but limited graft survival after purification of alginate for microencapsulation of pancreatic islets. *Diabetologia* **40**, 262-270 (1997).
203. Bunger, C.M., Gerlach, C., Freier, T., Schmitz, K.P., Pilz, M., Werner, C., Jonas, L., Schareck, W., Hopt, U.T., & De Vos, P. Biocompatibility and surface structure of chemically modified immunoisolating alginate-PLL capsules. *Journal of Biomedical Materials Research Part A* **67A**, 1219-1227 (2003).
204. Wei, O.Y. Artificial cell microcapsule for oral delivery of live bacterial cells for therapy: design, preparation, and in-vitro characterization. *Journal of pharmacy & pharmaceutical sciences* **7**, 315-324 (2004).
205. Haque, T., Chen, H., Ouyang, W., Martoni, C., Lawuyi, B., Urbanska, A.M., & Prakash, S. Superior Cell Delivery Features of Poly(ethylene glycol) Incorporated Alginate, Chitosan, and Poly-L-lysine Microcapsules. *Mol. Pharm* **2**, 29-36 (2005).
206. Jung, T., Kamm, W., Breitenbach, A., Kaiserling, E., Xiao, J.X., & Kissel, T. Biodegradable nanoparticles for oral delivery of peptides: is there a role for

- polymers to affect mucosal uptake? *European Journal of Pharmaceutics and Biopharmaceutics* **50**, 147-160 (2000).
207. Xiao,C.M. & Zhou,L.C. Chemical modification of the surface of calcium alginate gel beads. *Chinese Journal of Polymer Science* **22**, 183-186 (2004).
  208. Lee,C.S. & Chu,I.M. Characterization of modified alginate-poly-L-lysine microcapsules. *Artif. Organs* **21**, 1002-1006 (1997).
  209. Breguet,W., Gugerli,R., Perneti,M., von Stockar,U., & Marison,I.W. Formation of microcapsules from polyelectrolyte and covalent interactions. *Langmuir* **21**, 9764-9772 (2005).
  210. Shen,F., Li,A.A.H., Cornelius,R.M., Cirone,P., Childs,R.F., Brash,J.L., & Chang,P.L. Biological properties of photocrosslinked alginate microcapsules. *Journal of Biomedical Materials Research Part B-Applied Biomaterials* **75B**, 425-434 (2005).
  211. Khor,E. Chitin : fulfilling a biomaterials promise / Eugene Khor. (Amsterdam ; New York : Elsevier Science Ltd.,2001).
  212. Muzzarelli,R.A.A. & Muzzarelli,C. Chitosan chemistry: Relevance to the biomedical sciences. *Polysaccharides 1: Structure, Characterization and Use* **186**, 151-209 (2005).
  213. Singla,A.K. & Chawla,M. Chitosan: some pharmaceutical and biological aspects - an update. *Journal of Pharmacy and Pharmacology* **53**, 1047-1067 (2001).
  214. Sinha,V.R. Chitosan microspheres as a potential carrier for drugs. *International Journal of Pharmaceutics* **274**, 1-33 (2004).
  215. Koide,S.S. Chitin-chitosan: Properties, benefits and risks. *Nutrition Research* **18**, 1091-1101 (1998).
  216. De Rosa,M., Carteni,M., Petillo,O., Calarco,A., Margarucci,S., Rosso,F., De Rosa,A., Farina,E., Grippo,P., & Peluso,G. Cationic polyelectrolyte hydrogel fosters fibroblast spreading, proliferation, and extracellular matrix production: Implications for tissue engineering. *Journal of Cellular Physiology* **198**, 133-143 (2004).
  217. Mao,J.S., Cui,Y.L., Wang,X.H., Sun,Y., Yin,Y.J., Zhao,H.M., & De Yao,K. A preliminary study on chitosan and gelatin polyelectrolyte complex cytocompatibility by cell cycle and apoptosis analysis. *Biomaterials* **25**, 3973-3981 (2004).
  218. Risbud,H., Hardikar,A., & Bhonde,R. Chitosan-polyvinyl pyrrolidone hydrogels as candidate for islet immunoisolation: In vitro biocompatibility evaluation. *Cell Transplantation* **9**, 25-31 (2000).

219. Risbud,M., Bhonde,M., & Bhonde,R. Chitosan-polyvinyl pyrrolidone hydrogel does not activate macrophages: Potentials for transplantation applications. *Cell Transplantation* **10**, 195-202 (2001).
220. Chenite,A., Chaput,C., Wang,D., Combes,C., Buschmann,M.D., Hoemann,C.D., Leroux,J.C., Atkinson,B.L., Binette,F., & Selmani,A. Novel injectable neutral solutions of chitosan form biodegradable gels in situ. *Biomaterials* **21**, 2155-2161 (2000).
221. Li,J.L., Pan,J.L., Zhang,L.G., Guo,X.J., & Yu,Y.T. Culture of primary rat hepatocytes within porous chitosan scaffolds. *Journal of Biomedical Materials Research Part A* **67A**, 938-943 (2003).
222. Pan,J.L., Bao,Z.M., Li,J.L., Zhang,L.G., Wu,C., & Yu,Y.T. Chitosan-based scaffolds for hepatocyte culture. *Asbm6: Advanced Biomaterials Vi* **288-289**, 91-94 (2005).
223. Risbud,M.V., Bhonde,M.R., & Bhonde,R.R. Effect of chitosan-polyvinyl pyrrolidone hydrogel on proliferation and cytokine expression of endothelial cells: Implications in islet immunoisolation. *Journal of Biomedical Materials Research* **57**, 300-305 (2001).
224. Wang,Y.C., Kao,S.H., & Hsieh,H.J. A chemical surface modification of chitosan by glycoconjugates to enhance the cell-biomaterial interaction. *Biomacromolecules* **4**, 224-231 (2003).
225. Zhu,J.H., Wang,X.W., Ng,S., Quek,C.H., Ho,H.T., Lao,X.J., & Yu,H. Encapsulating live cells with water-soluble chitosan in physiological conditions. *Journal of biotechnology* **117**, 355-365 (2005).
226. Zielinski,B.A. & Aebischer,P. Chitosan As A Matrix for Mammalian-Cell Encapsulation. *Biomaterials* **15**, 1049-1056 (1994).
227. Sashiwa,H., Kawasaki,N., Nakayama,A., Muraki,E., Yajima,H., Yamamori,N., Ichinose,Y., Sunamoto,J., & Aiba,S. Chemical modification of chitosan. Part 15: Synthesis of novel chitosan derivatives by substitution of hydrophilic amine using N-carboxyethylchitosan ethyl ester as an intermediate. *Carbohydrate Research* **338**, 557-561 (2003).
228. Kubota,N., Tatsumoto,N., Sano,T., & Toya,K. A simple preparation of half N-acetylated chitosan highly soluble in water and aqueous organic solvents. *Carbohydrate Research* **324**, 268-274 (2000).
229. Shi,X.W., Du,Y.M., Sun,L.P., Zhang,B.Z., & Dou,A. Pnlvelectrolvt complex beads composed of water-soluble chitosan/alginate: Characterization and their protein release behavior. *Journal of Applied Polymer Science* **100**, 4614-4622 (2006).

230. Zeng,R., Fu,H., & Zhao,Y.F. Synthesis of novel biomimetic Zwitterionic phosphorylcholine-bound chitosan derivative. *Macromolecular Rapid Communications* **27**, 548-552 (2006).
231. Holappa,J., Nevalainen,T., Soininen,P., Masson,M., & Jarvinen,T. Synthesis of novel quaternary chitosan derivatives via N-chloroacyl-6-O-triphenylmethylchitosans. *Biomacromolecules* **7**, 407-410 (2006).
232. Bartkowiak,A. & Hunkeler,D. New microcapsules based on oligoelectrolyte complexation. *Bioartificial Organs II: Technology, Medicine, and Materials* **875**, 36-45 (1999).
233. Lee,J.S., Cha,D.S., & Park,H.J. Survival of freeze-dried *Lactobacillus bulgaricus* KFRI 673 in chitosan-coated calcium alginate microparticles. *Journal of Agricultural and Food Chemistry* **52**, 7300-7305 (2004).
234. Shu,X.Z. & Zhu,K.J. The release behavior of brilliant blue from calcium-alginate gel beads coated by chitosan: the preparation method effect. *European Journal of Pharmaceutics and Biopharmaceutics* **53**, 193-201 (2002).
235. Gaserod,O., Sannes,A., & Skjak-Braek,G. Microcapsules of alginate-chitosan. II. A study of capsule stability and permeability. *Biomaterials* **20**, 773-783 (1999).
236. Bartkowiak,A. & Hunkeler,D. Alginate-oligochitosan microcapsules: A mechanistic study relating membrane and capsule properties to reaction conditions. *Chemistry of Materials* **11**, 2486-2492 (1999).
237. Yan,X.L., Khor,E., & Lim,L.Y. Chitosan-alginate films prepared with chitosans of different molecular weights. *Journal of Biomedical Materials Research* **58**, 358-365 (2001).
238. Cruz,M.C.P., Ravagnani,S.P., Brogna,F.M.S., Campana,S.P., Trivino,G.C., Lisboa,A.C.L., & Mei,L.H.I. Evaluation of the diffusion coefficient for controlled release of oxytetracycline from alginate/chitosan/poly(ethylene glycol) microbeads in simulated gastrointestinal environments. *Biotechnology and Applied Biochemistry* **40**, 243-253 (2004).
239. Chen,H., Ouyang,W., Lawuyi,B., Martoni,C., & Prakash,S. Reaction of chitosan with genipin and its fluorogenic attributes for potential microcapsule membrane characterization. *Journal of Biomedical Materials Research Part A* **75A**, 917-927 (2005).
240. Chen,H., Ouyang,W., Lawuyi,B., Halim,T., & Prakash,S. A new method for microcapsule characterization: fluorogenic genipin can be used to characterize polymeric microcapsule membranes. *Applied Biochemistry and Biotechnology* (in press) (2006).

241. Ma,X.J., Vacek,I., & Sun,A. Generation of Alginate-Poly-L-Lysine-Alginate (APA) Biomicroscopies - the Relationship Between the Membrane Strength and the Reaction Conditions. *Artificial Cells Blood Substitutes and Immobilization Biotechnology* **22**, 43-69 (1994).
242. Thu,B., Bruheim,P., Espevik,T., Smidsrod,O., Soonshiong,P., & Skjakbraek,G. Alginate polycation microcapsules .1. Interaction between alginate and polycation. *Biomaterials* **17**, 1031-1040 (1996).
243. Bartkowiak,A. & Hunkeler,D. Alginate-oligochitosan microcapsules. II. Control of mechanical resistance and permeability of the membrane. *Chemistry of Materials* **12**, 206-212 (2000).
244. Hugerth,A., Caram-Lelham,N., & Sundelof,L.O. The effect of charge density and conformation on the polyelectrolyte complex formation between carrageenan and chitosan. *Carbohydrate Polymers* **34**, 149-156 (1997).
245. Chen,S.C., Wu,Y.C., Mi,F.L., Lin,Y.H., Yu,L.C., & Sung,H.W. A novel pH-sensitive hydrogel composed of N,O-carboxymethyl chitosan and alginate cross-linked by genipin for protein drug delivery. *Journal of Controlled Release* **96**, 285-300 (2004).
246. Dastan,T. & Turan,K. In vitro characterization and delivery of chitosan-DNA microparticles into mammalian cells. *Journal of Pharmacy and Pharmaceutical Sciences* **7**, 205-214 (2004).
247. Kovacs-Nolan,J. & Mine,Y. Microencapsulation for the gastric passage and controlled intestinal release of immunoglobulin Y. *Journal of Immunological Methods* **296**, 199-209 (2005).
248. Yin,C., Chia,S.M., Quek,C.H., Yu,H.R., Zhuo,R.X., Leong,K.W., & Mao,H.Q. Microcapsules with improved mechanical stability for hepatocyte culture. *Biomaterials* **24**, 1771-1780 (2003).
249. Quek,C.H., Li,J., Sun,T., Ling,M., Chan,H., Mao,H.Q., Gan,L.M., Leong,K.W., & Yu,H. Photo-crosslinkable microcapsules formed by polyelectrolyte copolymer and modified collagen for rat hepatocyte encapsulation. *Biomaterials* **25**, 3531-3540 (2004).
250. Chia,S.M., Wan,A.C.A., Quek,C.H., Mao,H.Q., Xu,X., Shen,L., Ng,M.L., Leong,K.W., & Yu,H. Multi-layered microcapsules for cell encapsulation. *Biomaterials* **23**, 849-856 (2002).
251. Orive,G., Hernandez,R.M., Gascon,A.R., Igartua,M., & Pedraz,J.L. Development and optimisation of alginate-PMCG-alginate microcapsules for cell immobilisation. *International Journal of Pharmaceutics* **259**, 57-68 (2003).

252. Lacik,I., Brissova,M., Anilkumar,A.V., Powers,A.C., & Wang,T. New capsule with tailored properties for the encapsulation of living cells. *Journal of Biomedical Materials Research* **39**, 52-60 (1998).
253. Bartkowiak,A., Canaple,L., Ceausoglu,I., Nurdin,N., Renken,A., Rindisbacher,L., Wandrey,C., Desvergne,B., & Hunkeler,D. New multicomponent capsules for immunoisolation. *Bioartificial Organs II: Technology, Medicine, and Materials* **875**, 135-145 (1999).
254. Bucko,M. Immobilization of a whole-cell epoxide-hydrolyzing biocatalyst in sodium alginate-cellulose sulfate-poly(methylene-co-guanidine) capsules using a controlled encapsulation process. *Enzyme and Microbial Technology* **36**, 118-126 (2005).
255. Bucko,M., Vikartovska,A., Gemeiner,P., Lacik,I., Kollarikova,G., & Marison,I.W. *Nocardia tartaricans* cells immobilized in sodium alginate-cellulose sulfate-poly(methylene-co-guanidine) capsules: mechanical resistance and operational stability. *Journal of Chemical Technology and Biotechnology* **81**, 500-504 (2006).
256. Dautzenberg,H., Schuldt,U., Grasnack,G., Karle,P., Muller,P., Lohr,M., Pelegri,M., Piechaczyk,M., Rombs,K.V., Gunzburg,W.H., Salmons,B., & Saller,R.M. Development of cellulose sulfate-based polyelectrolyte complex microcapsules for medical applications. *Bioartificial Organs II: Technology, Medicine, and Materials* **875**, 46-63 (1999).
257. Dautzenberg,H., Schuldt,U., Lerche,D., Woehlecke,H., & Ehwald,R. Size exclusion properties of polyelectrolyte complex microcapsules prepared from sodium cellulose sulphate and poly[diallyldimethylammonium chloride]. *Journal of Membrane Science* **162**, 165-171 (1999).
258. Zhang,J., Yao,S.J., & Guan,Y.X. Preparation of macroporous sodium cellulose sulphate/poly(dimethyldiallylammonium chloride) capsules and their characteristics. *Journal of Membrane Science* **255**, 89-98 (2005).
259. Boninsegna,S., Bosetti,P., Carturan,G., Dellagiacoia,G., Dal Monte,R., & Rossi,M. Encapsulation of individual pancreatic islets by sol-gel SiO<sub>2</sub>: A novel procedure for perspective cellular grafts. *Journal of biotechnology* **100**, 277-286 (2003).
260. Desai,T.A., West,T., Cohen,M., Boiarski,T., & Rampersaud,A. Nanoporous microsystems for islet cell replacement. *Advanced Drug Delivery Reviews* **56**, 1661-1673 (2004).
261. Hennink,W.E. & van Nostrum,C.F. Novel crosslinking methods to design hydrogels. *Advanced Drug Delivery Reviews* **54**, 13-36 (2002).
262. Richert,L., Boulmedais,F., Lavallo,P., Mutterer,J., Ferreux,E., Decher,G., Schaaf,P., Voegel,J.C., & Picart,C. Improvement of stability and cell adhesion properties of polyelectrolyte multilayer films by chemical cross-linking. *Biomacromolecules* **5**, 284-294 (2004).

263. Kumbar,S.G., Kulkarni,A.R., & Aminabhavi,T.M. Crosslinked chitosan microspheres for encapsulation of diclofenac sodium: effect of crosslinking agent. *Journal of Microencapsulation* **19**, 173-180 (2002).
264. Kurillova,L., Gemeiner,P., Vikartovska,A., Mikova,H., Rosenberg,M., & Ilavsky,M. Calcium pectate gel beads for cell entrapment. 6. Morphology of stabilized and hardened calcium pectate gel beads with cells for immobilized biotechnology. *Journal of Microencapsulation* **17**, 279-296 (2000).
265. Marchais,H. Cross-linking of hard gelatin carbamazepine capsules: effect of dissolution conditions on in vitro drug release. *European journal of pharmaceutical sciences* **19**, 129-132 (2003).
266. Meyer,M.C. The effect of gelatin cross-linking on the bioequivalence of hard and soft gelatin acetaminophen capsules. *Pharmaceutical research* **17**, 962-966 (2000).
267. Ofner,C.M. Crosslinking studies in gelatin capsules treated with formaldehyde and in capsules exposed to elevated temperature and humidity. *Journal of Pharmaceutical Sciences* **90**, 79-88 (2001).
268. Zhang,Y.J., Guan,Y., & Zhou,S.Q. Single component chitosan hydrogel microcapsule from a layer-by-layer approach. *Biomacromolecules* **6**, 2365-2369 (2005).
269. Cruise,G.M., Hegre,O.D., Lamberti,F.V., Hager,S.R., Hill,R., Scharp,D.S., & Hubbell,J.A. In vitro and in vivo performance of porcine islets encapsulated in interfacially photopolymerized poly(ethylene glycol) diacrylate membranes. *Cell Transplantation* **8**, 293-306 (1999).
270. Wang,M.S., Childs,R.F., & Chang,P.L. A novel method to enhance the stability of alginate-poly-L-lysine-alginate microcapsules. *Journal of Biomaterials Science-Polymer Edition* **16**, 91-113 (2005).
271. Lu,M.Z., Lan,H.L., Wang,F.F., & Wang,Y.J. A novel cell encapsulation method using photosensitive poly(allylamine alpha-cyanocinnamylideneacetate). *Journal of Microencapsulation* **17**, 245-251 (2000).
272. Lee,K.Y., Bouhadir,K.H., & Mooney,D.J. Controlled degradation of hydrogels using multi-functional cross-linking molecules. *Biomaterials* **25**, 2461-2466 (2004).
273. Srivastava,R., Brown,J.Q., Zhu,H.G., & McShane,M.J. Stabilization of glucose oxidase in alginate microspheres with photoreactive diazoresin nanofilm coatings. *Biotechnology and Bioengineering* **91**, 124-131 (2005).
274. Pastoriza-Santos,I. Core-shell colloids and hollow polyelectrolyte capsules based on diazoresins. *Advanced functional materials* **11**, 122-128 (2001).

275. Cellesi, F. Towards a fully synthetic substitute of alginate: Optimization of a thermal gelation/chemical cross-linking scheme ("Tandem" gelation) for the production of beads and liquid-core capsules. *Biotechnology and Bioengineering* **88**, 740-749 (2004).
276. Dobashi, T., Furukawa, T., Ichikawa, K., & Narita, T. Coupling of chemical cross-linking, swelling, and phase separation in microencapsulation. *Langmuir* **18**, 6031-6034 (2002).
277. Qiu, B. A hydrogel prepared by in situ cross-linking of a thiol-containing poly(ethylene glycol)-based copolymer: a new biomaterial for protein drug delivery. *Biomaterials* **24**, 11-18 (2003).
278. Nishi, C., Nakajima, N., & Ikada, Y. In-Vitro Evaluation of Cytotoxicity of Diepoxy Compounds Used for Biomaterial Modification. *Journal of Biomedical Materials Research* **29**, 829-834 (1995).
279. Sung, H. W., Huang, D. M., Chang, W. H., Huang, R. N., & Hsu, J. C. Evaluation of gelatin hydrogel crosslinked with various crosslinking agents as bioadhesives: In vitro study. *Journal of Biomedical Materials Research* **46**, 520-530 (1999).
280. Friess, W. Collagen - biomaterial for drug delivery. *European Journal of Pharmaceutics and Biopharmaceutics* **45**, 113-136 (1998).
281. Sung, H. W., Liang, I. L., Chen, C. N., Huang, R. N., & Liang, H. F. Stability of a biological tissue fixed with a naturally occurring crosslinking agent (genipin). *Journal of Biomedical Materials Research* **55**, 538-546 (2001).
282. Djerassi, C., Gray, J. D., & Kincl, F. A. Naturally Occurring Oxygen Heterocyclics .9. Isolation and Characterization of Genipin. *Journal of Organic Chemistry* **25**, 2174-2177 (1960).
283. Imanishi, Y. Herb medicine Inchin-ko-to (TJ-135) regulates PDGF-BB-dependent signaling pathways of hepatic stellate cells in primary culture and attenuates development of liver fibrosis induced by thioacetamide administration in rats. *Journal of hepatology* **41**, 242-250 (2004).
284. Koo, H. J. Antiinflammatory effects of genipin, an active principle of gardenia. *European journal of pharmacology* **495**, 201-208 (2004).
285. Sakaida, I. Herbal medicine inchin-ko-to (TJ-135) prevents liver fibrosis and enzyme-altered lesions in rat liver cirrhosis induced by a cholinedeficient (L)-amino acid-defined diet. *Journal of hepatology* **38**, 762-769 (2003).
286. Shoda, J. Genipin enhances Mrp2 (Abcc2)-mediated bile formation and organic anion transport in rat liver. *Hepatology* **39**, 167-178 (2004).

287. Yamazaki,M., Chiba,K., Mohri,T., & Hatanaka,H. Cyclic GMP-dependent neurite outgrowth by genipin and nerve growth factor in PC12h cells. *European journal of pharmacology* **488**, 35-43 (2004).
288. Park,J.E. Isolation and characterization of water-soluble intermediates of blue pigments transformed from geniposide of *Gardenia jasminoides*. *Journal of Agricultural and Food Chemistry* **50**, 6511-6514 (2002).
289. Touyama,R., Takeda,Y., Inoue,K., Kawamura,I., Yatsuzuka,M., Ikumoto,T., Shingu,T., Yokoi,T., & Inouye,H. Studies on the Blue Pigments Produced from Genipin and Methylamine .1. Structures of the Brownish-Red Pigments, Intermediates Leading to the Blue Pigments. *Chemical & Pharmaceutical Bulletin* **42**, 668-673 (1994).
290. Sung,H.W., Huang,R.N., Huang,L.L.H., Tsai,C.C., & Chiu,C.T. Feasibility study of a natural crosslinking reagent for biological tissue fixation. *Journal of Biomedical Materials Research* **42**, 560-567 (1998).
291. Mi,F.L., Sung,H.W., & Shyu,S.S. Synthesis and characterization of a novel chitosan-based network prepared using naturally occurring crosslinker. *Journal of Polymer Science Part A-Polymer Chemistry* **38**, 2804-2814 (2000).
292. Mi,F.L., Shyu,S.S., & Peng,C.K. Characterization of ring-opening polymerization of genipin and pH-dependent cross-linking reactions between chitosan and genipin. *Journal of Polymer Science Part A-Polymer Chemistry* **43**, 1985-2000 (2005).
293. Huang,L.L.H., Sung,H.W., Tsai,C.C., & Huang,D.M. Biocompatibility study of a biological tissue fixed with a naturally occurring crosslinking reagent. *Journal of Biomedical Materials Research* **42**, 568-576 (1998).
294. Liu,B.S., Yao,C.H., Chen,Y.S., & Hsu,S.H. In vitro evaluation of degradation and cytotoxicity of a novel composite as a bone substitute. *Journal of Biomedical Materials Research Part A* **67A**, 1163-1169 (2003).
295. Sung,H.W., Huang,R.N., Huang,L.L.H., & Tsai,C.C. In vitro evaluation of cytotoxicity of a naturally occurring cross-linking reagent for biological tissue fixation. *Journal of Biomaterials Science-Polymer Edition* **10**, 63-78 (1999).
296. Butler,M.F., Ng,Y.F., & Pudney,P.D.A. Mechanism and kinetics of the crosslinking reaction between biopolymers containing primary amine groups and genipin. *Journal of Polymer Science Part A-Polymer Chemistry* **41**, 3941-3953 (2003).
297. Sung,H.W., Chang,W.H., Ma,C.-Y., & Lee,M.-H. Crosslinking of biological tissues using genipin and/or carbodiimide. *Journal of Biomedical Materials Research* **64A**, 427-438 (2003).
298. Bigi,A., Cojazzi,G., Panzavolta,S., Roveri,N., & Rubini,K. Stabilization of gelatin films by crosslinking with genipin. *Biomaterials* **23**, 4827-4832 (2002).

299. Jin,J., Song,M., & Hourston,D.J. Novel chitosan-based films cross-linked by genipin with improved physical properties. *Biomacromolecules* **5**, 162-168 (2004).
300. Chang,Y., Liang,H.C., Wei,H.J., Chu,C.P., & Sung,H.W. Tissue regeneration patterns in acellular bovine pericardium implanted in a canine model as a vascular patch. *Journal of Biomedical Materials Research Part A* **69A**, 323-333 (2004).
301. Chen,Y.S., Chang,J.Y., Cheng,C.Y., Tsai,F.J., Yao,C.H., & Liu,B.S. An in vivo evaluation of a biodegradable genipin-cross-linked gelatin peripheral nerve guide conduit material. *Biomaterials* **26**, 3911-3918 (2005).
302. Mwale,F., Iordanova,M., Demers,C.N., Steffen,T., Roughley,P., & Antoniou,J. Biological evaluation of chitosan salts cross-linked to genipin as a cell scaffold for disk tissue engineering. *Tissue Engineering* **11**, 130-140 (2005).
303. Yao,C.H., Liu,B.S., Hsu,S.H., & Chen,Y.S. Calvarial bone response to a tricalcium phosphate-genipin crosslinked gelatin composite. *Biomaterials* **26**, 3065-3074 (2005).
304. Mi,F.L. Synthesis and characterization of a novel chitosan-gelatin bioconjugate with fluorescence emission. *Biomacromolecules* **6**, 975-987 (2005).
305. Ko,C.S. Immobilized cells biocatalyst for the production of S-acetylthio-2-methyl propionic acid. *Enzyme and Microbial Technology* **35**, 619-623 (2004).
306. Chen,H.M., Ouyang,W., Lawuyi,B., & Prakash,S. Genipin cross-linked alginate-chitosan microcapsules: Membrane characterization and optimization of cross-linking reaction. *Biomacromolecules* **7**, 2091-2098 (2006).
307. Orive,G., Hernandez,R.M., Gascon,A.R., Igartua,M., & Pedraz,J.L. Survival of different cell lines in alginate-agarose microcapsules. *European journal of pharmaceutical sciences* **18**, 23-30 (2003).
308. Brissova,M., Lacik,I., Powers,A.C., Anilkumar,A.V., & Wang,T. Control and measurement of permeability for design of microcapsule cell delivery system. *Journal of Biomedical Materials Research* **39**, 61-70 (1998).
309. Nurdin,N., Canaple,L., Bartkowiak,A., Desvergne,B., & Hunkeler,D. Capsule permeability via polymer and protein ingress/egress. *Journal of Applied Polymer Science* **75**, 1165-1175 (2000).
310. Grigorescu,G., Rehor,A., & Hunkeler,D. Polyvinylamine hydrochloride-based microcapsules: polymer synthesis, permeability and mechanical properties. *Journal of Microencapsulation* **19**, 245-259 (2002).
311. Yao,S.J., Guan,Y.X., & Lin,D.Q. Mass transfer behavior of solutes in NaCS-PDMAAC capsules. *Industrial & Engineering Chemistry Research* **45**, 1811-1816 (2006).

312. Mei,L.H. & Yao,S.J. Cultivation and modelling of encapsulated *Saccharomyces cerevisiae* in NaCS-PDMDAAC polyelectrolyte complexes. *Journal of Microencapsulation* **19**, 397-405 (2002).
313. Merrett,K., Cornelius,R.M., McClung,W.G., Unsworth,L.D., & Sheardown,H. Surface analysis methods for characterizing polymeric biomaterials. *Journal of Biomaterials Science-Polymer Edition* **13**, 593-621 (2002).
314. Chen,Y.Q., Sun,D.X., Su,J., & Yang,J. Theoretical calculation and experiments of diameter of calcium alginate gel microspheres. *Chemical Journal of Chinese Universities-Chinese* **24**, 481-484 (2003).
315. Su,J.F. Preparation and characterization of double-MF shell microPCMs used in building materials. *Journal of Applied Polymer Science* **97**, 1755-1762 (2005).
316. Maruyama,O., Yamane,T., Nishida,M., Aouidef,A., Tsutsui,T., Jikuya,T., & Masuzawa,T. Fractural characteristic evaluation of a microcapsule suspension using a rotational shear stressor. *Asaio Journal* **48**, 365-373 (2002).
317. Zimmermann,H., Hillgartner,M., Manz,B., Feilen,P., Brunnenmeier,F., Leinfelder,U., Weber,M., Cramer,H., Schneider,S., Hendrich,C., Volke,F., & Zimmermann,U. Fabrication of homogeneously cross-linked, functional alginate microcapsules validated by NMR-, CLSM- and AFM-imaging. *Biomaterials* **24**, 2083-2096 (2003).
318. Araki,T., Hitchcock,A.P., Shen,F., Chang,P.L., Wang,M., & Childs,R.F. Quantitative chemical mapping of sodium acrylate- and N-vinylpyrrolidone-enhanced alginate microcapsules. *Journal of Biomaterials Science-Polymer Edition* **16**, 611-627 (2005).
319. Kim,B.S. Effect of organic solvent on the permeability and stiffness of polyelectrolyte multilayer microcapsules. *Macromolecules* **38**, 5214-5222 (2005).
320. Lamprecht,A., Schafer,U.F., & Lehr,C.-M. Characterization of microcapsules by confocal laser scanning microscopy: structure, capsule wall composition and encapsulation rate. *European Journal of Pharmaceutics and Biopharmaceutics* **49**, 1-9 (2000).
321. Lamprecht,A., Schafer,U.F., & Lehr,C.-M. Visualization and quantification of polymer distribution in microcapsules by confocal laser scanning microscopy (CLSM). *International Journal of Pharmaceutics* **196**, 223-226 (2000).
322. Rahman,N.A. & Mathiowitz,E. Localization of bovine serum albumin in double-walled microspheres. *Journal of Controlled Release* **94**, 163-175 (2004).
323. Chen,H.M., Ouyang,W., Lawuyi,R., Lim,T., & Prakash,S. A new method for microcapsule characterization - Use of fluorogenic genipin to characterize polymeric

- microcapsule membranes. *Applied Biochemistry and Biotechnology* **134**, 207-221 (2006).
324. Fery,A., Dubreuil,F., & Mohwald,H. Mechanics of artificial microcapsules. *New Journal of Physics* **6**, (2004).
325. Sukhorukov,G.B., Fery,A., Brumen,M., & Mohwald,H. Physical chemistry of encapsulation and release. *Physical Chemistry Chemical Physics* **6**, 4078-4089 (2004).
326. Andrei,D.C., Briscoe,B.J., Luckham,P.F., & Williams,D.R. The deformation of microscopic gel particles. *Journal de Chimie Physique et de Physico-Chimie Biologique* **93**, 960-976 (1996).
327. Gauthier,M.A., Luo,J., Calvet,D., Ni,C., Zhu,X.X., Garon,M., & Buschmann,M.D. Degree of crosslinking and mechanical properties of crosslinked poly(vinyl alcohol) beads for use in solid-phase organic synthesis. *Polymer* **45**, 8201-8210 (2004).
328. Rosinski,S. Characterization of microcapsules: recommended methods based on round-robin testing. *Journal of Microencapsulation* **19**, 641-659 (2002).
329. Lebedeva,O.V. Mechanical properties of polyelectrolyte-filled multilayer microcapsules studied by atomic force and confocal microscopy. *Langmuir* **20**, 10685-10690 (2004).
330. Klemenz,A. Investigation of elasto-mechanical properties of alginate microcapsules by scanning acoustic microscopy. *Journal of Biomedical Materials Research* **65A**, 237-243 (2003).
331. Leblond,F.A. Quantitative method for the evaluation of biomicrocapsule resistance to mechanical stress. *Biomaterials* **17**, 2097-2102 (1996).
332. Van Raamsdonk,J.M. & Chang,P.L. Osmotic pressure test: A simple, quantitative method to assess the mechanical stability of alginate microcapsules. *Journal of Biomedical Materials Research* **54**, 264-271 (2001).
333. Schuldt,U. Characterization methods for microcapsules. *Minerva Biotechnologica* **12**, 249-264 (2000).
334. Rosinski,S., Lewinska,D., Wojcik,M., Orive,G., Pedraz,J.L., & Werynski,A. Mass transfer characteristics of poly-lysine, poly-ornithine and poly-methylene-co-guanidine membrane coated alginate microcapsules. *Journal of Membrane Science* **254**, 249-257 (2005).
335. Stewart,W.W. & Swaisgood,H.E. Characterization of Calcium Alginate Pore Diameter by Size-Exclusion Chromatography Using Protein Standards. *Enzyme and Microbial Technology* **15**, 922-927 (1993).

336. Coromili, V. & Chang, T.M.S. Polydisperse Dextran As A Diffusing Test Solute to Study the Membrane-Permeability of Alginate Polylysine Microcapsules. *Biomaterials Artificial Cells and Immobilization Biotechnology* **21**, 427-444 (1993).
337. Dembczynski, R. Determination of pore diameter and molecular weight cut-off of hydrogel-membrane liquid-core capsules for immunoisolation. *Journal of biomaterials science. Polymer edition* **12**, 1051-1058 (2001).
338. Vandebossche, G.M.R., Vanoostveldt, P., & Remon, J.P. A Fluorescence Method for the Determination of the Molecular-Weight Cutoff of Alginate-Polylysine Microcapsules. *Journal of Pharmacy and Pharmacology* **43**, 275-277 (1991).
339. Georgieva, R., Moya, S., Hin, M., Mitlohner, R., Donath, E., Kiesewetter, H., Mohwald, H., & Baumler, H. Permeation of macromolecules into polyelectrolyte microcapsules. *Biomacromolecules* **3**, 517-524 (2002).
340. King, A., Strand, B., Rokstad, A.M., Kulseng, B., Andersson, A., Skjak-Braek, G., & Sandler, S. Improvement of the biocompatibility of alginate/poly-L-lysine/alginate microcapsules by the use of epimerized alginate as a coating. *Journal of Biomedical Materials Research Part A* **64A**, 533-539 (2003).
341. King, A., Andersson, A., Strand, B.L., Lau, J., Skjak-Braek, G., & Sandler, S. The role of capsule composition and biologic responses in the function of transplanted microencapsulated islets of Langerhans. *Transplantation* **76**, 275-279 (2003).
342. Orive, G., Ponce, S., Hernandez, R.M., Gascon, A.R., Igartua, M., & Pedraz, J.L. Biocompatibility of microcapsules for cell immobilization elaborated with different type of alginates. *Biomaterials* **23**, 3825-3831 (2002).
343. Lacik, I., Anilkumar, A.V., & Wang, T.G. A two-step process for controlling the surface smoothness of polyelectrolyte-based microcapsules. *Journal of Microencapsulation* **18**, 479-490 (2001).
344. Bungler, C.M., Tiefenbach, B., Jahnke, A., Gerlach, C., Freier, T., Schmitz, K.P., Hopt, U.T., Schareck, W., Klar, E., & De Vos, P. Deletion of the tissue response against alginate-PLL capsules by temporary release of co-encapsulated steroids. *Biomaterials* **26**, 2353-2360 (2005).
345. Luca, G., Calvitti, M., Neri, L.M., Becchetti, E., Capitani, S., Basta, G., Angeletti, G., Fanelli, C., Brunetti, P., & Calafiore, R. Sertoli cell-induced reversal of adult rat pancreatic islet beta-cells into fetal-like status: Potential implications for islet transplantation in type I diabetes mellitus. *Journal of Investigative Medicine* **48**, 441-448 (2000).
346. Liu, Z.C. & Chang, T.M.S. Coencapsulation of hepatocytes and bone marrow stem cells: In vitro conversion of ammonia and in vivo lowering of bilirubin in hyperbilirubemia Gunn rats. *International Journal of Artificial Organs* **26**, 491-497 (2003).

347. Liu,Z.C. & Chang,T.M.S. Transdifferentiation of bioencapsulated bone marrow cells into hepatocyte-like cells in the 90% hepatectomized rat model. *Liver Transplantation* **12**, 566-572 (2006).
348. Liu,Z.C. & Chang,T.M.S. Transplantation of bioencapsulated bone marrow stem cells improve hepatic regeneration and survival of 90% hepatectomized rats: A preliminary report. *Artificial Cells Blood Substitutes and Biotechnology* **33**, 405-410 (2005).
349. Zhang,H., Sun,L., Wang,W., & Ma,X. Quantitative analysis of fibrosis formation on the microcapsule surface with the use of picro-sirius red staining, polarized light microscopy, and digital image analysis. *Journal of Biomedical Materials Research Part A* **76A**, 120-125 (2006).
350. Roth,D.J., Jansen,E.D., Powers,A.C., & Wang,T.G. A novel method of monitoring response to islet transplantation: Bioluminescent imaging of an NF-kB transgenic mouse model. *Transplantation* **81**, 1185-1190 (2006).
351. Weber,L.M., He,J., Bradley,B., Haskins,K., & Anseth,K.S. PEG-based hydrogels as an in vitro encapsulation platform for testing controlled beta-cell microenvironments. *Acta Biomaterialia* **2**, 1-8 (2006).
352. Tamber,H., Johansen,P., Merkle,H.P., & Gander,B. Formulation aspects of biodegradable polymeric microspheres for antigen delivery. *Advanced Drug Delivery Reviews* **57**, 357-376 (2005).
353. Prakash,S. & Bhatena,J. Live bacterial cells as orally delivered therapeutics. *Expert opinion on biological therapy* **5**, 1281-1301 (2005).
354. Saavedra,J.M. Microbes to fight microbes: a not so novel approach to controlling diarrheal disease. *J. Pediatr. Gastroenterol. Nutr.* **21**, 125-129 (1995).
355. Saavedra,J.M. & Tschernia,A. Human studies with probiotics and prebiotics: clinical implications. *British Journal of Nutrition* **87**, S241-S246 (2002).
356. Prakash,S. & Chang,T.M. Microencapsulated genetically engineered live E. coli DH5 cells administered orally to maintain normal plasma urea level in uremic rats. *Nat. Med.* **2**, 883-887 (1996).
357. Hansen,L.T., Allan-Wojtas,P.M., Jin,Y.L., & Paulson,A.T. Survival of Ca-alginate microencapsulated Bifidobacterium spp. in milk and simulated gastrointestinal conditions. *Food Microbiology* **19**, 35-45 (2002).
358. Ishibashi,N. & Yamazaki,S. Probiotics and safety. *American Journal of Clinical Nutrition* **73**, 465S-470S (2001).

359. Prakash,S. & Chang,T.M. Microencapsulated genetically engineered live E. coli DH5 cells administered orally to maintain normal plasma urea level in uremic rats. *Nat. Med.* **2**, 883-887 (1996).
360. Jones,M.L., Chen,H., Ouyang,W., Metz,T., & Prakash,S. Microencapsulated Genetically Engineered Lactobacillus plantarum 80 (pCBH1) for Bile Acid Deconjugation and Its Implication in Lowering Cholesterol. *J. Biomed. Biotechnol.* **2004**, 61-69 (2004).
361. Chang,T.M.S. & Prakash,S. Procedures for microencapsulation of enzymes, cells and genetically engineered microorganisms. *Molecular Biotechnology* **17**, 249-260 (2001).
362. Dhoot,N.O. & Wheatley,M.A. Microencapsulated Liposomes in controlled drug delivery: Strategies to modulate drug release and eliminate the burst effect. *Journal of Pharmaceutical Sciences* **92**, 679-689 (2003).
363. Prabakaran,M. & Mano,J.F. Chitosan-based particles as controlled drug delivery systems. *Drug Delivery* **12**, 41-57 (2005).
364. Drury,J.L. & Mooney,D.J. Hydrogels for tissue engineering: scaffold design variables and applications. *Biomaterials* **24**, 4337-4351 (2003).
365. De Smet,I., Van Hoorde,L., De Saeyer,N., Vande Woestyne,M., & Verstraete,W. In vitro study of bile salt hydrolase (BSH) activity of BSH isogenic Lactobacillus plantarum 80 strains and estimation of cholesterol lowering through enhanced BSH activity. *Microbial Ecology in Health and Disease* **7**, 315-329 (1994).
366. Liu,X.D., Xue,W.M., Liu,Q., Yu,W.T., Fu,Y.L., Xiong,X., Ma,X.J., & Yuan,Q. Swelling behaviour of alginate-chitosan microcapsules prepared by external gelation or internal gelation technology. *Carbohydrate Polymers* **56**, 459-464 (2004).
367. Dunny,G.M. & Leonard,B.A.B. Cell-cell communication in gram-positive bacteria. *Annual Review of Microbiology* **51**, 527-564 (1997).
368. Drotleff,S., Lungwitz,U., Breunig,M., Dennis,A., Blunk,T., Tessmar,J., & Gopferich,A. Biomimetic polymers in pharmaceutical and biomedical sciences. *European Journal of Pharmaceutics and Biopharmaceutics* **58**, 385-407 (2004).
369. Uludag,H. & Sefton,M.V. Colorimetric Assay for Cellular-Activity in Microcapsules. *Biomaterials* **11**, 708-712 (1990).
370. P.M.M.Schrooyen , R.van der Meer , & C.G.de Kruif Microencapsulation: its application in nutrition. *Proceedings of the Nutrition Society* **60**, 475-479 (2001).
371. Tsuji K. Microencapsulation of pesticides and their improved handling safety. *J Microencapsulation* **18**, 137-147 (2001).

372. Nelson,G. Application of microencapsulation in textiles. *International Journal of Pharmaceutics* **242**, 55-62 (2002).
373. Park,J.K. & Chang,H.N. Microencapsulation of microbial cells. *Biotechnology Advances* **18**, 303-319 (2000).
374. Ko,J.A., Park,H.J., Hwang,S.J., Park,J.B., & Lee,J.S. Preparation and characterization of chitosan microparticles intended for controlled drug delivery. *International Journal of Pharmaceutics* **249**, 165-174 (2002).
375. Speer,D.P., Chvapil,M., Eskelson,C.D., & Ulreich,J. Biological Effects of Residual Glutaraldehyde in Glutaraldehyde-Tanned Collagen Biomaterials. *Journal of Biomedical Materials Research* **14**, 753-764 (1980).
376. Chen,HM., Jones,L.M., Ouyang,W., Metz,T., Martoni,C., Haque,T., Cohen,R., & Prakash,S. Design, preparation and in-vitro characterization of genipin cross linked alginate-chitosan microcapsules for live cell encapsulation for cell therapy. *Cell Biochemistry and Biophysics* (**accepted**), (2005).
377. Lakowicz,J.R. Principles of fluorescence spectroscopy. (New York : Kluwer Academic/Plenum,1999).
378. Lamprecht,A., Yamamoto,H., Takeuchi,H., & Kawashima,Y. Observations in simultaneous microencapsulation of 5-fluorouracil and leucovorin for combined pH-dependent release. *European Journal of Pharmaceutics and Biopharmaceutics* **59**, 367-371 (2005).
379. Schmitt,C., Sanchez,C., Lamprecht,A., Renard,D., Lehr,C.M., de Kruif,C.G., & Hardy,J. Study of [beta]-lactoglobulin/acacia gum complex coacervation by diffusing-wave spectroscopy and confocal scanning laser microscopy. *Colloids and Surfaces B: Biointerfaces* **20**, 267-280 (2001).
380. Akao,T., Kobashi,K., & Aburada,M. Enzymic studies on the animal and intestinal bacterial metabolism of geniposide. *Biol. Pharm. Bull.* **17**, 1573-1576 (1994).
381. Touyama,R., Inoue,K., Takeda,Y., Yatsuzuka,M., Ikumoto,T., Moritome,N., Shingu,T., Yokoi,T., & Inouye,H. Studies on the Blue Pigments Produced from Genipin and Methylamine .2. on the Formation Mechanisms of Brownish-Red Intermediates Leading to the Blue Pigment Formation. *Chemical & Pharmaceutical Bulletin* **42**, 1571-1578 (1994).
382. Fujikawa,S., Nakamura,S., & Koga,K. Genipin, A New Type of Protein Crosslinking Reagent from Gardenia Fruits. *Agricultural and Biological Chemistry* **52**, 869-870 (1988).
383. Cole,E.T., Scott,R.A., Cade,D., Connor,A.L., & Wilding,I.R. In vitro and in vivo pharmacoscintigraphic evaluation of ibuprofen hypromellose and gelatin capsules. *Pharmaceutical research* **21**, 793-798 (2004).

384. Kaul,G. & Amiji,M. Tumor-targeted gene delivery using poly(ethylene glycol)-modified gelatin nanoparticles: In vitro and in vivo studies. *Pharmaceutical research* **22**, 951-961 (2005).
385. Thanou,M. & Duncan,R. Polymer-protein and polymer-drug conjugates in cancer therapy. *Curr. Opin. Investig. Drugs* **4**, 701-709 (2003).
386. Kruckeberg,S. Chances and limits of microencapsulation in progressive food industry. *Chemie-Ingenieur-Technik* **75**, 1733-1740 (2003).
387. Hua,L. Microencapsulation and culture in vitro of rat pinealocytes. *The International journal of artificial organs* **26**, 958-964 (2003).
388. Fu,S.H. Impact of cracks in alginate microcapsules on the survival of pancreatic islets. *Transplantation Proceedings* **35**, 496 (2003).
389. Peirone,M.A., Delaney,K., Kwiecin,J., Fletch,A., & Chang,P.L. Delivery of recombinant gene product to canines with nonautologous microencapsulated cells. *Human Gene Therapy* **9**, 195-206 (1998).
390. Chen,H., Ouyang,W., Jones,M., Martoni,C., Haque,T., Cohen,R., & Prakash,S. Novel polymeric microcapsules for live cell encapsulation and therapy: preparation and characterization of genipin cross-linked alginate-chitosan microcapsules. *Cell Biochemistry and Biophysics* (in press) (2006).
391. Kuijpers,A.J., van Wachem,P.B., van Luyn,M.J.A., Plantinga,J.A., Engbers,G.H.M., Krijgsveld,J., Zaat,S.A.J., Dankert,J., & Feijen,J. In vivo compatibility and degradation of crosslinked gelatin gels incorporated in knitted Dacron. *Journal of Biomedical Materials Research* **51**, 136-145 (2000).
392. Deng,P. The Application of statistical methods on determination and data analysis. (Beijing:Chemical Industry Publishing Company.,1984).
393. Varde,N.K. & Pack,D.W. Microspheres for controlled release drug delivery. *Expert opinion on biological therapy* **4**, 35-51 (2004).
394. Fournier,E., Passirani,C., Montero-Menei,C.N., & Benoit,J.P. Biocompatibility of implantable synthetic polymeric drug carriers: focus on brain biocompatibility. *Biomaterials* **24**, 3311-3331 (2003).
395. Hunkeler,D. Objectively assessing bioartificial organs. *Annals of the New York Academy of Sciences* **944**, 456-471 (2001).
396. Hsu,B.R.S., Ho,Y.S., Fu,S.H., Huang,Y.Y., Chiou,S.C., & Huang,H.S. Membrane compactness affects the integrity and immunoprotection of alginate-poly-L-lysine-alginate microcapsules. *Transplantation Proceedings* **27**, 3227-3231 (1995).

397. Hari,P.R., Chandy,T., & Sharma,C.P. Chitosan/calcium alginate microcapsules for intestinal delivery of nitrofurantoin. *Journal of Microencapsulation* **13**, 319-329 (1996).
398. Zhou,Y., Martins,E., Groboillot,A., Champagne,C.P., & Neufeld,P.C. Spectrophotometric quantification of lactic bacteria in alginate and control of cell release with chitosan coating. *Journal of Applied Microbiology* **84**, 342-348 (1998).
399. Paik,Y.S., Lee,C.M., Cho,M.H., & Hahn,T.R. Physical stability of the blue pigments formed from geniposide of gardenia fruits: Effects of pH, temperature, and light. *Journal of Agricultural and Food Chemistry* **49**, 430-432 (2001).
400. Mi,F.L., Tan,Y.C., Liang,H.C., Huang,R.N., & Sung,H.W. In vitro evaluation of a chitosan membrane cross-linked with genipin. *Journal of Biomaterials Science-Polymer Edition* **12**, 835-850 (2001).
401. Liang,H.C., Chang,W.H., Lin,K.J., & Sung,H.W. Genipin-crosslinked gelatin microspheres as a drug carrier for intramuscular administration: In vitro and in vivo studies. *Journal of Biomedical Materials Research Part A* **65A**, 271-282 (2003).
402. Chang,W.H., Chang,Y., Chen,Y.C., & Sung,H.W. Hemoglobin polymerized with a naturally occurring crosslinking agent as a blood substitute: In vitro and in vivo studies. *Artificial Cells Blood Substitutes and Immobilization Biotechnology* **32**, 243-262 (2004).
403. Liang,H.C., Chang,Y., Hsu,C.K., Lee,M.H., & Sung,H.W. Effects of crosslinking degree of an acellular biological tissue on its tissue regeneration pattern. *Biomaterials* **25**, 3541-3552 (2004).
404. Smidsrod,O. & Skjakbraek,G. Alginate As Immobilization Matrix for Cells. *Trends in Biotechnology* **8**, 71-78 (1990).
405. Darrabie,M.D., Kendall,W.F., & Opara,E.C. Characteristics of poly-L-ornithine-coated alginate microcapsules. *Biomaterials* **26**, 6846-6852 (2005).
406. Frigon,R.P., Leypoldt,J.K., Uyeji,S., & Henderson,L.W. Disparity Between Stokes Radii of Dextrans and Proteins As Determined by Retention Volume in Gel-Permeation Chromatography. *Analytical Chemistry* **55**, 1349-1354 (1983).
407. Salminen,S. & Gueimonde,M. Human studies on probiotics: What is scientifically proven. *Journal of food science* **69**, M137-M140 (2004).
408. Lin,Y.H., Liang,H.F., Chung,C.K., Chen,M.C., & Sung,H.W. Physically crosslinked alginate/N,O-carboxymethyl chitosan hydrogels with calcium for oral delivery of protein drugs. *Biomaterials* **26**, 2105-2113 (2005).
409. Pillay,V. & Fassihi,R. In vitro release modulation from crosslinked pellets for site-specific drug delivery to the gastrointestinal tract - II. Physicochemical

- characterization of calcium-alginate, calcium-pectinate and calcium-alginate-pectinate pellets. *Journal of Controlled Release* **59**, 243-256 (1999).
410. El Gibaly, I. Development and in vitro evaluation of novel floating chitosan microcapsules for oral use: comparison with non-floating chitosan microspheres. *International Journal of Pharmaceutics* **249**, 7-21 (2002).
411. Brown, J. The effect of cross-linking on the in vivo disintegration of hard gelatin capsules. *Pharmaceutical research* **15**, 1026-1030 (1998).
412. Desai, K.G.H. & Park, H.J. Encapsulation of vitamin C in tripolyphosphate cross-linked chitosan microspheres by spray drying. *Journal of Microencapsulation* **22**, 179-192 (2005).
413. Schultz, M., Watzl, S., Oelschlaeger, T.A., Rath, H.C., Gottl, C., Lehn, N., Scholmerich, J., & Linde, H.J. Green fluorescent protein for detection of the probiotic microorganism *Escherichia coli* strain Nissle 1917 (EcN) in vivo. *Journal of Microbiological Methods* **61**, 389-398 (2005).
414. Mi, F.L., Tan, Y.C., Liang, H.F., & Sung, H.W. In vivo biocompatibility and degradability of a novel injectable-chitosan-based implant. *Biomaterials* **23**, 181-191 (2002).
415. Berrada, N., Lemeland, J.F., Laroche, G., Thouvenot, P., & Piaia, M. Bifidobacterium from Fermented Milks - Survival During Gastric Transit. *Journal of Dairy Science* **74**, 409-413 (1991).
416. Berg, J.O., Nord, C.E., & Wadstrom, T. Formation of glycosidases in batch and continuous cultures of *bacteroides fragilis*. *Applied Environmental Microbiology* **35**, 269-273 (1978).
417. Lamprecht, A., Yamamoto, H., Takeuchi, H., & Kawashima, Y. Design of pH-sensitive microspheres for the colonic delivery of the immunosuppressive drug tacrolimus. *European Journal of Pharmaceutics and Biopharmaceutics* **58**, 37-43 (2004).
418. Reddy, T. & Tammishetti, S. Gastric resistant microbeads of metal ion cross-linked carboxymethyl guar gum for oral drug delivery. *Journal of Microencapsulation* **19**, 311-318 (2002).
419. Delie, F. Evaluation of nano- and microparticle uptake by the gastrointestinal tract. *Advanced Drug Delivery Reviews* **34**, 221-233 (1998).
420. NARAYANI, R. & Rao Panduranga, K. Polymer-coated gelatin capsules as oral delivery devices and their gastrointestinal-tract behavior in humans. *Journal of biomaterials science. Polymer edition* **7**, 39-48 (1995).

421. Sato, Y. Pharmacoscintigraphic evaluation of riboflavin-containing microballoons for a floating controlled drug delivery system in healthy humans. *Journal of Controlled Release* **98**, 75-85 (2004).
422. Wilding, I.R. In vivo disintegration profiles of encapsulated and nonencapsulated sumatriptan: Gamma scintigraphy in healthy volunteers. *The Journal of clinical pharmacology* **45**, 101-105 (2005).
423. Molly, K., Vandewoestyne, M., Desmet, I., & Verstraete, W. Validation of the Simulator of the Human Intestinal Microbial Ecosystem (Shime) Reactor Using Microorganism-Associated Activities. *Microbial Ecology in Health and Disease* **7**, 191-200 (1994).
424. Hirayama, K. & Rafter, J. The role of lactic acid bacteria in colon cancer prevention: mechanistic considerations. *Antonie Van Leeuwenhoek International Journal of General and Molecular Microbiology* **76**, 391-394 (1999).
425. Simon, G.L. & Gorbach, S.L. Intestinal Flora in Health and Disease. *Gastroenterology* **86**, 174-193 (1984).
426. von Wright, A. & Bruce, A. Genetically modified microorganisms and their potential effects on human health and nutrition. *Trends in Food Science & Technology* **14**, 264-276 (2003).
427. Champagne, C.P., Gaudy, C., Poncelet, D., & Neufeld, R.J. Lactococcus-Lactis Release from Calcium Alginate Beads. *Applied and Environmental Microbiology* **58**, 1429-1434 (1992).
428. Chen, H., Ouyang, W., & Prakash, S. Influences of complexation reaction variables on alginate-chitosan microcapsules: visualization and optimization. (*Under preparation*) (2006).
429. Cui, J.H., Goh, J.S., Kim, P.H., Choi, S.H., & Lee, B.J. Survival and stability of bifidobacteria loaded in alginate poly-l-lysine microparticles. *International Journal of Pharmaceutics* **210**, 51-59 (2000).
430. Hansen, L.T., Allan-Wojtas, P.M., Jin, Y.L., & Paulson, A.T. Survival of Ca-alginate microencapsulated Bifidobacterium spp. in milk and simulated gastrointestinal conditions. *Food Microbiology* **19**, 35-45 (2002).
431. Hannoun, B.J.M. & Stephanopoulos, G. Diffusion-Coefficients of Glucose and Ethanol in Cell-Free and Cell-Occupied Calcium Alginate Membranes. *Biotechnology and Bioengineering* **28**, 829-835 (1986).
432. Prakash, S and Jones, M. Bacterial cells for bile acid intake and/or lowering cholesterol: immobilized, microencapsulated. US Provisional. 02098 . 2-28-0003.
- Ref Type: Patent

433. Lee, K.Y. & Heo, T.R. Survival of *Bifidobacterium longum* immobilized in calcium alginate beads in simulated gastric juices and bile salt solution. *Applied and Environmental Microbiology* **66**, 869-873 (2000).
434. Shah, N.P. Probiotic bacteria: Selective enumeration and survival in dairy foods. *Journal of Dairy Science* **83**, 894-907 (2000).
435. Leung, K.T., So, J.S., Kostrzynska, M., Lee, H., & Trevors, J.T. Using a green fluorescent protein gene-labeled p-nitrophenol-degrading *Moraxella* strain to examine the protective effect of alginate encapsulation against protozoan grazing. *Journal of Microbiological Methods* **39**, 205-211 (2000).
436. Tharmaraj, N. & Shah, N.P. Selective enumeration of *Lactobacillus delbrueckii* ssp *bulgaricus*, *Streptococcus thermophilus*, *Lactobacillus acidophilus*, bifidobacteria, *Lactobacillus casei*, *Lactobacillus rhamnosus*, and propionibacteria. *Journal of Dairy Science* **86**, 2288-2296 (2003).
437. Nassif, N., Roux, C., Coradin, T., Rager, M.N., Bouvet, O.M.M., & Livage, J. A sol-gel matrix to preserve the viability of encapsulated bacteria. *Journal of Materials Chemistry* **13**, 203-208 (2003).
438. Wright, K.M., Coleman, H.P., Mackle, A.R., Parker, M.L., Brocklehurst, T.F., Wilson, D.R., & Hills, B.P. Determination of mean growth parameters of bacterial colonies immobilized in gelatin gel using a laser gel-cassette scanner. *International Journal of Food Microbiology* **57**, 75-89 (2000).

## **APPENDICES**

1. Compliance Certificate for the Use of Microorganisms and Other Biohazards
2. Copyright material
3. Signed coauthor waivers